Spacetime Geometry from Quantum Circuits and Berry Phases in AdS/CFT

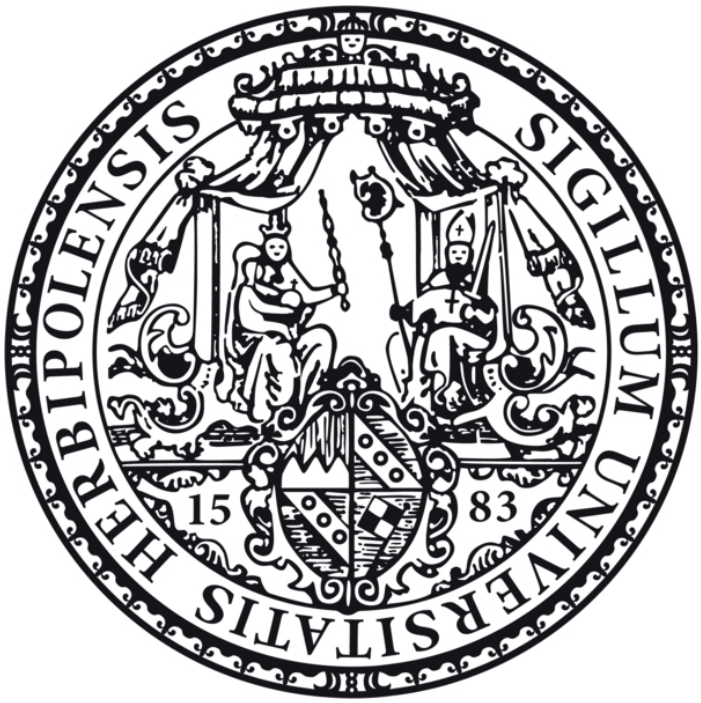

Dissertation zur Erlangung des naturwissenschaftlichen Doktorgrades
an der Fakultät für Physik und Astronomie
der Julius-Maximilians-Universität Würzburg

vorgelegt von

Anna-Lena Weigel

aus Bad Hersfeld

Würzburg, im Juli 2023

Eingereicht bei der Fakultät für Physik und Astronomie am

_____

Gutachter der Dissertation

1. Gutachter: Prof. Dr. Johanna Erdmenger
2. Gutachter: Prof. Dr. Björn Trauzettel
3. Gutachter: _____

Prüfer des öffentlichen Promotionskolloquiums

1. Prüfer: Prof. Dr. Johanna Erdmenger
2. Prüfer: Prof. Dr. Björn Trauzettel
3. Prüfer: _____
4. Prüfer: _____
5. Prüfer: _____

Tag des öffentlichen Promotionskolloquiums

_____

Doktorurkunde ausgehändigt am

_____

Abstract

One of the fundamental challenges in theoretical physics is to develop a complete, consistent theory of quantum gravity. In the last 25 years, the AdS/CFT correspondence has proven itself as an invaluable tool in this endeavor. The correspondence states that a d-dimensional conformal field theory (CFT) is dual to a gravity theory in $(d+1)$-dimensional Anti-de Sitter (AdS) space. Studying quantum information measures in the context of AdS/CFT has been very successful in understanding the fundamental nature of spacetime: Quantum information measures in the CFT are associated with the geometry of the dual AdS space.

I build on these successes in this thesis by establishing new relations between quantum information measures in a two-dimensional CFT and geometric objects in a three-dimensional AdS space. I focus on two quantum information measures: the computational cost of quantum circuits in a CFT and Berry phases in two entangled CFTs. In particular, I show that these quantities are associated with geometric objects in the dual AdS space.

The first part of this thesis focuses on quantum circuits in the CFT. Within AdS/CFT, it is conjectured that the computational complexity of quantum circuits in the CFT may be represented as a geometric object in the dual AdS space. There are multiple proposals, referred to as holographic complexity proposals, for geometric objects dual to the complexity. It is unclear, however, how the associated quantum circuit in the CFT is built and how its associated complexity is measured. To make progress in verifying the conjecture, I study quantum circuits implementing conformal transformations in the CFT. I employ the Fubini-Study distance as a cost measure, which yields the complexity when minimized, to measure the cost of such a quantum circuit. The Fubini-Study distance measures the distance between states on the projective Hilbert space, i.e. the space of physically indistinguishable states. The first essential step toward verifying the holographic complexity proposals is to find a gravity dual to a quantum circuit. I present a recipe in this thesis for implementing a quantum circuit built from conformal transformations in the CFT in the dual gravity theory. In particular, the quantum circuit is encoded in the time evolution of the dual AdS spacetime. Employing this gravity dual to a quantum circuit, the computational cost measured in terms of the Fubini-Study distance between states on the projective Hilbert space may be written as a geometric object in the dual spacetime that is given in terms of spacelike geodesics and metric components. This gravity dual to the CFT cost measure holds in the vacuum AdS spacetime, conical defect, and black hole

geometries. This result presents the first derivation of a holographic dual to a CFT cost function from first principles. Furthermore, the gravity dual to a quantum circuit introduced in this thesis provides the basis for deriving CFT duals to the holographic complexity conjectures.

In the second part, I investigate the implications of a non-traversable spacetime wormhole in AdS space for the dual CFTs. A spacetime wormhole in AdS is dual to two entangled CFTs that are causally disconnected. Such a wormhole gives rise to the factorization problem: an apparent factorization of the CFT Hilbert space between the two entangled copies of the CFT but a non-factorized dual gravity Hilbert space in the presence of a wormhole.

To make progress in understanding this problem, it is of essential importance to illuminate how the different Hilbert space structures arise. As a first step, I introduce Berry phases in the CFT as quantum information measures sensitive to the spacetime wormhole in the dual gravity theory. In particular, there are three different Berry phases probing the wormhole – Virasoro, modular, and gauge Berry phases – that each arise from different transformations in the CFT. For each Berry phase, I discuss which features of the dual spacetime wormhole they probe. Furthermore, I interpret the three Berry phases in view of the factorization puzzle and show that they arise from non-factorized classical CFT phase spaces. The non-factorized phase spaces emerge from a non-trivial center in the operator algebra of the CFT that is related to the spacetime wormhole.

Finally, I relate these results to recent progress in applying von Neumann algebras to AdS/CFT. These algebras were first considered in the context of algebraic quantum field theory and now present an essential tool in understanding the properties of operator algebras in a semiclassical and quantum gravity setup. In particular, I show that the Berry phases probe different features of the von Neumann algebras describing the operator algebras of the gravity theory and dual CFT. Moreover, I discuss a relation between Berry phases and missing information for a local observer. These results illuminate the source of the factorization puzzle and allow me to suggest steps to resolve it.

This thesis is based on the following original works:

[1]: J. Erdmenger, M. Flory, M. Gerbershagen, M. P. Heller, and A.-L. Weigel. "Exact Gravity Duals for Simple Quantum Circuits". In: *SciPost Phys.* **13** (2022), p. 061. arXiv: 2112.12158 [hep-th]

[2]: J. Erdmenger, M. Gerbershagen, M. P. Heller, and A.-L. Weigel. "From Complexity Geometry to Holographic Spacetime". In: *arXiv* (Nov. 2022). arXiv: 2212.00043 [hep-th]

[3]: S. Banerjee, M. Dorband, J. Erdmenger, R. Meyer, and A.-L. Weigel. "Berry phases, wormholes and factorization in AdS/CFT". in: *JHEP* **08** (2022), p. 162. arXiv: 2202.11717 [hep-th]

[4]: S. Banerjee, M. Dorband, J. Erdmenger, and A.-L. Weigel. "Geometric Phases Characterise Operator Algebras and Missing Information". In: *arXiv* (May 2023). arXiv: 2306.00055 [hep-th]

Zusammenfassung

Eine der grundlegenden Herausforderungen der theoretischen Physik ist es, eine vollständige, konsistente Theorie der Quantengravitation zu entwickeln. In den letzten 25 Jahren hat sich die AdS/CFT-Korrespondenz als besonders wertvoll für dieses Ziel erwiesen. Die Korrespondenz sagt aus, dass eine d-dimensionale konforme Feldtheorie (CFT) zu einer $(d+1)$-dimensionalen Gravitationstheorie im Anti-de-Sitter-Raum (AdS-Raum) dual ist. Zuletzt war insbesondere die Untersuchung von Quanteninformationsmaßen in AdS/CFT erfolgreich, um die fundamentale Natur der Raumzeit zu verstehen: Quanteninformationsmaße in der CFT wurden mit geometrischen Objekten im AdS-Raum assoziiert.

In dieser Arbeit baue ich auf diesen Erfolgen auf, indem ich neue Beziehungen zwischen Quanteninformationsmaßen in zweidimensionalen CFTs und geometrischen Objekten im dreidimensionalen AdS-Raum herstelle. Ich betrachte zwei Quanteninformationsmaße: die Rechenkosten eines Quantenschaltkreises in der CFT und Berry-Phasen in zwei verschränkten CFTs. Insbesondere zeige ich, dass diese Größen mit geometrischen Objekten im AdS-Raum assoziiert sind.

Der erste Teil dieser Arbeit beschäftigt sich mit Quantenschaltkreisen in der CFT. Im Rahmen der AdS/CFT-Korrespondenz wird vorgeschlagen, dass die Komplexität eines Quantenschaltkreises in der CFT durch ein geometrisches Objekt im dualen AdS-Raum dargestellt werden kann. Es gibt verschiedene Hypothesen, genannt holographische Komplexitätsvermutungen, die geometrische Objekte als Duale zur Komplexität vorschlagen. Es ist jedoch unklar, wie der entsprechende Quantenschaltkreis in der CFT aufgebaut ist und wie die assoziierte Komplexität gemessen wird. Um Fortschritte in der Überprüfung der holographischen Komplexitätsvermutungen zu machen, untersuche ich Quantenschaltkreise, die konforme Transformationen in der CFT implementieren. Um die Kosten eines solchen Quantenschaltkreises zu messen, verwende ich die Fubini-Study-Metrik als Kostenfunktion. Die Komplexität entspricht dann der minimierten Kostenfunktion. Die Fubini-Study-Metrik misst die Distanz zwischen Zuständen auf dem projektiven Hilbertraum, d.h. die Distanz zwischen physikalisch unterscheidbaren Zuständen.

Ein erster essentieller Schritt für die Verifizierung der holographischen Komplexitätsvermutungen ist es, ein holographisches Dual für einen Quantenschaltkreis zu finden. In dieser Arbeit entwickle ich ein Prinzip für die Konstruktion eines Quantenschaltkreises in der dualen Gravitationstheorie, der konforme Transformationen implementiert. Der Quantenschaltkreis kann insbesondere als Zeitevolution in der dualen Gra-

vitationstheorie dargestellt werden. Ich verwende dieses Gravitationsdual, um zu zeigen, dass die mit der Fubini-Study-Metrik gemessenen Kosten der Distanz zwischen Zuständen auf dem projektiven Hilbertraum ein geometrisches Objekt in der dualen Raumzeit sind. Insbesondere sind die Kosten durch raumartige Geodäten und Metrikkomponenten darstellbar. Das Gravitationsdual zu der CFT-Kostenfunktion ist im Vakuum-AdS-Raum, für konischen Defekt und in Schwarzen Loch-Geometrien gültig. Dieses Ergebnis ist somit die erste Herleitung für ein holographisches Dual zu einer CFT-Kostenfunktion basierend auf grundlegenden Prinzipien. Weiterhin erlaubt das hier vorgestellte Gravitationsdual zu einem Quantenschaltkreis prinzipiell die Herleitung von CFT-Dualen zu den holographischen Komplexitätsmaßen.

Im zweiten Teil dieser Arbeit beschäftige ich mich mit den Auswirkungen von nicht-transversablen Wurmlöchern im AdS-Raum auf die konformen Feldtheorien. Ein Wurmloch in AdS ist dual zu zwei verschränkten CFTs, die durch einen Ereignishorizont kausal getrennt sind. Ein solches Wurmloch führt auf das Faktorisierungsproblem: eine scheinbare Faktorisierung des Hilbertraums der beiden verschränkten CFTs, während der duale Hilbertraum des Gravitationssystems mit Wurmloch nicht faktorisiert.

Die Lösung dieses Problems erfordert zu verstehen, warum die Hilberträume eine unterschiedliche Struktur haben. Als ersten Schritt führe ich Berry-Phasen als Quanteninformationsmaß in der CFT ein, das durch die Anwesenheit eines Wurmlochs beeinflusst wird. Insbesondere zeige ich, dass drei verschiedene Berry-Phasen, die zu unterschiedlichen Symmterietransformationen gehören, die Anwesenheit des Wurmlochs im Gravitationsdual charakterisieren – Virasoro-, modulare und Eich-Berry-Phasen. Für jede dieser Berry-Phasen diskutiere ich, welche Eigenschaften des Wurmloches sie anzeigen. Weiterhin interpretiere ich die drei Berry-Phasen im Kontext des Faktorisierungsproblems und zeige, dass die Berry-Phasen von einem nicht-faktorisierten klassischen Phasenraum stammen. Die nicht-faktorisierten Phasenräume weisen auf ein nicht-triviales Zentrum der Operatoralgebra der CFT hin, das seinen Ursprung im dualen Wurmloch hat.

Als letztes stelle ich einen Zusammenhang zwischen diesen Ergebnissen und kürzlichen Fortschritten in der Anwendung von von Neumann-Algebren auf die AdS/CFT-Korrespondenz her. Diese Algebren stammen ursprünglich aus der algebraischen Quantenfeldtheorie und stellen aktuell ein wichtiges Werkzeug für das Verständnis der Eigenschaften von Operatoralgebren im semiklassischen und Quantengravtionsbereich dar. Insbesondere zeige ich, dass Berry-Phasen Eigenschaften der von Neumann-Algebren charakterisieren. Weiterhin diskutiere ich einen Zusammenhang zwischen

von Neumann-Algebren und fehlenden Informationen für einen lokalen Beobachter. Diese Ergebisse illustrieren die Ursache des Faktorisierungsproblems und erlauben mir, Schritte für dessen Lösung vorzuschlagen.

Diese Arbeit basiert auf den folgenden Originalveröffentlichungen:

[1]: J. Erdmenger, M. Flory, M. Gerbershagen, M. P. Heller, and A.-L. Weigel. "Exact Gravity Duals for Simple Quantum Circuits". In: *SciPost Phys.* **13** (2022), p. 061. arXiv: 2112.12158 [hep-th]

[2]: J. Erdmenger, M. Gerbershagen, M. P. Heller, and A.-L. Weigel. "From Complexity Geometry to Holographic Spacetime". In: *arXiv* (Nov. 2022). arXiv: 2212.00043 [hep-th]

[3]: S. Banerjee, M. Dorband, J. Erdmenger, R. Meyer, and A.-L. Weigel. "Berry phases, wormholes and factorization in AdS/CFT". in: *JHEP* **08** (2022), p. 162. arXiv: 2202.11717 [hep-th]

[4]: S. Banerjee, M. Dorband, J. Erdmenger, and A.-L. Weigel. "Geometric Phases Characterise Operator Algebras and Missing Information". In: *arXiv* (May 2023). arXiv: 2306.00055 [hep-th]

Contents

1 Introduction

The many mysteries of quantum gravity

The most fundamental developments in theoretical physics over a little more than the last century have been the development of quantum mechanics [5–9], special relativity [10, 11], and general relativity [12–15]. Quantum mechanics explains the properties of materials at the atomic and subatomic level. As such, it has for instance been essential in understanding the different conductivity properties of conductors and semiconductors. Its applications in technology are vast and ever-increasing. Examples include semiconductors that are a part of even the most basic electronic devices but also advanced technology such as quantum computers. Similarly, special relativity provides a framework to fully understand classical electrodynamics and is the foundation for the precision of modern GPS systems. From a theoretical point of view, the unification of the principles of quantum mechanics with those of special relativity gave rise to quantum field theory (QFT). QFT finds application in many fields in physics ranging from condensed matter to particle physics. In condensed matter physics, it played a fundamental role in the prediction of the quantum Hall effect [16] and its subsequent measurement [17]. In particle physics, it is the fundamental ingredient in the standard model [18]. The existence of the final proposed standard-model particle – the Higgs boson – was detected in 2012 [19–21].

A further essential development is general relativity. A first fundamental test of its predictions was the procession of mercury [14]. Furthermore, it predicted the existence of black holes [22, 23]. Recently, the mass of the supermassive black hole in our own galaxy [24] has been measured. Additionally, the existence of gravitational waves has been experimentally verified [25]. Yet, general relativity stands apart from quantum mechanics. So far, these two theories have resisted attempts to unify them consistently. A consistent unification of quantum mechanics and general relativity forms the basis for a theory of quantum gravity that describes the fundamental nature of space and time. Attempts to define such theories include string theory [26] and loop quantum gravity [27]. Despite these advances, understanding quantum gravity is one of the fundamental open questions in theoretical physics. One of the main obstacles is that quantum physics and general relativity appear to possess a vastly different and at times mutually exclusive playbook. For instance, quantum field theory is renormalizable, i.e.

a finite number of terms can be subtracted from the action of a given theory to remove divergences. General relativity, on the other hand, is non-renormalizable, implying an infinite number of terms are necessary to remove divergences. Another example of the apparently contradictory principles of quantum mechanics and general relativity is the behavior of the entropy. The entropy in a QFT scales with the volume and is thus extensive. On the other hand, the thermal entropy of a black hole in general relativity scales with the area of the horizon [23, 28, 29],

$$S_{\mathrm{BH}} = \frac{A}{4G_N}. \tag{1.1}$$

In statistical mechanics, the entropy is a measure of the number of states accessible to a system. However, in general relativity, the black hole is described by only three numbers: the charge, the angular momentum, and the mass. This is not compatible with an entropy that scales with the area of the black hole and is thus very large. It is assumed that the black hole entropy (1.1) counts the number of black hole microstates[30]. These are the quantum states from which the black hole may have formed within a given framework of quantum gravity[1].

Our limited understanding of quantum gravity gives rise to important puzzles. The most prominent one is the black hole information paradox [31], which consists of an inconsistency when considering the quantum mechanics of black holes in a spacetime described by general relativity. Black holes are objects that have a temperature [23] and obey the laws of thermodynamics [28, 32]. These properties allow black holes to evaporate. During its evaporation, the black hole emits thermal radiation, called Hawking radiation. If a black hole is formed by an object that is described by a pure state , then after it has evaporated only thermal Hawking radiation remains. Therefore, a black hole that was initially described by a pure state has evolved into a mixed state after its evaporation. This behavior violates unitarity and is called the black hole information paradox. An understanding of quantum gravity is therefore essential to make progress in black hole physics, but also in inflationary cosmology to describe the singularity from which our universe formed. Therefore, black holes and cosmology present ideal candidates to understand the fundamental properties a theory of quantum gravity must obey. We will focus our discussion on black holes. Progress toward understanding quantum gravity is driven by two important developments, the holographic principle [33] and the AdS/CFT correspondence [34].

[1] The authors of [30], for instance, employ string theory to derive the area law from the number of black hole microstates.

The holographic principle

The holographic principle [33], proposed in 1994, forms the basis for much of the progress that has been made over the last thirty years in understanding the principles of quantum gravity. An important ingredient to the holographic principle is the Bekenstein bound [35], proposed more than a decade earlier, which states that the entropy of a spacetime region cannot exceed its area A,

$$S \leq \frac{A}{4G_N}. \tag{1.2}$$

This implies that the entropy of a spacetime region is maximal if it contains a black hole that fits exactly into this region.

Based on the Bekenstein bound and the concept that the entropy counts the number of degrees of freedom of a system, [36] and [33] argued that quantum gravity is described by far fewer degrees of freedom than we might think: To fully capture the physics of a bounded spacetime volume, it is sufficient to consider the degrees of freedom in the area of its boundary. Or more general, the degrees of freedom of quantum gravity in $d+1$ dimensions are fully described by those on a d-dimensional surface bounding the spacetime region. In this sense, spacetime is a hologram of a lower-dimensional theory that captures the same physics. The most concrete and well-understood example of the holographic principle is the AdS/CFT correspondence. It is one of the most important developments in theoretical physics in the last 25 years. The correspondence was proposed by Maldacena in the seminal paper [34] in 1997 and states that a gravity theory in $(d+1)$-dimensional Anti-de Sitter space (AdS), a hyperbolic space, is dual to a conformal field theory (CFT) on flat Minkowski space in d dimensions that lives at the boundary of the AdS spacetime. The gravity theory is a certain type of string theory and is referred to as the bulk. A particularly remarkable feature of the AdS/CFT correspondence is that it proposes we may describe quantum gravity in terms of a theory that knows absolutely nothing about it since the dual CFT is a theory without gravity. Yet, we may use both theories to describe exactly the same physics, and the dynamics of the gravity theory are encoded fully in the dual CFT. Tests of the correspondence are typically performed in the semiclassical limit since the full quantum string theory on a curved spacetime is still poorly understood. In this limit, we consider quantum fields on a classical Einstein gravity background to perform explicit calculations. However, it is expected that the duality continues to hold in the quantum gravity regime. Another unique aspect of AdS/CFT is that both theories on either side of the correspondence exist as independent theories. In this re-

spect, the correspondence goes far beyond previous bulk-to boundary correspondences. To illustrate this, let us consider bulk-boundary correspondences in condensed-matter physics [37]. In a topological insulator, the existence of a topological invariant in the bulk leads to a physical observable in the boundary. Note that these boundary observables do not exist without the bulk. In contrast, the AdS/CFT correspondence relates two independent theories that exist and are well-defined without the other.

The AdS/CFT correspondence has been the driving force behind progress towards understanding quantum gravity. A particularly fruitful approach presents the introduction of concepts from quantum information theory, which has lead to significant advances in understanding black hole physics, including the information paradox, and how the bulk spacetime and its dynamics are encoded in the dual CFT.

It from Qubit: Spacetime from quantum information

Many of the earlier works [38–40] on AdS/CFT rely heavily on a particular string theory and its field content and similarly for the dual CFT. More recently, further progress was obtained by introducing concepts of quantum information into AdS/CFT. This approach is promising as quantum information measures are not sensitive to details of the theory such as the field content, but only to the information stored within a state or subregion. This opens up a path to draw very general lessons about the nature of quantum gravity from the correspondence. Quantum information associated to a state is for instance its entanglement structure or its quantum computational complexity. Complexity quantifies the most efficient way to create a state from an initial simple reference state by acting on the reference state with unitary transformations, called gates, chosen from a predefined gate set. In a quantum system describing a single spin, we may for instance ask how difficult it is to transform a spin-up state into a spin-down state using transformations built from Pauli matrices. This is accomplished by finding the most efficient unitary operation that transforms the reference state into the desired target state. The definition of the most efficient unitary strongly depends on the choice of gate set and reference state. If the set of gates are restricted to symmetry transformations, the shortest path in the group manifold from the identity transformation to the transformation that yields the desired target state or the distance between the reference state and target state on the projective Hilbert space present good choices. The states on which these gates act describe qubits. The qubits inherit their name from their classical counterparts – the bits – which are the foundation of classical computers. Quantum computational complexity is an information measure with a classical analog, but the complexity of quantum states is far larger

due to the existence of superpositions. Whereas a classical bit only takes the values zero or one, the qubit may be described by any superposition of these two states. Superpositions increase the complexity of a state as more information is stored in them and thus more complex operations are necessary to obtain such a state from a simple reference state.

In contrast, entanglement is a purely quantum phenomenon without any classical analog. This is a first hint that entanglement may play an integral part in understanding quantum gravity. Entanglement is the source of measurable correlations between a composite system consisting of system A and system B, even if there is no classical interaction between these systems. The defining property of entanglement is that the state describing both system A and B cannot be written as a product of a state in A and a state in B. Therefore, the state does not factorize between A and B. Entanglement is quantifiable by the entanglement entropy $S = -\mathrm{tr}(\rho_A \log(\rho_A))$, where ρ_A is the reduced density matrix associated to system A. In AdS/CFT, we may for instance consider a subregion on a static slice in the CFT (system A) and its complement (system B) and ask how we calculate the same quantity in the dual AdS gravity theory. The answer is as surprising as it is simple: The entanglement entropy of the subregion A in the CFT is given by the area of the minimal surface γ in AdS – the Ryu-Takayanagi surface – that is anchored in the boundary CFT in the subregion A [41, 42],

$$S = \frac{\mathrm{Area}(\gamma)}{4G_N}. \tag{1.3}$$

Covariant generalizations [43] and quantum corrections [44–46] to this formula are also known. The most remarkable aspect of (1.3) is that it is another instance, in addition to the black hole entropy and the Bekenstein bound, where the entropy is related to an area. Furthermore, (1.3) is a first indication that the bulk geometry is emergent from entanglement in the CFT, an idea first proposed in [47]: If the entanglement between the subregions is reduced, the area in (1.3) shrinks. This is illustrated in fig. 1.1. Ultimately, the area vanishes if there is no entanglement. The two subsystems then become 'squeezed off', and there are two disconnected geometries, one for system A and another one for system B. This idea of an emergent bulk geometry from entanglement in the dual CFT was made precise in the ER=EPR conjecture [48], which links entanglement to spacetime wormholes. ER is the wormhole (or the Einstein-Rosen bridge) and EPR refers to maximally entangled states called Bell states or EPR pairs. A prime example of this conjecture is the eternal AdS black hole. In contrast to the evaporating black holes that give rise to the black hole information paradox, eternal black holes are in thermal equilibrium with their surroundings and

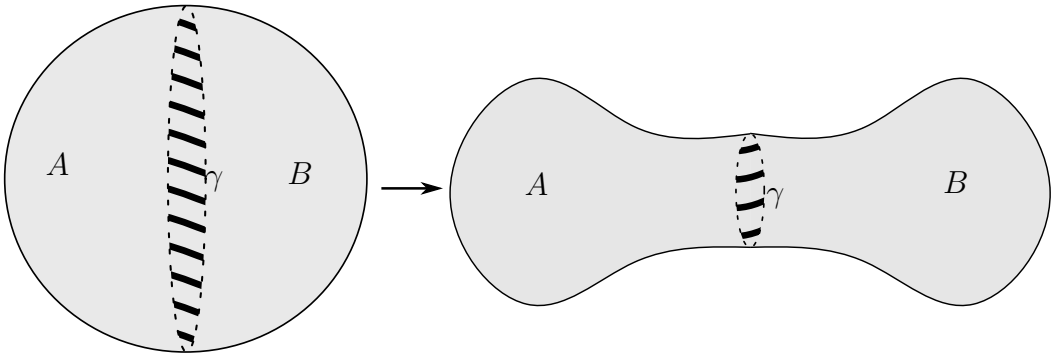

Fig. 1.1.: A sketch illustrating how entanglement gives rise to geometry in AdS/CFT: For illustration, let us assume that the CFT lives on a manifold represented by a sphere, and the dual gravity theory lives in the interior of the sphere. We then bipartition the sphere into two subsystems A and B that each live on a half-sphere. The holographic entanglement entropy between two subsystems A and B is given by the area of the minimal surface γ that connects the subregions A and B through the interior of the sphere. If the entanglement between regions A and B is reduced, the area of γ decreases until the regions become disconnected and the entanglement entropy vanishes. The subsystems A and B then live on disconnected manifolds. This illustrates that spacetime is emergent from entanglement.

thus do not evaporate. The eternal AdS black hole is the maximal extension of the Schwarzschild black hole in AdS and has two exterior regions, which are conjectured to be smoothly connected through a non-traversable wormhole. Since there are two exterior regions in this AdS space, there are also two boundaries. This eternal AdS black hole is then described in terms of two dual CFTs. In particular, the eternal AdS black hole is dual to the maximally entangled thermofield-double (TFD) state in the CFTs [49],

$$|\mathrm{TFD}\rangle = \frac{1}{\sqrt{Z}} \sum_n e^{-\beta \frac{E_n}{2}} |E_n\rangle_L |E_n\rangle_R \quad \text{with} \quad Z = \sum_n e^{-\beta E_n}. \tag{1.4}$$

Clearly, this state is not a product state between the energy-eigenstates $|E_n\rangle_R$ in the right CFT and $|E_n\rangle_L$ in the left CFT and is thus entangled. It is in fact a generalization of an EPR state.

The holographic entanglement entropy of the TFD state (1.4) was computed in [50] and was shown to be given in terms of a Ryu-Takayanagi surface that connects both boundaries through the interior of the black hole for early times. Similarly, correlation functions between operators in the left and right CFT are given in terms of geodesics connecting both boundaries through the black hole interior [51]. All this provides evidence that the interpretation of the black hole interior in terms of a smooth wormhole

geometry is sensible and that the existence of the wormhole is linked to entanglement in the CFT.

To summarize, there is clear evidence within AdS/CFT that entanglement in the CFT gives rise to a connected bulk spacetime. This idea has been studied extensively and has been made much more concrete. The boundary subregion for which we calculate the entanglement entropy is dual to a bulk subregion defined in terms of the domain of dependence of the Ryu-Takayanagi surface called the entanglement wedge [52]. Furthermore, a general prescription for obtaining bulk operators in this subregion in terms of CFT operators in the boundary subregion has been found [46, 53–59]. Another important lessons is that the bulk information is stored in the CFT in a redundant way that can be described in terms of quantum error correcting codes [60–62], which also have their origin in information theory. As a consequence, the AdS/CFT correspondence may be viewed as a quantum error correction code. In particular, quantum information can be retrieved via quantum recovery channels [63, 64]. This progress in understanding AdS/CFT as a quantum information/geometry correspondence culminated in showing that unitary black hole evaporation is possible [65] employing a generalization of the Ryu-Takayanagi surfaces [45, 66] in (1.3) and a particular quantum recovery channel [64]. This presents significant progress towards resolving the black hole information paradox. The guiding principle is that space and time are not a fundamental ingredients to a theory of quantum gravity but rather are emergent [47, 48, 67, 68] in certain limits of quantum gravity [69, 70]. Furthermore, the ideas relating quantum information and geometry are so general that the lessons learned about quantum gravity are most likely generalizable to more general frameworks than the AdS/CFT correspondence.

Holographic quantum circuits and the factorization puzzle

In light of these developments, this thesis is devoted to establishing new relations between quantum information measures in the CFT and geometric objects in the AdS gravity theory with the aim of further illuminating how quantum information stored in the CFT encodes the geometry of the AdS bulk spacetime. In particular, we study two quantum information measures in the CFT – the computational cost of quantum circuits and Berry phases – and demonstrate which features of the bulk geometry they probe.

We employ quantum circuits built from conformal symmetry transformations in a two-dimensional CFT and measure the computational cost of these circuits in terms of the distance between the reference and target state on the projective Hilbert space.

This distance measure is called the Fubini-Study distance. We then present an approach that allows to implement the CFT quantum circuit in the dual bulk spacetime. We accomplish this by encoding the evolution of the quantum circuit as a time evolution of the bulk spacetime. This construction presents a means to derive holographic duals to quantum information measures. We demonstrate this by deriving the holographic dual to the Fubini-Study distance. In particular, we show that the dual bulk object is geometric and may be written in terms of spacelike geodesics. This result presents the first derivation of a holographic dual to a CFT cost measure from first principles. It furthermore shows that the cost of a quantum circuit implementing conformal symmetry transformations measured by the Fubini-Study distance is geometric. We therefore find further evidence that quantum information content of the CFT is encoded geometrically in the AdS bulk.

The second quantum information measure we study is the Berry phase. We introduce Berry phases in the CFT as a probe that is sensitive to the presence of a bulk wormhole. In particular, we discuss three different types of Berry phases. Each Berry phase arises from different mechanisms which range from conformal symmetry transformations to gauge transformations and parallel transport of intervals in the CFT. We illustrate that the bulk wormhole is encoded in each of the CFT Berry phases and draw conclusions about the structure of the CFT and bulk Hilbert spaces. In particular, we demonstrate that the Berry phase encodes the microscopic structure of the CFT Hilbert space and comment on the implications of factorization properties of the CFT and bulk Hilbert spaces. Our results establish that Berry phases are an important tool in understanding the structure of the Hilbert space and therefore the factorization properties of the bulk and boundary Hilbert spaces in the presence of a bulk wormhole.

Let us now continue with two important developments that followed from the study of entanglement and its relation to the emergence of spacetime, which are of essential importance in this thesis:

First, it became clear in a series of papers [43, 50, 71, 72] that employing only entanglement as a probe of the bulk spacetime, some regions of the bulk spacetime cannot be reconstructed. The entanglement entropy exhibits phase transitions that make some regions inaccessible. A particularly relevant example for this thesis is the transition observed in [50]: Under time evolution, the Ryu-Takayanagi surface calculating the entanglement entropy between subregions in the left and right CFT stretches through the bulk wormhole at early times in the evolution and shows a linear growth with time that is associated with the growth of the wormhole. However, when the wormhole exceeds a certain size, the Ryu-Takayanagi surface jumps to a

configuration that lies outside the black hole horizon and thus is no longer sensitive to the growth of the wormhole. This immediately raises the question which CFT observable quantifies the growth of the wormhole at later times. It was proposed in [73, 74] that an appropriate measure is the complexity of the dual TFD state under time evolution. This raises two questions. First, how do we define complexity in the CFT? The authors of [75] introduced the notion of circuit complexity in a two-dimensional CFT based on previous works [76–79]. In this proposal gates are built from symmetry transformations and the complexity is associated to a geodesic with respect to a distance measure in the group manifold. And secondly, what is the bulk observable that is dual to the complexity of the CFT state and probes the growth of the wormhole? There exist an ever-increasing number of holographic complexity proposals [80–84], which range from observables defined on codimension-one to codimension-zero surfaces in the bulk. The holographic complexity proposals are conjectured and CFT evidence of their correctness is scarce. Note that so far there exists only a single map between CFT and holographic complexity derived in [85]. The authors employed the Fubini-Study metric, the distance between states on the projective Hilbert space, as a cost measure in the CFT. The results for the map between holographic and CFT complexity achieved in [85], however, are very specific to global symmetry transformations in excited CFT states and their holographic dual. One of the fundamental challenges of obtaining results with general validity is that in the CFT quantum circuits are parameterized by an auxiliary circuit parameter that is unrelated to the physical time of the bulk and boundary theories in AdS/CFT. Therefore, only the complexity of the circuit rather than the evolution of the circuit itself between the reference and target state can be mapped to gravity.

One of the main results of this thesis is that we identify the external parameter with the physical time by encoding the evolution of the quantum circuit as a time evolution in the CFT. Within the AdS_3/CFT_2 correspondence, this allows us to derive a gravity dual to a quantum circuit. In this way, we derive a generalizable holographic dual to a complexity geometry. The dual geometry in principle allows to map holographic complexity proposals to the CFT and CFT complexity measures to bulk observables. Building on previous work [85–87], we demonstrate the power of our construction by deriving a holographic dual to Fubini-Study distance as a cost measure for the quantum circuit that is valid for symmetry transformations in two-dimensional CFTs in states that are dual to Bañados geometries [88]. This presents the first derivation of a dual to a CFT cost measure from first principles.

Secondly, a further important issue that arises from viewing spacetime as emergent and in particular from the ER=EPR proposal is the factorization puzzle [89, 90]: The

TFD state (3.2.1) is an entangled state given in terms of a factorized Hilbert space for the left and right CFT. The factorization of the left and right CFT Hilbert spaces reflects that there is no interaction between both CFTs as they are causally separated by the black hole in the dual bulk geometry. On the other hand, the entanglement between the CFTs induces a classically connected spacetime geometry through the presence of a wormhole in the bulk. The connectedness is essential to obtain for instance geodesics through the wormhole which yield correlation functions in the dual CFT and implies that the bulk Hilbert space cannot be written in terms of a factorized Hilbert space between the left and right black hole interior. Similar to the black hole information paradox, the problem arises when we consider gravity in the semiclassical limit as we do not understand quantum gravity sufficiently. Recent progress toward resolving the factorization puzzle has been made by rephrasing the CFT and bulk operators and the Hilbert space on which they act in terms of abstract von Neumann algebras [69, 70, 91–95]. Von Neumann algebras were initially studied in the 1930s and 40s in a series of papers [96–104]. These algebras describe the general properties of operators in quantum mechanics and local regions in a QFT at the abstract level. For instance, operator algebras are distinguished by whether an irreducible representations exists, they have a non-trivial center or a trace is well-defined on the algebra. In turn, these properties allow fundamental statements about entanglement and the Hilbert space structure of a QFT or a quantum mechanical system. Since the factorization problem is centered around entanglement and the Hilbert space structure of the CFT and gravity theory, von Neumann algebras have recently become an essential tool in understanding the general properties of the CFT and gravity theory Hilbert spaces. The von Neumann algebras that correctly describe the bulk and boundary operator algebras in a semicalssical limit have very different properties than those in the quantum regime. This helps illuminate the factorization problem. The discussion about the factorization problem has so far been centered around simpler toy models or von Neumann algebras at the abstract level.

In this thesis, we bridge the gap between both approaches by first demonstrating that we may define Berry phases in black hole backgrounds that are sensitive to the bulk wormhole. We show that there are different types of Berry phases that may be defined in AdS_3/CFT_2 depending on the choice of parameter or base space. We distinguish between Virasoro [105], modular [106–108], and gauge Berry phases. Virasoro Berry phases arise from conformal symmetry transformations in the CFT, modular Berry phases from parallel transport of intervals, and gauge Berry phases from an independent choice of time coordinate in the exterior regions of the black hole. We calculate these Berry phases in CFTs dual to the eternal AdS black hole geometry

and show that they probe the wormhole in different ways. Then, we interpret these Berry phases in the framework of von Neumann algebras, and demonstrate that Berry phases are linked to missing information for a local observer due to the presence of global symmetries. We argue that the Virasoro Berry phase is a genuine probe of non-factorization while the gauge and modular Berry phase do not probe factorization of the Hilbert space, but the existence of a non-trivial center in the von Neumann algebra if the bulk spacetime is considered in the semiclassical limit.

The results presented in this thesis have the following implications for future research:
In this thesis, we derive a gravity dual to a quantum circuit implementing conformal symmetry transformations and show that that the Fubini-Study distance for this quantum circuit has a geometric bulk dual valid for empty AdS, conical defect and BTZ geometries. Our approach is generalizable to circuits that include other operators beyond the energy-momentum tensor. We therefore provide a path to analyze quantum circuits that do not only generate symmetry transformations. Furthermore, it now in principle becomes possible to derive cost functionals associated to the holographic complexity=action and complexity=volume proposals from first principles.

Furthermore, by establishing Berry phases as probes of the bulk wormhole in the eternal AdS black hole geometry, we present a means to study the Hilbert space structure of the CFT in the presence of a wormhole. Our analysis shows that, contrary to current expectations, the classical CFT phase space and therefore the CFT Hilbert space does not factorize in the semiclassical limit of the gravity theory. In particular, we show that Berry phases provide a valuable tool in assessing the microscopic structure of the Hilbert space. Employing our results for the classical non-factorized phase space of the CFT, it would now be interesting to derive the quantum Hilbert space with the aim of ultimately deriving the TFD state defined on this non-factorized Hilbert space.

Outline and Results

Based on the preceding presentation of developments relevant for this thesis, we first introduce essential aspects of AdS/CFT and the holographic dictionary in chapter 2, before moving on to a review of recent progress in applying quantum information theory concepts in AdS/CFT in chapter 3. We then present our results in chapters 4 and 5. Therefore, the following structure for this thesis naturally presents itself:

- Chapter 2 is a review chapter, where we introduce fundamental aspects of the

AdS/CFT correspondence with a focus on AdS_3/CFT_2 and its two ingredients, two-dimensional CFTs and three-dimensional gravity. In sec. 2.1, we introduce aspects of two-dimensional CFTs that will be essential in this thesis. We continue by discussing relevant geometries in asymptotically AdS_3 space in sec. 2.2. In sec. 2.3, we introduce the AdS/CFT correspondence as an instance of the holographic principle and discuss aspects special to the AdS_3/CFT_2 correspondence. Of particular relevance in this thesis is the holographic energy-momentum tensor and its role in reconstructing the three-dimensional bulk spacetime. Furthermore, we discuss the relation between the AdS_3 geometries and the Virasoro coadjoint orbits of the CFT.

- Chapter 3 is a review chapter focused on quantum information in AdS/CFT with a focus on the role of entanglement and quantum computational cost associated to quantum circuits. In sec. 3.1, we discuss aspects of entanglement, including the entanglement entropy, the modular (or entanglement) Hamiltonian, and the holographic dual of the entanglement entropy. Sec. 3.2 focuses on the relation between entanglement in the CFT and the geometry of the dual bulk spacetime. In particular, we discuss that entanglement between two CFTs dual to a two-sided black hole with two exterior regions gives rise to a spacetime wormhole in the bulk. In sec. 3.3, we review that entanglement alone is not sufficient to reconstruct the bulk geometry as, for instance, the entanglement entropy does not probe the wormhole at late times. We then discuss holographic complexity conjectures that were proposed as probes of the wormhole and discuss a relevant proposal for determining the complexity of quantum circuits in QFTs in sec. 3.4.

- In chapter 4, we present new results published in [1] and [2] concerning quantum circuits and their quantum computational cost in a two-dimensional CFT and their holographic duals. We begin in sec. 4.1 by introducing the quantum circuits and cost function we employ in this thesis and discuss problems that arise when attempting to relate the quantum circuits to a gravity dual. In sec. 4.2, we then resolve these issues by implementing the quantum circuit as a time evolution of the CFT and derive a gravity dual to the circuit. In sec. 4.3, we employ the gravity dual to the circuit to derive a gravity dual to the Fubini-Study distance as a cost function in the CFT.

- In chapter 5, we present new results published in [3] and [4] focusing on the factorization puzzle in AdS/CFT. We begin by introducing the factorization puzzle in sec. 5.1 and Berry phases as a useful probe of factorization in sec. 5.2. We

then discuss three different types of Berry phases which are possible candidates to study the factorization puzzle: the Virasoro Berry phase in sec. 5.3, the modular Berry phase in sec. 5.4, and the gauge Berry phase in sec. 5.5. In sec. 5.6, we relate our results for the Berry phases to recent work on von Neumann algebras in AdS/CFT and single out the Virasoro Berry phases as a good candidate to study the factorization puzzle. We furthermore discuss that Berry phases are associated to missing information for a local observer.

In chapters 4 and 5, we therefore present the results of this thesis. There are four main results, which we now summarize:

- We derive a holographic dual to a quantum circuit in chapter 4. Current constructions of quantum circuits rely on a Hamiltonian that implements symmetry transformations in the CFT. The quantum circuit is parameterized by an auxiliary circuit parameter. We identify the circuit Hamiltonian with the physical Hamiltonian of the boundary CFT. The auxiliary circuit parameter is therefore identified with physical time, and the circuit is implemented as a non-trivial time evolution of the CFT. Since the energy-momentum tensor implementing the symmetry transformations is conserved with respect to this background metric, the circuit is encoded by a non-trivial foliation of the boundary spacetime. In AdS_3/CFT_2, the bulk geometry is fixed in the Fefferman-Graham expansion by the expectation value of the boundary energy-momentum tensor and the boundary metric, which are known from the time evolution implementing the circuit. We then give a prescription for deriving the bulk dual to the quantum circuit employing the Fefferman-Graham expansion. These results are published in [1].

- Employing the holographic dual to a quantum circuit, we derive a gravity dual to Fubini-Study distance from first principles in chapter 4. The Fubini-Study distance measure serves as the metric on the projective Hilbert space. We show that in the holographic dual to the quantum circuit, the Fubini-Study distance may be written as a geometric object given in terms of the length of a spacelike geodesic and the boundary metric. Our result holds for empty AdS, conical defect, and the Bañados-Teitelboim-Zanelli (BTZ) black string and black hole geometries. For empty AdS and the BTZ black string, which is a three-dimensional black hole with non-compact horizon, the dual to the Fubini-Study metric is given in terms of the shortest geodesics which are employed to derive the holographic entanglement entropy. For the topologically non-trivial spacetimes that constitute the conical defect and the BTZ black hole, non-minimal winding geodesics must be included to obtain the Fubini-Study metric. These results appear in [2].

- In chapter 5, we calculate three different types of Berry phases in two-dimensional CFTs dual to a bulk spacetime with a wormhole and show that all three Berry phases are sensitive to the presence of the wormhole. The Berry phases arise from different transformations. We distinguish the Virasoro Berry phase, the modular Berry phase, and the gauge Berry phase. The Virasoro Berry phase is obtained from conformal transformations in the CFT and yields a coupled Berry phase for entangled CFTs dual to the eternal AdS black hole with a wormhole. The coupling is given in terms of a phase space variable related to the black hole mass, which must be equal for observers in each CFT. The modular Berry phase is obtained from parallel transporting intervals in each of the CFTs dual to the eternal AdS black hole. The Berry phase is non-vanishing if there is a misalignment in the boundary times. This misalignment is possible due to the absence of a global Killing vector in the presence of a wormhole in the bulk. Similarly, the gauge Berry phases arises by only considering the misalignment of time coordinates. Since all three Berry phases exhibit features which are unique to the bulk wormhole, we conclude that they are all sensitive to the wormhole. These results are published in [3].

- We relate our results for the Berry phase to recent advances in understanding AdS/CFT from the perspective of von Neumann algebras in chapter 5. We argue that the Virasoro Berry phase is a genuine probe of the factorization of the Hilbert space and that a quantization of the base space for the fiber bundle of this Berry phase will yield a non-factorized boundary Hilbert space as expected from the dual bulk theory. We furthermore argue that the gauge and modular Berry phase probe the existence of a non-trivial center in the von Neumann algebra in the semiclassical bulk limit, but not the factorization of the Hilbert space itself. Both Berry phases may be removed by including perturbative corrections which remove the center of the von Neumann algebra. We furthermore establish a link between Berry phases and and missing information for a local observer. These results appear in [4].

This collection of results present essential steps in further illuminating the relation between quantum information and geometry which is a fundamental tool in understanding the fundamental nature of spacetime:

First, this thesis takes a huge step toward verifying holographic complexity proposals in AdS_3/CFT_2 by establishing a procedure to obtain holographic duals to a quantum circuit. The approach is simple in nature as it involves identifying the circuit Hamiltonian with the physical Hamiltonian of the CFT and employing known

entries in the holographic dictionary to obtain the dual bulk geometry. The gravity dual allows the derivation of CFT complexity measures from bulk objects and vice versa from first principles. We illustrate this on the example of the Fubini-Study cost measure, which is dual to a geometric object in the bulk. In addition to the quantum circuit and its gravity dual, the Fubini-Study cost and its dual bulk object therefore present new entries in the holographic dictionary. Employing our gravity dual to a circuit, it now becomes possible to derive the boundary cost functions associated the holographic complexity proposals.

Secondly, we introduce Berry phases as a quantum information measure probing the existence of a bulk wormhole in AdS/CFT. Depending on the type of Berry phase, it either vanishes or decouples in both CFTs if such a wormhole does not exist. Furthermore, we establish Berry phases as a tool in AdS/CFT that probes properties of von Neumann algebras describing the operator algebras in the bulk and boundary operators. Based on these results, we take two essential step in resolving the the factorization problem in AdS/CFT. First, we identify that the source of the factorization puzzle lies in inconsistent assumptions of the type of von Neumann algebra describing the operator algebras in the bulk and boundary operator algebras: in defining a factorized CFT Hilbert space, a type I von Neumann algebra is implicitly assumed, whereas the bulk Hilbert space assumes a type III von Neumann algebra. Secondly, we show that the Virasoro Berry phase for to entangled CFTs is defined on a non-factorized classical phase space. We expect that quanitizing this phase should yield the appropriate non-factorized Hilbert space associated to a type III von Neumann algebra in the CFT that is consistent with the dual gravity algebra. We therefore provide the ingredients to resolve the factorization problem.

Conventions

We will use natural units with $c = \hbar = k_B = 1$. The gravitational constant G_N is kept explicit and dimensionful. For Lorentzian metrics, we will employ the mostly-plus convention. Furthermore, we count space and time directions such that a d-dimensional CFT has $d-1$ space directions and one time direction.

2 The AdS/CFT Correspondence

The AdS/CFT correspondence proposed in [34, 38, 39] is the foundation of significant progress towards understanding quantum gravity. It is a particularly concrete and well-studied example of the holographic principle [33], which purports that degrees of freedom in a spacetime region in quantum gravity scale with the area of this spacetime region rather than with its volume. The AdS/CFT correspondence proposes a duality between two very different theories: a particular string theory on $(d+1)$-dimensional Anti-de Sitter (AdS) space and a d-dimensional conformal field theory (CFT). The AdS space on which the string theory lives is a hyperbolic space that solves the vacuum Einstein equations. Thus, one side of the duality is given by a gravity theory. The CFT lives at the asymptotic boundary of the AdS space and does not have gravitational degrees of freedom. Therefore, the AdS/CFT correspondence relates a gravity theory in $(d+1)$ dimensions to a theory without gravity in d dimensions. In this thesis, we work exclusively within the $\mathrm{AdS}_3/\mathrm{CFT}_2$ correspondence. This instance of the correspondence has very special features which make many problems tangible that are exceptionally hard in higher dimensions. Whereas a CFT in general dimensions d only has a finite-dimensional symmetry group, the symmetry group of conformal transformations is infinite dimensional in two spacetime dimensions. The enhanced symmetry provides additional structure that allows the reconstruction of the particular AdS_3 geometry only from the values of the conserved charges in the CFT and the fixed flat background metric of the AdS boundary on which the CFT lives. This map between CFT charges and asymptotically AdS geometries is of central importance in this thesis.

We begin in sec. 2.1 by introducing two-dimensional CFTs and highlight the differences to their higher-dimensional counterparts. In sec. 2.2, we introduce three-dimensional asymptotically AdS spacetimes, focusing on empty AdS_3, conical defects, and black holes in AdS_3. We then have all necessary ingredients to discuss the AdS/CFT correspondence in sec. 2.3. We give an overview of the correspondence in general dimensions and then move on to focus on details of the $\mathrm{AdS}_3/\mathrm{CFT}_2$ correspondence.

2.1. Two-dimensional Conformal Field Theory

In this section, we review relevant aspects of two-dimensional CFTs. In sec. 2.1.1, we take a more physical approach towards CFTs, discussing important fields and their transformation properties under conformal transformations as well as highest-weight representations. In sec. 2.1.2, we take a group theoretic approach to CFTs and introduce the geometric action on coadjoint orbits. This formalism is useful to study geometric and topological features of CFTs.

2.1.1. Fields and Generators

We begin by defining conformal symmetry in a general number of spacetime dimensions d and then move on to discuss the symmetry group in two dimensions. In the process, we will illuminate the special properties CFTs in two dimensions possess compared to their higher-dimensional counterparts and highlight important differences between the classical and quantum theory. The discussion in this section follows the standard works [109] and [110].

Classical conformal symmetry

Consider a d-dimensional spacetime with metric $g_{\mu\nu}(x)$ and coordinates x^μ, where $\mu \in \{0, \cdots, d-1\}$. A conformal transformation $x^\mu \to y^\mu$ is an invertible coordinate transformation that changes the metric only by a global scale factor,

$$g_{\mu\nu}(x) \to \Omega(x) g_{\mu\nu}(x). \tag{2.1.1}$$

Employing the convariant transformation property of the metric under coordinate transformations $x^\mu \to y^\mu$,

$$\tilde{g}_{\mu\nu}(y) = g_{\rho\sigma}(x) \frac{\partial x^\rho}{\partial y^\mu} \frac{\partial x^\sigma}{\partial y^\nu}, \tag{2.1.2}$$

we may derive a set of differential equations specifying the precise infinitesimal form of the conformal transformation. Under the infinitesimal conformal transformation $y^\mu(x) = x^\mu + \varepsilon a^\mu(x)$ with infinitesimal expansion parameter ε, $\Omega(x)$ may be expanded as follows:

$$\Omega(x) = 1 + \varepsilon\sigma(x) + \mathcal{O}(\epsilon^2), \tag{2.1.3}$$

where $\sigma(x)$ is to be determined. Combining (2.1.1) and (2.1.2) then yields that under the infinitesimal conformal transformation $y^\mu(x) = x^\mu + \varepsilon a^\mu(x)$, the following equation

holds to first order in ε,

$$\partial_\mu a_\nu + \partial_\nu a_\mu \stackrel{!}{=} \sigma(x) g_{\mu\nu}. \tag{2.1.4}$$

We may solve for $\sigma(x)$ and obtain

$$\sigma(x) = \frac{2}{d}\partial^\mu a_\mu(x). \tag{2.1.5}$$

Therefore, (2.1.4) may be written as

$$\partial_\mu a_\nu + \partial_\nu a_\mu = \frac{2}{d}\partial^\rho a_\rho(x). \tag{2.1.6}$$

Let us assume that the manifold is $\mathbb{R}^{1,d-1}$ with $g_{\mu\nu} = \eta_{\mu\nu} = \mathrm{diag}(-1, 1, \ldots 1)$. Then, from (2.1.6) we arrive at

$$\left(\eta_{\mu\nu}\partial^2 + (d-2)\partial_\mu\partial_\nu\right)(\partial^\rho a_\rho) = 0. \tag{2.1.7}$$

For general dimensions d, the solution to this differential equation is at most quadratic in x^μ, $a^\mu \sim \mathcal{O}(x^2)$. Indeed, it may be shown that the finite conformal transformations in d dimensions are given by the set of transformations,

$$\begin{aligned}
&x^\mu \to y^\mu = x^\mu + b^\mu, \\
&x^\mu \to y^\mu = \Lambda^\mu{}_\nu x^\nu, \quad (\Lambda^\mu{}_\nu \in SO(1, d-1)), \\
&x^\mu \to y^\mu = \lambda x^\mu, \\
&x^\mu \to y^\mu = \frac{x^\mu + b^\mu x^\rho x_\rho}{1 + 2b^\rho x_\rho + b^\sigma x_\sigma x^\rho x_\rho}.
\end{aligned} \tag{2.1.8}$$

These transformations form the group $SO(2, d)$, which is the symmetry group of conformal transformations in d dimensions.

Let us now examine (2.1.7) for $d = 2$. It is evident that $d = 2$ is a special case in which (2.1.7) simplifies considerably. We introduce coordinates x_0, x_1 and the Euclidean metric $g_{\mu\nu} = \delta_{\mu\nu}$. Then, (2.1.4) reduces to the set of equations

$$\partial_0 a_1 + \partial_1 a_0 = 0, \quad \partial_0 a_0 - \partial_1 a_1 = 0. \tag{2.1.9}$$

These are infinitesimal versions of the Cauchy-Riemann differential equations. Introducing coordinates on the complex plane $z = x_0 + ix_1$ and $\bar{z} = x_0 - ix_1$, the Cauchy-Riemann equations are solved by any infinitesimal holomorphic function $f(z) = z + \varepsilon a(z)$ and similarly for the antiholomophic sector. Let us assume we may Laurent expand the holomorphic function $a(z)$ around $z = 0$ on the complex plane,

$a(z) = \sum_n a_n z^{n+1}$. Since an infinite number of coefficients a_n is necessary to describe all possible holomorphic transformations, two-dimensional conformal transformations form an infinite group. Analogous considerations apply to the antiholomorphic sector. The generators of these coordinate transformations are given by

$$\ell_n = -z^{n+1}\partial_z, \qquad \bar{\ell}_n = -\bar{z}^{n+1}\partial_{\bar{z}}. \tag{2.1.10}$$

They satisfy the classical Witt algebra,

$$[\ell_n, \ell_m] = (n-m)\ell_{n+m}. \tag{2.1.11}$$

We conclude that a conformal transformation in $d = 2$ is any (anti-)holomorphic mapping $z \to f(z)$ that is analytic and invertible[1]. However, in general $f(z)$ is not well defined globally on the full complex plane. This becomes evident when expanding $a(z)$,

$$a(z)\partial_z = -\sum_n a_n \ell_n = \sum_n a_n z^{n+1}\partial_z, \tag{2.1.12}$$

which is non-singular at $z = 0$ only if $a_n = 0$ for all $n < -1$. By employing $z = -\frac{1}{w}$, we can furthermore see that $a(z)$ is only well defined at $z \to \infty$ if $a_n = 0$ for all $n > 1$. Therefore, the infinite-dimensional conformal symmetry group in two dimensions generates a local symmetry. Nevertheless, these considerations show that there is a subgroup of transformations called global conformal transformations that are defined everywhere on the complex plane. These global transformations are generated by the subgroup of generators with $n = \{-1, 0, 1\}$ and thus the set of generators $\{\ell_{-1}, \ell_0, \ell_1\}$ and $\{\bar{\ell}_{-1}, \bar{\ell}_0, \bar{\ell}_1\}$. The holomorphic subgroup generates the Möbius transformations,

$$z \to \frac{az+b}{cz+d} \quad \text{with} \quad ad - bc = 1, \tag{2.1.13}$$

which are well-defined everywhere on the complex plane and form the group $SL(2, \mathbb{C})$ with $a, b, c, d \in \mathbb{C}$. There is a similar transformation for the antiholomorphic coordinate. Both copies form the group $SL(2, \mathbb{C}) \times SL(2, \mathbb{C}) \cong SO(1, 3)$.

Quantum conformal symmetry and the Weyl anomaly

In the next step, we introduce two fields of the CFT which play a fundamental role in this thesis. The first one is the primary field $\phi(z, \bar{z})$, which is defined by its transfor-

[1] Invertibility is necessary to form a group.

mation property under conformal transformations,

$$\phi(z,\bar{z}) \to \left(\frac{\partial f}{\partial z}\right)^{h} \left(\frac{\partial \bar{f}}{\partial \bar{z}}\right)^{\bar{h}} \phi(f(z),\bar{f}(\bar{z})). \tag{2.1.14}$$

This field is used to define the highest-weight states of the CFT as follows:

$$\begin{aligned} |h,\bar{h}\rangle &= \phi(0,0)|0\rangle, \\ \langle h,\bar{h}| &= \lim_{z,\bar{z}\to\infty} z^{2h}\bar{z}^{2\bar{h}}\langle 0|\phi(z,\bar{z}), \end{aligned} \tag{2.1.15}$$

where we employed for the bra-state that $(\phi(\bar{z},z))^\dagger = \phi(\frac{1}{z},\frac{1}{\bar{z}})\frac{1}{z^{2h}}\frac{1}{\bar{z}^{2\bar{h}}}$ and the transformation property (2.1.14) under $w = \frac{1}{z}$ and $\bar{w} = \frac{1}{\bar{z}}$.

Another important field is the energy-momentum tensor $T_{\mu\nu}$, which is a conserved current of the CFT. Furthermore, conformal invariance requires that its trace vanishes, $T^{\alpha}{}_{\alpha} = 0$, since a non-vanishing trace would introduce a scale that breaks conformal invariance. From the conservation equation $\nabla^\mu T_{\mu\nu} = 0$ on the complex plane with covariant derivative ∇^μ and the tracelessness condition, we obtain $\partial_{\bar{z}} T_{zz} = 0 = \partial_z T_{\bar{z}\bar{z}}$. The energy-momentum tensor therefore reduces to a holomorphic and an antiholomorphic component, which we denote as follows:

$$T(z) \equiv T_{zz}(z) \quad , \quad \bar{T}(\bar{z}) \equiv T_{\bar{z}\bar{z}}(\bar{z}). \tag{2.1.16}$$

Its vacuum expectation value on the complex plane is given by

$$\langle 0|T(z)|0\rangle = 0 = \langle 0|\bar{T}(\bar{z})|0\rangle, \tag{2.1.17}$$

and the two-point function reads

$$\langle 0|T(z)T(w)|0\rangle = \frac{c/2}{(z-w)^4}, \quad \langle 0|\bar{T}(\bar{z})\bar{T}(\bar{w})|0\rangle = \frac{c/2}{(\bar{z}-\bar{w})^4}. \tag{2.1.18}$$

Under a conformal transformation $z \to f(z)$, the energy-momentum tensor transforms as

$$T(z) = (\partial_z f)^2 T(f(z)) + \frac{c}{12}\{f,z\}, \tag{2.1.19}$$

where $\{f,z\}$ denotes the Schwarzian derivative,

$$\{f,z\} = \frac{\partial_z^3 f}{\partial_z f} - \frac{3}{2}\left(\frac{\partial_z^2 f}{\partial_z f}\right)^2. \tag{2.1.20}$$

The transformation of $\bar{T}(\bar{z})$ is analogous. It is useful to analyze (2.1.19) in more detail. Consider the conformal transformations $z \to f(z)$ and $\bar{z} \to \bar{f}(\bar{z})$ acting on the flat Euclidean metric $ds^2 = dzd\bar{z}$. The new metric follows from (2.1.2),

$$ds^2 = \partial_z f(z)\partial_{\bar{z}}\bar{f}(\bar{z})dzd\bar{z} = e^{2\omega(z,\bar{z})}dzd\bar{z}, \tag{2.1.21}$$

where

$$\omega(z,\bar{z}) = \frac{1}{2}(\log(\partial_z f(z)) + \log(\partial_{\bar{z}}\bar{f}(\bar{z}))). \tag{2.1.22}$$

The metric may therefore be returned to its original form $ds^2 = dzd\bar{z}$ by a local rescaling with $e^{-2\omega(z,\bar{z})}$,

$$ds^2 \to ds^2 e^{-2\omega(z,\bar{z})} = dzd\bar{z}. \tag{2.1.23}$$

Classically, the CFT action $S = \int d^2x\sqrt{g}\mathcal{L}$ with Lagrangian density $\mathcal{L}$ is invariant only if we apply both the conformal transformations, $z \to f(z)$ and $\bar{z} \to \bar{f}(\bar{z})$, and the Weyl rescaling $e^{-2\omega(z,\bar{z})}$. If we do not apply the Weyl rescaling, the determinant of the metric $\sqrt{g}$ gives an extra contribution to the action. Therefore, conformal invariance refers to the invariance of the action under *both* a conformal coordinate transformation $z \to f(z)$ and a Weyl rescaling (2.1.23). It is not sufficient simply to perform the coordinate transformation. This has implications for the transformation of the energy-momentum tensor as we now discuss.

Given coordinates $w^\mu = \{w = f(z), \bar{w} = \bar{f}(\bar{z})\}$ and $z^\rho = \{z, \bar{z}\}$, the transformation of the energy-momentum tensor under conformal transformations should intuitively follow from the covariant transformation property which tensors obey,

$$\tilde{T}_{\mu\nu}(w,\bar{w}) = T_{\rho\sigma}(z,\bar{z})\frac{\partial z^\rho}{\partial w^\mu}\frac{\partial z^\sigma}{\partial w^\nu}. \tag{2.1.24}$$

It is evident that in this manner, we reproduce only the first term in (2.1.19). To understand the second term, given in terms of the Schwarzian derivative, we need to take a detour. The Schwarzian derivative in (2.1.19) scales with the central charge c of the CFT. This term arises from a breaking of conformal invariance at the quantum level. To see this, consider a CFT on a curved two-dimensional manifold,

$$ds^2 = g_{\mu\nu}dx^\mu dx^\nu. \tag{2.1.25}$$

In two dimensions, we may always find a coordinate transformation that brings the metric into the form

$$ds^2 = e^{2\omega(z,\bar{z})}dzd\bar{z} \tag{2.1.26}$$

with Weyl factor $\omega(z,\bar{z})$. Therefore, any two-dimensional manifold is flat up to a Weyl factor. This Weyl factor then determines the curvature of the metric. In particular, the Ricci scalar R reads

$$\sqrt{g}R = -4\partial_z\partial_{\bar{z}}\omega. \tag{2.1.27}$$

It is clear that R only vanishes, i.e. the spacetime is flat, if the Weyl factor ω decomposes into a holomorphic and antiholomorphic part. The Weyl factor is then given by (2.1.22). A non-zero Ricci scalar R indicating a curved background introduces a scale in the CFT, which breaks conformal invariance. This breaking of conformal invariance is noticeable at the quantum level even for a CFT on a flat background. This becomes evident when considering the generating functional for a two-dimensional CFT on a curved background, which is invariant only up to an anomalous term induced by the Weyl rescaling of the metric. Given a two-dimensional CFT in an arbitrary background metric g with field content $\{X\}$ and action $S[g,X]$, the generating functional reads [111]

$$Z[g] = \int [\mathcal{D}X]_g \, e^{-S[g,X]} = e^{-W[g]}. \tag{2.1.28}$$

At the quantum level, a Weyl rescaling (2.1.23) induces a transformation of the generating functional [111–113],

$$Z[e^{2\omega}g] = e^{S_L} Z[g], \tag{2.1.29}$$

where S_L is the Liouville action [111],

$$S_L\left[\omega, g_{ab}\right] = \frac{c}{24\pi}\int d^2x\sqrt{g}\left[g^{\mu\nu}\partial_\mu\omega\partial_\nu\omega + e^{2\omega} + R_g\omega\right]. \tag{2.1.30}$$

Here, R_g denotes the Ricci scalar for the metric g before the Weyl rescaling is performed. We now assume that $g_{\mu\nu}dx^\mu dx^\nu = \partial_z f(z)\partial_{\bar{z}}\bar{f}(\bar{z})dzd\bar{z}$. Note that n-point correlation functions are obtained from the generating functional by varying n times with respect to the metric [112, 113],

$$\langle T_{\mu\nu}...T_{\rho\sigma}\rangle = \frac{4\pi}{Z[e^{2\omega}g]}\frac{\delta^n}{\delta g^{\mu\nu}...\delta g^{\rho\sigma}} Z[e^{2\omega}g]. \tag{2.1.31}$$

The expectation value for the energy-momentum tensor on a Weyl-rescaled metric then follows from a single variation with respect to the metric,

$$\langle T_{\mu\nu}\rangle = \frac{4\pi}{Z[e^{2\omega}g]}\frac{\delta}{\delta g^{\mu\nu}} Z[e^{2\omega}g]. \tag{2.1.32}$$

This yields [112, 113]

$$\langle T_{ij}\rangle_{e^{2\omega}g} = \langle T_{ij}\rangle_g + \frac{c}{6}\left(\partial_i\omega\partial_j\omega - \frac{1}{2}g_{ij}\partial^k\omega\partial_k\omega - \nabla_i\nabla_j\omega + g_{ij}\nabla^k\nabla_k\omega\right). \tag{2.1.33}$$

Upon contracting indices, the trace of the energy-momentum tensor reads [112, 113],

$$\langle T^{\mu}{}_{\mu}\rangle = -\frac{c}{12}R, \tag{2.1.34}$$

where $R = -8e^{-2\omega(z,\bar{z})}\partial_z\partial_{\bar{z}}\omega(z,\bar{z})$. This is called the *trace anomaly* or equivalently the *Weyl anomaly* as the non-vanishing trace originates from a Weyl rescaling of the metric. The anomaly appears only at the quantum level. Naively, we might think that the Weyl anomaly is not relevant on a flat background since (2.1.34) vanishes in this case. This reasoning is false, however. The two-point function involving $T^{\mu}{}_{\mu}$ follows from varying (2.1.34) with respect to a general metric $g^{\rho\sigma}$ and only then inserting the precise form of the metric. This gives a non-vanishing contribution to the two-point function even on a flat background.

We now have gathered all the ingredients to understand the transformation property of the energy-momentum tensor (2.1.19). Upon inserting (2.1.22) into (2.1.33) for T_{zz}, we obtain the Schwarzian term scaling with the central charge in (2.1.19). In summary, the first term in (2.1.19) is a consequence of the covariant tensor transformation under conformal coordinate transformations $z \to f(z)$, whereas the second term involving the Schwarzian derivative and the central charge is a consequence of the Weyl anomaly at the quantum level.

Moreover, the Weyl anomaly is also reflected in the algebra of the quantum symmetry generators. The classical Witt algebra (2.1.11) is modified by an additional term to include the central charge such that the quantum generators L_n satisfy the Virasoro algebra,

$$\begin{aligned}
[L_n, L_m] &= (n-m)L_{n+m} + \frac{c}{12}\left(n^3 - n\right)\delta_{n+m,0},\\
\left[\bar{L}_n, \bar{L}_m\right] &= (n-m)\bar{L}_{n+m} + \frac{c}{12}\left(n^3 - n\right)\delta_{n+m,0},\\
\left[L_n, \bar{L}_m\right] &= 0.
\end{aligned} \tag{2.1.35}$$

Note that the central term scaling with the central charge vanishes for the subgroup $\{L_{-1}, L_0, L_1\}$ forming $SL(2,\mathbb{C})$. This is precisely the subgroup that generates the global conformal transformations (2.1.13). Indeed, it is straightforward to show that the Schwarzian derivative in (2.1.19) also vanishes for these transformations, and therefore the energy-momentum tensor transforms in the usual covariant way without contributions from the Weyl anomaly for this subgroup. Hence, at the quantum level

the global conformal symmetry is not broken. Finally, the Virasoro generators L_n are related to the energy-momentum tensor by

$$T(z) = \sum_{n\in\mathbb{Z}} z^{-n-2} L_n, \quad \bar{T}(\bar{z}) = \sum_{n\in\mathbb{Z}} \bar{z}^{-n-2} \bar{L}_n. \tag{2.1.36}$$

The generators are Hermitian, $L_n^\dagger = L_{-n}$, and act on the highest-weight state $|h\rangle$ defined in (2.1.15) as follows:

$$\begin{aligned} &L_0|h\rangle = h|h\rangle, \\ &L_n|h\rangle = 0 \qquad\quad \text{for} \quad n > 0, \\ &L_n|h\rangle = |h+n\rangle \qquad \text{for} \quad n < 0. \end{aligned} \tag{2.1.37}$$

The action of $\bar{L}_n$ on $|\bar{h}\rangle$ is analogous.

Two-dimensional CFTs on the cylinder

In this thesis, we will often consider two-dimensional CFTs in Lorentzian signature on the cylinder. Let us begin with a CFT on Minkowski space $\mathbb{R}^{1,1}$. We choose the metric $ds^2 = -dx^+dx^- = -dt^2 + d\varphi^2$ in the light-cone coordinates $x^\pm = t \pm \varphi$ with time coordinate t and space coordinate φ. Then, the global conformal transformations (2.1.13) are given by

$$x^\pm \to \frac{ax^\pm + b}{cx^\pm + d}, \quad \text{where } a, b, c, d \in \mathbb{R} \quad \text{and} \quad ad - bc = 1. \tag{2.1.38}$$

Since $a, b, c, d \in \mathbb{R}$, these transformations form the group $SL(2,\mathbb{R})$ and are a composition of functions of the global conformal transformations (2.1.8) in two dimensions with real parameters. In particular, the global conformal group $SO(d,2)$ on a Lorentzian background in two dimensions is isomorphic to the group product $SO(2,2) \cong SL(2,\mathbb{R}) \times SL(2,\mathbb{R})$.

The cylinder is then obtained from the Minkowski plane by compactifying the spatial direction, $\varphi \sim \varphi + 2\pi$. To see the physical effects of this compactification, it is convenient to employ a map from the complex plane to the cylinder, $z = e^{t+i\varphi}$. This transformation maps the origin on the complex plane $z = 0$ to $t \to -\infty$ and $z \to \infty$ to $t \to \infty$. Employing the definition of highest-weight states on the complex plane (2.1.15), we find that on the cylinder bra-states are defined at $t \to -\infty$ and ket-states at $t \to \infty$.

Note that the periodic boundary conditions on φ introduce a scale into the system

that weakly breaks conformal invariance. Upon inserting $z = e^{t+i\varphi}$ into (2.1.19), we find that the expectation-value of the energy-momentum tensor on the cylinder is shifted by the central charge,

$$\langle h|T_{\text{cyl}}|h\rangle = z^2\langle h|T_{\text{plane}}|h\rangle - \frac{c}{24}. \tag{2.1.39}$$

The vacuum expectation value is obtained by setting $h = 0$ and employing (2.1.17). It is then clear that on the cylinder the vacuum expectation value of the energy-momentum tensor no longer vanishes, but is given in terms of the central charge, $\langle 0|T_{\text{cyl}}|0\rangle = -\frac{c}{24}$. This shift is induced by the Weyl anomaly. We will now examine two-dimensional CFTs from a more group theoretic approach.

2.1.2. Virasoro Coadjoint Orbits

Here, we take an abstract approach towards two-dimensional CFTs by investigating the underlying properties of their symmetry group, the Virasoro group. In particular, we will introduce the geometric action on coadjoint orbits of the symmetry group. This formalism was first developed in [114] and applied to the symmetry group of two-dimensional CFTs in [115–118]. The geometric action encodes important properties of the geometry and topology of the state space of the two-dimensional CFT as we will see in later chapters of this thesis. This section follows [105] and the excellent introduction [119] into this topic.

The Virasoro group and its algebra

In the mathematical approach, the conformal compactification of Minkowski space $\mathbb{R}^{1,1} \cong S^1 \times S^1$ is considered. Then, the group of classical conformal transformations on Minkowski space $\text{Conf}(\mathbb{R}^{1,1})$ is identified with the diffeomorphisms of the unit circle $\text{Diff}(S^1)$, $\text{Conf}(\mathbb{R}^{1,1}) \cong \text{Diff}(S^1) \times \text{Diff}(S^1)$. For details, we refer to [120]. We parameterize the unit circle as follows: $S^1 = \{e^{i\varphi} \in \mathbb{C} \mid \varphi \in [0, 2\pi[\}$. The orientation preserving diffeomorphisms of the unit circle form a group $\text{Diff}(S^1)$, which acts as

$$\varphi \to f(\varphi), \tag{2.1.40}$$

where

$$f'(\varphi) > 0, \quad f(\varphi + 2\pi) = f(\varphi) + 2\pi. \tag{2.1.41}$$

The Virasoro group $\widehat{\text{Diff}}(S^1)$ is the central extension of $\text{Diff}(S^1)$ reflecting that the quantum conformal group is centrally extended. The central extension is defined in

terms of two diffeomorphisms $f, g \in \mathrm{Diff}(S^1)$ by the Bott-cocycle, which maps two diffeomorphisms f, g to a real number [121],

$$C(f,g) \equiv -\frac{1}{48\pi}\int_0^{2\pi} d\varphi \log\left[f'(g(\varphi))\right]\frac{g''(\varphi)}{g'(\varphi)}. \tag{2.1.42}$$

The Virasoro group is then topologically $\widehat{\mathrm{Diff}}(S^1) = \mathrm{Diff}(S^1) \times \mathbb{R}$. Due to the central extension, group elements are pairs (f, α), where $f \in \mathrm{Diff}(S^1)$ and $\alpha \in \mathbb{R}$. Group multiplication is given by

$$(f,\alpha)\circ(g,\beta) \equiv (f\circ g, \alpha+\beta+C(f,g)). \tag{2.1.43}$$

Now let us consider the unitary representations U_f and U_g of two group elements $(f, 0)$ and $(g, 0)$ and act with these unitaries on the highest-weight state $|h\rangle$. Equation (2.1.43) then yields

$$U_g U_f |h\rangle = e^{icC(f,g)} U_{f\circ g}|h\rangle, \tag{2.1.44}$$

where c denotes the central charge. Therefore, the central extension contributes an additional phase that cannot be absorbed by redefining U_f.

We now move on to the Lie algebra. Let us first focus on the algebra for diffeomorphisms of the unit circle $\mathrm{Diff}(S^1)$ without central extension. Here, it is clear that Lie algebra elements are simply vector fields on the circle, which we denote by $X = X(\varphi)\partial_\varphi$. Fourier-expanding these vector fields yields

$$X = -i\sum_{n=-\infty}^{\infty} X_n e^{in\varphi}\partial_\varphi = \sum_{n=-\infty}^{\infty} X_n \ell_n. \tag{2.1.45}$$

Here, we introduced the generators $\ell_n = -ie^{in\varphi}\partial_\varphi$ of diffeomorphisms on the unit circle. It is straightforward to check that

$$[\ell_n, \ell_m] = (n-m)\ell_{n+m}. \tag{2.1.46}$$

This is the Witt algebra introduced in (2.1.11). To see precisely how the central extension appears in the Lie algebra, we need a Lie-algebra equivalent of (2.1.42). This equivalent is given in terms of two vector fields X, Y on the circle by the Gelfand-Fuks cocycle,

$$\mathrm{c}(X,Y) \equiv -\frac{1}{24\pi}\int_0^{2\pi} d\varphi X(\varphi) Y'''(\varphi). \tag{2.1.47}$$

Lie algebra elements of the centrally extended group $\widehat{\mathrm{Diff}}(S^1)$ are then given by pairs (X, α), where X denotes a vector field on the circle and α is again a real number. The

Lie bracket reads[2]

$$[(X,\alpha),(Y,\beta)] = (-[X,Y],\mathrm{c}(Y,X))\,. \tag{2.1.48}$$

In particular, for $\ell_n = -ie^{in\varphi}\partial_\varphi$ we obtain

$$\mathrm{c}\,(\ell_m,\ell_n) = \frac{m^3}{12}\delta_{m+n,0}. \tag{2.1.49}$$

Then,

$$[(\ell_n,\alpha),(\ell_m,\beta)] = \left((n-m)\ell_{n+m},\frac{m^3}{12}\delta_{m+n,0}\right). \tag{2.1.50}$$

Finally, (2.1.35) is obtained by defining a central operator $Z = (0,-i)$ such that we may expand $(X,\alpha) = \sum_m X_m\ell_m + i\alpha Z$. Employing (2.1.48) then yields

$$[\ell_m,\ell_n] = (m-n)\ell_{m+n} + \frac{Z}{12}m\left(m^2-1\right)\delta_{m+n,0}. \tag{2.1.51}$$

In a unitary representation $\mathfrak{u}$ of the Lie algebra, Z takes the value of the central charge $\mathfrak{u}[Z] = c\hat{I}$, where $\hat{I}$ is the identity operator. Furthermore, $\mathfrak{u}(\ell_n) \equiv L_n$. We then recover the Virasoro algebra (2.1.35). Note that the central charge operator commutes with L_n.

Coadjoint orbits and geometric action

Let us denote the centrally extended Lie algebra by $\hat{\mathfrak{g}}$. We may define a space dual to $\hat{\mathfrak{g}}$, which we denote by $\hat{\mathfrak{g}}^*$. The dual Lie algebra $\hat{\mathfrak{g}}^*$ is the space of linear maps $(p,c) : \hat{\mathfrak{g}} \to \mathbb{R}$, where $(p,c) \equiv (p(\varphi)d\varphi^2,c) \in \hat{\mathfrak{g}}^*$. For the Virasoro algebra, this map reads

$$\langle (p,c),(X,\beta)\rangle = \int d\varphi\, pX + c\beta, \tag{2.1.52}$$

where $(X,\beta) \in \hat{\mathfrak{g}}$ and $(p,c) \in \hat{\mathfrak{g}}^*$. This may seem rather abstract, but has an intuitive physical interpretation: The vector field X generates a symmetry on the unit circle, and the dual element p is a conserved vector with respect to the symmetry transformation generated by X. Then, $\langle p,X\rangle$ is the Noether charge associated to the symmetry generated by X. Since the Virasoro group is centrally extended, this Noether charge also receives a contribution from the central extension and is given by (2.1.52).

Given an element of the Lie algebra (X,β) and a group element (f,α), we may

[2] The additional sign in $-[X,Y]$ can be absorbed by a redefinition of the Lie bracket [119]. Here, it is convenient to keep it.

define the adjoint action of (f,α) on (X,β) as follows:

$$\mathrm{Ad}_{(f,\alpha)}(X,\beta) = \left(\mathrm{Ad}_f X, \beta - \frac{1}{24\pi}\int_0^{2\pi} d\varphi\,\{f,\varphi\}X(\varphi)\right). \tag{2.1.53}$$

Here, $\mathrm{Ad}_f X$ is the standard adjoint action for groups without central extension,

$$\mathrm{Ad}_f(X) = \frac{d}{d\tau}\bigg|_{\tau=0} f\cdot e^{\tau X}\cdot f^{-1} \quad \forall X\in\mathfrak{g}. \tag{2.1.54}$$

The coadjoint representation is then defined in terms of the map (2.1.52)

$$\left\langle \mathrm{Ad}^*_{(f,\alpha)}(b_0,c),(X,\beta)\right\rangle \equiv \left\langle (b_0,c), \mathrm{Ad}_{(f,\alpha)^{-1}}(X,\beta)\right\rangle, \tag{2.1.55}$$

where

$$\mathrm{Ad}^*_{(f,\alpha)}\, b_0 = \frac{1}{f'^2}\left(b_0 - \frac{c}{24\pi}\{f,\varphi\}\right). \tag{2.1.56}$$

Note that upon identifying b_0 with the expectation value of the energy-momentum tensor in the CFT,

$$b_0 = \frac{1}{2\pi}\langle h|T(\varphi)|h\rangle, \tag{2.1.57}$$

the coadjoint transformation (2.1.56) is simply the transformation property of the energy-momentum tensor under conformal transformations (2.1.19). Employing the coadjoint transformation (2.1.56), a codajoint orbit O_{b_0} is obtained by choosing an element of the dual Lie algebra $(b_0,c)\in\hat{\mathfrak{g}}^*$ and applying all possible group transformations of the Virasoro group to (b_0,c) by a coadjoint transformation,

$$O_{b_0} = \left\{ b = \mathrm{Ad}^*_{(f,\alpha)}\,(b_0,c) \mid (f,\alpha)\in\widehat{\mathrm{Diff}}(S^1)\right\}. \tag{2.1.58}$$

With the identification (2.1.57), the coadjoint orbit (2.1.58) is then given by all expectation values of the energy-momentum tensor that can be obtained by applying all conformal transformations. The orbits may be classified by the particular state in which the expectation value (2.1.57) is taken. For every choice of the value h in the state $|h\rangle$, we obtain a different orbit labeled by b_0 with $b_0 = \frac{1}{2\pi}\langle h|T(\varphi)|h\rangle = \frac{1}{2\pi}\left(h - \frac{c}{24}\right)$.

Note that there are certain group elements that leave the point on the orbit invariant, i.e. they satisfy

$$(b_0,c) = \mathrm{Ad}^*_{(h,\alpha)}\,(b_0,c). \tag{2.1.59}$$

The group elements h that satisfy this property form a subgroup of the Virasoro group. We denote this subgroup by H. Therefore, coadjoint orbits of the Virasoro group are manifolds $\widehat{\mathrm{Diff}}(S^1)/H$. The subgroup H is called the stabilizer group and

is either $SL(2,\mathbb{R})$ or $U(1)$, depending on the choice of b_0. This becomes evident with the identification (2.1.57): The state $|0\rangle$ is invariant under $SL(2,\mathbb{R})$; therefore b_0 is also invariant. All other states $|h\rangle$ with $h > 0$ are invariant under $U(1)$.

Furthermore, the coadjoint orbit (2.1.58) is a symplectic manifold, on which we may define a symplectic form. This symplectic form is called the Kirillov-Kostant symplectic form and is given by

$$\omega = -d\left\langle (b,c),(\theta,m_\theta)\right\rangle . \tag{2.1.60}$$

Here, (θ, m_θ) is the Maurer-Cartan form. This is a rather special Lie algebra element that tells us how two group elements are related. It may be derived as follows. Consider a path $(f(s'),\alpha(s'))$ through the Virasoro group, parameterized by s'. Then two group elements $(f_1,\alpha_1) = (f(s'),\alpha(s'))|_{s'=s}$ and $(f_2,\alpha_2) = (f(s'),\alpha(s'))|_{s'=\tau}$ are related as follows [122]:

$$(f(\tau),\alpha(\tau)) = e^{-\int_s^\tau ds'(\theta(s'),m_\theta(s'))}(f(s),\alpha(s)). \tag{2.1.61}$$

Multiplying by the inverse transformation $(f(s),\alpha(s))^{-1} = (f^{-1}(s),-\alpha(s))$ from the right and taking a derivative then yields the Maurer-Cartan form,

$$(\theta,m_\theta)_{f^{-1}} = \left(\frac{d}{ds}\bigg|_{s=\tau} f(\tau)\circ f^{-1}(s), \frac{d}{ds}\bigg|_{s=\tau} C\left(f(\tau)f^{-1}(s)\right)\right). \tag{2.1.62}$$

Evaluated explicitly using the notation $f^{-1} = F$ for the inverse diffeomorphism, the Maurer-Cartan form reads [116]

$$(\theta,m_\theta) = \left(\frac{\dot F}{F'}, \frac{1}{48\pi}\int_0^{2\pi} d\sigma \frac{\dot F}{F'}\left(\frac{F''}{F'}\right)'\right), \tag{2.1.63}$$

where $\dot F = \partial_\tau F$ and $F' = \partial_\varphi F$. Furthermore, we may define a symplectic potential for the symplectic form (2.1.60),

$$\alpha = -\left\langle (b,c),(\theta,m_\theta)\right\rangle , \tag{2.1.64}$$

such that at least locally $\omega = -d\alpha$. Here, d is the exterior derivative on the group manifold. We now have all the ingredients to define the geometric action of the Virasoro group on coadjoint orbits (2.1.58),

$$S = \int d\tau\, \alpha. \tag{2.1.65}$$

Employing (2.1.63) and rewriting $b = \mathrm{Ad}^*_{(f,\alpha)}(b_0,c)$ in terms of the inverse group

element F yields the geometric action for the Virasoro group as given in [116],

$$S = \int d\varphi \, \mathrm{d}\tau \left(-b_0(F) F' \dot{F} + \frac{c}{48\pi} \frac{\dot{F}}{F'} \left(\frac{F'''}{F'} - 2 \frac{F''^2}{F'^2} \right) \right). \tag{2.1.66}$$

Note that here we considered only one copy of the Virasoro group $\widehat{\mathrm{Diff}}(S^1) \times \widehat{\mathrm{Diff}}(S^1)$. The discussion for the second copy is analogous. Furthermore, note that while it is conventional in the literature to parameterize the circle by φ, we may equivalently choose x^+ or x^- on compactified Minkowski space. Both copies of $\widehat{\mathrm{Diff}}(S^1) \times \widehat{\mathrm{Diff}}(S^1)$ then correspond to the geometric action for the left- and right-moving sector in the CFT. The full geometric action is then given by

$$S = S_+ + S_-. \tag{2.1.67}$$

This concludes the discussion of two-dimensional CFTs.

2.2. Three-dimensional Anti-de Sitter Space

Here, we introduce three-dimensional Anti-de Sitter (AdS) spacetimes that are relevant in this thesis. Three-dimensional gravity is rather special as it has no propagating degrees of freedom and the Riemann tensor is completely fixed by the metric, $R_{\lambda\mu\nu\rho} = \Lambda \left(g_{\lambda\nu} g_{\mu\rho} - g_{\lambda\rho} g_{\mu\nu} \right)$ [119]. Nevertheless, solutions to Einstein's field equation,

$$R_{\mu\nu} - \frac{1}{2} R g_{\mu\nu} + \Lambda g_{\mu\nu} = 8\pi G_N \mathcal{T}_{\mu\nu}, \tag{2.2.1}$$

in three dimensions range from simple empty space solutions to black holes. Here, Λ denotes the cosmological constant, $\mathcal{T}_{\mu\nu}$ the bulk energy-momentum tensor[3], and R and $R_{\mu\nu}$ the Ricci scalar and curvature, respectively. The relative simplicity of three-dimensional gravity combined with the existence of non-trivial solutions such as black holes, provides an ideal setup to study gravitational systems that may be very complicated in higher dimensions. We are interested in solutions to (2.2.1) with constant negative Ricci curvature, $R = -6$. These solutions are the asymptotic AdS spacetimes. We discuss vacuum solutions with vanishing matter energy-momentum tensor $\mathcal{T}_{\mu\nu} = 0$ everywhere, which include empty AdS and black holes, and a special solution with $\mathcal{T}_{\mu\nu} = 0$ everywhere except at a single point, which gives rise to a conical

[3] The energy-momentum tensor in (2.2.1) is a source for matter content in the gravitational theory and is unrelated to the energy-momentum tensor of the two-dimensional CFT we encountered in sec. 2.1

defect geometry. Since three-dimensional gravity has no local degrees of freedom, these spacetimes are all locally equivalent to empty AdS, but differ from it globally. The metrics $g_{\mu\nu}$ we discuss have the general form

$$ds^2 = -f(r)dt^2 + \frac{1}{f(r)}dr^2 + r^2 d\varphi^2, \tag{2.2.2}$$

where t denotes the time, $r \in \mathbb{R}^+$ a radial coordinate and $\varphi \in [0, 2\pi)$ an angular coordinate. The solution are distinguished only by the function $f(r)$.

Embedding space and global AdS

Following [40, 123], we begin by considering the simplest asymptotically AdS vacuum solution to Einstein's field equations with maximal symmetry. The maximally symmetric solution of the form (2.2.2) is empty AdS with metric

$$ds^2 = -\left(1 + r^2\right) dt^2 + \left(1 + r^2\right)^{-1} dr^2 + r^2 d\varphi^2. \tag{2.2.3}$$

Another possibility to construct an AdS space that will be useful later in sec. 4.2.3 is to consider the $(2+2)$-dimensional Minkowski space $\mathbb{R}^{2,2}$ with metric

$$ds^2 = -dX_0^2 + dX_1^2 + dX_2^2 - dX_3^2. \tag{2.2.4}$$

AdS_3 is embedded in $\mathbb{R}^{2,2}$ as a hyperboloid satisfying

$$-X_0^2 + X_1^2 + X_2^2 - X_3^2 = -L^2. \tag{2.2.5}$$

By convention, we set the AdS radius L to $L = 1$. One possible solution to this constraint equation is given by

$$\begin{aligned} X_0 &= \cosh(\rho)\cos(t), \quad & X_3 &= \cosh(\rho)\sin(t), \\ X_1 &= \sinh(\rho)\cos(\varphi), \quad & X_2 &= \sinh(\rho)\sin(\varphi), \end{aligned} \tag{2.2.6}$$

where $\rho \geq 0$, $\varphi \in [0, 2\pi)$, and $t \in [0, 2\pi)$. The coordinates $\{\rho, \varphi, t\}$ are called global because they cover the full hyperboloid (2.2.5). Employing the metric (2.2.4) and the parameterization (2.2.6), we obtain the metric for global AdS,

$$ds^2 = -\cosh^2(\rho)dt^2 + d\rho^2 + \sinh(\rho)^2 d\varphi^2. \tag{2.2.7}$$

The spacetime is depicted in fig. 2.1. This metric is related to (2.2.3) by the coordinate

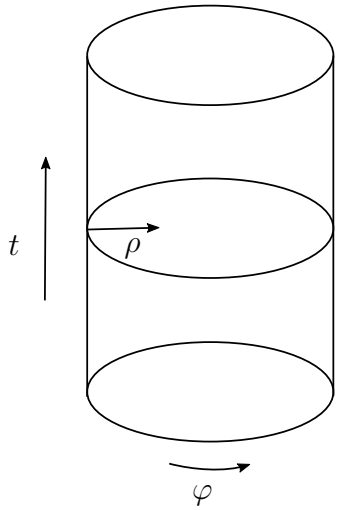

Fig. 2.1.: Empty AdS in global coordinates.

transformation $r = \sinh(\rho)$.

For the AdS/CFT correspondence, it is essential that the AdS spacetime has a boundary. This is easiest to see in conformally compactified coordinates. To this end, we set $\tanh(\chi) = \sinh(\rho)$ with $\chi \in [0, \frac{\pi}{2})$. Then, (2.2.7) becomes

$$ds^2 = \frac{1}{\cos(\chi)} \left(-dt^2 + d\theta^2 + \sin^2(\chi) d\varphi^2\right). \tag{2.2.8}$$

Note that we may add the point $\chi = \frac{\pi}{2}$ as spatial infinity. As we approach $\chi \to \frac{\pi}{2}$, the metric reduces to $ds^2 = -dt^2 + d\varphi^2$. Therefore, the boundary of AdS_3 is conformally compactified two-dimensional Minkowski space. So far, we have treated t as a periodic coordinate, which indicates closed timelike curves. To rid the spacetime of such an unwanted feature, we unwrap the angle such that $-\infty < t < \infty$. This corresponds to considering the universal cover of AdS_3. Let us comment on the Killing symmetries. AdS_3 is maximally symmetric with 6 Killing vectors. These Killing vectors correspond to time translations and spacetime rotations, and form the group $SO(2,2) \sim SL(2,\mathbb{R}) \times SL(2,\mathbb{R})$. A further useful parameterization that we will encounter is given by

$$\begin{aligned} X^0 &= \frac{1}{2r}\left(1 + r^2\left(\varphi^2 - t^2\right)\right), \\ X^1 &= r\varphi, \\ X^2 &= \frac{1}{2r}\left(1 + r^2\left(\varphi^2 - t^2\right)\right), \\ X^3 &= rt. \end{aligned} \tag{2.2.9}$$

Upon insertion into (2.2.4), this parameterization yields a metric of the form (2.2.2)

in Poincaré coordinates,

$$\mathrm{d}s^2 = \frac{1}{r^2}\, dr^2 + r^2 \left(-dt^2 + \mathrm{d}\varphi\right). \tag{2.2.10}$$

These coordinates cover only half of the hyperboloid (2.2.5). The boundary is located at $r \to \infty$. Furthermore, the spacetime (2.2.10) has a Killing horizon at $r = 0$, where the timelike Killing vector ∂_t vanishes.

The BTZ black hole

The BTZ black hole [124, 125] is the unique spherically-symmetric vacuum solution to (2.2.1) approaching empty AdS_3 at large values of the radial coordinate r. The metric for the uncharged, non-rotating black hole of mass m is given by

$$ds^2 = -\left(r^2 - r_h^2\right) dt^2 + \frac{1}{(r^2 - r_h^2)} dr^2 + r^2 d\varphi^2, \tag{2.2.11}$$

where $r_h = 2G_N m$ denotes the position of the horizon. The spacetime has two Killing vectors ∂_t and ∂_φ corresponding to mass and angular momentum conservation. The coordinates in (2.2.11) cover only the exterior region of the black hole $r > 2G_N m$ and have a coordinate singularity at $r = 2G_N m$. In contrast to its Minkowski counterparts, AdS_3 black holes do not have a curvature singularity at $r = 0$ since the Ricci scalar for an asymptotic AdS_3 spacetime is constant everywhere, and the BTZ black hole is locally isometric to empty AdS_3. However, there still is a causal singularity at $r = 0$ as ∂_φ becomes timelike. Furthermore, observe that for $m = -\frac{1}{4G}$, we recover (2.2.3). On the other hand, setting $m = 0$ yields (2.2.10). Therefore, empty AdS in Poincaré coordinates with metric (2.2.10) is sometimes referred to as the massless BTZ black hole.

While the metric (2.2.11) is suitable to describe physics in the black hole exterior region, we will be interested in applications where both the interior and exterior are relevant. Therefore, we need to choose a different set of coordinates which also cover the black hole interior. These are the Kruskal-Szekeres coordinates U, V. In these coordinates, lines of constant U and V are radial null geodesics obtained by first introducing a tortoise coordinate via $dr^* = \frac{dr}{r^2 - r_h^2}$ and then setting $U = -e^{-r_h}(t_R - r^*)$ and $V = e^{r_h}(t_R + r^*)$. The construction of the coordinates is described in detail in [126]. The new metric then reads

$$ds^2 = \frac{4dUdV}{(1+UV)^2} - \left(\frac{1-UV}{1+UV}\right)^2 d\varphi^2. \tag{2.2.12}$$

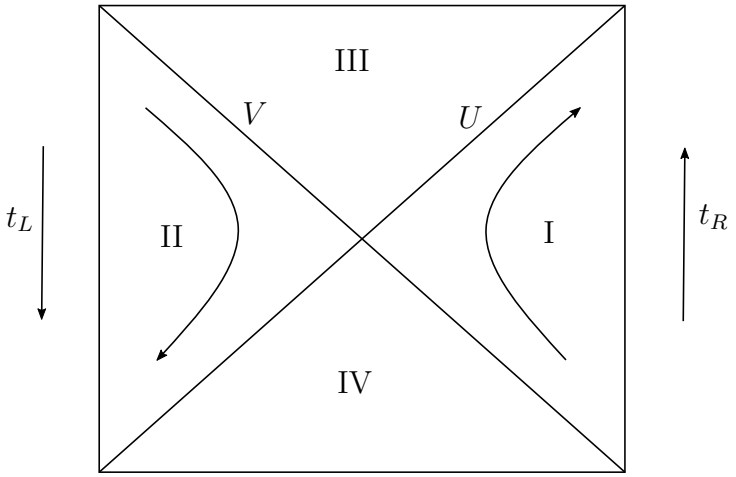

Fig. 2.2.: The eternal AdS black hole has two interior regions, III and IV, and two exterior regions, I and II. Each of the exterior regions has a boundary. Time runs downward on the left boundary and upward on the right boundary.

Its Penrose diagram is shown in fig. 2.2. The portion of spacetime covered by (2.2.11) corresponds to region I. For $r < 2G_N m$, the logarithm determining the tortoise coordinate r^* has a branch cut and we may either analytically continue to $U > 0$ or $U < 0$, which corresponds to regions III and IV, respectively. The singularity at $r = 0$ is given by $UV = 1$ in the new coordinates. Due to the analytical continuation, there exist two of those in U, V-coordinates, which correspond to the upper and lower horizontal lines in fig. 2.2. In this construction, in addition to the exterior region I, there is a second exterior region, region II in fig. 2.2, which is also asymptotically AdS. Since asymptotically AdS spacetimes have a Minkowski boundary and there are two such regions in fig. 2.2, the spacetime described by metric (2.2.12) has two boundaries. These are represented by the vertical straight lines in fig. 2.2. The horizon is given by $U = 0$ when approaching from the right exterior and $V = 0$ when approaching from the left exterior.

Further important properties of the black hole are its temperature and entropy. The temperature is given in terms of the mass m of the black hole [23, 32],

$$T_H = \frac{r_h}{2\pi}. \tag{2.2.13}$$

Its thermal radiation is the Hawking radiation of the black hole. Furthermore, the spacetime described by (2.2.12) is called the eternal AdS black hole in three dimensions. It is the maximal extension of (2.2.11) and is eternal in the sense that it does not evaporate as it is in thermal equilibrium with its own Hawking radiation. More generally, the black hole satisfies generalized laws of thermodynamics [23, 28, 29, 32].

In particular, it has an entropy,

$$S = \frac{A}{4G_N} = \frac{2\pi r_h}{4G_N}, \tag{2.2.14}$$

where A is the area of the black hole. Equation (2.2.14) is of fundamental importance in quantum gravity. In contrast, to the usual extensive entropy that scales with the volume, the black hole entropy (2.2.14) only scales with the area. Since the entropy can be interpreted as counting the degrees of freedom in a system, (2.2.14) implies that the black hole has microscopic degrees of freedom that are counted by the entropy. These microscopic degrees of freedom arise from the underlying theory of quantum gravity. It is an open question to understand how exactly these microstates look like. But the entropy (2.2.14) gives a first hint that degrees of freedom in quantum gravity scale with the area rather than the volume. We will later encounter the behavior (2.2.14) again in a much more general setting.

Conical defects

The final geometry that will be relevant in this thesis is the conical defect, which is a solution with a pointlike source. Therefore, the matter energy-momentum tensor $\mathcal{T}_{\mu\nu}$ does not vanish everywhere. The presentation follows [127]. The conical defect is obtained by solving (2.2.1) with an ansatz,

$$\begin{aligned} ds^2_{DJ} &= -N^2(r)dt^2 + \Phi(r)\left(dr^2 + r^2 d\tilde{\varphi}^2\right), \\ \mathcal{T}^{00} &= \frac{m}{\sqrt{-g}} N(r)\delta(r). \end{aligned} \tag{2.2.15}$$

The unspecified functions are given by [128]

$$\Phi(r) = \frac{\frac{4}{n^2}}{\Lambda r^2 \left((r/r_0)^{\frac{1}{n}} + (r/r_0)^{-\frac{1}{n}}\right)^2}, \quad N(r) = \frac{\left((r/r_0)^{\frac{1}{n}} - (r/r_0)^{-\frac{1}{n}}\right)}{\left((r/r_0)^{\frac{1}{n}} + (r/r_0)^{-\frac{1}{n}}\right)}, \tag{2.2.16}$$

where r_0 is an integration constant. With the identification

$$\sinh\rho = \frac{1}{2}\left(\left(\frac{r}{r_0}\right)^{\frac{1}{n}} + \left(\frac{r}{r_0}\right)^{-\frac{1}{n}}\right), \quad \varphi = \frac{\tilde{\varphi}}{n}, \tag{2.2.17}$$

we recover

$$ds^2 = -\cosh^2\rho dt^2 + d\rho^2 + \sinh^2\rho d\varphi^2, \quad \varphi \in \left[0, \frac{2\pi}{n}\right). \tag{2.2.18}$$

Therefore, a massive pointlike particle in AdS_3 generates a conical defect due to the

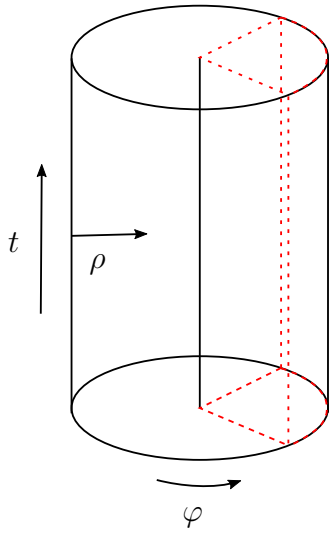

Fig. 2.3.: The conical defect is created by a massive particle in AdS which moves along the geodesic indicated by the black line at the center of AdS. The particle excises a wedge shown by the red dotted lines, creating a defect angle.

angular deficit $\frac{2\pi}{n}$. In this thesis, we will only consider the case, where $n \in \mathbb{Z}$ because only then will we have a dual CFT in the AdS/CFT correspondence. In particular, (2.2.18) implies that the conical defect is simply empty AdS_3 quotiented by the discrete symmetries $\mathbb{Z}_n$, $AdS_3/\mathbb{Z}_n$. The conical defect may be thought of as cutting a wedge from AdS, where the deficit angle is determined by the mass $m = -\frac{1}{8n^2 G_N}$ of the defect. A particle at the center of AdS, where $\rho = 0$, follows a timelike trajectory determined by the geodesic equation[4].

$$\frac{d^2X^\mu}{dt^2} = -\Gamma^\mu_{\alpha\beta}\frac{dX^\alpha}{dt}\frac{dX^\beta}{dt} + \Gamma^0_{\alpha\beta}\frac{dX^\alpha}{dt}\frac{dX^\beta}{dt}\frac{dX^\mu}{dt}. \tag{2.2.20}$$

For a massive particle in empty AdS (2.2.7), the geodesic is given by

$$X^\mu(t) = \begin{pmatrix} \rho(t) = 0 \\ t \\ \varphi(t) = 0 \end{pmatrix}, \tag{2.2.21}$$

[4]The geodesic equation for the geodesic parameterized by the physical time t follows from the textbook geodesic equation,

$$\frac{d^2X^\mu}{d\lambda^2} = -\Gamma^\mu_{\alpha\beta}\frac{dX^\alpha}{d\lambda}\frac{dX^\beta}{d\lambda}, \tag{2.2.19}$$

parameterized by the affine parameter λ by employing $d\lambda = Ldt$, where L is the particle Lagrangian in AdS_3 and $\frac{d^2t}{d\lambda^2} = -\Gamma^t_{\alpha\beta}\frac{dX^\alpha}{d\lambda}\frac{dX^\beta}{d\lambda}$.

which implies the particle moves on a straight line from past to future infinity. This timelike geodesic is the intersection of the faces of the wedge that is cut from empty AdS by the presence of the pointlike particle. The geometry is depicted in fig. 2.3.

2.3. The Holographic Principle

In this section, we introduce the theoretical foundation of this thesis – the AdS/CFT correspondence – as a concrete example of the holographic principle. At the center of the holographic principle is the Bekenstein bound [35], which states that the maximum entropy of a spacetime region bounded by a surface of area A is at most A,

$$S \leq \frac{A}{4G_N}. \tag{2.3.1}$$

The Bekenstein bound (2.3.1) can be understood from a simple thought experiment [33, 129]. We consider a spacetime region with some isolated matter bounded by an area A just large enough to contain the matter. We now add to this particular region matter to an extend that it collapses to form a black hole with a surface $A_{BH} = A$. Since the entropy of the initial matter configuration cannot be smaller than the black hole entropy, (2.3.1) must be true. Otherwise there would be a clear violation of the second law of thermodynamics. Furthermore, (2.3.1) implies that the entropy of a spacetime region is not extensive, i.e. it does not scale with the volume. The number of degrees of freedom in a spacetime region is then much smaller than we might naively expect and grows only with the area of the region. This realization leads to the holographic principle [33, 36]: A consistent theory of quantum gravity describing the physics in some spacetime region has an equivalent description in terms of some other theory utilizing only the degrees of freedom on the boundary of the spacetime region. Then, the black hole entropy (2.2.14) can be understood in terms of a much more fundamental statement: It is a consequence of the property of quantum gravity that degrees of freedom scale with the area rather than the volume of an enclosing surface. This peculiar scaling of the degrees of freedom implies that we may rephrase quantum gravity in terms of a theory in one dimension less. An example of a concrete realization of this holographic principle is the AdS/CFT correspondence.

2.3.1. Realizing the Holographic Principle: The AdS/CFT Correspondence

We begin with a general introduction into the AdS/CFT correspondence and then refine statements on concrete examples of the correspondence with a focus on $\mathrm{AdS}_3/\mathrm{CFT}_2$, which is the focus of this thesis.

General overview

The AdS/CFT correspondence [34] is the prime example of a realization of the holographic principle. It is a conjecture that purports a duality between a theory of quantum gravity on $\mathrm{AdS}_{d+1} \times M$, where M is a compact manifold, and a d-dimensional CFT on $\mathbb{R} \times S^{d-1}$. This duality implies that the degrees of freedom of the theory of quantum gravity on $\mathrm{AdS}_{d+1} \times M$ may be described by those of a d-dimensional CFT on $\mathbb{R} \times S^{d-1}$. It is essential to the correspondence that AdS_{d+1} has a d-dimensional boundary, as we discussed on the example of AdS_3 in sec. 2.2, since this is where the CFT lives. The $(d+1)$-dimensional space on which the gravity theory lives is referred to as the bulk, whereas the d-dimensional space on which the CFT lives is called the boundary. Furthermore, the duality implies that there is a map between observables in the CFT and those in the quantum gravity theory. This map is called the holographic dictionary and can be put in a single equation: The partition function of the quantum gravity theory is equal to the generating functional of the dual CFT, $\mathcal{Z}_{\text{quantum gravity}} = \mathcal{Z}_{\text{CFT}}$, upon specifying boundary conditions for the quantum gravity partition function. In principle, expectation values and correlation functions of operators may be derived from the partition functions and must be equal for dual operators. However, the quantum gravity partition function $\mathcal{Z}_{\text{quantum gravity}}$ is generally not known. Therefore, a semiclassical approximation with quantum fields on a classical Einstein gravity background and the appropriate limit in the CFT is typically considered. We will come back to these statements and make them more precise after we motivate the AdS/CFT correspondence from the behavior of D-branes in string theory.

Motivation: The two faces of a D-brane

The theory of quantum gravity relevant for the AdS/CFT correspondence is type IIB string theory with string-coupling constant g_s and string length l_s. Within this theory, we may define Dp-branes. These branes are $(p+1)$-dimensional dynamical hypersurfaces on which strings end. The 'D' stands for Dirichlet and specifies the

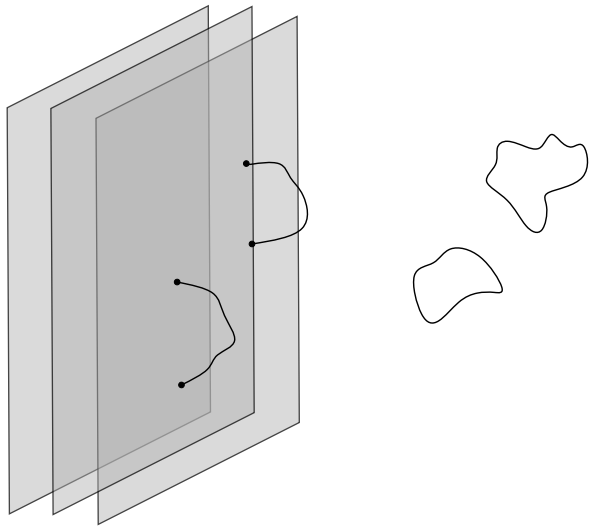

Fig. 2.4.: In the open-string picture, valid in the weak-coupling limit $g_sN \ll 1$, D-branes are hypersurfaces on which open string end. Closed strings propagate in the background.

boundary condition for the string. The Dp-branes have two different interpretations depending on whether we take a weak-coupling limit $g_sN \ll 1$ or a strong-coupling limit $g_sN \gg 1$, where N denotes the number of branes. The main motivation behind the AdS/CFT correspondence arises by considering the branes in these limits.

We begin with the weak-coupling limit $g_sN \ll 1$ of type IIB string theory and N coinciding Dp-branes in (9+1)-dimensional Minkowski space. The presence of the branes breaks Lorentz symmetry from $SO(1,9)$ to $SO(1,p)\times SO(9-p)$. Furthermore, we take a low-energy limit $E \ll \frac{1}{l_s}$, which implies we only consider massless string excitations. The setup is shown in fig. 2.4. Then, type IIB string theory may be described by an effective action consisting of open and closed string contributions as well as interactions between them,

$$S = S_{\text{closed}} + S_{\text{open}} + S_{\text{int}}. \tag{2.3.2}$$

The relevant part of the closed string action is given by

$$S_{\text{closed}} = \frac{1}{(2\pi)^7 l_s^8} \int d^{10}x \sqrt{-g} e^{-2\Phi} \left(R + 4(\partial\Phi)^2\right), \tag{2.3.3}$$

where Φ is the dilaton. Note that (2.3.3) does not reproduce the usual Einstein term in the action. This, however, can be straightforwardly achieved by going from string

to Einstein frame using $g_{\mu\nu} \to g_{\mu\nu}\sqrt{g_s e^{-\Phi}}$,

$$S_{\text{closed}} = \frac{1}{(2\pi)^7 g_s^2 l_s^8} \int \mathrm{d}^{10}x \, \sqrt{-g} \, (R + 4\partial_\mu \Phi \partial^\mu \Phi) + \cdots . \tag{2.3.4}$$

Employing $2\kappa^2 = (2\pi)^7 g_s^2 l_s^8$ and expanding around small metric perturbations $g_{\mu\nu} = \eta_{\mu\nu} + \kappa h_{\mu\nu}$, we find

$$S_{\text{closed}} \sim -\frac{1}{2} \int \mathrm{d}^{10}x \, \partial_\mu h \partial^\mu h + \mathcal{O}(\kappa). \tag{2.3.5}$$

In the low-energy limit, $\kappa \to 0$. Therefore, we obtain a kinetic term for a freely propagating graviton. The full closed-string action describes a type IIB supergravity theory on $(9+1)$-dimensional flat Minkowski space. Furthermore, to lowest order the interaction term is of order $\mathcal{O}(\kappa)$ and therefore vanishes in the limit $\kappa \to 0$. This indicates that open and closed strings decouple at low energies.

Next, we consider the open-string action. Recall that open strings end on the N coinciding Dp-branes. We denote the coordinates in the direction of the brane by $a, b \in \{0, 1, ..., p\}$ and those transverse to the brane by $i, j \in \{p+1, ..., 9\}$. At low energies, the action of a single Dp-brane is given by the Dirac-Born-Infeld action,

$$S_{\text{DBI}} = -\frac{1}{(2\pi)^3 l_s'^4 g_s} \int dx^{p+1} e^{-\Phi} \sqrt{-\det\left(\mathcal{P}(g)_{ab} + 2\pi\alpha' F_{ab}\right)}. \tag{2.3.6}$$

The field F_{ab} is associated to a $U(1)$ gauge field living on the brane, and the pullback $\mathcal{P}(g)_{ab}$ is given by $\mathcal{P}(g)_{ab} = g_{\mu\nu} \frac{\partial X^\mu}{\partial \xi^a} \frac{\partial X^\nu}{\partial \xi^b} = g_{ab} + g_{ij} \frac{\partial x^i}{\partial \xi^a} \frac{\partial x^j}{\partial \xi^b}$. We now associate a scalar field ϕ to the transverse directions by the expansion $x^i = c^i + 2\pi l_s^2 \phi^i(x)$. Furthermore, we set the dilaton to $\Phi = g_s$ and expand the metric with $g = \eta + \kappa h$. Then to lowest order in l_s, the non-trivial terms in the Dirac-Born-Infeld action for a single brane read

$$S_{\text{DBI}} = -\frac{1}{2\pi g_s} \int dx^{p+1} \frac{1}{4} \left[F^{ab} F_{ab} + \frac{1}{2} \sum_i \partial_a \phi^i \partial^a \phi^i \right]. \tag{2.3.7}$$

The story for N coinciding branes is more complicated. First of all, for N branes we have gauge group $(U(1))^N$. But if we consider a stack of N coinciding Dp-branes, the gauge group enhances to $U(N)$ since strings can then stretch between these coinciding branes and are labeled by the Chan-Paton factors λ_{kl}. The indices of the Chan-Paton factors indicate that the string begins on the k-th brane and ends on the l-th brane. For N branes, there are N^2 index combinations, which implies a $U(N)$ gauge symmetry. Furthermore, this new gauge symmetry is non-Abelian. Therefore, we must replace ordinary derivatives in (2.3.7) with covariant derivatives $D_a = \partial_a + i[A_a, \cdot]$ and rather than a single gauge field and field strength, there are N. Let T^n denote the $U(N)$

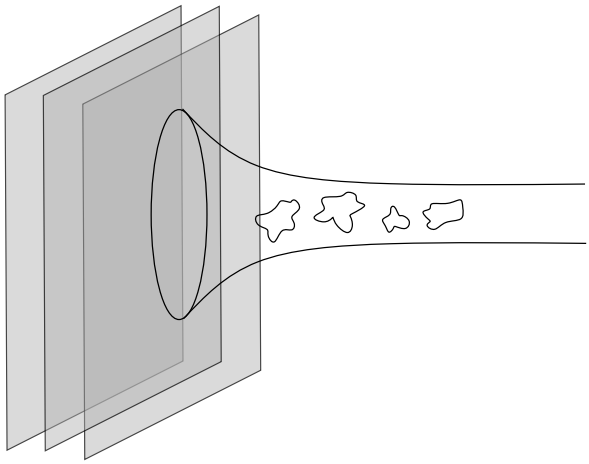

Fig. 2.5.: In the closed-string picture, valid in the strong-coupling limit $g_sN \gg 1$, D-branes source closed strings on a curved background geometry.

generators. Then, $A_a = \sum_{n=1}^{N} A_a^n T^n$ and $F_{ab} = \sum_{n=1}^{N} F_{ab}^n T^n$. Finally, there is an additional potential term $[\phi^i, \phi^j]^2$ for coinciding branes such that for N coinciding branes (2.3.7) becomes

$$S_{\text{open}} = -\frac{1}{2\pi g_s} \int dx^{p+1} \frac{1}{4} \operatorname{tr} \left[\sum_n F^{abn} F_{ab}^n + \frac{1}{2} \sum_i D_a \phi^i D^a \phi^i + \sum_{i,j} \left[\phi^i, \phi^j\right]^2 \right]. \quad (2.3.8)$$

This is the action of $\mathcal{N} = 4$ $U(N)$ Super-Yang-Mills theory upon identifying the Yang-Mills coupling $2\pi g_s = g_{\text{YM}}^2$. Therefore, type IIB string theory on $(9+1)$-dimensional Minkowski space reduces to a gauge theory at low energies in the weak coupling limit $g_sN \ll 1$.

In the strong-coupling limit $g_sN \gg 1$, the Dp-branes become sources for closed strings of type IIB supergravity. This setup is shown in fig. 2.5. The relevant part of the low-energy effective action is given by

$$S = \frac{1}{(2\pi)^7 l_s^8} \int d^{10}x \sqrt{-g} \left(e^{-2\Phi} \left(R + 4(\partial\Phi)^2 \right) - \frac{2}{(8-p)!} F_{p+2}^2 \right), \quad (2.3.9)$$

where Φ is the dilaton and $F_{p+2} = dA_{p+1}$ is the field strength to the $(p+1)$-form potential A_{p+1}. The potential A_{p+1} is associated to charges on the Dp-branes. Due to the presence of N Dp-branes, there are N units of charge,

$$Q = \frac{1}{2\kappa^2} \int_{S^{8-p}} {}^*F_{p+2} = N, \quad (2.3.10)$$

where $*$ is the hodge star. The general solution for the IIB supergravity equations of motion obtained from the action (2.3.9) is given by

$$\begin{aligned} ds^2 &= \frac{1}{\sqrt{H(r)}}\left(-dt^2+\sum_{i=1}^{p} dx^i dx^i\right)+\sqrt{H(r)}\left(dr^2+r^2\sum_{a=1}^{9-p-1} d\theta^a d\theta^a\right), \\ e^{\Phi} &= g_s H(r)^{\frac{3-p}{4}}. \end{aligned} \tag{2.3.11}$$

Here, θ_a are coordinates on a compact manifold. This general solution describes a black brane with blackening factor

$$H(r) = 1+\frac{L^{7-p}}{r^{7-p}}, \quad L^{7-p} = 2^{5-p}\pi^{\frac{5-p}{2}}\Gamma\left(\frac{7-p}{2}\right) g_s N l_s^{7-p}. \tag{2.3.12}$$

In contrast to a black hole, the black brane has a non-compact horizon. The location of the horizon is at $r=0$ in these coordinates.

There are two interesting limits for the metric in (2.3.11). The first one is the near-horizon limit $r \to 0$. In this case, $H(r) \sim \frac{L^{7-p}}{r^{7-p}}$, and we obtain the metric

$$\begin{aligned} ds^2 &= \frac{1}{\sqrt{\frac{L^{7-p}}{r^{7-p}}}}\left(-dt^2+\sum_{i=1}^{p} dx^i dx^i\right)+\sqrt{\frac{L^{7-p}}{r^{7-p}}}\left(dr^2+r^2\sum_{a=1}^{9-p-1} d\theta^a d\theta^a\right) \\ &= \left[\frac{1}{\sqrt{\frac{L^{7-p}}{r^{7-p}}}}\left(-dt^2+\sum_{i=1}^{p} dx^i dx^i\right)+\sqrt{\frac{L^{7-p}}{r^{7-p}}}dr^2\right]+\sqrt{\frac{L^{7-p}}{r^{7-p}}}r^2\sum_{a=1}^{9-p-1} d\theta^a d\theta^a. \end{aligned} \tag{2.3.13}$$

The terms in the square bracket are the AdS_{p+2} metric in Poincaré coordinates with radius of curvature L. The second one is the compact manifold M mentioned at the beginning of this section. Therefore, we obtain $\mathrm{AdS}_{p+2}\times M$ in the near-horizon region. The second interesting limit is $r \to \infty$. In this case, $H(r) \sim 1$ and we obtain a flat $(9+1)$-dimensional metric.

Note that energies in the near-horizon region can be arbitrarily high. Let us consider a string excitation with energy $l_s E_r$ at position r near the horizon. Even if this energy is large, an observer at radial infinity will see a low-energy mode since the blackening factor $H(r)$ leads to a gravitational red-shift. The energy perceived by an observer at infinity is then obtained from

$$E_\infty = \sqrt{-g_{00}}E_r = H(r)^{-\frac{1}{4}}E_r. \tag{2.3.14}$$

For fixed energy $l_s E_r$ in the near-horizon region, $E_\infty \to 0$ due to the gravitational red-shift. Therefore, an observer at infinity perceives two different low-energy excitations:

Low-energy modes propagating on flat Minkowski space far away from the branes and low-energy modes near the branes on $\mathrm{AdS}_{p+2} \times M$. The low-energy modes on Minkowski space have large wavelength compared to the branes, whereas the low-energy modes near the branes cannot escape the potential well. Therefore, the low-energy modes decouple. We now have all the ingredients to arrive at Maldacena's conjecture.

The original conjecture

So far, our discussion has been very general and presents the general approach to motivate the duality. The first instance of the correspondence presented in [34] is the $\mathrm{AdS}_5/\mathrm{CFT}_4$ correspondence. To arrive at its statement, we consider type IIB supergravity in $(9+1)$-dimensional Minkowski space with N coinciding $D3$-branes. This is precisely the setup we discussed above for general Dp-branes. Therefore, we simply set $p = 3$.

The strong-coupling limit $g_s N \gg 1$ then leads to the following result. In the near-horizon limit, the compact manifold M may be shown to be the 5-sphere S^5 such that we obtain type IIB supergravity on $\mathrm{AdS}_5 \times S^5$. The limit $r \to 0$ yields $(9+1)$-dimensional Minkowski space. In the weak-coupling limit $g_s N \ll 1$, we obtained $\mathcal{N} = 4$ $U(N)$ Super-Yang-Mills theory and $(9+1)$-dimensional Minkowski space in the preceding discussion. The conjecture then follows from the reasoning that if we obtain the same Minkowski spaces from type IIB string theory in both pictures, then type IIB supergravity on $\mathrm{AdS}_5 \times S^5$ must also be equal to $\mathcal{N} = 4$ $U(N)$ Super-Yang-Mills (SYM) theory upon identifying the free parameters g_{YM}, N, g_s, and $\frac{L}{l_s}$ in both theories as follows: $g^2_{\mathrm{YM}} = 2\pi g_s$ and $2g^2_{\mathrm{YM}} N = \frac{L^4}{l_s^4}$. It is useful to introduce the t'Hooft coupling $\lambda = g^2_{\mathrm{YM}} N = \frac{L^4}{2l_s^4}$.

The correspondence has several forms. In principle, it is expected to be valid for any values of the free parameters. For the values $g_s \neq 0$ and $\frac{l_s^2}{L^2}$ arbitrary, the string theory is quantum and in the dual SYM theory N and λ take any value. This is the AdS/CFT correspondence in its strongest form. However, this non-perturbative string theory is currently not well understood. Therefore, to perform calculations, we have to take certain limits. We obtain a perturbative classical string theory by considering weak couplings $g_s N \ll 1$ while keeping $\frac{l_s^2}{L^2}$ fixed but arbitrary. In the dual CFT, this corresponds to large N at fixed λ. This is the strong form of the correspondence. Finally, we may also take the weak-coupling limit $g_s N \ll 1$ and send $\frac{l_s^2}{L^2} \to 0$. The latter is a point-particle limit since the string length l_s is very small compared to the radius of curvature of AdS. In this limit, the string theory becomes a classical

	t	x_1	x_2	x_3	x_4	x_5	x_6	x_7	x_8	x_9
N_1 $D1$-branes	•	•	-	-	-	-	-	-	-	-
N_5 $D5$-branes	•	•	-	-	-	-	•	•	•	•

Tab. 2.1.: Brane configuration for the D1-D5-brane system. A dot indicates that the brane extends in this direction. The directions (x_2, x_3, x_4, x_5) in which none of the branes extend are compact with topology T^4.

supergravity theory, where strings reduce to point particles. In the dual CFT, this implies a large-N and large-λ limit. The $\mathcal{N} = 4$ SYM theory is therefore strongly coupled. This is the weak form of the correspondence and the most useful one. While the gravity theory is weakly coupled, the dual theory is strongly coupled. We may then use the weakly coupled theory to perform computations that would otherwise be impossible in the strongly coupled theory.

In this thesis, we are interested in $\mathrm{AdS}_3/\mathrm{CFT}_2$. In this case, we do not consider a single type of brane, but the correspondence emerges from type IIB string theory in (9+1)-dimensional Minkowski space from a D1-D5 brane system. The overall procedure is nevertheless exactly the same as before.

$\mathrm{AdS}_3/\mathrm{CFT}_2$: The D1-D5-brane system

This discussion is based on [40, 130]. The $\mathrm{AdS}_3/\mathrm{CFT}_2$ correspondence follows from a D1-D5-brane system in 10 dimensions with coordinates (t, x^i), where $i \in \{1, ..., 9\}$. The branes are arranged as follows. There is a set of N_1 parallel D1 branes extending in the non-compact (t, x_1)-direction and another set of N_5 D5-branes in $(t, x_1, x_6, x_7, x_8, x_9)$-directions. Therefore, the branes share the direction x_1. The directions (x_2, x_3, x_4, x_5) are compact and have the topology of a four-torus T^4. The D5-brane wraps around the compact directions. None of the branes extend in the (x_2, x_3, x_4, x_5)-directions. The brane configuration is summarized in Table 2.1. The presence of the branes breaks the Lorentz symmetry of $SO(1, 9)$ to $SO(1, 1) \times SO(4)_E \times SO(4)_I$. Note that $SO(4)_I$ is a broken internal symmetry since the directions on the torus are compactified. The number of supersymmetry charges reduces from 32 to 8 with $\mathcal{N} = (4, 4)$ supersymmetry. $SO(4)_E$ corresponds to rotations in the directions (x_2, x_3, x_4, x_5) in which none of the branes extent. $SO(1, 1)$ generates boosts along the strings. The eight supercharges decompose into four left and four right spinors under $SO(1, 1)$, which gives rise to $\mathcal{N} = (4, 4)$ supersymmetry.

We now study this D1-D5 system as a solution to type IIB supergravity. This is the string-coupling limit $g_s N_{1/5} \gg 1$, where the branes are considered as sources for type

IIB strings. The solution to (2.3.9) is given by

$$\begin{aligned} ds^2 &= (H_1 H_5)^{-1/2} \left(-dt^2 + dx_5^2\right) + (H_1 H_5)^{1/2}\, dx^i dx^i + (H_1/H_5)^{1/2}\, ds_{T^4}^2, \\ F_3 &= 2Q_5 d\Omega_3 + 2Q_1 e^{-2\Phi} *_6 d\Omega_3, \\ e^{-2\Phi} &= H_5/H_1. \end{aligned} \tag{2.3.15}$$

Here, $d\Omega_3$ is the volume form of S^3 and $*_6$ the six-dimensional Hodge star. The harmonic functions read

$$H_{1,5} = 1 + \frac{Q_{1,5}}{r^2} \quad \text{with} \quad Q_1 = \frac{(2\pi)^4 g N_1 \alpha^3}{V_4}, \quad Q_5 = g N_5 \alpha'. \tag{2.3.16}$$

We now first take the near-horizon limit $r \to 0$. Then, the metric becomes

$$ds^2 = \frac{r^2}{L^2}\left(-dt^2 + dx_5^2\right) + \frac{L^2}{r^2} dr^2 + L^2 d\Omega_3^2 + (Q_1/Q_5)^{1/2}\, ds_{T^4}^2, \tag{2.3.17}$$

where

$$L^2 = (Q_1 Q_5)^{1/2} = e^{-\Phi}. \tag{2.3.18}$$

The resulting metric (2.3.17) is just AdS_3 in Poincaré coordinates (2.2.10) with radius of curvature L and contributions from S^3 and T^4. Therefore, we have obtained $AdS_3 \times S^3 \times T^4$ in the near-horizon limit. On the other hand, in the limit $r \to \infty$, the metric in (2.3.15) becomes

$$ds^2 = (-dt^2 + dx_5^2 + dx_i dx^i + ds_{T^4}^2). \tag{2.3.19}$$

This is a flat metric on $\mathbb{R}^{1,5}$ and a contribution from T^4.

We still need to obtain the two-dimensional CFT, which emerges from a weak string-coupling perspective of the $D1$-$D5$-branes at an IR fixed point. It may be shown that the open-string action for strings ending on the $D1$-$D5$-branes is given by $\mathcal{N} = 4$ $U(N_1) \times U(N_5)$ gauge theory with Lagrangian [131]

$$\begin{aligned} S = \frac{1}{g} \int & \operatorname{Tr}\left(F_{\alpha\beta} F^{\alpha\beta}\right) + \operatorname{Tr}\left(F'_{\alpha\beta} F'^{\alpha\beta}\right) + \operatorname{Tr}\left[\left(\partial_\alpha A_I + [A_\alpha, A_I]\right)^2\right] + \\ & + \operatorname{Tr}\left[\left(\partial_\alpha A'_I + [A'_\alpha, A'_I]\right)^2\right] + \left|\left(\partial_\alpha + A^a_\alpha T^a + A'^a_\alpha T^a\right)\chi\right|^2 + \sum_{aIJ} D^{a2}_{IJ}. \end{aligned} \tag{2.3.20}$$

Here, F, A are gauge fields of $U(N_1)$ and F', A' gauge fields of $U(N_5)$. Indices a run over both groups. Indices α label the direction of the $D5$-brane. Furthermore, χ^B_j is a spinor transforming under the $SO(4)_I$ internal symmetry labeled by Chan-Paton factors j for $U(N_1)$ and B for $U(N_5)$. Finally, $D_{IJ} = \frac{1}{2}\epsilon_{IJKL} D_{KL}$ is a self-dual antisymmetric tensor in $SO(4)_I$. The indices $\{I, J, K, L\}$ label directions transverse

to the brane.

There is a vector multiplet and a hypermultiplet, each consisting of four scalars and four fermions, which transform under the global $SO(4) \sim SU(2)_L \times SU(2)_R$ R-symmetry. The vector multiplets describe the motion of the brane in the transverse directions. The spinors give rise to a chiral anomaly by transforming chirally under $SU(2)_L$ with anomaly $k_a = N_1 N_5$. Furthermore, the $\mathcal{N} = 4$ $U(N_1) \times U(N_5)$ gauge theory has an IR fixed point. At this point, the $SU(2)_L \times SU(2)_R$ symmetry becomes the current algebra of the CFT and the chiral anomaly is related to the central charge of the CFT by $c = 6(k_a + 1)$. Employing the AdS radius (2.3.18) and the Newton constant $G_N = \frac{1}{4L^3}$, we obtain the central charge

$$c = \frac{3L}{2G_N}. \tag{2.3.21}$$

The result (2.3.21) predates the AdS/CFT correspondence and was first derived in [132]. It is universal for two-dimensional CFTs.

Finally, let us compare the symmetries of the gravity theory with its dual CFT. The full symmetry group of the emerging CFT in the IR limit is given by $SU(1,1|2)$ with bosonic symmetry group $SO(2,2) \times SO(4)$. In particular, $SO(2,2) \sim SL(2,\mathbb{R}) \times SL(2,\mathbb{R})$ are the symmetries generated by the global conformal generators $\{L_{-1}, L_0, L_1\}$ and match the Killing symmetries of AdS_3. Similarly, $SO(4) \sim SU(2)_L \times SU(2)_R$ is the global R-symmetry of the CFT. This symmetry matches the the rotation symmetry of the S^3 contribution to the $AdS_3 \times S^3 \times T^4$ topology.

2.3.2. The Holographic Dictionary

We introduce the holographic dictionary with a focus on the holographic energy-momentum tensor and its role in reconstructing the bulk spacetime from the CFT in AdS_3/CFT_2. These concepts are of fundamental importance in this thesis. The presentation follows [40, 123]. The proposed duality implies there is a one-to-one map between observables in the CFT and the gravity theory. In particular, the correspondence may be summarized in a single statement: The generating functional of n-point correlation functions in the CFT living in two dimensions is equal to the generating functional of the string partition function in three dimensions, provided that we identify boundary values of gravity fields ϕ with sources in the CFT ϕ_0, $\phi(\vec{x}, r)|_{r\to\infty} = \phi_0(\vec{x})$,

$$\left\langle e^{\int d^4x\, \phi_0(\vec{x})\mathcal{O}(\vec{x})} \right\rangle_{CFT} = \mathcal{Z}_{\text{string}}\ \left[\phi(\vec{x}, r)|_{r\to\infty} = \phi_0(\vec{x})\right]. \tag{2.3.22}$$

Here, r denotes the radial bulk coordinate with boundary at $r \to \infty$. Equation (2.3.22) is the AdS/CFT correspondence in its strongest form. The precise string partition function is not known, however. Therefore, we must content ourselves with a slightly weaker form of the correspondence, in which we take the semiclassical limit in the gravity theory. This corresponds to a saddle-point approximation of the string partition function, $\mathcal{Z}_{\text{string}}\ [\phi(\vec{x},r)|_{r\to\infty} = \phi_0(\vec{x})] = e^{-S\left[\tilde{\phi}(\vec{x},r)\right|_{r\to\infty}=\phi_0(\vec{x})\right]}$. The field $\tilde{\phi}$ is the gravity approximation of the string theory field ϕ. The weak form of the correspondence then states [38, 39],

$$\left\langle e^{\int d^4x\, \phi_0(\vec{x})\mathcal{O}(\vec{x})}\right\rangle_{CFT} = e^{-S_{\text{grav,on-shell}}\left[\tilde{\phi}(\vec{x},r)\right|_{r\to\infty}=\phi_0(\vec{x})\right]}, \tag{2.3.23}$$

where $S_{\text{grav,on-shell}}$ is the on-shell gravitational action. In this thesis, we will be interested in the energy-momentum tensor $T_{\mu\nu}$ of the two-dimensional CFT and its correlation functions. This operator is sourced by the boundary metric $g^{(0)}_{\mu\nu}$ of the space on which the CFT lives. We now discuss the holographic construction of the energy-momentum tensor.

Reconstructing the bulk from a two-dimensional CFT

If the only source in the CFT is the boundary metric $g^{(0)}_{\mu\nu}$, which sources the CFT energy-momentum tensor $T_{\mu\nu}$, then we may use a powerful technique – the Fefferman-Graham expansion – to reconstruct the bulk geometry. In particular, the only boundary data necessary are $g^{(0)}_{\mu\nu}$ and the expectation value of the energy-momentum tensor. In general dimensions, the Fefferman-Graham expansion only allows to reconstruct the bulk geometry in an asymptotic expansion near the boundary. On the other hand, for a two-dimensional boundary and a three-dimensional bulk geometry, the expansion terminates and we may reconstruct the full bulk geometry. Once we have identified the appropriate bulk geometry, we may use (2.3.23) to derive the holographic energy-momentum tensor. This is the CFT energy-momentum tensor that follows from the bulk gravitational action via (2.3.23). This section is based on the original works [133–135] and the excellent review [136].

We start with the right-hand side of (2.3.23). The gravitational bulk action is given by the Einstein-Hilbert action and the Gibbons-Hawking boundary term, the latter of which is essential since we consider a bulk theory with a boundary on which the CFT lives. Hence, the full gravitational action including the boundary terms is given by

$$S_{\text{gr}}[G] = \frac{1}{16\pi G_{\text{N}}}\left[\int_M \mathrm{d}^{d+1}x\sqrt{G}(R[G]-2\Lambda) - \int_{\partial M}\mathrm{d}^d x\sqrt{\gamma}2K\right], \tag{2.3.24}$$

where M denotes the gravitational space and ∂M its boundary. Furthermore, $\gamma_{\mu\nu}$ is the induced metric and $K = h_{ij}K^{ij}$ the trace of the extrinsic curvature K_{ij} on ∂M. To make the distinction between bulk and boundary directions clear, we now employ Greek indices for the bulk directions and Latin indices for the boundary directions in this section. As before, R and Λ denote the Ricci scalar and the cosmological constant, respectively. It is convenient to work with a metric in Fefferman-Graham gauge. This means that given a radial coordinate z and boundary coordinates x_i, we make an ansatz for the asymptotic AdS metric such that $g_{zx_i} = 0$ and $g_{zz} = \frac{1}{z^2}$. Then,

$$ds^2 = G_{\mu\nu}dx^\mu dx^\nu = \frac{1}{z^2}\left(dz^2 + g_{ij}(x,z)dx^i dx^j\right). \tag{2.3.25}$$

The coordinate z is related to the coordinate r in (2.2.10) by $z = \frac{1}{r^2}$ such that the boundary is now at $z \to 0$. Next, we expand the metric g_{ij} around the boundary metric $g^{(0)}_{ij}$. The choice of coordinate z is then particularly convenient since the expansion is given in powers of z around $z = 0$, which yields the Fefferman-Graham expansion [137],

$$g(x,z) = g_{(0)} + \cdots + z^d g_{(d)} + h_{(d)} z^d \log z^2 + \ldots. \tag{2.3.26}$$

Note that the logarithmic term only appears for even d and is related to the Weyl anomaly. The vacuum Einstein equations may now be solved order by order in z by inserting the ansatz (2.3.26) into the Einstein equations (2.2.1). In three dimensions, only a finite number of terms in the expansion are necessary to fully solve the Einstein equations. They are given by

$$\begin{aligned} g_{(2)ij} &= \frac{1}{2}\left(R g_{(0)ij} + t_{ij}\right), \\ g_{(4)ab} &= \frac{1}{4} g_{(2)ac} g^{cd}_{(0)} g_{(2)db}. \end{aligned} \tag{2.3.27}$$

Here, t_{ij} is an integration constant obtained when solving the Einstein equations that has to satisfy

$$\nabla^i t_{ij} = 0, \quad \operatorname{Tr} t = -R. \tag{2.3.28}$$

It will become clear later in this section how t_{ij} should be fixed.

It is a unique feature of AdS_3 that we obtain the full bulk spacetime from only three terms in the expansion. The solution is given by

$$ds^2 = \frac{dz^2}{z^2} + \frac{1}{z^2}\left(g_{(0)ab} + z^2 g_{(2)ab} + z^4 g_{(4)ab}\right) dx^a dx^b. \tag{2.3.29}$$

In higher dimensions, an infinite number of terms in the expansion are necessary to fully solve the Einstein equations. Therefore, we then only obtain the bulk metric in a region near the boundary.

Since we would like to derive the holographic energy-momentum tensor, (2.3.23) implies we should compute the on-shell gravitational action. We therefore evaluate (2.3.24) by inserting the solution (2.3.29). Note that the integrals in (2.3.24) are generally divergent. Therefore, we impose a cut-off at $z = \epsilon$ and introduce $g_{ij} = \frac{\kappa_{ij}}{z^2}$. We then find

$$\begin{aligned} S_{\text{reg}} &= \frac{1}{2\kappa}\int d^3x\sqrt{|G|}(R-2\Lambda) - \frac{1}{\kappa}\int_{z=\epsilon} d^dx\sqrt{|g|}K \\ &= -\frac{1}{16\pi G_{\text{N}}}\int \mathrm{d}^2x\left[\int_{z\geq\epsilon} dz\frac{4}{z^3}\sqrt{\det\kappa(x,z)} + \frac{4}{z^2}\sqrt{\det\kappa(x,z)} + \frac{2}{z}\partial_z\sqrt{\det\kappa(x,z)}\right]. \end{aligned} \tag{2.3.30}$$

The divergent terms in this action are given by

$$\begin{aligned} S_{\text{div}} &= -\frac{1}{2\kappa}\int_{z=\epsilon} d^2x\sqrt{|g^{(0)}|}\left(\epsilon^{-2}a_{(0)} - \log(\epsilon^2)a_{(2)}\right) \\ &= -\frac{1}{2\kappa}\int dx^2\sqrt{|g^{(0)}|}\left(-\frac{2}{\epsilon^2} + \frac{R^{(0)}}{2}\log(\epsilon^2)\right). \end{aligned} \tag{2.3.31}$$

The action may be renormalized by subtracting counterterms S_{ct}, which exactly cancel the divergences,

$$S_{\text{ct}} = -S_{\text{div}}. \tag{2.3.32}$$

The renormalized action then reads

$$S_{\text{ren}} = \lim_{\epsilon\to 0}(S_{\text{reg}} + S_{\text{ct}}). \tag{2.3.33}$$

The holographic energy-momentum tensor now follows from variation with respect to the boundary metric,

$$\langle T_{ij}\rangle = \frac{4\pi}{\sqrt{-g(0)}}\frac{\delta S_{\text{reg}}}{\delta g^{ij}_{(0)}} = \lim_{\epsilon\to 0}\frac{4\pi}{\sqrt{\det\kappa(x,\epsilon)}}\frac{\partial S_{\text{reg}}}{\partial\kappa^{ij}(x,\epsilon)}. \tag{2.3.34}$$

This yields

$$\langle T_{ij}\rangle = \frac{1}{16\pi G_{\text{N}}}t_{ij}. \tag{2.3.35}$$

Therefore, the undetermined integration constants t_{ij} in (2.3.27) are given by the components of the boundary energy-momentum tensor. This result has two important consequences. First, upon employing (2.3.27) we obtain the boundary energy-momentum

tensor in terms of bulk metric components,

$$\langle T_{ij}\rangle = \frac{2}{16\pi G_{\mathrm{N}}}\left(g_{(2)ij} - g_{(0)ij}\,\mathrm{Tr}\,g_{(2)}\right), \tag{2.3.36}$$

where the prefactor is related to the central charge by (2.3.21). Note in particular that upon taking the trace, we recover the Weyl anomaly (2.1.34),

$$\langle T^{i}_{\ i}\rangle = -\frac{c}{12}R. \tag{2.3.37}$$

It is a non-trivial check of the correspondence that we recover the correct Weyl anomaly from the holographic dictionary (2.3.23).

Secondly, now that we have determined the coefficients (2.3.27) and know that the integrations constants t_{ij} are given in terms of the boundary CFT energy-momentum tensor, we may employ these results to rewrite the general AdS_3 metric (2.3.29) only in terms of boundary quantities. This implies that the asymptotically AdS_3 bulk geometry is fixed completely by two boundary quantities:

1. the boundary metric $g^{(0)}_{ij}$ and
2. the expectation value of the boundary energy-momentum tensor $\langle T_{ij}\rangle$.

Therefore, we may reconstruct the bulk spacetime exclusively from CFT data. The complete set of bulk spacetimes obtained by choosing a flat boundary metric $g^{(0)}_{ij} = \eta_{ij}$ may then be parameterized by the expectation value of the energy-momentum tensor $\frac{c}{6}\langle T_{ij}\rangle = L_{\pm}(x^{\pm})$. Note that $\langle T_{+-}\rangle = 0$ on a flat background. Therefore, we only need two functions $L_{\pm}(x^{\pm})$ to parameterize the bulk geometries. The set of spacetimes obtained in this manner are called the Bañados geometries [88, 138],

$$ds^2 = \frac{dr^2}{r^2} - \left(rdx^{+} - \frac{L_{-}\left(x^{-}\right)dx^{-}}{r}\right)\left(rdx^{-} - \frac{L_{+}\left(x^{+}\right)dx^{+}}{r}\right). \tag{2.3.38}$$

Here, the coordinate system is chosen such that the boundary is located at $r \to \infty$ by setting $z^2 = \frac{1}{r^2}$. The set of geometries (2.3.38) includes the empty AdS, BTZ black hole, and conical defect geometries discussed in sec. 2.2. In particular, these spacetimes may be classified by the expectation value of the energy-momentum tensor $\frac{c}{6}\langle T_{ij}\rangle = L(x^{\pm})$. We also used $\langle T_{ij}\rangle$ to classify the coadjoint orbits of the Virasoro group in sec. 2.1.2. Thus, asymptotic AdS_3 geometries may be classified in terms of Virasoro coadjoint orbits [138–140]. We discuss this in detail in the next section.

2.3.3. The Phase Space of AdS_3 Geometries: Virasoro Coadjoint Orbits

Here, we review the classification of the phase space of AdS_3 geometries in terms of Virasoro coadjoint orbits as derived in [138–140]. This establishes a precise map between bulk geometries and CFT representations that is an essential ingredient in this thesis. The authors of [138–140] studied the effect of bulk diffeomorphisms $\xi(x^{\pm}, r)$ that do not vanish near the boundary of the spacetimes (2.3.38) and preserve the Fefferman-Graham form of the metric, $g_{rr} = \frac{1}{r^2}$ and $g_{r+} = g_{r-} = 0$. These conditions yield three equations for the diffeomorphism $\xi(x^{\pm}, r)$,

$$\begin{aligned} \mathcal{L}_\xi g_{rr} &= 0, \\ \mathcal{L}_\xi g_{r\pm} &= 0, \end{aligned} \tag{2.3.39}$$

where the Lie derivative of the metric reads $\mathcal{L}_\xi g_{\mu\nu} = \nabla_\mu \xi_\nu + \nabla_\nu \xi_\mu$. Solving these equations yields diffeomorphisms of the general form

$$\begin{aligned} \xi^z(r, x^{\pm}) &= r\omega(x^{\pm}), \\ \xi^a(r, x^{\pm}) &= \epsilon^a(x^b) - \partial_b \omega(x^{\pm}) \int_r^\infty \frac{dr'}{r'} \gamma^{ab}(r', x^c). \end{aligned} \tag{2.3.40}$$

Furthermore, the diffeomorphisms must respect the Brown-Henneaux boundary conditions [132] $g^{(0)}_{ab} = \eta_{ab}$, i.e. they must leave the boundary metric invariant. This is equivalent to requiring that $\mathcal{L}_\xi \gamma_{ab} = \mathcal{O}(r)$, which gives rise to the conformal Killing equations,

$$\mathcal{L}_\epsilon g^{(0)}_{ab} + 2\omega g^{(0)}_{ab} = 0. \tag{2.3.41}$$

Therefore, we may identify $\epsilon(x^{\pm})$ with a conformal vector field generating conformal transformation on the boundary and $\omega(x^{\pm})$ with the appropriate Weyl factor that ensures Brown-Henneaux boundary conditions are satisfied. In the dual bulk theory, we obtain the corresponding diffeomorphism ξ by integrating (2.3.40) for the Bañados geometries (2.3.38). This yields

$$\xi = -\frac{r}{2}\left(\epsilon'_+ + \epsilon'_-\right)\partial_r + \left(\epsilon_+ + \frac{r^2\epsilon''_- + L_-\epsilon''_+}{2\left(r^4 - L_+L_-\right)}\right)\partial_+ + \left(\epsilon_- + \frac{\ell^2 r^2 \epsilon''_+ + L_+\epsilon''_-}{2\left(r^4 - L_+L_-\right)}\right)\partial_-. \tag{2.3.42}$$

These bulk diffeomorphisms are defined not only asymptotically near the boundary but for the full range of the coordinates in (2.3.38). Under (2.3.42), the Bañados

geometries (2.3.38) transform as follows:

$$\delta_\xi g_{\mu\nu} = g_{\mu\nu}\left(L_+ + \delta_\xi L_+, L_- + \delta_\xi L_-\right) - g_{\mu\nu}\left(L_+, L_-\right), \tag{2.3.43}$$

$$\delta_\xi L_+ = \epsilon_+ \partial_+ L_+ + 2L_+\partial_+\epsilon_+ - \frac{1}{2}\partial_+^3\epsilon_+ \tag{2.3.44}$$

$$\delta_\xi L_- = \epsilon_- \partial_- L_- + 2L_-\partial_-\epsilon_- - \frac{1}{2}\partial_-^3\epsilon_-. \tag{2.3.45}$$

Note that $\delta_\xi L_-$ and $\delta_\xi L_-$ transform like the CFT energy-momentum tensor $T_{\mu\nu}$ in (2.1.19) under an infinitesimal conformal transformation $f(x^\pm) = x^\pm + \epsilon(x^\pm)$, where the quantum Weyl anomaly appears classically. This validates the identification $L_\pm(x^\pm) = \frac{c}{6}\langle T(x^\pm)\rangle$. Furthermore, the bulk vector fields (2.3.42) satisfy the classical Witt algebra (2.1.11) with respect to the adjusted Lie bracket,

$$\left[\xi\left(\epsilon_1; L\right), \xi\left(\epsilon_2; L\right)\right]_* = \left[\xi\left(\epsilon_1; L\right), \xi\left(\epsilon_2; L\right)\right] - \left(\delta^L_{\epsilon_1}\xi\left(\epsilon_2; L\right) - \delta^L_{\epsilon_2}\xi\left(\epsilon_1; L\right)\right), \tag{2.3.46}$$

where $\delta^L_{\epsilon_1}\xi\left(\epsilon_2; L\right) = \delta_{\epsilon_1} L\frac{\partial}{\partial L}\xi\left(\epsilon_2; L\right)$, and $\epsilon = (\epsilon_+, \epsilon_-)$ and $L = (L_+, L_-)$. The adjusted Lie bracket is necessary since L transforms under ξ. Therefore, this contribution has to be subtracted to ensure the bracket closes. The Fourier modes of (2.3.42) then satisfy

$$\left[\xi_m, \xi_n\right]_* = (m-n)\xi_{m+n}, \tag{2.3.47}$$

which is the Witt algebra (2.1.11).

The vector fields (2.3.42) allow us to classify the Bañados geometries (2.3.38). Some of the vector fields (2.3.42), which we denote by ζ, leave the metric invariant, i.e. they satisfy $\delta g_{\mu\nu} = \mathcal{L}_{\xi=\zeta}\, g_{\mu\nu} = 0$. These are the Killing vector fields of the given Bañados geometry. From (2.3.43), it follows that the Killing vector fields are precisely those that leave the energy-momentum tensor invariant $\delta_\zeta L = 0$. Furthermore, from the discussion of the Virasoro coadjoint orbits in sec. 2.1.2 we know these transformations form the stabilizer group of a particular coadjoint orbit. Therefore, the Killing symmetries of the bulk Bañados geometry correspond to the orbit stabilizer group in the CFT. For instance, the $U(1)$ Killing charges are given by

$$J_+ = \frac{1}{4G_N}L_+, \quad J_- = \frac{1}{4G_N}L_-. \tag{2.3.48}$$

Then the Bañados geometries are in one-to-one correspondence to Virasoro codjoint orbits: The expectation value of the energy-momentum tensor in the CFT fixes the particular orbit and the orbit stabilizer group. In the bulk, Bañados geometries are distinguished by their Killing charge, which is given in terms of the boundary energy-

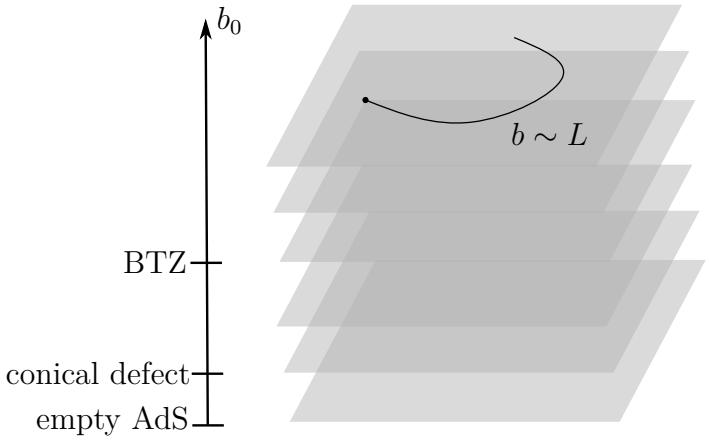

Fig. 2.6.: A schematic depiction of the classification of the AdS_3 phase space in terms of Virasoro coadjoint orbits: different orbits are labeled by b_0 and correspond to Bañados geometries with different Killing charges. Points b on the same orbit correspond to Bañados geometries with different values of the boundary energy-momentum tensor $L_\pm(x^\pm) = \frac{c}{6}\langle T(x^\pm)\rangle$ generated by non-trivial bulk diffeomorphisms ξ. These bulk diffeomorphisms generate a path from the orbit representative b_0 through the Bañados geometries belonging to the same coadjoint orbit. This is indicated by the black line starting from an orbit representative represented by the black dot. There are two copies of a coadjoint orbit, one for L_+ and one for L_-. We only show one copy which is representative for both.

momentum tensor in (2.3.48), and the Killing symmetries match the orbit stabilizer. The remaining vector fields (2.3.42) transform the bulk metric by transforming the energy-momentum tensor $L_\pm$, which corresponds to moving among a set of Bañados geometries that fall within the same coadjoint orbit in the CFT. The transformations of $L_\pm$ generated by the vector fields ξ may then be associated with points on the orbit via (2.1.58). The phase space structure is schematically depicted in fig. 2.6.

We may then establish the following correspondence between Virasoro coadjoint orbits and bulk geometries discussed in this thesis:

- The coadjoint orbit with representative $b_0 = \frac{1}{2\pi}\langle T\rangle = -\frac{c}{48\pi}$ corresponding to a CFT in the vacuum state $|0\rangle$ is dual dual to empty AdS. The CFT exhibits an $SL(2,\mathbb{R})$ symmetry, the dual spacetime an $SL(2,\mathbb{R})$ Killing symmetry.
- The coadjoint orbit with representative $b_0 = \frac{1}{2\pi}\langle T\rangle = \frac{1}{2\pi}\left(h - \frac{c}{24}\right)$, where $0 < h < \frac{c}{24}$, is dual to a conical defect geometry.
- The coadjoint orbit with representative $b_0 = \frac{1}{2\pi}\langle T\rangle = 0$ is dual to Poincaré AdS, also called the massless BTZ. The value of b_0 indicates $h = \frac{c}{24}$. This the black

hole threshold.

- The coadjoint orbit with representative $b_0 = \frac{1}{2\pi}\langle T\rangle = \frac{1}{2\pi}\left(h - \frac{c}{24}\right)$, where $h > \frac{c}{24}$, is dual to a BTZ black hole.

This correspondence between Virasoro coadjoint orbits – and by extension – representations of the CFT and Bañados geometries will be of fundamental importance in this thesis.

Entanglement and the Emergence of Spacetime

3

An important step in understanding quantum gravity is to shed light on black hole physics. Black holes present one of the few phenomena in which semiclassical gravity approximations fail to capture essential physics. In an additional development unrelated to the AdS/CFT correspondence at first, concepts from quantum information theory were applied to QFTs and gravity in attempts to understand black hole physics. In particular, the black hole information paradox has been a driving force in these developments. The black hole information paradox was raised by Hawking in [31], which predates the AdS/CFT correspondence by two decades: A black hole that is formed by an object described by a pure states evaporates by emitting Hawking radiation. Since Hawking radiation is thermal, the system has evolved from a pure to a mixed state, which is a clear violation of unitarity. To reconcile the seemingly contradictory experiences of an external and infalling observer, black hole complimentarity [141–143] introduced three axioms before the advent of AdS/CFT: (1) an external observer perceives pure Hawking radiation, (2) the radiation is emitted from the horizon, and (3) the infalling observer sees nothing extraordinary. Following these developments, the AdS/CFT correspondence [34, 38, 39] was introduced.

As we discussed in chapter 2, AdS/CFT is a realization of the holographic principle [33] which is motivated by the area law describing the quantum states of a black hole. AdS/CFT then provided a controllable framework in which assumptions about black hole physics could be tested. In [49], a CFT dual to an eternal (non-evaporating) AdS black hole was derived, which is the entangled TFD state (1.4). This was later followed by a prescription for the holographic entanglement entropy [41, 144]: Quite remarkably, the entanglement entropy of a CFT subregion is given in terms of the area of a minimal surface in the dual AdS spacetime. Therefore, geometry is related to quantum information. This is seen as a hint that spacetime is not fundamental but emergent from entanglement [47] and presented a fundamental step in understanding quantum gravity.

Since then, concepts from quantum information are gaining an ever-increasing role within the AdS/CFT correspondence. The discussion is centered around the idea that quantum information stored within the CFT gives rise to the AdS spacetime in the bulk. This approach to AdS/CFT is often called 'It from qubit' and is particularly

promising as there is no need to rely on aspects of string theory in the bulk or on specific field content in the dual CFT, which is in stark contrast to the original motivation of AdS/CFT in [34] that relies on very specific string theory and CFT details. Indeed, recent results suggest [145–150] that AdS/CFT is only a special instance of a much more general quantum information/geometry correspondence that may be generalized beyond AdS spaces. Understanding the relation between quantum information and geometry on the tangible example of AdS/CFT then not only provides methods and approaches that are generalizable to other theories, but also teaches us important general lessons about quantum gravity that do not rely on string theory.

In particular, the AdS/CFT correspondence provides a framework in which the black hole information paradox was resolved by showing that information is conserved. An essential tool in the resolution is the relation between entanglement and geometry. Within the unitary framework of AdS/CFT, it was proposed in [151] that black holes may be treated as quantum computers described by a state with a set of qubits, which are quantum analogues of classical bits. The black hole dynamics are then represented by unitary operations that act on an infalling state and scramble or randomize it by acting with the black hole's own qubits. This approach was then employed to test previous assumptions such as black hole complimentarity. It was established that when the black hole emits its qubits in Hawking radiation, the infalling state is encoded in the outgoing Hawking radiation. The central idea is that information about the original state is then recoverable from the entanglement created by the black hole. Important results in studying these aspects of black hole dynamics were obtained [152–156], and the solution to the black hole information paradox was obatined by showing that information about the infalling state may be recovered from Hawking radiation using quantum recovery channels [65] in AdS/CFT.

The success of applying quantum information concepts to AdS/CFT led to broad interest also outside black hole physics in quantum error correction [60, 61, 154], entanglement wedge reconstruction via quantum recovery channels [58, 63–66, 155, 157], the spread of information and scrambling [152, 158–160], and complexity [74, 75, 78, 81–84, 154, 161, 162]. We refer to [163] for a general overview. In particular, the AdS/CFT correspondence may be thought of as a quantum error correction code, where CFT data is stored in the bulk theory in a redundant way such that 'erasures' in bulk subregions do not immediately destroy the CFT information in a boundary subregion, i.e. CFT data can be reconstructed from multiple subregions in the bulk.

Since then the concepts of quantum information have also been successfully applied to eternal (non-evaporating) black holes. Entanglement plays a central role in constructing CFT duals to the eternal AdS black hole and in illuminating the role of

entanglement in the emergence of spacetime from quantum information. The eternal AdS black hole also provided evidence that entanglement alone is not sufficient to fully reconstruct spacetime [48, 50, 74]. This lead to the introduction of quantum computational complexity. The complexity of a quantum state is a measure of how hard it is to build the state of interest from a simple initial state using only simple operations.

Quantum information in AdS/CFT is by now an immensely large and very rapidly developing topic. In this thesis, we will focus on two information theoretic concepts – entanglement and quantum computational complexity – which are crucial in understanding AdS/CFT from an information theoretic perspective. In particular, we illustrated in the preceding paragraphs, these concepts play a crucial role in understanding the physics of evaporating and eternal black holes. We focus on the latter in this thesis.

The aim of this chapter is to introduce entanglement and the modular (or entanglement) Hamiltonian as well as complexity with a focus on their role in AdS/CFT. These quantum information measures will be of fundamental importance for the results obtained in this thesis.

We begin in sec. 3.1 by reviewing aspects of entanglement in quantum field theory (QFT) and the holographic bulk dual to the entanglement entropy in the boundary CFT. We then move on to discuss the emergence of the bulk spacetime from entanglement in the CFT in sec. 3.2. In sec. 3.3, we introduce holographic complexity as an important observable in reconstructing the bulk from quantum information, and then conclude this chapter by discussing complexity from a QFT perspective in sec. 3.4.

3.1. Entanglement

We begin in sec. 3.1.1 by reviewing entanglement and the entanglement entropy in quantum mechanics with a focus on a simple two-spin system. This allows us to introduce entanglement and an important entangled state, the EPR pair, in a conceptually simple framework. We will then discuss entanglement in QFT in sec. 3.1.2 and introduce the modular (or entanglement) Hamiltonian for a subregion. This operator will be of central importance in sec. 5.4. While calculating the entanglement entropy for a subregion in a continuous QFT is technically challenging, we will then see in sec. 3.1.3 that the calculation in the holographic dual gravitational theory in the bulk is straightforward. The holographic entanglement entropy provides evidence of a relation between quantum information and geometry and in particular the emergence of

spacetime from entanglement as it relates the entanglement entropy in a CFT subregion to the area of a minimal surface in the bulk homologous to the CFT subregion.

3.1.1. Entanglement in Quantum Mechanics

We briefly review entanglement and the entanglement entropy in quantum mechanics based on [164]. Entanglement is an intriguing property of quantum systems which has no classical analog and can occur in even the simplest of composite quantum systems such as a two-spin system. To define entanglement, we first consider the Hilbert space structure of a composite quantum system composed of two distinct systems A and B. We denote the Hilbert space of the individual systems by $\mathcal{H}_i$, where the index i labels the two systems. The Hilbert space of the composite system $\mathcal{H}_{\text{comp}}$ is then given by a tensor product of the Hilbert spaces of the individual systems, $\mathcal{H}_{\text{comp}} = \mathcal{H}_A \otimes \mathcal{H}_B$. A composite system is in an entangled state if the state cannot be written as a tensor product of states of the individual systems. Therefore, given states $|\psi\rangle_i$ for the individual systems, the composite system is entangled if $|\psi\rangle_{AB} \neq |\psi\rangle_A |\psi\rangle_B$. The state $|\psi\rangle_{AB}$ has a density matrix $\rho = (|\psi\rangle_{AB})({}_{AB}\langle\psi|)$. The amount of entanglement between A and B is then quantified by the entanglement entropy,

$$S = -\text{tr}_A(\rho_A \log \rho_A). \tag{3.1.1}$$

Here, ρ_A is the reduced density matrix obtained by tracing out the degrees of freedom in subsystem B, $\rho_A = \text{tr}_B(\rho)$. An illustrative example is the two-spin system. Each spin may be regarded as an individual quantum system with a Hilbert space spanned by the states $|\uparrow\rangle_i$ and $|\downarrow\rangle_i$ denoting spin up and down, respectively. For the composite system of two spins, we may then define a state

$$|\text{EPR}\rangle = \frac{1}{\sqrt{2}} \left(|\uparrow\rangle_A \otimes |\uparrow\rangle_B + |\downarrow\rangle_A \otimes |\downarrow\rangle_B \right). \tag{3.1.2}$$

It is impossible to write the state $|\text{EPR}\rangle$ as a tensor product $|\psi_{\text{comp}}\rangle = |\psi\rangle_A \otimes |\psi\rangle_B$ of a single spin state $|\psi\rangle_i$ from the individual systems. In particular, the state (3.1.2) is a maximally entangled EPR state. A generalization of this state to a CFT plays a fundamental role in the AdS/CFT correspondence as we will see in sec. 3.2. Maximally entangled states have maximal entropy $S = \log(d)$, where d is the dimension of the finite-dimensional Hilbert space. We now move on to discuss entanglement in continuous QFTs.

3.1.2. Entanglement in Quantum Field Theory

So far our discussion has been focused on a simple quantum mechanical example to introduce relevant aspects in conceptually simple terms. We now generalize the discussion to QFTs as we are ultimately interested in entanglement in AdS/CFT. In principle, the concepts introduced in the previous section apply to CFTs as well. Consider a constant time slice in a two-dimensional CFT on the cylinder in the vacuum. The constant time slice is simply a circle. This circle may be split into two subsystems A and B by choosing an interval $[u, v]$ on the circle to describe the subsystem A; the complement of A defines the subregion B. Since we defined the composite system AB on a constant timeslice of a CFT in the vacuum, the system AB is in state $|0\rangle$ with density matrix $\rho_{AB} = |0\rangle\langle 0|$. The reduced density matrix ρ_A follows by tracing out the degrees of freedom in region B, which is the complement of the interval $[u, v]$. While conceptually there is no difference in how the entanglement entropy and reduced density matrices are defined in quantum mechanics and QFT, explicit computations are extremely challenging in the latter. In quantum mechanics, the entanglement entropy is most easily calculated by determining the eigenvalues of the reduced density matrix, called the entanglement spectrum, since the Hilbert space is finite dimensional. On the other hand, in QFT the state of the system is described via a path integral by a wave function on a constant timeslice, and ρ_A is a continuum operator. This introduces many technical challenges in the computation of the entanglement entropy. See also [165] for a discussion. Of particular relevance in this thesis is the modular operator $K = K_A - K_{\bar{A}}$, which is formally defined in terms of the reduced density matrix ρ_A associate to a subregion A,

$$K_A = -\frac{1}{2\pi} \log(\rho_A), \tag{3.1.3}$$

and similarly for the complement $\bar{A}$ of the subregion A. The modular operator generates a generalized time evolution with respect to the modular time s with the unitary $U(s) = \rho^{is} = e^{-2\pi i s K}$. We will begin by first considering entanglement in the vacuum state in $(1+1)$-dimensional Minkowski space and derive the reduced density matrix and the associated modular operator. As we will see, the modular operator (3.1.3) has a straightforward interpretation in this case. The known modular operators and their associated charge, the modular Hamiltonian, that act locally in holographic two-dimensional CFTs then all follow from the modular Hamiltonian in $(1+1)$-dimensional Minkowski space [166]. Finally, we will briefly discuss how to calculate the entanglement entropy in QFTs using the replica trick [167].

Entanglement of the vacuum in (1+1)-dimensional Minkowski space and the modular Hamiltonian for a half-space

We derive the modular Hamiltonian for a half-space in $(1+1)$-dimensional Minkowski space based on [168, 169]. The vacuum state of a relativistic QFT is entangled. In particular, the vacuum state is so highly entangled that by acting with an operator $\mathcal{O}$ in a subregion A, we create a set of states that is dense in the Hilbert space. This is the Reeh-Schlieder theorem [170]. Figuratively speaking, due to entanglement, we can act with an operator here on earth and create the moon. This statement sounds intuitively wrong and there is a caveat. The operator $\mathcal{O}$ is not unitary and is therefore not an observable. A rather simple example to illustrate entanglement of the vacuum state that we will make repeated use of in sec. 5.4.1 is $(1+1)$-dimensional Minkowski space. We label the Minkowski coordinates by $\vec{x} = (t, x)$. The metric in these coordinates is given by

$$ds^2 = -dt^2 + dx^2. \tag{3.1.4}$$

We choose the $t = 0$ slice as the Cauchy surface on which we define initial values for fields and denote the vacuum state of a QFT by $|\Omega\rangle$. Given fields ϕ, a wave functional is obtained from the path integral

$$\Omega(\phi(x)) = \langle\Omega|\phi(x)\rangle = \int_{\phi(t=-\infty,x)=0}^{\phi(t=0,x)=\phi(x)} \mathcal{D}\phi\, e^{-S_E}, \tag{3.1.5}$$

where S_E is the Euclidean action with Euclidean time t_E obtained from the Wick rotation $t \to -it_E$. In Euclidean signature, the $(1+1)$-dimensional Minkowski space (3.1.4) is then given by the Euclidean plane $\mathbb{R}^2$. Our aim is to find the reduced density matrix ρ_R for the region $x > 0$. To this end we factorize the Hilbert space $\mathcal{H} = \mathcal{H}_L \otimes \mathcal{H}_R$, where $\mathcal{H}_L$ is acted on by fields ϕ_L with support only in $x < 0$ and $\mathcal{H}_R$ by fields ϕ_R with support only in $x > 0$. This is shown in fig. 3.1a. The density matrix ρ_R for the region $x > 0$ is obtained from

$$\rho_R(\phi'_R, \phi_R) = \mathrm{tr}_{\mathcal{H}_L} |\Omega\rangle\langle\Omega|, \tag{3.1.6}$$

where $|\Omega\rangle\langle\Omega|$ is given in terms of

$$\begin{aligned} |\Omega(\phi_L, \phi_R)\rangle &= \int \mathcal{D}\phi_L \mathcal{D}\phi_R \, \langle\phi_L, \phi_R|\Omega\rangle |\phi_L\phi_R\rangle, \\ \langle\Omega(\phi'_L, \phi'_R)| &= \int \mathcal{D}\phi'_L \mathcal{D}\phi'_R \, \langle\Omega|\phi'_L, \phi'_R\rangle \langle\phi'_L\phi'_R|. \end{aligned} \tag{3.1.7}$$

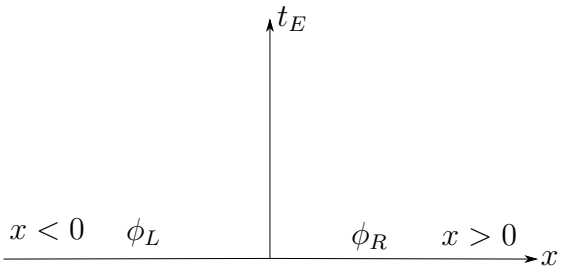

(a) We factorize the Hilbert space by defining fields ϕ_L that have support only in $x < 0$ and ϕ_R with support only in $x > 0$.

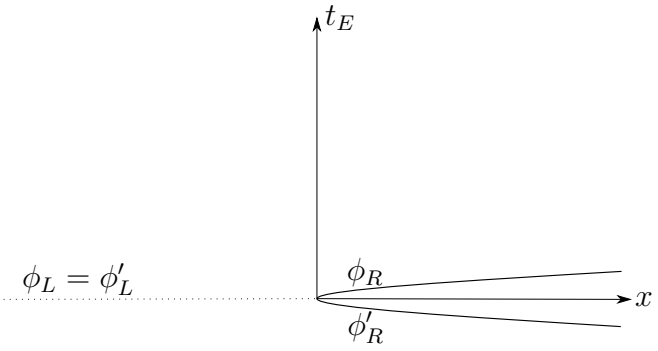

(b) The reduced density matrix ρ_R for the subregion $x > 0$ is obtained by first gluing surfaces on which ϕ_L and ϕ'_L are defined by setting $\phi_L = \phi'_L$ and integrating over ϕ_L.

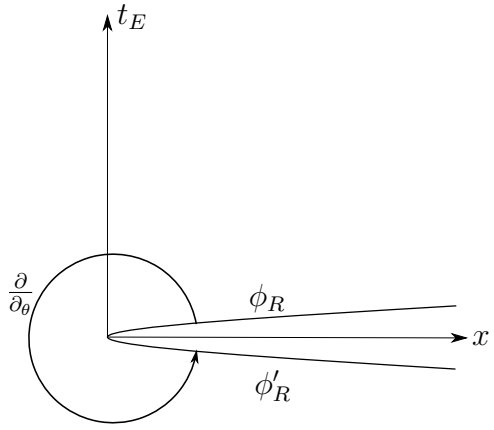

(c) The surfaces on which ϕ_R and ϕ'_R are defined are related by a 2π rotation on the Euclidean plane.

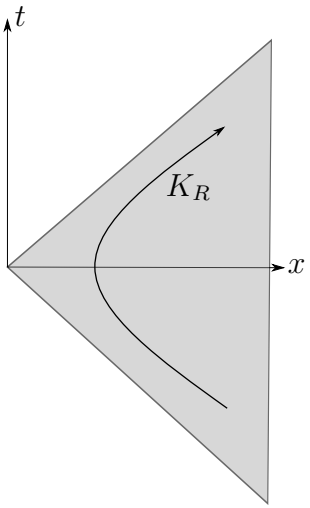

(d) The modular operator K_R is the Rindler boost in the right Rindler wedge shaded in gray. The accelerated observer moving along the boost orbit perceives the Rindler temperature $T = \frac{1}{2\pi}$.

Fig. 3.1.: Constructing the modular operator for a QFT in two-dimensional Minkowski space.

The trace over $\mathcal{H}_L$ in (3.1.6) is performed by first gluing ϕ_L and ϕ'_L surfaces, i.e. setting $\phi'_L = \phi_L$, and integrating over ϕ_L,

$$\rho_R(\phi'_R, \phi_R) = \int \mathcal{D}\phi_L \, |\Omega(\phi_L, \phi'_R)\rangle\langle\Omega(\phi_L, \phi_R)|. \tag{3.1.8}$$

The space on which we perform the path integral is depicted in fig. 3.1c. The path integral may also be interpreted as computing the matrix elements of an operator

between an initial state defined on the lower surface and a final state defined on the upper surface. The surfaces are related by a rotation with angle $\theta = 2\pi$ in the $t_E - x$-plane. The Euclidean rotation is generated by the operator $\partial_\theta = t_E\partial_x - x\partial_{t_E}$. Then, (3.1.8) may be written as

$$\rho_R = \int \mathcal{D}\phi'_R \mathcal{D}\phi_R \, \langle\phi_R|e^{2\pi\partial_\theta}|\phi'_R\rangle|\phi_R\rangle\langle\phi'_R| = e^{-2\pi K_R}, \tag{3.1.9}$$

where we set $-\partial_\theta = K_R$. In Lorentzian signature K_R is given by $K_R = -it\partial_x + ix\partial_t$, which is the generator of Lorentz boosts. Comparing with (3.1.3), we see that the modular operator for the half space $x > 0$ is just the boost operator. This result was first derived in [171]. In particular, the modular operator has a very nice physical interpretation: K_R is the generator of Rindler boosts in the right Rindler wedge as shown in fig. 3.1d and generates time evolution in the Rindler time. Therefore, the modular time in this example is the Rindler time. The Rindler boost generates the orbits of an observer with constant acceleration in Minkowski space. The accelerated observer perceives the Rindler horizon at $x = t$ and observes the Rindler temperature $T = \frac{1}{2\pi}$ through a process analogous to Hawking radiation of a black hole [172]. Thus, the Rindler temperature is an analog of the Hawking temperature of a black hole. A similar Rindler boost with opposite direction may be obtained in the left Rindler wedge $x < 0$ such that the full modular operator is given by

$$K = K_R - K_L. \tag{3.1.10}$$

The modular Hamiltonian, which is the conserved charge associated to the Rindler boost K_A is an integral of a weighted energy-momentum tensor over the initial value surface $x > 0$ at $t = 0$ [168],

$$H_{\text{mod},A} = \int_{t=0,x>0} dx\, xT_{tt}. \tag{3.1.11}$$

Note that in the literature, both the modular boost operator K as well as the conserved charge H_{mod} are commonly referred to as modular Hamiltonian. In this thesis, it is important to distinguish these operators. Therefore, we will only call the charge H_{mod} modular Hamiltonian and will refer to K as the modular operator. In general, it is extraordinarily difficult to find the modular Hamiltonian for a given theory and entangling surface. In two-dimensional CFTs, there are only a handful of known cases discussed in [166] for which its explicit form is known and its action is local. For all of these cases the modular Hamiltonian may be obtained via mappings from the Rindler

modular Hamiltonian. We will come back to this in sec. 5.4, where the modular Hamiltonian will feature extensively. While the modular Hamiltonian is often very hard to obtain, the reduced density matrix may generally be obtained following the procedure described here[1].

Entanglement entropy in QFT

From the reduced density matrix, we may then calculate the entanglement entropy. We will be rather brief since the technicalities are not relevant in this thesis. For a thorough discussion we refer to [165, 173]. To facilitate the calculation, the replica trick [167] is employed. Rather than finding the entanglement entropy directly, it is much more practical to compute the Renyi entropies,

$$S^{(q)} = \frac{1}{1-q} \log(\mathrm{tr}_A \rho_A^q). \tag{3.1.12}$$

Therefore, instead of obtaining $\log(\rho_A)$ directly, $\mathrm{tr}_A \rho_A^q$ with $q \in \mathbb{Z}_+$ is calculated first. This amounts to creating q copies of the system, hence the name replica trick. By identifying the entanglement interval endpoints in these q copies with twisted boundary conditions, a new manifold – the q-fold branch cover of the initial manifold – is created. On this new manifold, $\mathrm{tr}_A \rho_A^q$ is then evaluated. Upon analytic continuation of q to $q \in \mathbb{R}_+$, the entanglement entropy (3.1.1) is recovered in the limit $q \to 1$,

$$S = \lim_{q \to 1} S^{(q)}. \tag{3.1.13}$$

With this method, the entanglement entropy for an interval $[u, v]$ on a constant time slice in a two-dimensional CFT was evaluated in [167]. The result reads

$$S = \frac{c}{3} \log \frac{v-u}{\epsilon}. \tag{3.1.14}$$

The entanglement entropy (3.1.14) is universal for two-dimensional CFTs. Furthermore, it shows a UV divergence in the limit $\epsilon \to 0$ that is characteristic of any QFT. Therefore, when calculating the entanglement entropy for QFTs, a regulator ϵ has to be introduced. The UV divergence arises for the following reason: Upon considering two subsystems A and B, we assume that the QFT Hilbert space factorizes, $\mathcal{H} = \mathcal{H}_A \otimes \mathcal{H}_B$. However, this is not true in QFTs as there always are correlations between operators in the subregions due to entanglement. For this reason, the UV divergence in QFTs

[1] For this reason, the identification (3.1.3) is formal.

is universal[2].

While the replica trick provides a useful tool for calculating entanglement entropies in CFTs, the calculation is still fairly involved. However, as is often the case in AdS/CFT, calculations that are extremely challenging on one side of the duality become very simple in the dual theory. This is also the case for the entanglement entropy as we demonstrate in the next section.

3.1.3. Holographic Entanglement Entropy

In this section, we discuss the holographic dual of entanglement entropy in the CFT, which presents a prime example of the geometrization of quantum information and in particular the emergence of spacetime in AdS/CFT. A first hint that entropy manifests itself as a geometric quantity is given by the Bekenstein-Hawking thermal entropy of a black hole [29], which scales with the area of the black hole horizon as given in (2.2.14). It was conjectured in [41] and later derived in [174] that a similar geometric relation holds for the holographic dual of the entanglement entropy (3.1.1) for a subregion in the CFT. Consider a subregion A in a d-dimensional CFT. The holographic dual of the entanglement entropy S_A is given by the area of the minimal $(d-1)$-dimensional surface γ_A anchored in subregion A on the boundary [42, 175, 176],

$$S_A = \frac{\text{Area}(\gamma_A)}{4G_N}. \tag{3.1.15}$$

The minimal surface γ_A is called the Ryu-Takayanagi surface and is depicted in fig. 3.2a. For a holographic two-dimensional CFT, we should then be able to obtain (3.1.14) from the gravity theory employing (3.1.15). Since we considered an interval $[u, v]$ on a constant timeslice in a vacuum CFT, the holographic entanglement entropy can be obtained from the dual three-dimensional geometry. Following the discussion in sec. 2.3.3, the dual geometry is empty AdS_3. In three dimensions, the appropriate minimal codimension-two surface γ_A reduces to a geodesic. The holographic dual of the entanglement entropy S_A is then simply given in terms of the shortest geodesic in AdS_3 with endpoints $[u, v]$ in the CFT. This is visualized in fig. 3.2b. When calculating the length of the minimal geodesic, a UV cutoff is necessary since the CFT boundary is an infinite distance away from the bulk point of view. This UV cutoff can be identified with the UV cutoff in the field theory calculation. Upon identifying

[2] The origin of the UV divergence is not a property of states but rather a property of the algebra. Quantum mechanics is described by a profoundly different type of algebra than QFTs. In fact, the UV divergence is already build into the algebra in QFTs. For a more detailed discussion of the origin of the UV divergence, we refer to [168].

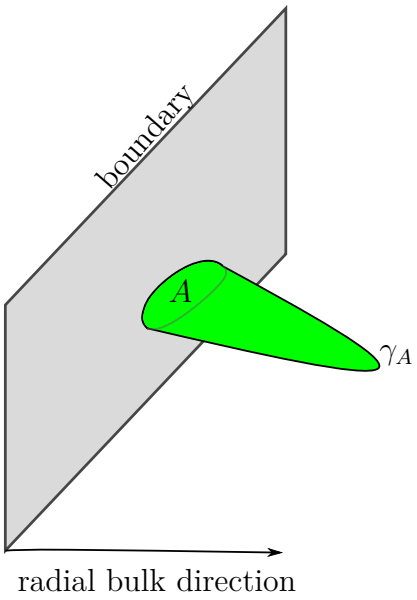

(a) The holographic entanglement entropy is given in terms of the area of the minimal codimension-two surface γ_A homologous to the boundary subregion A.

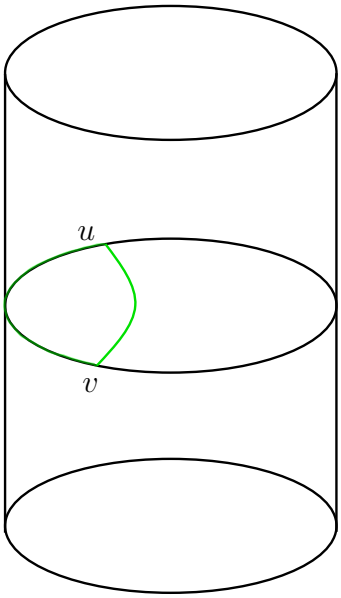

(b) In AdS_3, the codimension-two surface is a geodesic, and the length of the geodesic yields the holographic entanglement entropy for the boundary interval $[u, v]$.

Fig. 3.2.: Ryu-Takayanagi surfaces for holographic entanglement entropies.

$c = \frac{3}{2G_N}$, the holographic entanglement entropy reads [41]

$$S = \frac{c}{3} \log \frac{v-u}{\epsilon}. \tag{3.1.16}$$

This results matches (3.1.14), as expected. Appropriate covariant generalizations of (3.1.15) necessary to perform calculations in time-dependent backgrounds were presented in [176].

Finally, let us stress again that (3.1.15) shows that entanglement in the CFT manifests itself in the geometry of the bulk spacetime: Calculating the entanglement entropy associated to a subregion in the CFT corresponds to finding the area of a particular codimension-two subregion in the bulk. Therefore, in principle the bulk may be reconstructed simply from the knowledge of entanglement in the CFT[3] and causality constraints in the bulk [177–179]. These notions of bulk reconstruction were refined in a series of papers under the common theme entanglement-wedge reconstruction [46, 52–59]. Given a boundary subregion, the field theory information such as operators contained within this subregion are encoded in the entanglement wedge in the bulk, the domain of dependence of the Ryu-Takayanagi surface, and precise tools

[3] We will later see in sec. 3.3 that entanglement is not sufficient to reconstruct the full bulk spacetime in topologically non-trivial spacetimes.

were developed to reconstruct dual operators. Furthermore, the bulk information is stored redundantly in the CFT and can be retrieved with methods from quantum error correction [60–62], which are based on entanglement. There is a deep interplay between quantum information and geometry. In some sense, entanglement gives rise to spacetime itself as we will see in the next section.

3.2. Emergence of Spacetime from Entanglement: ER=EPR

In this section, we introduce the ER=EPR proposal for the eternal AdS black hole which forms the basis for many developments regarding entanglement and complexity in AdS/CFT, including the results of this thesis.

One of the fundamentally new ideas that arose from the AdS/CFT correspondence is that spacetime is emergent from quantum information. At the center of this proposal is the holographic entanglement entropy (3.1.15) which suggests that geometry and entanglement are intricately linked. The idea of an emergent spacetime from entanglement was first advocated in [47] on a simple toy model. Since the idea in [47] is not special to two-dimensional CFTs, we consider a d-dimensional CFT on the sphere S^d as the boundary. Then, the interior of the sphere represents the dual bulk geometry. Upon dividing the CFT into two subregions A and B, the entanglement entropy between those two subregions is holographically given by (3.1.15). Therefore, the entanglement is given by the area of the codimension-two surface anchored at the boundary at the entanglement cut that splits S^d into regions A and B. Next, we assume that the amount of entanglement decreases between regions A and B. Then, the area of the surface measuring the entanglement entropy in (3.1.15) decreases and the subregions A and B are pinched off. This is shown in fig. 1.1. In particular, if there is no entanglement between A and B, the surface measuring the entanglement entropy has vanishing area. This implies regions A and regions B become completely separated. The single boundary sphere S^d with a single bulk dual now becomes two boundary spheres with two disconnected bulk geometries. Hence, entanglement gives rise to spacetime itself. This idea can be made much more concrete on the example of the eternal AdS black hole. Let us therefore now introduce the holographic dual to the eternal AdS black hole, which forms the basis of the ER=EPR proposal [48] that we discuss afterwards.

The maximally entangled TFD state as the holographic dual to the eternal AdS black hole

This discussion is based on the original work [49] and the introduction [180]. According to our discussion in sec. 2.2, the eternal AdS black hole has two asymptotic boundaries and must therefore be dual to two CFTs, one on the left and one on the right boundary. We consider the $t = 0$ slice in the eternal AdS black hole geometry. Then, the dual CFT state is obtained as follows. At the $t = 0$ time slice, the black hole is described by the Hartle-Hawking state [181], which presents an initial condition for the time evolution of the black hole. We therefore want to construct a CFT state dual to the Hartle-Hawking state. In both the CFT and the bulk geometry, the future development is then given by time evolution. At the selected timeslice, each of the two CFTs lives on a space with the topology of a cylinder $\mathbb{R} \times S^1$ with a non-compact time direction and a compact spatial direction. The holographic dictionary implies that the gravitational path integral in the black hole geometry $\mathcal{M}$ with appropriate boundary conditions $\partial\mathcal{M} = \Sigma$ for the geometry of the boundary and the CFT path integral evaluated on the same boundary geometry must give the same result, $Z_{\text{grav}}[\partial\mathcal{M} = \Sigma] = Z_{\text{bdry}}[\Sigma]$. In the Euclidean signature, time is compact $t_E \sim t_E + \beta$, which is necessary to evaluate the path integral. The appropriate geometry is then $\Sigma = I_{\beta/2} \times S^1$ since it is half the Euclidean time circle $I_{\beta/2}$ that connects the boundary angular circles S^1 at the fixed time $t = 0$. The path integral then yields that the state dual to the eternal AdS black hole at $t = 0$ is the thermofield double (TFD) state [49],

$$|\text{TFD}\rangle = \frac{1}{\sqrt{Z}} \sum_n e^{-\beta \frac{E_n}{2}} |E_n\rangle_L |E_n\rangle_R \quad \text{with} \quad Z = \sum_n e^{-\beta E_n}, \tag{3.2.1}$$

where $|E_n\rangle_{L/R}$ are the energy eigenstates in the left and right CFT, respectively. The state is pure and maximally entangled, indicating that the eternal AdS black hole is dual to two maximally entangled CFTs. The TFD state (3.2.1) may be viewed as an initial condition for time evolution. The Lorentzian eternal AdS black hole at a later time t is then dual to the time-evolved TFD state. Non-trivial time-evolution is achieved with the Hamiltonian $H_L + H_R$, where $H_{L/R}$ is the Hamiltonian for the CFT on the left and right boundary, respectively. Note that evolution with the Hamiltonian $H_L - H_R$ is a symmetry of the system since time runs in opposite directions in the exterior regions of the eternal AdS black hole. Furthermore, upon tracing out one of the CFTs, we obtain the thermal density matrix of a single CFT,

$$\text{tr}_L(|\text{TFD}\rangle\langle\text{TFD}|) = \sum_n e^{-\beta E_n} |E_n\rangle_R \langle E_n|_R = \rho_T. \tag{3.2.2}$$

Holographically, tracing out the left CFT corresponds to removing the left side of the eternal AdS black hole. What remains is a single-sided AdS black hole, which is described by the thermal density matrix ρ_T [182] and thermal entropy given by the Bekenstein-Hawking entropy (2.2.14). The TFD state is then a purification of the single-boundary thermal system described by a mixed state with density matrix ρ_T. This purification is obtained by doubling the system and gives rise to the name TFD state. The idea of purifying the state in this manner was first proposed in [183] long before the AdS/CFT correspondence was conjectured.

ER=EPR

We now introduce the ER=EPR conjecture based on the original papers [47, 48]. The thermofield double state (3.2.1) is a maximally entangled state similar to the EPR pair (3.1.2) in the two-spin system in the sense that it may be viewed as a generalization of the two-spin EPR pair, where entanglement now is between two CFTs with n states $|E_n\rangle_{L/R}$. The entanglement generates correlations between the left and right CFTs even though there is no classical interaction between them: If we were to write down a Lagrangian for both CFTs, we would obtain two separate Lagrangians with no coupling between them because the CFTs are causally disconnected by the black hole horizon. An observer in the left CFT thus does not see an observer in the right CFT. Similarly, a bulk observer in the left exterior region of the black hole cannot communicate with an observer in the right exterior region. Nevertheless, the geometry of the eternal AdS black hole is a classically connected geometry, and correlation functions between operators in the left and right CFT are given in terms of geodesics connecting both boundaries through the black hole interior [51]. Based on these observations, it has been proposed that a useful way to think about the geometry of the eternal AdS black hole is to interpret it as two black holes, each living in their own spacetime with an asymptotic boundary, where the asymptotic regions are connected by a wormhole. Wormholes are solutions to Einstein gravity first discussed in [184] that connect two spacetime regions and are sometimes called ER bridges after the authors Einstein and Rosen. In particular, it is the entanglement between the CFTs in the left and right boundary that gives rise to the connected geometry formed by the wormhole. The notion that entanglement gives rise to a connected spacetime via wormholes is often referred to as ER=EPR, which is a short notation to indicate the holographic duality between the maximally entangled TFD state, the CFT generalization of the EPR pair (3.1.2), and the eternal AdS black hole. It is a concrete realization of the notion that spacetime is emergent from entanglement as proposed in [47]. A simple check that

without entanglement, there is no wormhole can be achieved by considering a product state in the CFT. To be concrete, we consider two CFTs, each in a vacuum state. According to our discussion in sec. 3.1.1, we may write the state of the full system as a product state between left and right CFT, $|0\rangle_L \otimes |0\rangle_R$, if there is no entanglement between the CFTs. Each of the vacuum states is dual to empty AdS. Therefore, the product state is dual to two empty AdS spaces. In contrast to the eternal AdS black hole, these do not form a single connected geometry.

Let us conclude by noting that there is evidence that ER=EPR applies to entanglement in general also outside holography. Concrete realizations of wormholes arising from entanglement in simple quantum systems without holographic duals were discussed in [185]. In contrast to the spacetime wormholes present if there is an actual bulk geometry, the wormholes in more general systems are purely topological. We will comment on this in more detail in sec. 5.

3.3. Entanglement is Not Enough: Holographic Computational Complexity

In this section, we introduce holographic complexity, one of the central topic of this thesis. As we discussed in sec. 3.1.3, the idea that entanglement gives rise to the bulk geometry was the foundation for many fruitful attempts to reconstruct the bulk geometry only from the entanglement structure of the dual CFT. However, in a series of papers [43, 71, 72], it became clear that entanglement is not sufficient to reconstruct the full bulk geometry. The fundamental obstruction is that the entanglement entropy (3.1.15) is given in terms of the *minimal* surface anchored in the boundary. In static geometries, these minimal surfaces are sufficient to reach every point in the dual AdS bulk spacetime in topologically simple spacetimes such as empty AdS [144, 186]. However, for the conical defect or the BTZ black hole, it was shown that there are entanglement shadows [43, 71] that cannot be probed with minimal surfaces. The reason is that the entanglement entropy exhibits phase transitions. Since the Ryu-Takayanagi surface is a minimal surface, it exhibits a transition from one surface to another if a certain system-dependent interval size is exceeded. This is shown on the example of the single-sided BTZ black hole in fig. 3.3. In contrast to the eternal black hole, the single-sided black hole has only one exterior region. As we now discuss, the entanglement entropy also exhibits a transition in the eternal AdS black hole geometry.

In [50], it was attempted to probe the interior of the eternal AdS black hole using

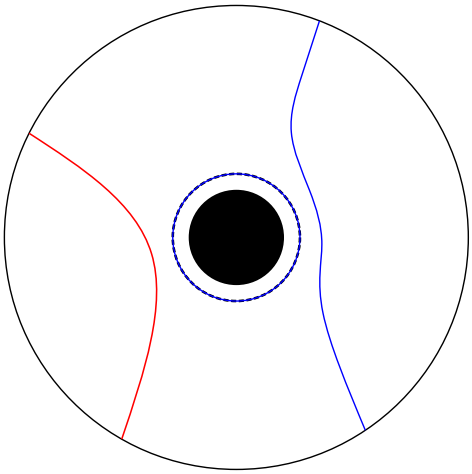

Fig. 3.3.: The Ryu-Takayanagi geodesics on a constant time slice in the single-sided BTZ black hole geometry for two different intervals: The red geodesic encloses a small interval. When the interval is increased to the endpoint of the blue configuration, the geodesic transitions to two disconnected geodesics, one for the smaller complement of the interval and one horizon-wrapping geodesic. The entanglement shadow is shown as the dotted line.

Ryu-Takayanagi surfaces. Since as discussed in sec. 3.2, the eternal AdS black hole is invariant under $H_L - H_R$, an explicit time dependence can be introduced by evolving with $H_L + H_R$. In the dual CFT, we then obtain a time-dependent TFD state $|\mathrm{TFD}(t_L, t_R)\rangle$. Upon choosing an interval on a constant time slice $t = t_L = t_R$ in the left and right CFTs, it is possible to calculate the entanglement entropy between both causally separated CFTs. The minimal Ryu-Takayanagi surface yielding the holographic entanglement entropy (3.1.15) between the CFTs is anchored in the constant time slice in the left and right CFT and goes through the wormhole. Therefore, upon evolving the entanglement entropy with time, its value should change with the size of the wormhole. Initially, the entanglement entropy grows linearly with time [50],

$$S_A^{(1)} = \frac{4\pi c}{3\beta} t + 4S_{\mathrm{div}}, \tag{3.3.1}$$

indicating a linear growth of the wormhole. Here, S_{div} denotes the UV-divergent contribution to the entanglement entropy. However, after the thermalization time t_*, the entanglement entropy stops to grow [50] and remains at a constant value. The wormhole, however, is expected to continue to grow. Similar to the entanglement shadows discussed before, the minimal surface yielding the entanglement entropy (3.3.1) transitions to two new minimal surfaces once the wormhole is so large that the area of the minimal surface becomes smaller if the minimal surface connects endpoints at the same

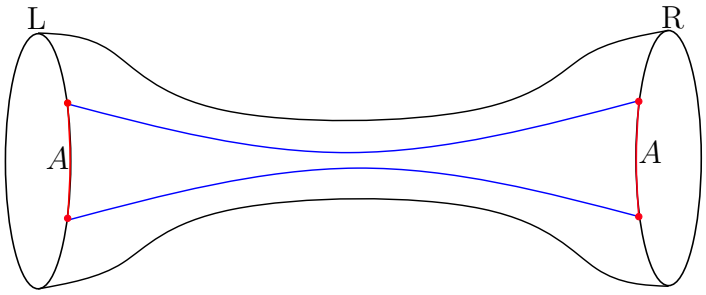

(a) Before the thermalization time, the Ryu-Takayanagi surfaces (blue) probe the growth of the wormhole.

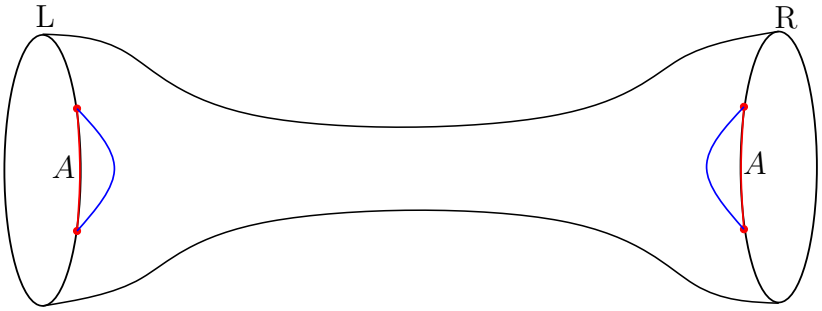

(b) When the thermalization time has passed, the Ryu-Takayanagi surfaces yielding the holographic entanglement entropy (blue) sit outside the wormhole and no longer probe the growth of the wormhole.

Fig. 3.4.: Transition between two minimal Ryu-Takayanagi surfaces (blue) yielding the holographic entanglement entropy for subregions A (red) in the left (L) and right (R) boundaries in the presence of a wormhole. The wormhole continuous to grow, but the growth can no longer be probed by the minimal Ryu-Takayanagi surfaces after the thermalization time.

boundary rather than at different boundaries. This is visualized in fig. 3.4. However, such a configuration does not probe the wormhole and therefore fails to capture the growth after the transition at the thermalization time t_*.

It is then apparent that the entanglement entropy in the CFT is not able to capture the linear growth of the wormhole after the thermalization time. The very principles of AdS/CFT, however, require that there is a CFT quantity that describes the wormhole at later times. Based on very fundamental considerations, the computational complexity of the dual CFT state has been proposed as a viable candidate. Let us review these considerations presented in [74, 80].

We assume that Alice is located in the left boundary. Bob is in the right exterior region and will at some point cross the black hole horizon. Alice now creates a perturbation $\mathcal{O}$ in the left CFT. As time evolves with $U = e^{i(H_L+H_R)t}$, the perturbation will grow according to $U\mathcal{O}U^\dagger$. Therefore, the perturbation and thus the operator $\mathcal{O}$ will become more complex. The growth of the complexity of this operator was first

linked to the size of the wormhole in [74]. How can we understand this growth of complexity? A useful model to describe black hole dynamics has been proposed in [151, 187–189]. Black hole dynamics can be sufficiently captured by a quantum computer with n qubits that scrambles (randomizes) infalling states very effectively. In particular, black holes implement unitary random quantum circuits. The quantum circuit consists of a sequence of unitary transformations that turn an initial pure state into a random state. This scrambling occurs at the scrambling time $t_{\text{scr}} \sim \log S$ [152], which is equal to the thermalization time t_* of the CFT. The black hole implements this quantum circuit in such a way that the transformations, called gates, act on no more that two qubits at a time. For a black hole with n qubits, this implies $\frac{n}{2}$ gates act in parallel. How does the perturbation $\mathcal{O}$ then spread through the wormhole? We assume that the perturbation $\mathcal{O}$ is initially localized to a single qubit. Then, the black hole implements $\frac{n}{2}$ parallel transformations U. After n layers of such parallel operations, $\mathcal{O}$ will have acted on every of the n qubits of the quantum computer. This happens precisely at the scrambling time. If we count the complexity of the operator as the number of such layers necessary, then $\mathcal{C}_{scr} = \log(n) = \log(S)$. But this is not the maximal complexity of the operator. Any unitary transformation can be approximated by an exponential number of gates. Therefore, $\mathcal{C}_{max} \sim e^n$. In contrast to the growth of the entanglement entropy, the complexity growth then does not stop at the scrambling time. Furthermore, since the black hole is modeled such that it implements a layer at every time step, the complexity satisfies $\mathcal{C} \propto t$ which agrees with the expected linear growth of the wormhole with time. We now make these statements precise. First of all, from the CFT point of view, the operator $\mathcal{O}$ is somewhat arbitrary. The eternal black hole is dual to the TFD state. So let us instead associate the complexity of the state under time evolution to the number of layers needed to implement the time evolution. This implies we aim to quantify the number of layers necessary to implement $U = e^{i(H_L+H_R)t}$ in order to obtain the time-evolved TFD state $|\text{TFD}(t_L, t_R)\rangle = e^{i(H_L+H_R)t}|\text{TFD}\rangle$. Then, all of the previous considerations still apply. In particular, it was argued in [80] that

$$\mathcal{C} = S|t_L + t_R|, \tag{3.3.2}$$

where the entropy S is given by the number of qubits n. After the initial linear growth, the growth stops at $t \sim e^S$ at which $\mathcal{C}_{\text{max}}$ is reached and stays constant until the quantum recurrence time $t \sim e^{e^S}$ after which $U \sim 1$ and the complexity reaches zero again.

Furthermore, the spread of a perturbation may also be associated to the evolution

of the state under

$$|\psi\rangle = U^\dagger \mathcal{O} U |\mathrm{TFD}\rangle. \tag{3.3.3}$$

We choose the operator $\mathcal{O}$ such that it only yields a small change in the state in a sense that we obtain a new state orthogonal to the original one but in which very few degrees of freedom were changed. As an illustrative example consider a spin chain, where we may apply a single Pauli operator σ_x on the n-th qubit in an n qubit state. Then, we only changed a single degree of freedom, but the new state is orthogonal to the original one. For such operators $\mathcal{O}$, it is natural to expect that the time evolution in $U^\dagger(t)\mathcal{O}U(t)$ still approximately cancels. This is not true, however, in chaotic systems such as black holes. After a small amount of time, the new state will be completely different from the old one. It is simplest to think of this in terms of an infection model [190]: When $\mathcal{O}$ acts, it first acts (i.e. infects) a single qubit. Since in a chaotic system, the infected qubit interacts with many other qubits, the infection – the size of $\mathcal{O}(t)$ measured by the norm of the commutator – will spread exponentially fast. If we now want to measure the complexity of the state obtained from acting with $\mathcal{O}(t) = U^\dagger(t)\mathcal{O}U(t)$ on the initial state, then we observe the switchback effect [80, 190]: The transformation $U^\dagger(t)\mathcal{O}U(t)$ does not effect most qubits shortly after it has acted on a single qubit since most qubits have not yet been transformed. Therefore, for these qubits, the action of $U(t)$ and $U^\dagger(t)$ cancels and does not contribute to the complexity. It takes until the scrambling time $t^* \propto \log S$ [73, 74] for the complexity to grow. This same behavior has been observed upon sending a shockwave into the black hole in [80]. Therefore, the action of the operator $\mathcal{O}$ may be thought of as sending a shockwave through the wormhole, which is the signal Bob receives when Alice sends her message from the left boundary.

To summarize, the linear growth of the complexity with time made it a prime candidate to study the linear growth of the black hole interior. Then, the logical next step is to find suitable observables in the gravity theory that probe the linear growth. Codimension-two surfaces such as the Ryu-Takayanagi surface were ruled out as a good candidate [50, 73]. There are only two conditions that this new bulk observable has to satisfy: It must be able to probe the linear growth in the black hole interior, and it must be sensitive to the switchback effect. These conditions are very general and led to a wide range of holographic complexity proposals that identify candidate bulk observables. These holographic complexity proposals use codimension-one or codimension-zero surfaces to probe the black hole interior. We give an overview.

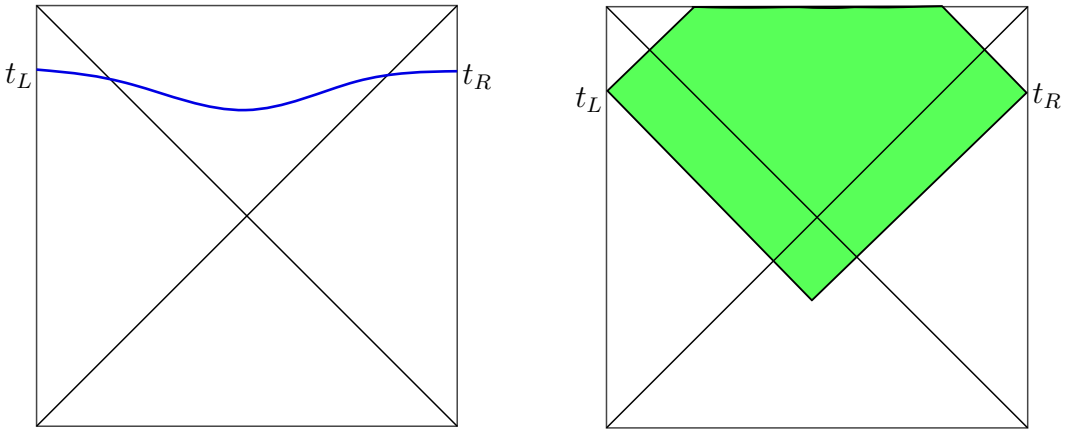

(a) In the CV proposal, the complexity of the TFD state at times t_L and t_R in the left and right boundary is given in terms of the maximal volume slice (blue) anchored in the boundary at the given times.

(b) In the CA proposal, the complexity of the dual TFD state is given in terms of the gravitational action on the Wheeler-de Witt patch (green region).

Fig. 3.5.: The complexity=volume (CV) and complexity=action (CA) proposals

Complexity = Volume

The complexity = volume proposal, or short CV, was put forward in [74]. The black hole interior is probed by the maximal-volume slice $\mathcal{V}$, which is a codimension-one slice in the bulk region $\mathcal{B}$ with boundary $\partial\mathcal{B} = \Sigma$ on which the dual CFT state is defined. In particular, the maximal volume slice asymptotes to the Cauchy slice Σ at the times t_L and t_R in the left and right boundary. The holographic complexity is then given by

$$C_\Sigma = \frac{\mathcal{V}_{\partial\mathcal{B}=\Sigma}}{G_N \ell}. \tag{3.3.4}$$

The length ℓ is introduced to give the complexity the dimension of a number, and its choice is arbitrary. Often it is set to the radius of curvature of AdS. This introduces an arbitrariness to the complexity. As we will see in the next section, this is not a fault but a feature of complexity that we will also encounter in the field theory approach. The CV proposal is shown in fig. 3.5a.

Complexity = Action

The complexity = action (CA) proposal [81, 161] conjectures that the CFT state defined on the Cauchy slice Σ is dual to the gravitational action evaluated on the

Wheeler-de Witt (WdW) patch,

$$C_\Sigma = \frac{S_{\text{WdW}}}{\pi}. \tag{3.3.5}$$

The WdW patch is a causal bulk region bounded by in- and outgoing lightrays from the boundary Cauchy slice Σ. The CA proposal is illustrated in fig. 3.5b.

There also exists a combination of the CV and CA proposal, called CV 2.0 [82], that defines the complexity of the field theory state to be the volume of the WdW patch.

Complexity = Anything

It was observed in [83] and [84] that in principle an infinite number of bulk observables satisfy linear growth and the switchback effect. The holographic complexity proposals were dubbed complexity = anything and are defined on codimension-one or zero surfaces in the bulk. The bulk observables in [83] are given by

$$O_{F_1,\Sigma_{F_2}}(\Sigma_{\text{CFT}}) = \frac{1}{G_{\text{N}}}\int_{\Sigma_{F_2}} d^d\sigma\sqrt{h}F_1\left(g_{\mu\nu};X^\mu\right), \tag{3.3.6}$$

where F_1 is an arbitrary scalar function depending on the metric and embedding of a codimension-one surface Σ_{F_2}, and $\sqrt{h}$ is the induced metric on the surface. On the other hand, bulk observables in [84] are defined in terms of a scalar function G_2 on a codimension-zero surface $\mathcal{M}$ and functions $F_{2,\pm}$ on the bounding Σ_+ and Σ_- surfaces,

$$\begin{aligned} W_{G_2,F_{2,\pm}}(\mathcal{M}) = &\int_{\Sigma_+} d^d\sigma\sqrt{h}F_{2,+}\left(g_{\mu\nu};X^\mu_+\right) + \int_{\Sigma_-} d^d\sigma\sqrt{h}F_{2,-}\left(g_{\mu\nu};X^\mu_-\right) \\ &+ \frac{1}{L}\int_{\mathcal{M}} d^{d+1}x\sqrt{g}G_2\left(g_{\mu\nu}\right). \end{aligned} \tag{3.3.7}$$

Here, we have kept the radius of curvature L of AdS explicit. The bulk surfaces are shown in fig. 3.6. Finally, note that all of these proposals are conjectures. To check them, a notion of complexity in quantum field theory is necessary.

3.4. Quantum Circuits in QFT

In this section, we introduce the final ingredient for this thesis, which is a notion of complexity for a QFT state based on quantum circuits. As we discussed in the previous section, there are a vast number of holographic complexity proposals that relate the complexity of the time-evolved TFD state to a geometric object in the bulk theory that probes the growth of the wormhole. How then do we define the complexity

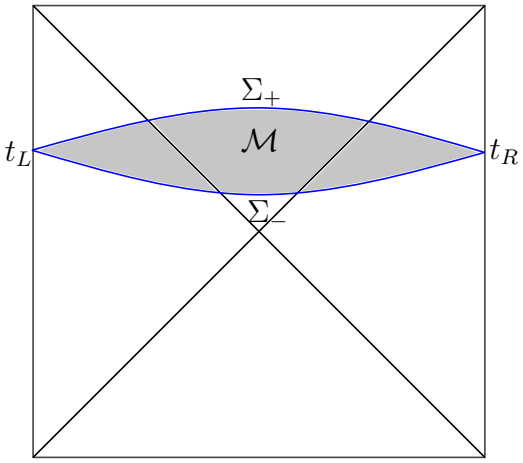

Fig. 3.6.: The complexity = anything proposal (3.3.7) is defined on a codimension-zero bulk slice $\mathcal{M}$ bounded by two surfaces $\Sigma_\pm$. The complexity of the TFD state at times t_L and t_R is given in terms of scalar functions defined on $\mathcal{M}$ and $\Sigma_\pm$.

of a field theory state? Complexity arises from a notion of computational cost, which is essential in information theory. It helps us determine the most computationally efficient way to implement an operation. In quantum information theory, the quantum computational cost assigns a number to the question how hard it is to create the desired target state from a simple reference state using only transformations from a predefined gate set [191, 192]. Therefore, we need three ingredients: a simple reference state, a set of unitary transformations called gates and a cost measure. The cost measure associates a computational cost to every gate we apply and the complexity is obtained by minimizing the cost over the possible gates that create the target state from the reference state. In particular, the sequence of transformations we apply constitutes a quantum circuit and is optimal once the cost is minimized. The three ingredients reference state, gate set, and cost measure present three choices we can make to obtain complexity. This immediately implies that the complexity is not a unique number but depends on all of these choices, which makes it hard to find the 'correct' definition of complexity implicitly used in the holographic complexity proposals in sec. 3.3. In quantum information theory, gates usually implement discrete transformations such that the target state is only reached within a certain tolerance. However, we aim to define complexity for a continuous CFT. It was proposed by Nielsen in [76, 77, 193] on the example of an n-qubit system that when the gate set is restricted to symmetry transformations of the system – for n-qubits this is $SU(2^n)$ – the continuity of symmetry groups can be exploited to recast the problem of finding the optimal circuit to one of finding geodesics. Given a reference state $|\psi_R\rangle$, we aim to generate

the target state $|\psi_T\rangle$ by applying the circuit U,

$$|\psi_T\rangle = U|\psi_R\rangle. \tag{3.4.1}$$

The circuit U is a unitary transformation composed of a sequence of transformations parameterized by the circuit parameter τ and is generated by a circuit Hamiltonian $Q(\tau)$,

$$U = \overleftarrow{\mathcal{P}} \exp\left[i \int d\tau\, Q(\tau)\right], \tag{3.4.2}$$

where $\overleftarrow{\mathcal{P}}$ denotes path ordering. Individual gates are then given by $U(\tau + d\tau) = e^{iQ(\tau)d\tau}U(\tau)$. If we restrict the gate set to symmetry transformations, the circuit Hamiltonian may be written in terms of the symmetry generators J_I of the symmetry group,

$$Q(\tau) = \sum_I V^I(\tau) J_I. \tag{3.4.3}$$

Here, $V^I(\tau)$ are gate velocities which specify at which time step τ in the quantum circuit a certain generator is applied and by how much. Finally, we need to assign computational cost C to the circuit U. This is achieved by choosing a cost function F that assigns cost to every transformation $U(\tau)$ along the circuit and then integrating over the circuit time necessary to reach the target state,

$$C = \int d\tau\, \mathcal{F}(U(\tau), v). \tag{3.4.4}$$

The cost function may depend on both $U(\tau)$ and the tangent vector along the circuit v. Furthermore, the following properties are expected of a reasonable cost function: It must be smooth and positive, and vanish if and only if $v = 0$. Furthermore, it must be positively homogeneous $\mathcal{F}(U, \lambda v) = \lambda \mathcal{F}(U, v)$ and must satisfy the triangle inequality in the second argument, $\mathcal{F}(U, v + v') \leq \mathcal{F}(U, v) + \mathcal{F}(U, v')$. These are the properties of a Finsler geometry [194], a generalized Riemann geometry, where the norm on the tangent space is not necessarily induced by a metric. Therefore, to optimize the circuit, we find the shortest geodesic in the Finsler geometry. The length of the geodesic is then equal to the complexity,

$$\mathcal{C} = \min C. \tag{3.4.5}$$

Possible choices for the cost function $\mathcal{F}$ proposed in [76, 77, 193] are the one- and two-norm,

$$\mathcal{F}_1(U, V) = \sum_I \left|V^I\right|, \qquad \mathcal{F}_2(U, V) = \sqrt{\sum_I (V^I)^2}. \tag{3.4.6}$$

The circuit approach to complexity presented here was first studied for free field theories in [78, 195–198]. In particular, the inhomogenous cost $\mathcal{F}_\kappa \equiv \sum_I \left|V^I(s)\right|^\kappa$ was shown to exhibit the same UV divergence as the CA and CV proposals in [195]. The agreement, however, is only qualitative. Furthermore, in [78, 79] state-dependent cost functions such as for instance $\mathcal{F} = \langle\psi(\tau)|Q(\tau)|\psi(\tau)\rangle$ were proposed. Building on the results of [79], [75] introduced the first notion of complexity in a two-dimensional CFT. In [75], gates are built from the energy-momentum tensor of the CFT to generate conformal transformations, and complexity is linked to geodesics in the Virasoro group manifold. This approach formed the basis for the works [86, 87, 122, 199], which examined the complexity and properties of various cost functions in a CFT. It emerged that in order to make contact with holographic complexity measures, the cost measure must be invariant under global symmetry transformations as these correspond to Killing symmetries in the bulk. Maps between CFT complexities for conformal transformations and the CV and CA proposals were achieved with limited success in [162, 200–203]. Complexity for CFTs in higher dimensions was introduced in [85], and generalizations to mixed states were studied in [204–207]. While the notion of circuit complexity is the focus of this thesis, alternative approaches such as path integral complexity and their dual prescriptions [111, 175, 208–217] as well as Krylov complexity [209, 218–225] are also pursued. For a comprehensive review we refer to [226].

Despite these advances, the holographic complexity proposals have not yet been verified. In fact, apart from [85] no precise map between a CFT cost function for a quantum circuit and a geometric object in the bulk has been achieved. We now present a general framework, which allows the derivation of such maps from first principles.

4 Holographic Quantum Circuits

Within the AdS/CFT correspondence, every bulk observable has a dual in the CFT which yields the same value. Matching observables represent corresponding entries in the holographic dictionary. Due to our limited understanding of the correspondence, especially beyond the semiclassical approximation, the entries in the holographic dictionary are far from complete. A prime example of a bulk observable lacking a precise CFT dual is holographic complexity. In sec. 3.3, we learned that there are in principle an infinite number of holographic complexity proposals that exhibit the switchback effect and linear growth. The CFT duals to these observables are generally unknown. Promising advances toward defining complexity in the CFT were made with the general framework of circuit complexity discussed in sec. 3.4, using only the CFT energy-momentum tensor in the circuit. However, it has so far been exceptionally hard to derive a map between complexity measures in the CFT and holographic complexity measures. Within circuit complexity this was achieved for the first time in [85], but the result is specific to the system and not straightforwardly generalizable. A major obstacle toward deriving such a map is the existence of an auxiliary circuit parameter in the CFT description of the quantum circuit that has no analog in the dual gravity theory. We show that this problem may be solved by identifying the auxiliary parameter with the physical time of the boundary CFT. This identification allows us to implement the quantum circuit as a non-trivial time evolution of the boundary CFT such that every time slice in the CFT corresponds to the appropriate state generated by the quantum circuit. We then draw on known entries in the holographic dictionary to derive the bulk spacetime dual to the time-evolving boundary CFT implementing the circuit. Therefore, we construct a bulk dual to a quantum circuit. This bulk dual presents a general framework that allows the derivation of maps between CFT cost functions and bulk observables from first principles for the first time. We demonstrate the power of this construction by deriving a holographic dual to the Fubini-Study distance cost function which is the metric on the projective Hilbert space of the CFT. In particular, we show that the dual bulk observable is a complicated geometric object given in terms of spacelike geodesics anchored in the boundary CFT. Our dual for the Fubini-Study distance is valid for general conformal transformations generated by the energy-momentum tensor of the CFT in the dual empty AdS, conical defect, and BTZ geometries.

We begin in sec. 4.1 by introducing CFT quantum circuits generated by the energy-momentum tensor and the Fubini-Study metric as a cost measure for the circuit. In sec. 4.2, we then elaborate how the circuit may be implemented as a time evolution of the boundary CFT and describe the construction of the dual spacetime geometry in the bulk. Furthermore, we discuss our construction for circuits built from global conformal transformations initially considered in [85] and highlight important differences to [85]. In sec. 4.3, we then derive the gravity dual to the Fubini-Study cost measure in the gravity dual to a quantum circuit we obtained in sec. 4.2. The new results presented in this chapter appeared in [1, 2].

4.1. Quantum Circuits in Two-dimensional CFTs

In this section, we introduce the quantum circuits and cost function for which we later derive holographic duals. Following the approach to quantum circuits based on symmetry transformations presented in sec. 3.4, we begin in sec. 4.1.1 by introducing quantum circuits in the CFT that are generated by the energy-momentum tensor. In sec. 4.1.2, we introduce the Fubini-Study distance function as the cost measure we choose to study. Since the Fubini-Study metric is the natural metric on the projective Hilbert space, the cost function has certain desirable properties which we discuss. In sec. 4.1.3, we comment on the issues that arise when constructing a dual geometry for a quantum circuit parameterized by an auxiliary time coordinate. This motivates the implementation of the quantum circuit as a time evolution in later sections.

4.1.1. Quantum Circuits for Conformal Transformations

While many holographic complexity proposals exist, the precise definition of complexity in the dual CFT remains unclear. A first step has been taken in [75]. The authors considered quantum circuits implementing conformal transformations in the CFT based on the framework presented in sec. 3.4. The conformal transformations f are continuously parameterized by the circuit parameter τ, $x^+ \to f(\tau, x^+)$, where the coordinates $x^\pm = t \pm \varphi$ parameterize the two-dimensional manifold on which the CFT lives. We may think of $f(\tau, x^+)$ as a path through the Virasoro group manifold starting from the identity transformation $f(\tau = 0, x^+) = x^+$ at $\tau = 0$ to some conformal transformation $f(\tau = T, x^+) = f(x^+)$ after a finite circuit time T. We know from sec. 2.1 that conformal transformations are generated by the energy-momentum tensor. In the framework of sec. 3.4, the quantum circuit is generated by a circuit Hamiltonian (3.4.3) given in terms of the symmetry generator. The circuit Hamilto-

nian implementing conformal transformations is therefore given by

$$Q(\tau) = -\int d\varphi\, \epsilon(\tau, x^+) T(x^+), \tag{4.1.1}$$

where $\epsilon(\tau, x^+)$ are some yet-to-be-determined gate velocities that are given in terms of the conformal transformation $f(\tau, x^+)$. We employ the following notation for the components of the energy-momentum tensor in this section:

$$T(x^+) \equiv T_{++}(x^+), \quad \bar{T}(x^-) \equiv T_{--}(x^-). \tag{4.1.2}$$

The quantum circuit is obtained by evolving a reference state $|\psi_R\rangle$ which we choose to be the highest weight state $|h\rangle$ with the circuit Hamiltonian (4.1.1) for the duration T of the circuit,

$$|\psi_T\rangle = e^{i\int_0^T d\tau \int_0^{2\pi} d\varphi\, \epsilon(\tau,x^+) T(x^+)} |h\rangle. \tag{4.1.3}$$

A suitable choice of reference state is the highest-weight state $|h\rangle$. In the next step, the gate velocities are determined such that (4.1.3) implements a particular conformal transformation $x^+ \to f(\tau, x^+)$. An infinitesimal layer of the circuit (4.1.3) is obtained from

$$|\psi(\tau + d\tau)\rangle = e^{-iQ(\tau)d\tau} |\psi(\tau)\rangle \tag{4.1.4}$$

and must implement the step

$$f(\tau + d\tau, x^+) = e^{\epsilon(\tau,x^+)d\tau} f(\tau) \tag{4.1.5}$$

in the group manifold. Expanding (4.1.5) to first order in $d\tau$ then yields

$$\epsilon(\tau, f(\tau, x^+)) = \dot{f}(\tau, x^+), \tag{4.1.6}$$

where $\dot{f}$ denotes the derivative with respect to the first argument. We now group multiply by the inverse transformation $F(\tau, x^+)$ defined as $f(\tau, F(\tau, x^+)) = x^+$. Employing $\dot{f}(\tau, F(\tau, x^+)) = -\frac{\dot{F}(\tau,x^+)}{F'(\tau,x^+)}$, where F' denotes the derivative with respect to the second argument, we obtain

$$\epsilon(\tau, x^+) = -\frac{\dot{F}(\tau, x^+)}{F'(\tau, x^+)}. \tag{4.1.7}$$

This is just the Maurer-Cartan form (2.1.63) without central extension. Note that it is possible to include the central extension, but this only yields an additional global phase which does not physically change the state and thus does not contribute to

complexity. For details, we refer to [122]. Therefore, the circuit (4.1.3) then takes us from the reference state along a trajectory

$$|\psi_T\rangle = U_{f(T)}|h\rangle, \quad \text{where} \quad U_{f(T)} = e^{-i\int_0^T d\tau \int_0^{2\pi} d\varphi \frac{\dot{F}(\tau,x^+)}{F'(\tau,x^+)} T(x^+)}, \tag{4.1.8}$$

through the Hilbert space of a single Verma module. The circuit takes us from the reference state at $\tau = 0$ to a target state $|\psi_T\rangle$ that is determined by the conformal transformation $f(\tau = T, x^+) = f(x^+)$. The trajectory through the Hilbert space is thus determined by the reference state $|h\rangle$ and the path $f(\tau, x^+)$ through the conformal group manifold.

4.1.2. The Cost Function: Fubini-Study Distance

Next, we specify the cost function with respect to which we would like to measure the cost of reaching a particular target state $|\psi_T\rangle$ from a reference state $|h\rangle$. A suitable choice is the Fubini-Study distance, which has been studied extensively for the circuits (4.1.3) in [86, 87]. It measures the distance between states on the projective Hilbert space. The projective Hilbert space is equipped with a metric – the Fubini-Study metric. This metric may be derived by considering two infinitesimally close states in the Hilbert space. In our quantum circuit (4.1.3), the states $|\psi(\tau)\rangle$ and $|\psi(\tau + d\tau)\rangle$ are infinitesimally close. The overlap between those two states defines the fidelity [227–229],

$$F = |\langle\psi(\tau)|\psi(\tau + d\tau)\rangle|. \tag{4.1.9}$$

Next, we use that the time evolution of the state along the circuit is governed by the Schödinger equation,

$$\frac{\partial}{\partial\tau}|\psi(\tau)\rangle = -iQ(\tau)|\psi(\tau)\rangle, \tag{4.1.10}$$

where $Q(\tau)$ is the circuit Hamiltonian (4.1.1). Then, to second order in $d\tau$ (4.1.9) is given by

$$F = 1 - \frac{1}{2}\mathcal{F}_{\text{FS}}\, d\tau^2, \tag{4.1.11}$$

where

$$\mathcal{F}_{\text{FS}} = \langle\psi(\tau)|Q(\tau)Q(\tau)|\psi(\tau)\rangle - |\langle\psi(\tau)|Q(\tau)|\psi(\tau)\rangle|^2 \tag{4.1.12}$$

is the Fubini-Study distance measure. The Fubini-Study metric then reads

$$ds^2 = \mathcal{F}_{\text{FS}}\, d\tau^2 = (\langle\psi(\tau)|Q(\tau)Q(\tau)|\psi(\tau)\rangle - |\langle\psi(\tau)|Q(\tau)|\psi(\tau)\rangle|^2)d\tau^2. \tag{4.1.13}$$

We alluded that the Fubini-Study metric is a metric on the projective Hilbert space. This has important consequences for how exactly quantum computational cost is counted. The Fubini-Study metric does not distinguish between states that only differ by a global phase. In quantum mechanics, states $|\psi\rangle$ that only differ by a phase belong to the same ray $[\psi]$, $[\psi] = \left\{|\psi\rangle = e^{i\theta}|\Phi\rangle \mid \theta \in \mathbb{R}\right\}$ [119]. These rays define the projective Hibert space. Recalling our discussion in sec. 2.1.2, this implies that diffeomorphisms $f(\tau, x^+)$ that belong to the stabilizer group U(1) for a reference state $|h\rangle$ with $h > 0$ or SL(2,$\mathbb{R}$) for the reference state $|0\rangle$ are assigned zero cost. This was shown in [86, 87]. The property of assigning zero cost to global phases is a desirable feature in any cost function: Transformations which yield global phases in the reference state do not lead to physically distinguishable target states as the phase does not effect measurements. For example, the transformation $f(\tau, x^+) = x^+ + \alpha(x^+)$ is generated only by L_0. The gate for this transformation reads

$$Q(\tau) = \dot{\alpha}(\tau) L_0. \tag{4.1.14}$$

This yields the target state

$$|\psi_T\rangle = e^{i\int_0^T d\tau\, \dot{\alpha}(\tau) L_0}|h\rangle = e^{i\alpha(T)(h-c/24)}, \tag{4.1.15}$$

where in the last step we used (2.1.37) and assumed that $\alpha(0) = 0$. Clearly, the reference state $|h\rangle$ and the target state $|\psi_T\rangle$ only differ by a global phase and are therefore physically indistinguishable. In contrast to, for example, $\langle\psi(\tau)|Q(\tau)|\psi(\tau)\rangle$, the Fubini-Study metric does not measure such phases since it is a metric on the projective Hilbert space.

In order to obtain the explicit form of (4.1.12), it is convenient to rewrite the expectations values in terms of the reference state. Any state $|\psi(\tau)\rangle$ along the circuit is obtained by time-evolving the reference state $|h\rangle$ according to (4.1.8) for the specified amount of time τ. Therefore, the Fubini-Study distance may be written as

$$\mathcal{F}_{\text{FS}} = \langle h|U^\dagger_{f(\tau)} Q(\tau) U_{f(\tau)} U^\dagger_{f(\tau)} Q(\tau) U_{f(\tau)}|h\rangle - |\langle h|U^\dagger_{f(\tau)} Q(\tau) U_{f(\tau)}|h\rangle|^2. \tag{4.1.16}$$

We now define the transformed circuit Hamiltonian $\tilde{Q}(\tau) = U^\dagger_{f(\tau)} Q(\tau) U_{f(\tau)}$. As the quantum circuit implements conformal transformations, the transformed circuit Hamiltonian $\tilde{Q}(\tau)$ may be obtained by combining (4.1.1) with the transformation of

the energy-momentum tensor under conformal transformations (2.1.19). This yields

$$\tilde{Q}(\tau) = -\int_0^{2\pi} \frac{d\varphi}{2\pi} \frac{\dot{f}(\tau, x^+)}{f'(\tau, x^+)} \left(T(x^+) - \frac{c}{12}\{f(x^+), x^+\} \right). \tag{4.1.17}$$

Thus, the Fubini-Study distance may be written as

$$\mathcal{F}_{\text{FS}} = \iint_0^{2\pi} \frac{d\varphi_1 d\varphi_2}{4\pi^2} \frac{\dot{f}(\tau, x_1^+)}{f'(\tau, x_1^+)} \frac{\dot{f}(\tau, x_2^+)}{f'(\tau, x_2^+)} (\langle h|T(x_1^+)T(x_2^+)|h\rangle - \langle h|T(x_1^+)|h\rangle\langle h|T(x_2^+)|h\rangle). \tag{4.1.18}$$

The one-point function $\langle h|T(x^+)|h\rangle$ may be evaluated by making use of (2.1.37), whereas the two-point function on the cylinder is given by

$$\langle h|T(x_1^+)T(x_2^+)|h\rangle = \left(h - \frac{c}{24}\right)^2 + \frac{c}{32\sin((x_1^+ - x_2^+)/2)^4} - \frac{h}{2\sin((x_1^+ - x_2^+)/2)^2}. \tag{4.1.19}$$

Putting everything together, the Fubini-Study distance for the circuit (4.1.3) is given by[1]

$$\mathcal{F}_{\text{FS}} = \iint_0^{2\pi} d\varphi_1 d\varphi_2 \frac{\dot{f}(\tau, \varphi_1)}{f'(\tau, \varphi_1)} \frac{\dot{f}(\tau, \varphi_2)}{f'(\tau, \varphi_2)} \left(\frac{c}{32\sin((\varphi_1 - \varphi_2)/2)^4} - \frac{h}{2\sin((\varphi_1 - \varphi_2)/2)^2} \right). \tag{4.1.21}$$

This result, derived in [86, 87], is of central importance in this thesis as we will derive a bulk dual to (4.1.21) in sec. 4.3.

4.1.3. Holographic Duals to a Quantum Circuit: A Sequence of Geometries

The circuit (4.1.3) is parameterized by an auxiliary circuit parameter τ that is unrelated to the physical spacetime coordinates $x^\pm = t \pm \varphi$ of the CFT. Given a particular diffeomorphism $f(\tau, x^+)$, the circuit (4.1.3) generates a sequence of states $|\psi(\tau)\rangle$. In

[1] Note that in this form the Fubini-Study distance cannot be evaluated due to divergences in the limit $x_1^+ \to x_2^+$. In [86, 87], differential regularization was employed to obtain milder divergences that can be integrated over,

$$\begin{aligned} &\iint_0^{2\pi} d\varphi_1 d\varphi_2 \frac{\dot{f}(\tau, \varphi_1)}{f'(\tau, \varphi_1)} \frac{\dot{f}(\tau, \varphi_2)}{f'(\tau, \varphi_2)} \left(\frac{c}{32\sin((\varphi_1 - \varphi_2)/2)^4} - \frac{h}{2\sin((\varphi_1 - \varphi_2)/2)^2} \right) \\ &\overset{!}{=} \iint_0^{2\pi} d\varphi_1 d\varphi_2 \log\left(\sin\left(\frac{\varphi_1 - \varphi_2}{2}\right)^2\right) \left(-\frac{c}{24}\partial_{\varphi_1}^2 \frac{\dot{f}(\tau, \varphi_1)}{f'(\tau, \varphi_1)} \partial_{\varphi_2}^2 \frac{\dot{f}(\tau, \varphi_2)}{f'(\tau, \varphi_2)} \right. \\ &\qquad \left. + \left(\frac{c}{24} - h\right) \partial_{\varphi_1} \frac{\dot{f}(\tau, \varphi_1)}{f'(\tau, \varphi_1)} \partial_{\varphi_2} \frac{\dot{f}(\tau, \varphi_2)}{f'(\tau, \varphi_2)} \right). \end{aligned} \tag{4.1.20}$$

particular, the states $|\psi(\tau)\rangle$ all belong to the same Verma module and consequently to the same coadjoint orbit. For every state $|\psi(\tau)\rangle$ along the circuit, we may assign an expectation value of the energy-momentum tensor,

$$\langle\psi(\tau)|T(x^+)|\psi(\tau)\rangle = \langle h|U^\dagger_{f(\tau)}T(x^+)U_{f(\tau)}|h\rangle. \tag{4.1.22}$$

Let us assume for concreteness that $h = 0$ such that the reference state is the vacuum state $|0\rangle$. Therefore, the circuit (4.1.3) may also be thought of as generating a path on the vacuum coadjoint orbit, where the path is given by $f(\tau, x^+)$. The orbit label b_0 given in (2.1.57) is the expectation value of the energy-momentum tensor in the reference state $|0\rangle$, which then evolves according to (4.1.22) along the circuit. We may now employ the duality between Virasoro coadjoint orbits and Bañados geometries described in sec. 2.3.3 to establish a dual description of the circuit (4.1.3). The coadjoint orbit for a CFT in the vacuum is dual to an empty AdS geometry. Upon applying the circuit (4.1.3) to the vaccum reference state, a sequence of Bañados geometries (2.3.38) is generated, where the geometry is specified by the expectation value of the energy-momentum tensor,

$$L(\tau, x^+) = \frac{6}{c}\langle\psi(\tau)|T(x^+)|\psi(\tau)\rangle = \frac{6}{c}\langle 0|U^\dagger_{f(\tau)}T(x^+)U_{f(\tau)}|0\rangle. \tag{4.1.23}$$

The Bañados geometries are then related to empty AdS by conformal transformations. These geometries all have the same SL(2,$\mathbb{R}$) Killing charges associated to global AdS, but differ by the value of $L(x^+)$ and $L(x^-)$. Since τ parameterizes the conformal transformation, we obtain a different value for $L(x^+)$ and $L(x^-)$ for every fixed value of τ along the circuit. The dual state in the boundary CFT is defined on a constant time slice. Since physical time has no special meaning in this circuit, the choice of time slice is arbitrary; for simplicity, we choose $t = 0$. This is depicted in fig. 4.1. Note that the sequence of geometries generated by the circuit (4.1.3) is disconnected as τ is an external parameter from the point of view of the bulk geometry. It is then difficult to make contact with holographic complexity proposals. In particular, the circuit dynamics cannot be related to the bulk geometry, which makes it hard to understand how features of CFT cost functions translate to properties of bulk complexity measures. We therefore now establish a CFT circuit that has a single dual holographic geometry, thus in principle allowing the derivation of holographic duals to CFT cost functions and of CFT duals to holographic complexity proposals from first principles.

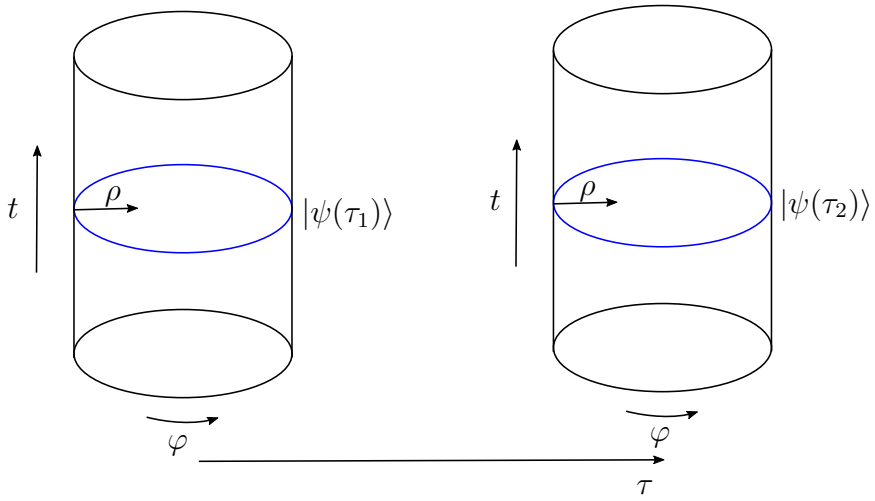

Fig. 4.1.: The circuit generates a sequence of dual geometries parameterized by the auxiliary circuit parameter τ. The states are defined on a constant time slice in the physical time shown in blue. This choice of timeslice is arbitrary for the circuit.

4.2. Dual Spacetime to a Quantum Circuit

The aim of this section is to construct a quantum circuit with a single connected holographic dual geometry. This can only be achieved if the states $|\psi(\tau)\rangle$ generated by the circuit (4.1.3) are no longer parameterized by an external parameter τ. Therefore, we demand that instead the states are parameterized by the physical time t such that we obtain a sequence of states $|\psi(t)\rangle$. This implies we have to identify the circuit parameter τ with the physical time t, $\tau = t$. Since we would like to implement the same circuit as given by (4.1.3), the sequence of states between $0 \leq t \leq T$ generated by (4.1.3) must be the same as in the new circuit construction after identifying $\tau = t$. This may be achieved by identifying the physical Hamiltonian governing time evolution in the CFT with the circuit Hamiltonian $Q(\tau = t)$,

$$Q(t) \stackrel{!}{=} H(t). \tag{4.2.1}$$

The circuit (4.1.3) implements conformal transformations. Therefore, the condition (4.2.1) implies that $H(t)$ cannot be the standard time evolution operator $\tilde{H} = L_0 + \bar{L}_0$ when the circuit acts between $0 \leq t \leq T$ as it generates a global symmetry that leaves the reference state $|0\rangle$ invariant. Instead, the correct Hamiltonian $H(t)$ must generate a non-trivial time evolution of the background metric on which the CFT lives such that at any given constant time slice between $0 \leq t \leq T$, the CFT is in the appropriate state $|\psi(t)\rangle$. This is ensured by (4.2.1). We furthermore demand that

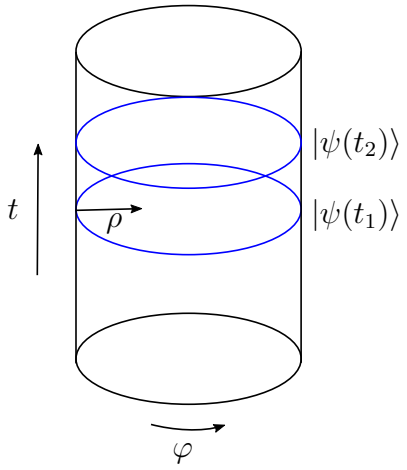

Fig. 4.2.: The circuit is encoded in the time evolution of the boundary spacetime. States in the circuit are defined on constant time slices in the boundary.

before the circuit starts acting at $t = 0$ the CFT is in the reference state and after the circuit is complete at $t = T$, it remains in the target state $|\psi_T\rangle$. This implies that for $t < 0$ and $t > T$, the Hamiltonian reduces to the ordinary time evolution operator $H(t) = \tilde{H} = L_0 + \bar{L}_0$. The new circuit construction is depicted schematically in fig. 4.2. The boundary conditions at $t = 0$ and $t = T$ as well as (4.2.1) then allow us to derive a holographic dual bulk geometry to the quantum circuit. We now proceed as follows: We first derive the time-dependent boundary metric on which the CFT lives from the condition (4.2.1) in sec. 4.2.1 and then proceed to derive the dual bulk geometry in sec. 4.2.2.

4.2.1. A Quantum Circuit as Time Evolution of the Boundary Spacetime

We now encode the evolution of the quantum circuit (4.1.3) as an evolution of the CFT with physical time t by enforcing the condition (4.2.1). This implies that the spacetime on which the CFT lives evolves under time evolution and is explicitly time dependent between $0 \leq t \leq T$. Therefore, we must first determine the appropriate form of the time-evolution operator on such a time-dependent background geometry.

Time Evolution in a time-dependent flat background metric

The general form of the Hamiltonian is given by [81, 136],

$$H(t, \varphi) = \int d\Sigma^{\mu}(t, \varphi) T_{\mu\nu}(t, \varphi) \xi^{\nu}(t, \varphi), \tag{4.2.2}$$

where $d\Sigma^\mu(t,\varphi)$ is the integration measure on a hypersurface Σ normal to the time translation vector $\xi^\nu(t,\varphi)$ that maps a point on the constant time slice Σ_t along $\xi^\nu(t,\varphi)$ to a new slice Σ_{t+dt}. Since any metric in two dimensions may be written as $ds^2 = \Omega(t,\varphi)(-dt^2+d\varphi^2)$, it follows that $d\Sigma^\mu(t,\varphi) = \sqrt{g_{\varphi\varphi}}n^\mu d\varphi$ and thus the general form of the Hamiltonian generating time evolution is given by

$$H(t) = \int d\varphi \sqrt{g_{\varphi\varphi}} T_{\mu\nu}(t,\varphi)\xi^\mu(t,\varphi)n^\nu(t,\varphi). \tag{4.2.3}$$

Here, ξ^μ generates time translations and thus satisfies

$$\xi^\mu \partial_\mu = \partial_t. \tag{4.2.4}$$

The normal vector n^μ is fixed by

$$n_\mu = N\partial_\mu t \quad \text{and} \quad n^\mu n_\mu = -1. \tag{4.2.5}$$

Let us first examine the simplest background metric, which is the standard two-dimensional flat Lorentzian metric $ds^2 = -dt^2 + d\varphi^2$. Since $n_\mu = (1,0)$ in this background, the Hamiltonian generating time evolution is given by

$$H(t) = \int_0^{2\pi} \frac{d\varphi}{2\pi} T^t{}_t. \tag{4.2.6}$$

Rewriting the Hamiltonian in terms of the more standard T_{++}, T_{--} and T_{+-} components yields

$$H = -\int \frac{d\varphi}{2\pi}\left(T_{++}(x^+) + T_{--}(x^-) + 2T_{+-}(x^+,x^-)\right). \tag{4.2.7}$$

The careful reader might notice that (4.2.7) does not seem to be equal to the CFT textbook Hamiltonian (compare for instance [109]), which is given by

$$H(t) = L_0 + \bar{L}_0 = -\int \frac{d\varphi}{2\pi}\left(T_{++}(x^+) + T_{--}(x^-)\right). \tag{4.2.8}$$

In contrast to (4.2.7), T_{+-} does not appear in the textbook expression (4.2.8). We now argue that T_{+-} may be dropped from (4.2.7) since it does not contribute to the time evolution. To show this, we may for instance consider the time evolution of the T_{++} component of the energy-momentum tensor,

$$T_{++}(t) = e^{iH(t)}T_{++}(t=0)e^{-iH(t)}, \tag{4.2.9}$$

and expand (4.2.9) to first order,

$$T_{++}(t) = (1 + iH(t))T_{++}(t=0)(1 - iH(t)) = T_{++}(t=0) + i[H(t), T_{++}(t=0)]. \tag{4.2.10}$$

We are interested in the term

$$[H(t), T_{++}(t=0)] = [\int \frac{d\varphi}{2\pi} \left(T_{++}(x^+) + T_{--}(x^-) + 2T_{+-}(x^+, x^-)\right), T_{++}(t=0)]. \tag{4.2.11}$$

The commutator may be determined from the two-point functions $H(t)T_{++}(t=0)$ and $T_{++}(t=0)H(t)$. We focus on the role of the T_{+-}-contribution in $H(t)$ in these two-point functions. Note that the two-point function on the complex plane is given only by a contact term [112] , $T_{z\bar{z}}T_{ww} = -\frac{c}{12}\partial_z^2\delta^{(2)}(z-w)$ with $z = it+\varphi$ and $\bar{z} = -it+\varphi$. This implies that $T_{+-}T_{++} \propto \delta(t)$. Therefore, in the time evolution (4.2.9) T_{+-} contributes with contact terms that are only non-vanishing at $t = 0$. This in turn indicates that the contribution from T_{+-} in (4.2.9) lies outside the range of the t-coordinate in which we evolve in time since at $t = 0$ $H(t)$ does not yet act on $T_{++}(t=0)$. Conclusively, we may disregard the T_{+-} contribution in the Hamiltonian and work with the standard textbook Hamiltonian

$$H(t) = -\int \frac{d\varphi}{2\pi} \left(T_{++}(x^+) + T_{--}(x^-)\right). \tag{4.2.12}$$

Note that this argument holds for any flat background metric and therefore we drop T_{+-} from (4.2.2). We now move on to find the Hamiltonian for a general two-dimensional flat background.

The most general two-dimensional flat metric is obtained from $ds^2 = -dx^+dx^-$ by applying the diffeomorphisms $x^+ \to y(x^+, x^-)$ and $x^- \to v(x^+, x^-)$,

$$ds^2 = -\frac{\partial y}{\partial x^+}\frac{\partial v}{\partial x^+}(dx^+)^2 - \left(\frac{\partial y}{\partial x^+}\frac{\partial v}{\partial x^-} + \frac{\partial y}{\partial x^-}\frac{\partial v}{\partial x^+}\right)dx^+dx^- - \frac{\partial y}{\partial x^-}\frac{\partial v}{\partial x^-}(dx^-)^2. \tag{4.2.13}$$

This geometry is flat but time dependent since $x^\pm = t \pm \varphi$. The transformation of the energy-momentum tensor under $x^+ \to y(x^+, x^-)$ and $x^- \to v(x^+, x^-)$ is obtained

from $T_{ab}dx^a dx^b = \tilde{T}_{cd}d\tilde{x}^c d\tilde{x}^c$, which yields

$$\begin{aligned} T_{++}(x^+,x^-) &= \left(\frac{\partial y}{\partial x^+}\right)^2 T_{yy} + \left(\frac{\partial v}{\partial x^+}\right)^2 T_{vv} + 2\frac{\partial y}{\partial x^+}\frac{\partial v}{\partial x^+}T_{yv}, \\ T_{--}(x^+,x^-) &= \left(\frac{\partial y}{\partial x^-}\right)^2 T_{yy} + \left(\frac{\partial v}{\partial x^-}\right)^2 T_{vv} + 2\frac{\partial y}{\partial x^-}\frac{\partial v}{\partial x^-}T_{yv}, \\ T_{+-}(x^+,x^-) &= \frac{\partial y}{\partial x^+}\frac{\partial y}{\partial x^-}T_{yy} + \frac{\partial v}{\partial x^+}\frac{\partial v}{\partial x^-}T_{vv} + \left(\frac{\partial y}{\partial x^+}\frac{\partial v}{\partial x^-} + \frac{\partial v}{\partial x^+}\frac{\partial y}{\partial x^-}\right)T_{yv}. \end{aligned} \tag{4.2.14}$$

The time evolution operator (4.2.6) for the general flat metric (4.2.13) is then given by

$$H(t) = \int \frac{d\varphi}{2\pi}\sqrt{|g|}\left(\left(g^{++}+g^{+-}\right)\left(T_{++}+T_{+-}\right) + \left(g^{--}+g^{+-}\right)\left(T_{--}+T_{+-}\right)\right). \tag{4.2.15}$$

Inserting (4.2.13) and (4.2.14) into (4.2.15) yields the Hamiltonian

$$\begin{aligned} H(t) &= \int \frac{d\varphi}{2\pi}\left(\left(\frac{\partial y}{\partial x^+}\right)^2 - \left(\frac{\partial v}{\partial x^-}\right)^2\right)T_{yy} + \left(\left(\frac{\partial v}{\partial x^-}\right)^2 - \left(\frac{\partial v}{\partial x^+}\right)^2\right)T_{vv} \\ &= -\int \frac{d\varphi}{2\pi}\partial_\varphi y \partial_t y T_{yy} + \partial_\varphi v \partial_t v T_{vv}. \end{aligned} \tag{4.2.16}$$

Note that we dropped T_{yv} as it does not contribute to the time evolution. Equation (4.2.16) is our final result for the Hamiltonian governing time evolution in the general two-dimensional metric (4.2.13). In the next step, we determine the diffeomorphisms y and v such that (4.2.1) is satisfied.

A Hamiltonian implementing quantum circuits

To find the diffeomorphisms y and v, we compare the circuit Hamiltonian $Q(t)$ with the Hamiltonian (4.2.16). After a change of variables $x^+ \to f(t,x^+)$, the left-moving component of $Q(t)$ reads

$$Q_+(t) = -\int \frac{d\varphi}{2\pi}\epsilon(t,x^+)T_{++}(x^+) \to Q_+(t) = -\int \frac{d\varphi}{2\pi}(\partial_\varphi f)\epsilon(t,f(t,x^+))T_{ff}(f(t,x^+)). \tag{4.2.17}$$

An analogous contribution may be obtained from the right-moving sector under the change of coordinates $x^- \to \bar{f}(t,x^-)$. The full circuit Hamiltonian then reads

$$Q(t) = Q_+(t) + Q_-(t)$$

$$= -\int \frac{d\varphi}{2\pi}(\partial_\varphi f \epsilon(t, f(t, x^+)))T_{ff}(f(t, x^+)) - \int \frac{d\varphi}{2\pi}(\partial_\varphi \bar{f})\epsilon(t, \bar{f}(t, x^-))T_{\bar{f}\bar{f}}(\bar{f}(t, x^-)). \tag{4.2.18}$$

For simplicity, we assume that Q_- implements a trivial transformation $x^- \to x^-$ such that the circuit Hamiltonian for the right-moving sector reduces to the ordinary time-evolution operator after the identification $\tau = t$. Then,

$$Q(t) = -\int \frac{d\varphi}{2\pi}\left(\partial_\varphi f \epsilon(t, f(t, x^+))T_{ff}(f(t, x^+)) + T_{--}(x^-)\right). \tag{4.2.19}$$

Upon comparing (4.2.16) with (4.2.19), the condition (4.2.1) then yields the equations

$$\begin{aligned} \partial_\varphi y \partial_t y T_{yy} &= \partial_\varphi f \epsilon(t, f) T_{ff}, \\ \partial_\varphi v \partial_t v T_{vv} &= T_{--}. \end{aligned} \tag{4.2.20}$$

In the final step, we now employ (4.1.6) which fixes $\epsilon(t, f(t, x^+)) = \partial_t f(t, x^+)$ after identifying $\tau = t$. Therefore, the diffeomorphisms $y(x^+, x^-)$ and $v(x^+, x^-)$ are given by

$$y(x^+, x^-) = f(x^+, x^-), \qquad v(x^+, x^-) = x^-. \tag{4.2.21}$$

We then obtain the following result: The Hamiltonian which implements the circuit (4.1.3) as a time evolution of the boundary spacetime is given by

$$H(t) = -\int \frac{d\varphi}{2\pi}\left(\partial_\varphi f \partial_t f T_{ff} + T_{--}\right). \tag{4.2.22}$$

It is straightforward to check that (4.2.22) indeed satisfies the condition (4.2.1) by rewriting $H(t)$ in terms of the inverse diffeomorphism $F(t, x^+)$ with $F(t, f(t, x^+)) = x^+$. The inverse diffeomorphism of $v(t, x^-) = x^-$ is trivial. Employing the relations $\partial_\varphi f(t, F) = \frac{1}{\partial_\varphi F}$ and $\dot{f}(t, F) = -\frac{\dot{F}}{F'}$, where $\dot{f}(t, F)$ and $\dot{F}(t, x^+)$ are derivatives with respect to the first argument and $F'(t, x^+)$ with respect to the second argument, yields

$$H(t) = \int \frac{d\varphi}{2\pi}\left(\frac{\partial_t F(t, \varphi)}{\partial_\varphi F(t, \varphi)} T_{++} - T_{--}\right). \tag{4.2.23}$$

This agrees with (4.1.1) after the identification $\tau = t$. The time evolution of the reference state $|h\rangle$ with (4.2.22) then implements a quantum circuit

$$|\psi(t)\rangle = e^{-i\int_0^t dt' H(t')}|h\rangle \tag{4.2.24}$$

that yields the same sequence of states as the circuit (4.1.3). The states are defined

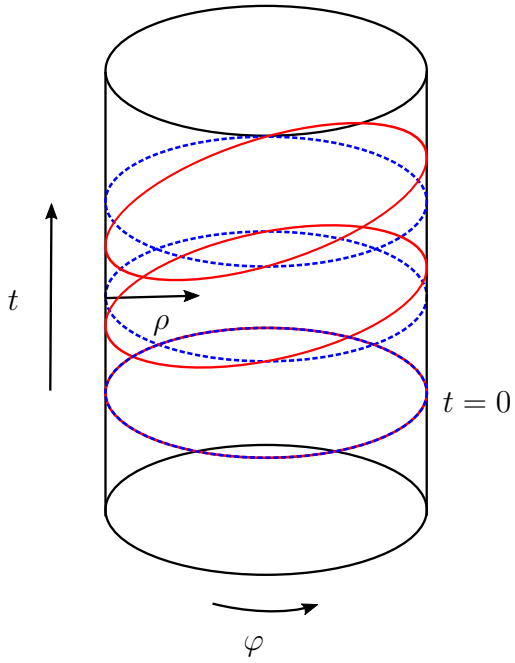

Fig. 4.3.: Constant time slices in the original geometry (blue, dotted) and in the new time-dependent geometry (red) implementing the quantum circuit: At the beginning of the circuit at $t = 0$ both coordinate systems match, then the geometry is foliated differently in the time-dependent circuit geometry.

on constant time slices of the boundary spacetime.

We may now employ the diffeomorphisms v and y determined in (4.2.21) to derive the boundary metric on which the CFT lives as it evolves with $H(t)$ and the energy-momentum tensor that is conserved on this background. The boundary metric follows from (4.2.13) and reads

$$ds^2 = -\left(\frac{1}{2}\left(\dot{f}(t,x^+) + 2f'(t,x^+)\right)dx^+ + \frac{1}{2}\dot{f}(t,x^+)dx^-\right)dx^-. \tag{4.2.25}$$

Therefore, the circuit generates a highly non-trivial evolution of the boundary spacetime which is now explicitly time-dependent. We have thus found a circuit construction implementing quantum circuits as a time evolution of the boundary spacetime. In particular, the boundary spacetime is flat at all times such that the circuit is obtained by a specific time foliation of the flat boundary spacetime. For illustration, the foliation in (x^+, x^-)-coordinates is depicted in fig. 4.3. Next, let us assume that the reference state is the vacuum state $|0\rangle$. Then, employing (4.2.14), the expectation value of the

energy-momentum tensor in the background (4.2.25) reads

$$\begin{aligned}\langle T_{++}\rangle &= -\frac{c}{24}\frac{1}{4}\left(\dot{f}(t,x^+)+2f'(t,x^+)\right)^2,\\ \langle T_{+-}\rangle &= -\frac{c}{24}\frac{1}{4}\left(\dot{f}(t,x^+)+2f'(t,x^+)\right)\dot{f}(t,x^+),\\ \langle T_{--}\rangle &= -\frac{c}{24}\left(1+\frac{1}{4}\dot{f}(t,x^+)^2\right).\end{aligned} \tag{4.2.26}$$

By construction, the circuit generated by the Hamiltonian (4.2.22) must yield the same target state $|\psi_T\rangle$ at $t = T$. After the circuit is implemented at $t = T$, the diffeomorphism becomes constant in time such that $\dot{f}(t, x^+) = 0$. The expectation value of the energy-momentum tensor (4.2.26) must then be equal to the one generated by (4.1.3), which is given by

$$\langle T_{++}\rangle = -\frac{c}{24}f'_{\text{final}}\left(x^+\right)^2 + \frac{c}{12}\left\{f_{\text{final}}\left(x^+\right), x^+\right\}, \quad \langle T_{+-}\rangle = 0, \quad \langle T_{--}\rangle = -\frac{c}{24}, \tag{4.2.27}$$

where $f_{\text{final}}\left(x^+\right) = f(t = T, x^+)$. However, (4.2.26) reduces to

$$\langle T_{++}\rangle = -\frac{c}{24}f'_{\text{final}}\left(x^+\right)^2, \quad \langle T_{+-}\rangle = 0, \quad \langle T_{--}\rangle = -\frac{c}{24}. \tag{4.2.28}$$

Clearly, the Schwarzian term is missing in (4.2.28). Furthermore, at the end of the circuit, the boundary metric (4.2.25) reduces to $ds^2 = -f'_{\text{final}}dx^+dx^-$ rather than the desired $ds^2 = -dx^+dx^-$. We discussed in sec. 2.1 that a Weyl rescaling of the metric,

$$ds^2 \to e^{2\omega(x^+,x^-)}ds^2, \tag{4.2.29}$$

yields the Schwarzian derivative since the energy-momentum tensor transforms as (2.1.33). The appropriate Weyl factor that recovers the metric $ds^2 = -dx^+dx^-$ and the expectation value (4.2.27) follows from imposing that the metric remains flat under the Weyl rescaling, i.e. the Ricci scalar vanishes. Under a general Weyl transformation, the Ricci scalar transforms as $R \to e^{-2\omega}\left(R - 2\nabla_i\nabla^i\omega\right)$ [112]. From these conditions, we find that the appropriate Weyl factor is then given by [1]

$$\omega(x^+, x^-) = -\frac{1}{2}\log f'_{\text{final}}\left(F_{\text{final}}\left(f(t, x^+)\right)\right). \tag{4.2.30}$$

This concludes our discussion of the circuit construction implementing quantum circuits as time evolution of the boundary spacetime. We now have all necessary ingredients to obtain a bulk dual for this quantum circuit.

4.2.2. Gravity Dual to a Circuit

In the quantum circuit generated by the Hamiltonian (4.2.22), the energy-momentum tensor of the CFT is sourced by the non-trivial boundary metric (4.2.25). In sec. 2.3.2, we discussed that in pure gravity in AdS_3/CFT_2 the bulk spacetime may be reconstructed from the CFT energy-momentum tensor and the boundary metric as its source employing the Fefferman-Graham expansion (2.3.29). Therefore, we now take the Weyl-rescaled boundary metric and the appropriate Weyl-rescaled energy-momentum tensor obtained from the construction in the previous section and compute the Fefferman-Graham coefficients (2.3.27). Inserting the coefficients in the metric (2.3.29) then yields the dual bulk spacetime to the quantum circuit generated by the Hamiltonian (4.2.22). By this construction, the time foliation of the boundary spacetime is continued into the bulk geometry in such a manner that the bulk spacetime is foliated according to the evolution of the quantum circuit.

As we have now developed a method that yields a bulk dual to a quantum circuit, we may in principle derive bulk duals to CFT complexity measures and vice versa. This is a significant step toward verifying the holographic complexity conjectures discussed in sec. 3.3 and studying the relation between CFT complexity and holographic complexity measures since our proposal allows for explicit computations both in the bulk and boundary that can be related directly to one another. Before we demonstrate the power of our proposal by deriving a bulk dual to the Fubini-Study distance (4.1.12), we discuss our construction on an illustrative example and draw some important lessons from it.

4.2.3. Circuits with Time-dependent Diffeomorphisms: Lessons from SL(2,R) and U(1) Circuits

When implementing the circuit construction of sec. 4.2.1 for a particular diffeomorphism several subtleties arise. The first one concerns the choice of transformation $f(t, x^+)$. Given a diffeomorphism $f(\tau, x^+)$ in the original circuit (4.1.3), the diffeomorphism which implements the circuit with Hamiltonian (4.2.22) is not obtained by simply identifying $\tau = t$ in $f(\tau, x^+)$. Instead the diffeomorphisms $f(\tau, x^+)$ appearing in the original circuit construction (4.1.3) and the diffeomorphisms $f(t, x^+)$ in the new circuit construction (4.2.22) must have the same Fourier modes to ensure (4.2.1) is satisfied. We therefore now denote the diffeomorphism appearing in the new circuit by $\tilde{f}$ since it is in general not the same diffeomorphism as the one obtained by simply identifying $\tau = t$ in $f(\tau, x^+)$. Let us understand this in more detail. We first go back to

the original circuit construction, in which the circuit parameter and the physical time are not identified. Two diffeomorphisms in the circuit (4.1.3) are related by (4.1.5). This leads to $\epsilon(\tau, x^+)$ given by (4.1.7). In particular, the Fourier modes of $\epsilon(\tau, x^+)$ determine which state $|\psi(\tau)\rangle$ is generated at a particular time step by

$$Q(\tau) = -\int d\varphi\, \epsilon(\tau, x^+) T(x^+) = -\sum_n \epsilon_{-n}(\tau) L_n, \tag{4.2.31}$$

where the Virasoro generators act as (2.1.37) on a state. On the other hand, after identifying $\tau = t$ two diffeomorphisms are related by

$$\tilde{f}(t + dt, x^+ + dt) = e^{\tilde{\epsilon}(t,x^+)dt} \tilde{f}(t, x^+) \tag{4.2.32}$$

since $x^+ = t + \varphi$. To first order in dt, this yields

$$\partial_t \tilde{f}(t, x^+) = \dot{\tilde{f}}(t, x^+) + \tilde{f}'(t, x^+) = \tilde{\epsilon}(t, \tilde{f}(t, x^+)), \tag{4.2.33}$$

where $\dot{\tilde{f}}(t, x^+)$ is the derivative with respect to the first argument and $\tilde{f}'(t, x^+)$ with respect to the second argument. $\tilde{\epsilon}(t, x^+)$ may then be obtained by rewriting (4.2.33) in terms of the inverse diffeomorphism $\tilde{F}(t, x^+)$,

$$\tilde{\epsilon}(t, x^+) = \dot{\tilde{f}}(t, \tilde{F}(t, x^+)) + \tilde{f}'(t, \tilde{F}(t, x^+)) = -\frac{\dot{\tilde{F}}(t, x^\pm)}{\tilde{F}'(t, x^\pm)} + \frac{1}{\tilde{F}'(t, x^\pm)}. \tag{4.2.34}$$

Therefore, given a diffeomorphism $f(\tau, x^+)$ with inverse $F(\tau, x^+)$ in the original circuit (4.1.3), the diffeomorphism $\tilde{f}(t, x^+)$ that implements the same circuit with circuit Hamiltonian (4.2.22) after setting $\tau = t$ may be found from the condition

$$\epsilon_{-n} = \int_0^{2\pi} \frac{d\varphi}{2\pi} \frac{\dot{F}(\tau, x^\pm)}{F'(\tau, x^\pm)} e^{in\varphi}\Big|_{\tau=t} \stackrel{!}{=} \int_0^{2\pi} \frac{d\varphi}{2\pi} \left(\frac{\dot{\tilde{F}}(t, x^\pm)}{\tilde{F}'(t, x^\pm)} - \frac{1}{\tilde{F}'(t, x^\pm)} \right) e^{in\varphi}. \tag{4.2.35}$$

This ensures that $Q(\tau)$ and $Q(t) = H(t)$ generate the same circuit.

The second subtlety in the new circuit generated by $Q(t)$ follows directly from (4.2.35). Consider a U(1) transformation $F(\tau, x^+) = x^+ + \alpha(\tau)$. In the circuit (4.1.3), this transformation is generated by L_0. Since the reference state $|0\rangle$ is an eigenstate of L_0, the circuit generates a phase, see also (4.1.15). The U(1) transformation is a Killing symmetry of the dual AdS_3 bulk geometry. Therefore, this transformation does not generate a sequence of different geometries as discussed in sec. 4.1.3 since we remain in the same AdS geometry. In the new circuit generated by $H(t)$, the corresponding diffeomorphism may be determined from (4.2.35). We obtain $\tilde{F}(t, x^+) =$

$x^+ + \beta(t)$, where $\beta(t) = \alpha(t) + t$. This still leaves the reference state invariant as the transformation implements the same circuit with respect to the circuit Hamiltonian $H(t)$. However, the new transformation $\tilde{F}(t, x^+)$ is now coordinate-dependent and thus no longer a Killing symmetry of the global AdS_3 geometry dual to the reference state $|0\rangle$. Therefore, transformations that are Killing symmetries of the bulk spacetime with respect to the circuit generated by $Q(\tau)$ in general are mapped to transformations that are no longer symmetries with respect to the circuit generated by $H(t)$.

Application to an SL(2,R) circuit

To illustrate our circuit construction on an explicit example, we now apply the SL(2,$\mathbb{R}$) circuit studied in [85] to our construction. The circuits in [85] are parameterized in terms of three independent parameters $\gamma_R(\tau), \zeta(\tau), \zeta^*(\tau)$,

$$|\psi(\tau)\rangle = U(\tau)|h\rangle, \quad U(\tau) = e^{i\zeta(\tau)L_{-1}} e^{i\gamma(\tau)L_0} e^{i\zeta_1(\tau)L_1}, \tag{4.2.36}$$

where $\gamma = \gamma_R + i\gamma_I$ with $\gamma_I = -\log(1 - |\zeta|^2)$ and $\zeta_1 = \zeta^* e^{i\gamma_R}$ to ensure the circuit is unitary. The circuit implements the conformal transformation

$$F(\tau, x^+) = -i \log\left(\frac{i e^{i\left(x^+ + \gamma_R(\tau)\right)} - \zeta(\tau)}{i + e^{i(x^+ + \gamma_R(\tau))}\zeta^*(\tau)}\right). \tag{4.2.37}$$

An infinitesimal layer of the circuit is obtained from

$$U(\tau + d\tau) = e^{-i\epsilon_1(\tau)L_{-1}d\tau} e^{-i\epsilon_0(\tau)L_0 d\tau} e^{-i\epsilon_{-1}(\tau)L_1 d\tau} U(\tau), \tag{4.2.38}$$

where

$$\epsilon_n(\tau) = -\int \frac{d\varphi}{2\pi} \frac{\partial_\tau F(\tau, \varphi)}{\partial_\varphi F(\tau, \varphi)} e^{in\varphi}. \tag{4.2.39}$$

This illustrates that the diffeomorphism $\tilde{F}$ in our circuit must have Fourier modes (4.2.35) to ensure the circuit implements the same sequence of states. The Fourier modes for the transformation (4.2.37) read

$$\begin{aligned}
\epsilon_{-1}(\tau) &= -\frac{e^{-i\gamma_R(\tau)}\dot{\zeta}(\tau)}{1 - |\zeta(\tau)|^2} \\
\epsilon_0(\tau) &= -\frac{i\zeta(\tau)\dot{\zeta}^*(\tau) + \dot{\gamma}_R(\tau)(1 - |\zeta(\tau)|^2) - i\zeta^*(\tau)\dot{\zeta}(\tau)}{1 - |\zeta(\tau)|^2} \\
\epsilon_1(\tau) &= -\frac{e^{i\gamma_R(\tau)}\dot{\zeta}^*(\tau)}{1 - |\zeta(\tau)|^2},
\end{aligned} \tag{4.2.40}$$

and the Fubini-Study metric obtained from (4.1.12) is given by [85]

$$\mathrm{d}s^2_{FS} = 2h\left[\frac{\mathrm{d}\zeta\mathrm{d}\zeta^*}{(1-|\zeta|^2)^2} + \frac{\mathrm{d}\bar{\zeta}\mathrm{d}\bar{\zeta}^*}{\left(1-|\bar{\zeta}|^2\right)^2}\right]. \tag{4.2.41}$$

We now determine the diffeomorphism $\tilde{F}$ that satisfies (4.2.35) with Fourier modes (4.2.40). Since the new diffeomorphism $\tilde{F}$ must still be an SL(2,$\mathbb{R}$) transformation, we have to ensure that ϵ_n has only three Fourier modes $n = \{-1, 0, 1\}$. We therefore first choose a general parameterization for the SL(2,$\mathbb{R}$) transformation. A convenient choice is

$$\tilde{F}(t, x^{\pm}) = -i\log\left(\frac{ie^{i(x^+ + \alpha_R(t))} - \beta(t)}{i + e^{i(x^+ + \alpha_R(t))}\beta^*(t)}\right), \tag{4.2.42}$$

where $\alpha_R(t)$ is real. We now split $\beta(t)$ into a real and imaginary part, $\beta(t) = \beta_R(t) + i\beta_I(t)$ and determine the unknown functions such that (4.2.35) is satisfied. This yields

$$\tilde{F}(t, x^{+}) = -i\log\left(\frac{ie^{i(x^+ + \alpha_R(t))} - \zeta(t)}{i + e^{i(x^+ + \alpha_R(t))}\zeta^*(t)}\right), \tag{4.2.43}$$

where $\alpha_R(t) = t + \gamma_R(t)$. Therefore, the transformation implementing the circuit in [85] as a time evolution of the boundary geometry is identical to (4.2.37) up to a time shift originating from identifying $\tau = t$. Furthermore, upon determining the inverse diffeomorphism $\tilde{f}(t, x^+)$ and inserting it into (4.2.43) with the identification $\tau = t$, we recover (4.2.41) with τ replaced by t. The authors of [85] derived a gravitational dual to (4.2.41) that we will now discuss in the context of our circuit construction.

Holographic dual to Fubini-Study distance for SL(2,R) circuits

The authors in [85] considered the SL(2,$\mathbb{R}$) circuit when acting on a highest-weight state $|h\rangle$ that is dual to a conical defect geometry and therefore a massive particle in AdS_3. The circuit (4.2.36) may then be interpreted in the sequence of disconnected geometries discussed in sec. 4.1.3, where for every infinitesimal layer of the circuit, a new AdS_3 geometry with a particle is generated in conformally transformed coordinates. In the global AdS_3 coordinates (2.2.7), the coordinates transform as follows

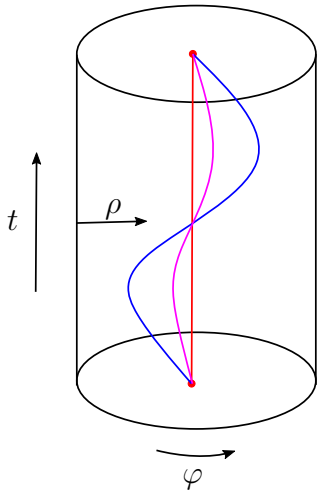

Fig. 4.4.: The initial straight-line trajetory of a particle in empty AdS (red) is boosted by an SL(2,ℝ) transformation. Boosts with different parameters yield different circular trajectories (pink, blue).

under a conformal transformation:

$$\begin{aligned} t &\to \frac{f(\tau,x^+)+\bar{f}(\tau,x^-)}{2}, \\ \varphi &\to \frac{f(\tau,x^+)-\bar{f}(\tau,x^-)}{2}, \\ \rho &\to \rho - \frac{1}{2}\log(f'(\tau,x^+)\bar{f}'(\tau,x^-)). \end{aligned} \tag{4.2.44}$$

Therefore, for every τ there is a new geometry. In the coordinates (2.2.7), the massive particle giving rise to the conical defect geometry moves along the trajectory (2.2.21). In the new coordinates, the particle then moves along the same trajectory in different coordinates. Note, however, that AdS_3 has an SL(2,ℝ) isometry. Therefore, the new sequence of geometries may alternatively be described by boosting the massive particle with trajectory (2.2.21) with an SL(2,ℝ) boost rather than transforming the coordinates. This yields a family of particle trajectories in global AdS_3 that encode the particular conical defect geometry dual to the circuit generated by (4.2.36) in the boosted trajectories. An illustration of the boosted trajectories is shown in fig 4.4. Of course, transforming the coordinate system and boosting the trajectory are equivalent descriptions of the same system since one corresponds to a passive transformation, whereas the other one is an active transformation. The authors in [85] then observed that the Fubini-Study metric (4.2.41) may be recovered from the family of boosted particle trajectories in AdS_3. Given a geodesic X^A in the covering space (2.2.4), the Fubini-Study metric is given in terms of the spacelike components X^a of the timelike

trajectory,

$$\mathrm{d}s^2_{\mathrm{FS}} = \frac{h}{2}\left(\delta X^2_{\mathrm{perp,min}} + \delta X^2_{\mathrm{perp,max}}\right), \tag{4.2.45}$$

where $X_{\mathrm{perp,min\,/\,max}}$ are the minimal and maximal perpendicular distance between two infinitesimally close geodesics in the embedding space (2.2.4). We give an explicit formula for the geodesics $X^A(t)$ in app. A.1.

The main drawback of this construction of a dual to the Fubini-Study distance is the lack of generalizability beyond conical defect geometries and SL(2,$\mathbb{R}$) transformations since the derivation of the dual makes explicit use of the SL(2,$\mathbb{R}$) boost isometries of global AdS_3. Furthermore, in our construction the SL(2,$\mathbb{R}$) transformations are no longer isometries of AdS_3 for a general choice of function $\zeta(t), \gamma(t)$ since the diffeomorphisms become explicitly coordinate dependent after identifying $\tau = t$. Nevertheless, the Fubini-Study metric still exhibits the isometries of the dual state. Therefore, in our circuit construction, which implements the circuit as a time evolution of the bulk spacetime, we should choose a geometric object that is invariant under these isometries. This is no longer true of timelike trajectories for particles due to the explicit time dependence of the transformations, but still holds for spacelike geodesics.

4.3. Gravity Dual to Fubini-Study Distance

In this section, we derive a dual to the Fubini-Study distance as a cost measure for general diffeomorphisms $x^+ \to f(t, x^+)$ in our circuit construction that holds beyond SL(2,$\mathbb{R}$) transformations and is valid for empty AdS, the conical defect, and BTZ geometries. The dual bulk observable to the Fubini-Study distance we obtain is a complicated geometric object given in terms of spacelike geodesics anchored in the boundary at the points where the energy-momentum tensor is inserted. This is the first construction of a dual to a CFT cost function that follows from first principles.

General approach

We begin by considering a trivial evolution of the circuit with the standard Hamiltonian (4.2.8). When the circuit acts on the vacuum state $|0\rangle$, a trivial time evolution is generated. In the dual bulk spacetime, the time evolution with (4.2.8) is an isometry of the global AdS_3 bulk geometry. The Fubini-Study metric (4.1.12) vanishes for such transformations. However, the connected energy-momentum tensor two-point function $\langle 0|T(x_1^+)T(x_2^+)|0\rangle_{\mathrm{conn}} = \langle 0|T(x_1^+)T(x_2^+)|0\rangle - \langle 0|T(x_1^+)|0\rangle\langle 0|T(x_2^+)|0\rangle$ in the

vacuum does not vanish and reads

$$\langle 0|T(x_1^+)T(x_2^+)|0\rangle_{\text{conn}} = \frac{c}{32\sin((x_1^+ - x_2^+)/2)^4}. \tag{4.3.1}$$

This two-point function may be written in terms of a spacelike geodesic in empty AdS. The procedure to obtain the geodesic length of a spacelike geodesic in a general static geometry such as empty AdS or the conical defect is described in app. A.2. The length of the geodesic in the empty AdS geometry (2.2.3) is then obtained by setting $\alpha = 1$ in (A.2.5), which yields the result

$$L = \log\left[\frac{\sin\left(\left(x_1^+ - x_2^+\right)/2\right)\sin\left(\left(x_1^- - x_2^-\right)/2\right)}{\epsilon_{\text{UV}}^2}\right] = \log\left[\frac{\cos(\varphi_1-\varphi_2)-\cos(t_1-t_2)}{2\epsilon_{\text{UV}}^2}\right], \tag{4.3.2}$$

where ϵ_{UV} is a UV cutoff. We then find that we may write the connected two-point function (4.3.1) as follows:

$$\begin{aligned}\langle T(x_1^+)T(x_2^+)\rangle_{\text{conn}} + \langle \bar{T}(x_1^-)\bar{T}(x_2^-)\rangle_{\text{conn}} &= \frac{c}{2}\left(\left(\partial_{x_1^+}\partial_{x_2^+}L\right)^2 + \left(\partial_{x_1^-}\partial_{x_2^-}L\right)^2\right)\\ &= \frac{c}{4}\left(\partial_{t_1}\partial_{t_2}L\partial_{\varphi_1}\partial_{\varphi_2}L + \partial_{t_1}\partial_{\varphi_2}L\partial_{t_2}\partial_{\varphi_1}L\right).\end{aligned} \tag{4.3.3}$$

Next, we apply this observation to our circuit construction from sec. 4.2.2. The circuit geometry is obtained from the transformations $x^+ \to f(t,x^+)$ and $x^- \to \bar{f}(t,x^-)$. From (4.2.25), we then obtain the metric tensor in t,φ-coordinates,

$$g_{ij}^{(0)}(t,\varphi) = -\begin{pmatrix}\partial_t f(t,\varphi)\partial_t\bar{f}(t,\varphi) & \frac{1}{2}\left(\partial_t f(t,\varphi)\partial_\varphi\bar{f}(t,\varphi) + \partial_\varphi f(t,\varphi)\partial_t\bar{f}(t,\varphi)\right)\\ g_{t\varphi}^{(0)} & \partial_\varphi f(t,\varphi)\partial_\varphi\bar{f}(t,\varphi)\end{pmatrix}. \tag{4.3.4}$$

We now write the Fubini-Study distance as an integral over the Hamiltonian densities $\mathcal{H}$ associated to the physical Hamiltonian governing time evolution in the spacetime. This yields

$$\begin{aligned}F_{\text{FS}}(t) &= \int d\varphi_1 \int d\varphi_2 \sqrt{g_{(0)}(t,\varphi_1)}\sqrt{g_{(0)}(t,\varphi_2)}\,\langle \mathcal{H}(t,\varphi_1)\,\mathcal{H}(t,\varphi_2)\rangle\\ &= \int d\varphi_1 \int d\varphi_2\,\big(\partial_{\varphi_1}f_1\partial_{t_1}f_1\partial_{\varphi_2}f_2\partial_{t_2}f_2\,\langle T(f_1)\,T(f_2)\rangle\\ &\qquad + \partial_{\varphi_1}\bar{f}_1\partial_{t_1}\bar{f}_1\partial_{\varphi_2}\bar{f}_2\partial_{t_2}\bar{f}_2\langle\bar{T}(\bar{f}_1)\bar{T}(\bar{f}_2)\rangle\big),\end{aligned} \tag{4.3.5}$$

where the index i in f_i refers to the coordinate dependence, for example $f_1 \equiv f(t,\varphi_1)$. In the next step, we combine the result (4.3.3) for the connected two-point function under a trivial time evolution with our knowledge of the background metric (4.3.4) and

the Hamiltonian two-point function in (4.3.5). In this manner, we obtain an expression for the Hamiltonian densities in terms of spacelike geodesics in the dual bulk geometry with boundary metric (4.3.4),

$$\begin{aligned}
&\sqrt{g_{(0)}\left(t_1,\varphi_1\right)}\sqrt{g_{(0)}\left(t_2,\varphi_2\right)}\left\langle\mathcal{H}\left(t_1,\varphi_1\right)\mathcal{H}\left(t_2,\varphi_2\right)\right\rangle \\
&= \frac{c}{4}\sum_{k=0}^{n_{\max}}\Big[\left(\partial_{\varphi_1}\partial_{\varphi_2}L_{(k)}\right)\left(\partial_{t_1}\partial_{t_2}L_{(k)}\right)+\left(\partial_{\varphi_1}\partial_{t_2}L_{(k)}\right)\left(\partial_{t_1}\partial_{\varphi_2}L_{(k)}\right) \\
&\quad -\frac{1}{2}g^{(0)}_{t_1\varphi_1}g^{(0)}_{t_2\varphi_2}g^{ij}_{(0)}\left(t_1,\varphi_1\right)g^{kl}_{(0)}\left(t_2,\varphi_2\right)\left(\partial_i\partial_k L_{(k)}\right)\left(\partial_j\partial_l L_{(k)}\right)\Big] \\
&= \mathcal{F}_{\text{bulk}}\,.
\end{aligned} \tag{4.3.6}$$

The sum is necessary to obtain the correct Fubini-Study metric in geometries with non-trivial topologies, where winding geodesics with winding numbers k become relevant. We sum over all winding geodesics to the maximal winding number $n_{\max}$, which is system dependent. In geometries with trivial topologies, the sum reduces to a single term as winding geodesics do not exist. We will explain this in detail when discussing concrete examples below. The bulk dual to Fubini-Study distance is then obtained by identifying $t_1 = t_2 = t$ after evaluating the derivatives in (4.3.6) and integrating over the spacelike boundary direction,

$$\begin{aligned}
F_{\text{FS}}(t) &= \int d\varphi_1\int d\varphi_2\sqrt{g_{(0)}\left(t,\varphi_1\right)}\sqrt{g_{(0)}\left(t,\varphi_2\right)}\left\langle\mathcal{H}\left(t,\varphi_1\right)\mathcal{H}\left(t,\varphi_2\right)\right\rangle \\
&= F_{\text{bulk}}\left(t\right) = \int d\varphi_1\int d\varphi_2\,\mathcal{F}_{\text{bulk}}\,,
\end{aligned} \tag{4.3.7}$$

We now show that (4.3.6) holds for empty AdS, the conical defect, and the BTZ black string geometries.

Empty AdS

The geodesic length in the transformed empty AdS bulk geometry with boundary metric (4.3.4) is straightforwardly obtained from (4.3.2) since scalars such as the geodesic length do not transform under coordinate transformations. Therefore, we may simply replace $x^+ \to f(t,x^+)$, $x^- \to \bar{f}(t,x^-)$ in (4.3.2) and transform the cutoff ϵ_{UV}. Since the Fubini-Study metric does not depend on the bulk cutoff, the cutoff term is irrelevant and vanishes when evaluating (4.3.6). We therefore from now on employ the regularized length L_{reg}, which is the geodesic length without its divergent piece,

$$L_{\text{reg}} = \log\left[\sin\left(\left(f\left(t_1,\varphi_1\right)-f\left(t_2,\varphi_2\right)\right)/2\right)\sin\left(\left(\bar{f}(t_1,\varphi_1)-\bar{f}(t_2,\varphi_2)\right)/2\right)\right]. \tag{4.3.8}$$

Note that empty AdS is a topologically trivial geometry since there are no defects or other punctures. In such a geometry, winding geodesics do not exists and the sum in (4.3.6) reduces to a single term. Inserting the geodesic length (4.3.8) and the metric tensor (4.3.4) into (4.3.6) then yields

$$\begin{aligned}\mathcal{F}_{\text{bulk}} &= \\ \partial_{\varphi_1} f_1 \partial_{t_1} f_1 \partial_{\varphi_2} f_2 \partial_{t_2} f_2 &\frac{c}{32 \sin((f(t_1,\varphi_1) - f(t_2,\varphi_2))/2)^4} \\ +\partial_{\varphi_1} \bar{f}_1 \partial_{t_1} \bar{f}_1 \partial_{\varphi_2} \bar{f}_2 \partial_{t_2} \bar{f}_2 &\frac{c}{32 \sin((\bar{f}(t_1,\varphi_1) - \bar{f}(t_2,\varphi_2))/2)^4}.\end{aligned} \tag{4.3.9}$$

The same result is obtained by first transforming (4.3.1), which yields

$$\langle 0|T(f(t_1,\varphi_1))T(f(t_2,\varphi_2))|0\rangle_{\text{conn}} = \frac{c}{32 \sin((f(t_1,\varphi_1) - f(t_2,\varphi_2))/2)^4}, \tag{4.3.10}$$

and similarly for $\langle 0|\bar{T}(\bar{f}(t_1,\varphi_1))\bar{T}(\bar{f}(t_2,\varphi_2))|0\rangle_{\text{conn}}$, and then inserting this result into (4.3.5). Therefore, we have shown that (4.3.6) holds true for empty AdS. We now continue with the conical defect geometry.

Conical defect

For the conical defect, we may either obtain the geodesics from the procedure in app. A.2 by setting $\alpha = \frac{1}{n^2}$ or by making use of the fact that empty AdS is the n-fold cover of the conical defect [71]. The geodesic length is then given by

$$L_{\text{reg}} = \log\left[\sin\left(\frac{x_1^+ - x_2^+ + 2\pi k}{2n}\right)\sin\left(\frac{x_1^- - x_2^- + 2\pi k}{2n}\right)\right]. \tag{4.3.11}$$

The conical defect is a geometry with non-trivial topology induced by the point particle. It was shown in [71] that in such geometries there are multiple geodesics that connect the same points in the boundary. These geodesics have different winding numbers k, which range from $k = 0$ to $n - 1$, where n is given in terms of the mass of the point particle $m = -\frac{1}{4n^2}$. An example of a winding geodesic on a constant time slice is shown in fig. 4.5. Following the same procedure as before, the geodesic length in the transformed geometry is given by

$$L_{\text{reg}} = \log\left[\sin\left(\frac{f(t_1,\varphi_1) - f(t_2,\varphi_2) + 2\pi k}{2n}\right)\sin\left(\frac{\bar{f}(t_1,\varphi_1) - \bar{f}(t_2,\varphi_2) + 2\pi k}{2n}\right)\right]. \tag{4.3.12}$$

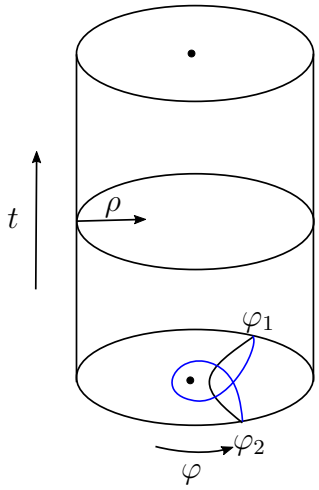

Fig. 4.5.: An example of a winding (blue) and non-winding (black) spacelike geodesic ending at the same endpoints φ_1 and φ_2 on the boundary in a conical defect geometry.

Inserting the geodesic length into (4.3.6) yields

$$\begin{aligned}&\mathcal{F}_{\text{bulk}} = \\ &\sum_{k=0}^{n-1}\left(\partial_{\varphi_1}f_1\partial_{t_1}f_1\partial_{\varphi_2}f_2\partial_{t_2}f_2\frac{c}{32\sin\left(\left(f(t_1,\varphi_1)-f(t_2,\varphi_2)+2\pi k\right)/(2n)\right)^4}\right. \\ &\left.+\,\partial_{\varphi_1}\bar{f}_1\partial_{t_1}\bar{f}_1\partial_{\varphi_2}\bar{f}_2\partial_{t_2}\bar{f}_2\frac{c}{32\sin((\bar{f}(t_1,\varphi_1)-\bar{f}(t_2,\varphi_2)+2\pi k)/(2n))^4}\right).\end{aligned} \tag{4.3.13}$$

In the final step, we evaluate the sum over the different winding numbers. We are not aware that an analytic expression for the sum exists and therefore proceed numerically. We checked for maximal winding numbers up to $n_{\max} = n-1 = 1000$ that

$$\begin{aligned}&\sum_{k=0}^{n-1}\frac{c}{32\sin\left(\left(f(t_1,\varphi_1)-f(t_2,\varphi_2)+2\pi k\right)/(2n)\right)^4} \\ &=\frac{c}{32\sin\left(\left(f(t_1,\varphi_1)-f(t_2,\varphi_2)\right)/2\right)^4}-\frac{c}{48}\left(1-\frac{1}{n^2}\right)\frac{1}{\sin\left(\left(f(t_1,\varphi_1)-f(t_2,\varphi_2)\right)/2\right)^2}.\end{aligned} \tag{4.3.14}$$

Therefore, the bulk dual to the Fubini-Study distance is given by

$$\begin{aligned}&\mathcal{F}_{\text{bulk}} = \\ &\partial_{\varphi_1}f_1\partial_{t_1}f_1\partial_{\varphi_2}f_2\partial_{t_2}f_2\left(\frac{c}{32\sin\left(\left(f_1-f_2\right)/2\right)^4}-\frac{c}{48}\left(1-\frac{1}{n^2}\right)\frac{1}{\sin\left(\left(f_1-f_2\right)/2\right)^2}\right) \\ &+\partial_{\varphi_1}\bar{f}_1\partial_{t_1}\bar{f}_1\partial_{\varphi_2}\bar{f}_2\partial_{t_2}\bar{f}_2\left(\frac{c}{32\sin((\bar{f}_1-\bar{f}_2)/2)^4}-\frac{c}{48}\left(1-\frac{1}{n^2}\right)\frac{1}{\sin((\bar{f}_1-\bar{f}_2)/2)^2}\right).\end{aligned} \tag{4.3.15}$$

In the dual CFT, the two-point function of the energy-momentum tensor for the conical defect is obtained by setting $h = \frac{c}{24}\left(1 - \frac{1}{n^2}\right)$ [138]. Therefore, we find from (4.1.19) that the connected two-point function in the transformed coordinates reads

$$\begin{aligned} &\langle h|T\left(f(t_1,\varphi_1)\right)T\left(f(t_2,\varphi_2)\right)|h\rangle \\ &= \frac{c}{32\sin((f(t_1,\varphi_1)-f(t_2,\varphi_2))/2)^4} - \frac{c}{48}\left(1-\frac{1}{n^2}\right)\frac{1}{\sin(f(t_1,\varphi_1)-f(t_2,\varphi_2)/2)^2}. \end{aligned} \tag{4.3.16}$$

Upon inserting (4.3.16) and its right-moving counterpart into (4.3.5), we find that the result agrees with (4.3.15).

BTZ black string

The BTZ black string geometry is obtained from the BTZ black hole (2.2.11) by unwrapping the angle such that $-\infty < \varphi < \infty$. The horizon is therefore non-compact. This implies that in contrast to the black hole the geometry of the black string is topologically trivial, and there are no winding geodesics. There are two dual CFTs living on the asymptotic boundary regions. Following the procedure outlined in app. A.2 with $\alpha = -m$ for the BTZ black string, we obtain two different types of geodesics: There are geodesics that connect boundary points at the same boundary, and ones that connect points across the horizon in the left and right boundary by stretching between both boundaries. Both types of geodesics have different geodesic length,

$$\begin{aligned} &\text{between boundaries: } L_{\text{reg}} = \log\left[2\cosh\left(\frac{\pi}{\beta}(x_1^+ - x_2^+)\right)\cosh\left(\frac{\pi}{\beta}(x_1^- - x_2^-)\right)\right], \\ &\text{same boundary: } L_{\text{reg}} = \log\left[2\sinh\left(\frac{\pi}{\beta}(x_1^+ - x_2^+)\right)\sinh\left(\frac{2\pi}{\beta}(x_1^- - x_2^-)\right)\right]. \end{aligned} \tag{4.3.17}$$

In the transformed coordinates, the geodesic lengths are straightforwardly obtained. For instance, the geodesic length for the geodesic stretching between both boundaries reads

$$L_{\text{reg}} = \log\left[2\sinh\left(\frac{\pi}{\beta}\left(f_1 - f_2\right)\right)\sinh\left(\frac{\pi}{\beta}\left(\bar{f}_1 - \bar{f}_2\right)\right)\right]. \tag{4.3.18}$$

Upon inserting the two types of geodesics into (4.3.6), we find that the Fubini-Study distance is given in terms of geodesics that stretch between both boundaries,

$$\begin{aligned}\mathcal{F}_{\text{bulk}} &= \\ &\frac{c}{32}\left(\frac{2\pi}{\beta}\right)^4 \partial_{\varphi_1} f_1 \partial_{t_1} f_1 \partial_{\varphi_2} f_2 \partial_{t_2} f_2 \frac{1}{\sinh^4\left(\frac{\pi}{\beta}\left(f(t_1,\varphi_1)-f(t_2,\varphi_2)\right)\right)} \\ &+\frac{c}{32}\left(\frac{2\pi}{\beta}\right) \partial_{\varphi_1} \bar{f}_1 \partial_{t_1} \bar{f}_1 \partial_{\varphi_2} \bar{f}_2 \partial_{t_2} \bar{f}_2 \frac{1}{\sinh^4\left(\frac{\pi}{\beta}\left(\bar{f}(t_1,\varphi_1)-\bar{f}(t_2,\varphi_2)\right)\right)}.\end{aligned} \tag{4.3.19}$$

This result may be verified from the CFT perspective by inserting the connected two-point function for the energy-momentum tensor for a CFT dual to the BTZ black string into (4.3.5). The CFT is thermal with a temperature matching the Hawking-temperature T_{H} of the BTZ black string. Its two-point function is obtained by mapping the vacuum two-point function (2.1.18) with $z = e^{\frac{2\pi}{\beta}(\varphi+it_E)}$ to the cylinder with compact Euclidean time direction $t_E \sim t_E + \beta$ and $t_E = -it$, where $\beta = \frac{1}{T_{\text{H}}}$. In the transformed coordinates, this yields

$$\langle T\left(f(t_1,\varphi_1)\right) T\left(f(t_2,\varphi_2)\right)\rangle_\beta = \frac{c}{32}\left(\frac{2\pi}{\beta}\right)^4 \frac{1}{\sinh^4\left(\frac{\pi}{\beta}\left(f(t_1,\varphi_1)-f(t_2,\varphi_2)\right)\right)}. \tag{4.3.20}$$

The right-moving component is obtained analogously. Upon inserting the thermal two-point function into (4.3.5), we have verified the result (4.3.19). Therefore, we have shown that (4.3.6) holds true in a BTZ black string geometry for a geodesic connecting points in the left and right boundary by stretching through the bulk. The result may furthermore be generalized to the BTZ black hole geometry with compact horizon by including winding geodesics. This is straightforwardly accomplished by replacing $\varphi_1 - \varphi_2 \to \varphi_1 - \varphi_2 + 2\pi k$ and summing over winding numbers.

4.4. Summary and Discussion

In this chapter, we derived a holographic dual to quantum circuits that employ the CFT energy-momentum tensor to generate the circuits. The construction involves identifying the auxiliary circuit parameter τ with the physical time t. In the next step, the circuit Hamiltonian $Q(t)$ is then identified with the physical Hamiltonian generating time evolution in the CFT to find the diffeomorphisms that implement the circuit generated by $Q(t)$ as a time evolution of the background metric. Once the diffeomorphisms are identified, the sequence of states $|\psi(t)\rangle$ generated by the circuit

is then encoded in the time evolution of the boundary spacetime on which the CFT lives. Furthermore, the evolution of the energy-momentum tensor is fixed as well by our construction as it is conserved with respect to the background metric. In three-dimensional gravity, the energy-momentum tensor and the boundary metric are sufficient to reconstruct the dual bulk geometry. This allows us to derive a bulk dual to a quantum circuit from the Fefferman-Graham expansion. Since the boundary metric is flat at all times, the circuit is encoded in the choice of time foliation in the boundary and dual bulk geometry. We discussed our circuit construction on the example of SL(2,$\mathbb{R}$) circuits acting on an excited state dual to a conical defect that were studied in [85] and commented on the construction of a dual to the Fubini-Study distance in terms of timelike geodesics presented in [85] for this special class of circuits within our new circuit construction. We argued that the approach in [85] is not convenient in our framework. In particular, timelike geodesics are no longer invariant under U(1) transformations in our dual geometry to the circuit since the transformations become explicitly coordinate-dependent. Instead we proposed spacelike geodesics as a natural invariant object and showed that we may employ these to construct a dual to Fubini-Study distance from first principles. Our dual to Fubini-Study distance is valid for general diffeomorphisms beyond SL(2,$\mathbb{R}$) transformations and is applicable in empty AdS, conical defect, and BTZ geometries.

It is evident that the dual bulk object (4.3.6) is geometric as it is constructed in terms of the length of spacelike geodesics and the boundary metric. However, it is currently not clear whether (4.3.6) may be rewritten in terms of a simpler geometric object. We can already exclude the volume as a possible candidate as the volume is UV divergent and does not agree with the Fubini-Study distance as shown in [1]. A good starting point to make progress is empty AdS, where the dual is given in terms of Ryu-Takayanagi geodesics yielding the entanglement entropy. These geodesics define the kinematic space, which is the set of intervals $[\varphi_1, \varphi_2]$ on a constant time slice in the CFT. In [230, 231] for instance, the volume of a subregion Q on kinematic space was defined in terms of the spacelike geodesics length,

$$V_Q \propto \int_{G_Q} d\varphi_1 d\varphi_2 \lambda_Q \partial_{\varphi_1} \partial_{\varphi_2} L, \tag{4.4.1}$$

where Q is the subregion of interest, λ_Q the length of the part of the geodesic that intersects Q, and G_Q the set of all geodesics intersecting Q. It would then be interesting to understand if (4.3.6) may be rewritten in terms of a simpler geometric object on kinematic space and how it fits within the existing holographic complexity proposals discussed in sec. 3.3. For instance, the geodesics contributing to the bulk dual (4.3.6)

form a codimension-zero surface filling a spacetime region over a time-band determined by the length of the circuit. In contrast, the complexity=anything proposal [84] defines the holographic complexity as an observable on a codimension-zero surface that asymptotes to a single constant time slice in the boundary.

Furthermore, we would like to comment that our construction is special to three bulk dimensions as in higher dimensions, the Fefferman-Graham expansion that is essential in obtaining the dual bulk geometry does not terminate after a finite number of terms [135]. It is not immediately clear if or how our construction may be extended to higher dimensions. Finally, we consider only circuits with energy-momentum tensor insertions. However, our construction is general enough to include other fields. For instance, by allowing heavy primary fields to act in the circuit, shockwave geometries [80] may be studied from the CFT point of view. These are essential to study the switchback effect. In these geometries, (4.3.6) is no longer true as we consider only circuits with energy-momentum tensor insertions. It would be interesting to derive the dual to Fubini-Study distance once primary fields are included in the circuit.

The Eternal Black Hole: Factorization and Berry Phases

5

The eternal black hole and its CFT dual, the TFD state (3.2.1), raise an interesting conundrum within the AdS/CFT correspondence. The CFT Hilbert space on which the TFD state is defined is a tensor product of the Hilbert space of the left and right CFT. On the other hand, the presence of the wormhole – a classically connected geometry – in the dual bulk spacetime prevents a similar factorization of the bulk Hilbert space. Since both theories are dual, we would expected that they have the same Hilbert space structure. This apparent contradiction is called the *factorization problem*. This problem was first observed in [232] and studied in [89, 90, 233–235] for gauge theory toy models and lower-dimensional gravity theories such as AdS_2, where explicit calculations are more manageable. The factorization problem has its origin in the semiclassical approximation of AdS/CFT that is employed when performing calculations [89]. It is expected that in a full quantum version, the problem is not present. In particular, it is expected that the factorization of the CFT Hilbert space does not hold in general [91]. Since it is extremely difficult to make progress in the appropriate quantum treatment without understanding quantum gravity, calculations have been focused on understanding the implications of explicitly factorizing the bulk Hilbert space manually [234, 236]. In this section, we take a different approach. We argue that the non-factorization of the bulk Hilbert space induced by the wormhole may be treated as a topological problem. The topology of a wormhole representing the connected bulk spacetime is different from the topology of a disconnected spacetime that gives rise to a factorized Hilbert space. Therefore, we propose that the wormhole may be probed by a topological quantity. Based on results for topological wormholes in quantum mechanical systems [185], we employ Berry phases as probes of the spacetime wormhole in the eternal AdS black hole geometry. We show that we may distinguish three types of Berry phases that are sensitive to the presence of the wormhole: The Virasoro Berry phase which arises from independent conformal transformations in each boundary CFT, the gauge Berry phase obtained from an independent choice of time coordinate in each boundary, and the modular Berry phase obtained from parallel transport of intervals on a constant time slice.

We then employ recent results [69, 70, 91] that discuss the algebra of bulk operators in the exterior regions of the eternal AdS black hole in the abstract language of von

Neumann algebras to interpret our results. For the Virasoro Berry phase, we show that upon taking appropriate boundary limits, the non-factorization of the boundary Hilbert space may be seen from this Berry phase even in the semiclassical approximation. We then argue that quantizing the base space of the fiber bundle from which the Berry phase is obtained yields the appropriate non-factorized CFT Hilbert space expected from the dual bulk theory. We furthermore illustrate that the factorization problem has its origin in the type of von Neumann algebra that is implicitly assumed when defining the TFD Hilbert space. Employing von Neumann algebras, we furthermore argue that the gauge and modular Berry phases do not probe the factorization of the Hilbert space but the presence of a non-trivial center in the von Neumann algebra describing the wormhole geometry in the semiclassical limit. Finally, we comment that Berry phases are related to missing information from global symmetries for a local observer.

We review the arguments behind the factorization problem in sec. 5.1. In sec. 5.2, we introduce Berry phases as measures of non-factorization based on the proposal [185]. In sec. 5.3, we calculate the Virasoro Berry phase in the presence of a wormhole and demonstrate that the Berry phase couples both CFTs. In sec. 5.4, we show that modular Berry phases are also sensitive to the bulk wormhole. In sec. 5.5, we discuss gauge Berry phases. Finally, we interpret our results in the language of von Neumann algebras in sec. 5.6 and elaborate on the relation to missing information. The new results presented in this chapter appeared in [3, 4].

5.1. The Factorization Problem

Here, we explain the factorization problem in detail on two examples considered in the literature [89, 90]. The factorization problem arises from the ER=EPR proposal presented in sec. 3.2. Let us begin by first considering the CFT perspective. The CFTs dual to the eternal AdS black hole are in the maximally entangled TFD state (3.2.1) built from energy-eigenstates $|E_n\rangle$ of a CFT on the right boundary and its identical copy on the left boundary of the eternal AdS black hole. Since the CFTs are causally separated by the black hole horizon in the bulk, there is no classical interaction between them, and the Hilbert space of both CFTs is expected to have a tensor product structure $\mathcal{H}_L \otimes \mathcal{H}_R$. Quantum correlations, on the other hand, are clearly present between the CFTs and have their origin in the highly entangled nature of the TFD state. We would like to stress the difference between state and Hilbert space factorization. The TFD state is an entangled state, which cannot be written as

a tensor product of states in the left and right CFTs, $|\text{TFD}\rangle \neq |E_n\rangle_L \otimes |E_n\rangle_R$. This non-factorization of the state gives rise to quantum correlations between the left and right CFT. A factorization of the full Hilbert space $\mathcal{H}_L \otimes \mathcal{H}_R$ of the CFTs, on the other hand, implies the absence of classical interactions between the theories. It is the factorization of the CFT Hilbert space that gives rise to the factorization puzzle. This may be seen by considering the dual bulk perspective. ER=EPR implies the presence of a wormhole in the bulk geometry. Therefore, the eternal AdS black hole is a single classically connected geometry. Furthermore, the connectedness of the bulk geometry is essential in defining bulk duals to correlation functions for operators in the left and right CFT. These duals include, for example, geodesics that stretch through the wormhole. The existence of such objects implies that the Hilbert space of the effective low-energy bulk theory that emerges in the semiclassical limit cannot factorize in a left and right Hilbert space. This contradiction in the structure of the bulk and CFT Hilbert spaces is the factorization puzzle.

An illustrative example considered in [89] is a Wilson line connecting the two boundaries through a wormhole in the presence of a U(1) gauge theory in the eternal AdS black hole background. This is a theory of electromagnetism on an eternal AdS black hole geometry. The Wilson line $\mathcal{W}$ in a charge-q representation along the curve C is given in terms of the gauge potential A_μ,

$$\mathcal{W}(C) = e^{iq\int_C A}. \tag{5.1.1}$$

In an eternal AdS black hole geometry, the Wilson line may for instance connect both boundaries through the wormhole. Upon acting with the Wilson line on the Hartle-Hawking state describing the bulk at a given constant time slice, an electric flux through the wormhole is created. The existence of such a Wilson line is therefore directly linked to the existence of the wormhole and hence a connected bulk geometry. In AdS/CFT, the Wilson line should have a dual representation in terms of CFT operators. But the Wilson line cannot be straightforwardly written in terms of factorized CFTs. When cutting the Wilson lines, we obtain operators that are not invariant under gauge transformations in the left or right CFTs separately. We then create additional charged states in each CFT.

Furthermore, the factorization problem also emerges without a gauge theory in the black hole background. This brings us to a second example illustrating the factorization problem. A tangible toy model that is often considered is JT gravity on AdS_2 [89, 90]. The action is given by the Einstein-Hilbert action coupled to a dynamical scalar field called the dilaton. For details, we refer to [237]. This setup was employed to

study the factorization problem in [90]. The solution to the gravitational action is a two-sided black hole in AdS_2 with two boundaries. The authors of [90] considered the phase space of the model and its quantization. The phase space is given in terms of the full system Hamiltonian $H = H_L + H_R$, where $H_{L/R}$ is the Hamiltonian of the left/right boundary theory, and a time shift δ. The time shift is a relative shift between the time coordinates in the left and right boundaries. It was shown that the symplectic form on the phase space is given by

$$\omega = d\delta \wedge dH. \tag{5.1.2}$$

This result implies that the classical phase space as well as the quantized Hilbert space cannot be written in terms of a tensor product required for factorization. A simple argument given in [238] is that the time shift δ is not a local variable of the left or right CFT, but a non-local shift that cannot be measured by a single observer. Since the time shift is between the left and right boundary, which are separated by the horizon of the black hole, no single observer can measure it. Instead two observers must enter the wormhole and compare their clocks when they meet inside the wormhole. This will allow them to measure the time shift.

The source of the factorization problem lies in an incomplete understanding of the bulk and boundary theories. In sec. 2.3.2, we discussed that the holographic dictionary for the AdS/CFT correspondence is employed in a semiclassical limit since the full quantum theory is poorly understood. In this low-energy limit, the bulk theory reduces from a theory of quantum gravity to an effective field theory, where we lose access to UV degrees of freedom. It has been suggested in [89] that these UV degrees of freedom are essential to fully capture low-energy dynamics in the CFTs. It is expected that the factorization puzzle does not appear in the fully quantum version of AdS/CFT, where all degrees of freedom are taken into account. The semiclassical wormhole is a first hint that there are degrees of freedom in the CFT that couple both theories, which we simply cannot see in the approximation we consider.

Since it is hard to make progress without a well-understood theory of quantum gravity, we take another approach. It was proposed in [185] that wormholes give rise to Berry phases in the partition function describing the system. We calculate these Berry phases for CFTs dual to the eternal AdS black hole and show that parameters that are unique to wormhole geometries give rise to the CFT Berry phases, indicating that parameters related to the connected bulk geometry also appear in the dual CFT. We then interpret these Berry phases in the context of the factorization problem and propose steps to resolve it.

Before we calculate these Berry phases for the wormhole geometry of the eternal AdS black hole in AdS_3, we first provide a brief review of Berry phases with a focus on two-dimensional CFTs and discuss the relation between wormholes and the Berry phase.

5.2. Wormholes and the Berry Phase

We now introduce two ingredients we employ in this chapter to study how the bulk wormhole appears in the dual CFTs in AdS_3/CFT_2. The first one is the Berry phase, which we discuss in sec. 5.2.1. Berry phases may be calculated for symmetry groups [239] including the Virasoro group [105]. These Berry phases are obtained from paths through the group manifold and are a generalization of the well-known Berry phases that arise from a parameter-dependent Hamiltonian. It is then possible to obtain a Berry phase for a two-dimensional CFT. In sec. 5.2.2, we discuss a general relation between Berry phases and wormholes established in [185, 238, 240]. At the center of the argument is the non-factorization of the path integral defining the partition function if the phase space is topologically non-trivial. Non-factorization is induced by a topology-dependent phase term given in terms of the symplectic form on the phase space, which has a natural interpretation as a Berry phase.

5.2.1. Berry Phases for Symmetry Groups

In this section, we introduce Berry phases for symmetry groups. In particular, we demonstrate that the well-known Berry phase for a spin in a magnetic field may be recast as a Berry phase in an SU(2) group manifold. We then focus on Berry phases in two-dimensional CFTs [105]. The concepts introduced in this section are essential to later derive Virasoro Berry phases in CFTs dual to the eternal AdS black hole. The presentation follows [105].

The prototypical Berry phase [241] arises when the system Hamiltonian depends on a time-dependent external parameter, for instance the magnetic field. This external parameter varies adiabatically in time in such a manner that it traces out a closed path $\gamma(t)$ in parameter space. The time-dependent Hamiltonian $H(\gamma(t))$ then has time-dependent energy-eigenvalues $E_n(\gamma(t))$ and eigenstates $|\psi_n(\gamma(t))\rangle$. For an adiabatic evolution, n does not change. We then obtain a sequence of states

$$|\psi(t)\rangle = e^{i\eta_n(t)}|\psi_n(\gamma(t))\rangle. \tag{5.2.1}$$

The phase $\eta_n(t)$ follows from inserting $|\psi(t)\rangle$ into the Schrödinger equation and taking the expectation value by multiplication with $\langle\psi_n(\gamma(t))|$. The result is given in terms of two contributions,

$$\eta_n(T) = -\int_0^T dt\, E_n(\gamma(t)) + i\int_0^T dt\, \langle\psi_n(\gamma(t))\,|\partial_t|\,\psi_n(\gamma(t))\rangle\,. \tag{5.2.2}$$

The first term is dynamical as it arises from the Hamiltonian and is of no further interest to us. On the other hand, the second term is purely geometric as it originates from the parameter-dependence of the state, and is called the Berry phase $\mathcal{B}$,

$$\mathcal{B} = \oint_\gamma A = i\int_0^T dt\, \langle\psi_n(\gamma(t))\,|\partial_t|\,\psi_n(\gamma(t))\rangle\,. \tag{5.2.3}$$

Here, A denotes the Berry connection. Furthermore, in order for the Berry phase to be a well-defined gauge-invariant object, the path γ must be closed.

Let us understand (5.2.3) in more detail in the context of fiber bundles. The parameter space is a manifold $\mathcal{M}$, called the base space of the fiber bundle, where each point corresponds to a particular value of the parameter. To obtain the Berry phase, we move along a path $\gamma(t)$ through points in the parameter space $\mathcal{M}$. To each point along this path, we may associate a unique state $|\psi_n(\gamma(t))\rangle$ on the projective Hilbert space $\mathcal{PH}$. The projective Hilbert space is formed by rays $[\psi] = \{|\psi\rangle = e^{i\eta}|\Phi\rangle \mid \eta \in \mathbb{R}\}$, where all states that differ only by a phase from $|\psi_n(\gamma(t))\rangle$ are represented by the same state $|\psi_n(\gamma(t))\rangle$. In the full Hilbert space $\mathcal{H}$, however, each representative $|\psi_n(\gamma(t))\rangle$ on the projective Hilbert space may carry an additional phase $e^{i\eta(\gamma)}|\psi_n(\gamma(t))\rangle$, where $\eta \in \mathbb{R}$. These phases are generated by operators that are eigenoperators for the state $|\psi_n(\gamma(t))\rangle$. Therefore, the state $|\psi_n(\gamma(t))\rangle$ has a gauge symmetry with a gauge group generated by the subgroup of eigenoperators of $|\psi_n(\gamma(t))\rangle$. This gauge group forms the fiber $\mathcal{K}$ over the base space $\mathcal{M}$. The fiber and the base space form the fiber bundle. This is illustrated in fig. 5.1. We may then define a bundle connection A given by

$$A = \langle\psi_n(\gamma(t))\,|d|\,\psi_n(\gamma(t))\rangle\,, \tag{5.2.4}$$

where d is the exterior derivative in the fiber bundle. The curvature F is obtained from $F = dA$. Upon rewriting $d = dt\frac{d}{dt}$, the fiber connection is simply the Berry connection in (5.2.3). For a more thorough introduction to fiber bundles, we refer to [242]. The Berry phase then arises due to the gauge symmetry at every point along the closed path $\gamma(t)$ in $\mathcal{M}$. When the path is lifted from the base space $\mathcal{M}$ into the bundle, the path is no longer closed since the state $|\psi_n(\gamma(t=0))\rangle$ at the beginning

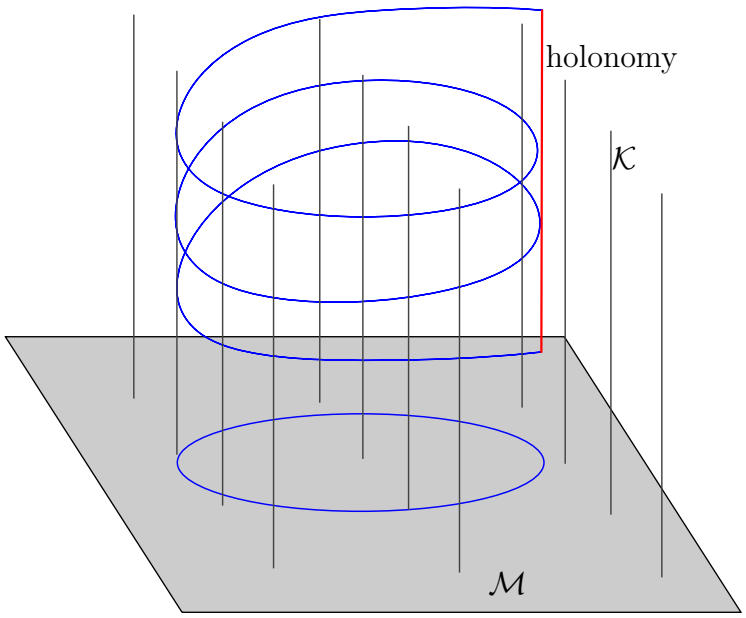

Fig. 5.1.: A fiber bundle with base manifold $\mathcal{M}$ and fiber $\mathcal{K}$. The Berry phases is obtained from a closed path in parameter space, which is the base manifold. For every point in the base manifold there is a unique state in the projective Hilbert space $\mathcal{PH}$, but there is a phase ambiguity in the full Hilbert space $\mathcal{H}$. The phase ambiguity is represented by the fiber $\mathcal{K}$. The lift of the closed path into the fiber bundle is then no longer closed. The Berry phases measures the holonomy shown in red.

of the path and the state at the end of the path at $t = T$ differ by an overall phase $|\psi_n(\gamma(t = T))\rangle = e^{i\eta}|\psi_n(\gamma(t = 0))\rangle$. This is the holonomy induced by the non-trivial curvature of the bundle.

This notion of a Berry phase may be generalized to symmetry groups [105, 239]. We consider a symmetry group G with group elements g and a highest-weight state $|\psi\rangle$. We now consider a path $g(t)$ through the group manifold. This generates a sequence of states $|\psi(t)\rangle = U_{g(t)}|\psi\rangle$. Let us now assume the group has a one-parameter subgroup J formed by operators that only generate phases in the state $|\psi\rangle$ and that the generator of this subgroup is the Hamiltonian H. Note that the choice of Hamiltonian is not unique. Rather than H, we may as well choose $\tilde{H} = U_g^\dagger H U_g$, where U_g is a unitary representation of the group element g. There are some group elements j in G, however, that leave the Hamiltonian invariant and only generate a phase in the state $|\psi\rangle$. These are precisely the transformations that belong to the one-parameter subgroup J generated by the Hamiltonian. Therefore, the fiber $\mathcal{K}$ is formed by the group J and the base space is the manifold $\mathcal{M} = \frac{G}{J}$.

At every point along the path $g(t)$, the state $|\psi(t)\rangle$ picks up an additional phase due to the gauge symmetry generated by H. If the group path is closed in the base space,

the state will then not return to its initial form $|\psi\rangle$, but differ by a phase, $|\psi\rangle \to e^{i\eta}|\psi\rangle$. We may interpret the choice of the phase for every state $|\psi(t)\rangle$ along the path as a choice of reference frame for the state. This is analogous to the choice of Lorentz frame in general relativity. And just as in general relativity, where the curvature of the spacetime induces a holonomy, the curvature of the state space gives rise to a holonomy, which is the Berry phase. Analogous to (5.2.3), the Berry connection for the symmetry group is given by

$$A = i\langle\psi(t)|d|\psi(t)\rangle = i\langle\psi|U^\dagger dU|\psi\rangle, \tag{5.2.5}$$

and the Berry phase is again obtained by integrating over the closed group path in $\mathcal{M} = \frac{G}{J}$. In particular, $U^\dagger dU$ is the Maurer-Cartan form θ in a unitary representation of the Lie algebra $\mathfrak{g}$ of the group G. Therefore, we may rewrite the connection as

$$A = i\langle\psi|\mathfrak{u}(\theta)|\psi\rangle. \tag{5.2.6}$$

Before we delve into the Berry phase for a two-dimensional CFT with Virasoro symmetry, let us consider the simpler example of an $SU(2)$ Berry phase.

For illustration: SU(2) Berry phase

Let us assume that a spin is aligned with the z-axis in a three-dimensional Cartesian coordinate system and the Hamiltonian of the system is proportional to the Pauli matrix σ_3. The Hamiltonian varies in time when applying group transformations $g \in SU(2)$ due to $\tilde{H} \propto U^\dagger_{g(t)}\sigma_3 U_{g(t)}$. This setup corresponds to a spin in a magnetic field that changes direction. The highest-weight state is given by $|j\rangle$ for a spin-j representation and is invariant under transformations generated by $J_3 = \frac{i}{2}\sigma_3$. Therefore, the fiber $\mathcal{K}$ is $U(1)$. The set of transformations forming the base space $\mathcal{M} = \frac{G}{\mathcal{K}}$ that physically changes the state $|j\rangle$ is then $\frac{SU(2)}{U(1)} = S^2$. We parameterize a group element on the 2-sphere S^2 as follows:

$$g_{(\theta,\varphi)} = \begin{pmatrix} \cos(\theta/2) & -e^{-i\varphi}\sin(\theta/2) \\ e^{i\varphi}\sin(\theta/2) & \cos(\theta/2) \end{pmatrix}. \tag{5.2.7}$$

From the group element, we obtain the Maurer-Cartan form, which we may express in terms of the Pauli matrices σ_i,

$$\begin{aligned}\theta &= g^{-1}_{(\theta,\varphi)} dg_{(\theta,\varphi)} \\ &= \frac{i}{2}\left[(\cos\varphi\sin\theta d\varphi + \sin\varphi d\theta)\sigma_1 + (\sin\varphi\sin\theta d\varphi - \cos\varphi d\theta)\sigma_2 + (1-\cos\theta)d\varphi\sigma_3\right].\end{aligned} \tag{5.2.8}$$

The Berry connection then follows from evaluating (5.2.6) and reads $A = -j(1-\cos\theta)d\varphi$. Employing $F = dA$, we find that the Berry curvature is just the volume form on the two-sphere

$$F = -j\sin\theta\, d\theta \wedge d\varphi, \tag{5.2.9}$$

and the Berry phase is given by

$$\mathcal{B} = \oint_\gamma A = \int_\Sigma F = -j\,\mathrm{area}(\Sigma), \tag{5.2.10}$$

where Σ is the surface on S^2 enclosed by the path γ.

Virasoro Berry phase

For the Virasoro Berry phase [105], we draw on the discussion of Virasoro coadjoint orbits in sec. 2.1.2. Since the Virasoro group $\widehat{\mathrm{Diff}}(S^1)$ is centrally extended, group elements are pairs (f,λ) with f a diffeomorphisms of the unit circle and $\lambda \in \mathbb{R}$. As usual, we denote highest-weight states by $|h\rangle$ if $h > 0$ and by $|0\rangle$ if $h = 0$. The stabilizer subgroups that generate the gauge redundancy are SL(2,$\mathbb{R}$) for $|0\rangle$ and U(1) for $|h\rangle$. Furthermore, the Maurer-Cartan form for groups with central extensions also receives a contribution from the central extension, (θ, m_θ). Therefore, the Berry connection for centrally extended groups is given by

$$A = i\langle h|\mathfrak{u}(\theta) + c\mathfrak{u}(m_\theta)|h\rangle, \tag{5.2.11}$$

where c is the central charge of the CFT. We discussed in sec. 2.1.2 how to derive the Maurer-Cartan form and now employ the result (2.1.63) to obtain the Berry phase. The Berry connection follows from (5.2.11) and (2.1.63),

$$A = -\frac{1}{2\pi}\int_0^{2\pi} d\varphi \frac{\dot{f}(t,\varphi)}{f'(t,\varphi)}\left(\left[h - \frac{c}{24} + \frac{c}{24}\left(\frac{f''}{f'}\right)'\right]\right), \tag{5.2.12}$$

where we employed that the inverse group element $F(t,\varphi)$ and the group element $f(t,\varphi)$ are related by $F(t, f(t,\varphi)) = \varphi$. Note that the Berry connection is equal to

the symplectic form α on coadjoint orbits of the Virasoro group defined in (2.1.64),

$$A = \alpha = -\langle (b,c),(\theta,m_\theta)\rangle\,. \tag{5.2.13}$$

This implies that the Berry curvature F is given by the Kirillov-Kostant symplectic form (2.1.60) on the coadjoint orbit, $F = \omega$. Furthermore, the Berry phase is given by the geometric action (2.1.66) on the orbit written in terms of the group element f and an additional boundary term,

$$\begin{aligned}\mathcal{B} &= \int dt\, A(f(t)) = \int dt\, \alpha \\ &= -\frac{1}{2\pi}\int_0^T dt \int_0^{2\pi} d\varphi \frac{\dot f}{f'}\left[h - \frac{c}{24} + \frac{c}{24}\left(\frac{f''}{f'}\right)'\right] + \left(h-\frac{c}{24}\right) f^{-1}(0, f(T,0)).\end{aligned} \tag{5.2.14}$$

The boundary term is necessary since the group path we consider is not in the base space but in the full Virasoro group manifold and therefore ensures that a path in the fiber does not contribute to the Berry phase as its projection onto the base manifold is simply a point. The relation between the coadjoint orbits and the Berry phase can be understood as follows: The Berry phase is generated by a closed group path through the manifold $\mathcal{M} = \frac{\widehat{\text{Diff}}(S^1)}{\mathcal{K}}$, where the fiber $\mathcal{K}$ is either U(1) or SL(2,$\mathbb{R}$) in fig. 5.1. These are precisely the coadjoint orbits of the Virasoro group discussed in sec. 2.1.2. The Kirillov-Kostant symplectic form on the orbit then serves as the natural Berry curvature. The Virasoro Berry phase may be thought of as probing the geometry of the state space of the CFT since quantizing the orbit gives rise to the states that are generated by moving along a path on the orbit.

Just as $\frac{\widehat{\text{Diff}}(S^1)}{\mathcal{K}}$ is a coadjoint orbit of the Virasoro group, so is $\frac{SU(2)}{U(1)} = S^2$ for SU(2). These orbits form symplectic manifolds with a symplectic form that is equal to the Berry curvature. The analogy between the symplectic form on coadjoint orbits and Berry curvature holds for general symmetry groups. However, the Berry phase is only non-trivial (non-vanishing) if the symplectic form is not exact, i.e. the identification $\omega = d\alpha$ does not hold globally. If $\omega = d\alpha$ globally, the Berry phase vanishes as the surface integral over the curvature may be written globally as an integral over a closed loop, which vanishes. For SU(2), it is particularly easy to see that the symplectic form or Berry curvature is not exact as it is the volume form of the 2-sphere, and volume forms are by definition never exact. The Virasoro symplectic form is not exact due to the presence of defects [138, 185].

5.2.2. Berry Phases from Wormholes

In [185], it was proposed that Berry phases are intricately linked to wormholes. This observation, which we now motivate, then allows us to study how the bulk wormhole appears in the dual CFTs by calculating CFT Berry phases in the presence of a bulk wormhole in AdS_3/CFT_2.

The relation between wormholes and Berry phases is very general as it holds not only within the AdS/CFT correspondence, but extends to systems that do not have a gravitational dual as well. Rather surprisingly, wormholes may appear via Berry phases in very simple quantum systems such as a quantum mechanical harmonic oscillator [185] or a two-spin system [243]. In contrast to the geometric spacetime wormholes that appear in AdS/CFT in the gravitational bulk theory, wormholes that appear in theories without gravity such as the harmonic oscillator are purely topological.

To illustrate how these wormholes arise even in systems without gravity and how they are linked to Berry phases, we consider the simplest case of a general one-dimensional quantum system as presented in [185]. The generalization to higher dimensions is straightforward. We assume that the one-dimensional quantum system is obtained by quantizing the classical phase space spanned by generalized coordinates and momenta, which we collectively denote by x^a. The symplectic form on the phase space may then be written as $\omega = \omega_{ab} dx^a \wedge dx^b$. Furthermore, the thermal partition function of the system is given by $Z(\beta) = \mathrm{tr}(e^{-\beta H})$, where H is the system Hamiltonian and β the inverse temperature corresponding to the periodicity of the Euclidean time circle. The partition function may be written in terms of a path integral [185, 244]

$$Z(\beta) = \int \mathcal{D}x\, e^{-S} = \int \mathcal{D}x\, e^{-(\int_D \omega - \oint_{\partial D} H dt)}. \tag{5.2.15}$$

Here, S denotes the action, and ∂D, which is simply the thermal circle in a one-dimensional system, is the boundary of the disk D. If the symplectic form ω is exact, we may find a symplectic potential globally and thus $\int_D \omega = \oint_{\partial D} \alpha$. A well-known example is the symplectic form of a particle given by $\omega = dp \wedge dq$. The potential $\alpha = p\, dq$ is globally defined and hence the partition function reduces to $Z(\beta) = \int \mathcal{D}x\, e^{-\oint_{\partial D}(p\dot{q} - H)dt}$ [244]. Note that because the integral reduces to a boundary integral over ∂D, the topology of D is irrelevant. This is no longer true if the symplectic form ω is not globally exact. In this case $\int_D \omega$ does not reduce to a boundary integral, and the integral thus depends on the particular topology of D. We may now introduce wormhole topologies into such a system by evaluating the integral not on D, but a connected geometry Σ_n with n thermal circles at the boundary. For such a setup, the

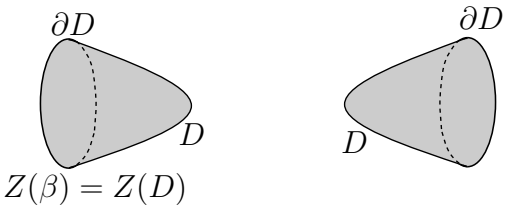

(a) For two disconnected geometries, the partition function factorizes as the integral over the symplectic form ω is exact in such systems, and the integral $\int_D \omega = \oint_{\partial D} \alpha$ reduces to a boundary integral independent of the topology of D.

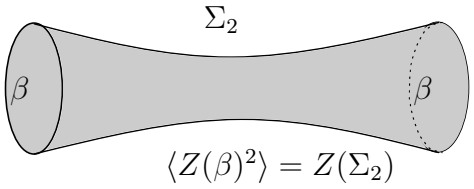

(b) For the wormhole topology Σ_2, the partition function does not factorize, and $\int_{\Sigma_2} \omega$ does not reduce to a boundary integral. In particular, $\int_{\Sigma_2} \omega$ yields a Berry phase.

Fig. 5.2.: Factorization properties of the partition function in trivial and non-trivial topologies.

partition function is given by

$$\langle Z(\beta)^n \rangle = Z(\Sigma_n) = \int \mathcal{D}x\, e^{-(\int_{\Sigma_n} \omega - \oint_{\partial \Sigma_n} H dt)}. \tag{5.2.16}$$

In particular, the partition function does not factorize into individual contributions since it is evaluated on a connected wormhole topology.

Let us now assume that we consider a phase space, where the symplectic form is exact. Then, $\int_{\Sigma_n} \omega$ no longer depends on the topology Σ_n and reduces to a boundary integral. We therefore obtain a factorized system $\langle Z(\beta^n) \rangle = \langle Z(\beta) \rangle^n$ and the connected wormhole topology is replaced by factorized disks, where only the boundary is relevant. Therefore, non-factorization of the partition function indicating the presence of a wormhole may be probed with the term $e^{\int \omega}$ in the partition function. Since this term arises from a non-exact symplectic form, it has the natural interpretation of a Berry phase. This is illustrated in fig. 5.2. The Berry curvature F is then equal to the symplectic form ω on the phase space.

We now calculate these wormhole Berry phases for CFTs dual to the eternal AdS black hole and identify parameters that indicate the presence of a bulk wormhole also in the dual CFTs.

5.3. Spacetime Wormholes from Virasoro Berry Phases

The relation between Berry phases and wormholes presented for generic quantum systems in sec. 5.2.2 is also applicable to AdS/CFT. We may therefore make progress

in understanding the factorization problem by illuminating the implications of the bulk wormhole in the dual CFTs. To this end, we now derive Virasoro Berry phases in the presence of a bulk wormhole. In particular, we focus on the Berry curvature. Since the Berry curvature is given in terms of the symplectic form on the phase space, we now determine the latter. Given a set of phase space variables x^a, the symplectic form follows from the system Hamiltonian by evaluating

$$\dot{x}^a = \left(\omega^{-1}\right)^{ab} \partial_b H. \tag{5.3.1}$$

Therefore, to obtain the symplectic form and thereby the Berry curvature in the CFTs dual to an eternal AdS black hole, the following steps are necessary:

1. The bulk action for an eternal AdS black hole is derived. Since three-dimensional gravity is topological, the bulk action reduces to a boundary action for the CFTs upon specifying boundary values for the bulk fields.

2. The Hamiltonian is obtained from the boundary action for the CFTs derived in step 1. With this Hamiltonian, we may then calculate the symplectic form on the phase space by employing (5.3.1).

For step 1, we may employ the results of [245], where the bulk action for the eternal AdS black hole was derived from Chern-Simons theory on a manifold $\mathcal{M} = \mathbb{R} \times \Sigma$ that is equivalent to a wormhole topology Σ at every constant time slice. The Chern-Simons action is given in terms of the gauge connection A,

$$S_{\text{CS}}[A] = \frac{k}{4\pi} \int_{\Sigma \times \mathbb{R}} \text{tr} \left(A \wedge dA + \frac{2}{3} A \wedge A \wedge A \right), \tag{5.3.2}$$

where k is the Chern-Simons level. Since three-dimensional gravity has no propagating degrees of freedom and is thus purely topological, we may deform the manifold $\mathcal{M}$ without changing the boundary conditions at the two asymptotic boundaries or the topology. At a given constant time slice, the wormhole is topologically equivalent to an annulus. This is shown in fig. 5.3. It is therefore appropriate to evaluate (5.3.2) on a manifold $\mathcal{M}$ given by the annulus times the time direction. In particular, the action for the eternal AdS black hole in three dimensions is obtained by imposing asymptotic AdS_3 boundary conditions on $\text{SL}(2,\mathbb{R}) \times \text{SL}(2,\mathbb{R})$ Chern-Simons theory on an annulus times time topology [245]. The action for the CFTs at the asymptotic boundaries follows by setting boundary values for the bulk fields. With this results, we may then proceed with step 2 and apply (5.3.1).

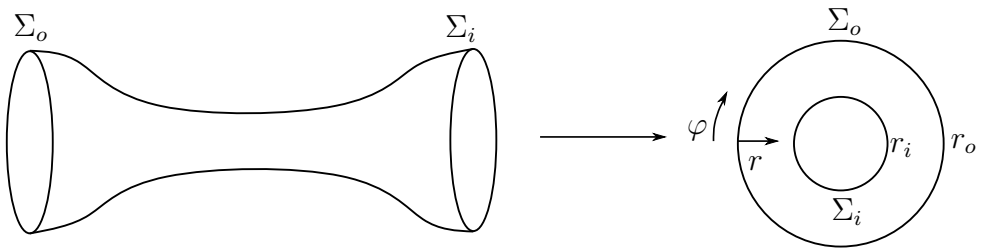

Fig. 5.3.: A constant time slice in the eternal AdS black hole geometry corresponds to a wormhole. Topologically, the wormhole is equivalent to an annulus, where Σ_o and Σ_i represent the two boundaries on which the CFTs live. The coordinate r denotes the radial bulk direction; φ denotes the angular boundary direction on the constant time slice.

Before we derive the symplectic form and therefore the Berry curvature for the eternal AdS black hole, we begin with a simpler (non-holographic) Abelian example of U(1) Chern-Simons theory on the annulus. Topologically, this theory is similar to SL(2,$\mathbb{R}$) Chern-Simons theory on the annulus and we may interpret the annulus as a topological but not a spacetime wormhole in this example. We will see that for this reason U(1) Chern-Simons theory captures the essential features we expect of the actual spacetime wormhole Berry phase associated to the eternal AdS black hole obtained from the non-Abelian SL(2,$\mathbb{R}$) Chern-Simons theory on the annulus.

5.3.1. Toy Model: U(1) Theory on the Annulus

We now derive the Berry connection for U(1) Chern-Simons theory on an annulus representing a topological wormhole. For this toy model, step 1 was calculated in [245]. Since the subtleties that arise when evaluating the action (5.3.2) on an annulus are essential to obtain the correct Berry curvature in step 2, we briefly review how the bulk and boundary actions are obtained.

The Chern-Simons action for a single U(1)-valued gauge field on the annulus is given by

$$S_{[CS]} = \frac{k}{2\pi} \int dt dr d\varphi \left(A_\varphi \partial_t A_r + A_t F_{r\varphi} \right), \tag{5.3.3}$$

where the field strength is given by $F_{r\varphi} = \partial_r A_\varphi - \partial_\varphi A_r$. The annulus has an inner boundary at the value $r = r_i$ of the radial coordinate and an outer boundary at $r = r_o$. Moreover, the non-contractible circle is along the φ-direction on the annulus. This is also shown in fig. 5.3. The equation of motion obtained from (5.3.3) for A_t yields $F_{r\varphi} = 0$. From this condition, the remaining components of the gauge field are given

in terms of a field $\mu(r,t,\varphi)$ by

$$A_r = \partial_r \mu(r,t,\varphi), \quad A_\varphi = \partial_\varphi \mu(r,t,\varphi) + k(t,\varphi). \tag{5.3.4}$$

Note that on the annulus topology, $\oint A_\varphi$ is non-trivial due to the non-contractible circle along the φ-direction and measures the holonomy k_0. Therefore, $k(t,\varphi)$ is parameterized as $k(t,\varphi) = \partial_\varphi \lambda(t,\varphi) + k_0$, which yields the non-trivial holonomy k_0,

$$\oint A_\varphi = 2\pi k_0. \tag{5.3.5}$$

In the next step, boundary conditions are imposed on the U(1) Chern-Simons action such that time evolution is upward on both boundaries. This corresponds to the conditions $A_t = A_\varphi$ at the outer boundary and $A_t = -A_\varphi$ at the inner boundary. To ensure the variation of the action vanishes after the boundary conditions are imposed, the following term is added to the action,

$$S_{\text{add}} = \frac{k}{2\pi} \oint H, \qquad H = \oint d\varphi \, (A_\varphi)^2 \Big|_{r=r_o} + \oint d\varphi \, (A_\varphi)^2 \Big|_{r=r_i}. \tag{5.3.6}$$

Finally, upon inserting the solution (5.3.4) into the action and specifying the boundary values of $\mu(r,t,\varphi)$ as $\mu(r=r_i,t,\varphi) = \Phi(t,\varphi)$ and $\mu(r=r_o,t,\varphi) = \Psi(t,\varphi)$, the action reduces to a boundary term [245],

$$\begin{aligned} S = \frac{k}{4\pi} \Big(\int dt \left[\oint d\varphi \, (\partial_\varphi \Phi \partial_t \Phi) - H_\Phi \right] + \int dt \left[- \oint d\varphi \, (\partial_\varphi \Psi \partial_t \Psi) - H_\Psi \right] \\ + 2 \int dt \left[\oint d\varphi k_0 \, (\partial_t \Phi - \partial_t \Psi) - H_0 \right] \Big). \end{aligned} \tag{5.3.7}$$

The full Hamiltonian is given by [245]

$$\begin{aligned} H &= H_\Phi + H_\Psi + H_0 \\ H_\Phi = \int d\varphi \, (\partial_\varphi \Phi)^2, \quad H_\Psi &= \int d\varphi \, (\partial_\varphi \Psi)^2, \quad H_0 = 2\pi \, (k_0)^2. \end{aligned} \tag{5.3.8}$$

The first line in (5.3.7) is the sum of two free chiral boson actions with one chiral boson Φ at the inner boundary at $r = r_i$ and another Ψ at the outer boundary at $r = r_o$. In addition to these standard terms, there is a term involving the holonomy k_0 in (5.3.7). In particular, the holonomy couples both chiral bosons Φ and Ψ. Therefore, the action is not a simple sum of two decoupled chiral bosons living on the left and right boundary. The holonomy k_0 is an additional dynamical variable of the theory

with canonical conjugate,

$$\Pi_0 = \frac{\partial L}{\partial \dot{k}_0} = -\frac{k}{2\pi}\oint d\varphi\,(\Phi - \Psi)\,, \tag{5.3.9}$$

where L is the Lagrangian of the action (5.3.7). The conjugate momentum Π_0 has a particularly interesting interpretation as we now discuss. Since we consider Chern-Simons theory on the annulus, the setup is topologically equivalent to a wormhole with boundaries Σ_i at r_i and Σ_o at r_o on either end of the wormhole, see fig. 5.3. In the presence of such a wormhole, there exist radial Wilson lines threading the wormhole. These radial Wilson lines are anchored at both boundaries and read

$$\mathcal{W} = \mathcal{P}e^{-\int_{r_o}^{r_i} dr A_r} = e^{-(\Phi-\Psi)}, \tag{5.3.10}$$

where in the last step we used (5.3.4) and the boundary values of μ. Therefore, the conjugate momentum Π_0 to the holonomy k_0 is given in terms of the radial Wilson line threading the wormhole. The phase space variables are then given by $x^a = (\Phi, \Pi_\Phi, \Psi, \Pi_\Psi, k_0, \Pi_0)$, where Π_Φ is the canonical momentum to the chiral boson Φ and similarly for Π_Ψ.

We now proceed with step 2 and employ (5.3.1) to derive the symplectic form and therefore the Berry curvature on the phase space from the full Hamiltonian (5.3.8) of the system. To this end, we first compute the canonical momenta Π_Φ and Π_Ψ as well as the time derivatives $\dot{\Pi}_0$ and $\dot{k}_0$ from the Lagrangian L of the action (5.3.7) and the Hamiltonian (5.3.8),

$$\begin{aligned}
\Pi_\Phi &= \frac{\partial L}{\partial \dot{\Phi}} = \frac{k}{4\pi}\int d\varphi\,(\partial_\varphi \Phi + 2k_0)\,,\\
\Pi_\Psi &= \frac{\partial L}{\partial \dot{\Psi}} = \frac{k}{4\pi}\int d\varphi\,(\partial_\varphi \Psi - 2k_0)\,,\\
\dot{\Pi}_0 &= \frac{\partial H}{\partial k_0} = \frac{k}{2\pi}k_0,\\
\dot{k}_0 &= \frac{\partial H}{\partial \Pi_0} = 0.
\end{aligned} \tag{5.3.11}$$

We now begin determining components of ω_{ab} from (5.3.1) starting with $x^a = \Phi$. Then, (5.3.1) reads

$$\begin{aligned}
\partial_t \Phi &= (\omega^{-1})^{\Phi b}\partial_b H\\
&= (\omega^{-1})^{\Phi\Phi}\partial_\Phi H + (\omega^{-1})^{\Phi\Psi}\partial_\Psi H + (\omega^{-1})^{\Phi\Pi_\Phi}\partial_{\Pi_\Phi} H\\
&+(\omega^{-1})^{\Phi\Pi_\Psi}\partial_{\Pi_\Psi} H + (\omega^{-1})^{\Phi\Pi_0}\partial_{\Pi_0} H + (\omega^{-1})^{\Phi k_0}\partial_{k_0} H.
\end{aligned} \tag{5.3.12}$$

We now first employ that ω_{ab} is antisymmetric. Therefore, contributions with $a = b$ such as $(\omega^{-1})^{\Phi\Phi}$ must vanish. Secondly, we exploit that the left-hand side in (5.3.12)

only depends on Φ. Therefore, the right-hand side of (5.3.12) can also only depend on Φ and not for instance on Ψ since these are independent variables. This immediately implies that the only possible non-vanishing contributions are

$$\partial_t \Phi = (\omega^{-1})^{\Phi\Pi_\Phi} \partial_{\Pi_\Phi} H + (\omega^{-1})^{\Phi\Pi_0} \partial_{\Pi_0} H. \tag{5.3.13}$$

Upon employing (5.3.11), we find that the term involving $(\omega^{-1})^{\Phi\Pi_0}$ vanishes. Furthermore, the only non-vanishing contribution in $\partial_{\Pi_\Phi} H$ comes from H_Φ. We therefore find

$$\partial_t \Phi = \partial_{\Pi_\Phi} H = (\omega^{-1})^{\Phi\Pi_\Phi} \partial_{\Pi_\Phi} H \quad \Rightarrow (\omega^{-1})^{\Phi\Pi_\Phi} = 1. \tag{5.3.14}$$

For the remaining five phase space variables $x^a = (\Pi_\Phi, \Psi, \Pi_\Psi, k_0, \Pi_0)$, we proceed similarly and find

$$(\omega^{-1})^{\Psi\Pi_\Psi} = 1, \quad (\omega^{-1})^{k_0\Pi_0} = 1. \tag{5.3.15}$$

The other components may be fixed by employing the antisymmetric properties of the symplectic form or by explicit calculation. Inverting ω^{-1} then yields the symplectic form for $U(1)$ Chern-Simons theory on the annulus,

$$\omega = d\Pi_\Phi \wedge d\Phi + d\Pi_\Psi \wedge d\Psi + d\Pi_0 \wedge dk_0. \tag{5.3.16}$$

Note that the first two contributions $d\Pi_\Phi \wedge d\Phi + d\Pi_\Psi \wedge d\Psi$ seem analogous to the standard symplectic form for a single particle in quantum mechanics $\omega = dp \wedge dq$. However, the third term in (5.3.16) indicates that the phase space is not simply the sum of two manifolds – one for the left and one for the right boundary – but that there is a single phase space due to the presence of the holonomy k_0 and the radial Wilson line related to Π_0 that couple the boundaries. In particular, k_0 and Π_0 indicate the presence of a topological wormhole since the radial Wilson line threading the wormhole can only be present if the wormhole exists. A simple thought experiment illustrates this. Let as assume that rather than a wormhole corresponding to an annulus topology, we consider a disk topology. The disk has no non-contractible cycles and therefore $k_0 = 0$, i.e. the disk does not have a holonomy. Similarly a radial Wilson line as its canonical conjugate does not exist. In this case, (5.3.16) reduces to two decoupled symplectic forms,

$$\omega_{\text{disk}} = d\Pi_\Phi \wedge d\Phi + d\Pi_\Psi \wedge d\Psi. \tag{5.3.17}$$

This corresponds to the case, where the partition function in sec. 5.2.2 does not depend on the topology but reduces to a boundary integral over the boundary of the disk since the symplectic form (5.3.17) is exact. The Berry phase then vanishes. On

the other hand, on the annulus representing the wormhole topology, the symplectic form (5.3.16) gains additional contributions from the holonomy and the radial Wilson line. Both of these are non-local from the boundary point of view as they cannot be written in terms of the boundary fields on a single boundary. This is precisely the condition discussed in sec. 5.2.2: We obtain a non-trivial Berry phase with Berry curvature (5.3.16) if the symplectic form depends on topological information related to the wormhole rather than only on local boundary fields. Furthermore, the action (5.3.7) is a boundary action and (5.3.16) the corresponding symplectic form on the phase space. This indicates that the classical phase space as well as the quantum mechanical Hilbert space obtained by quantizing the phase space do not factorize in terms of a Hilbert space for the left boundary and a Hilbert space for the right boundary. It may be shown that the boundary theories for U(1) Chern-Simons theory on the annulus are two U(1) Kac-Moody algebras whose Hilbert spaces are known [245]. These are algebras of conformal field theories with an additional U(1) symmetry. For details we refer to [109]. In particular, in the presence of the annulus with symplectic form (5.3.16), the non-factorized Hilbert space arises from the manifold $\mathcal{M} = \frac{\widehat{LG}\times\widehat{LG}}{U(1)}$, where $\widehat{LG}$ denotes the centrally extended $U(1)$ Kac-Moody group. The common $U(1)$ quotient prevents factorization due to the presence of the holonomy k_0. On the other hand, for (5.3.17), the manifold is $\mathcal{M} = \frac{\widehat{LG}}{U(1)} \times \frac{\widehat{LG}}{U(1)}$, which is factorized.

This concludes the discussion of the U(1) Chern-Simons theory toy model on the annulus. We will now employ the same procedure to derive the symplectic form for SL(2,$\mathbb{R}$) Chern-Simons theory on the annulus with asymptotic AdS_3 boundary conditions, which describes the eternal AdS_3 black hole. We will see that while the results are very similar additional steps are necessary due to the non-Abelian group SL(2,$\mathbb{R}$).

5.3.2. The Eternal AdS Black Hole: SL(2,R) Theory on the Annulus

Here, we derive the Berry curvature for the CFTs dual to the eternal AdS_3 black hole. The eternal black hole may be obtained from SL(2,$\mathbb{R}$)$\times$ SL(2,$\mathbb{R}$) Chern-Simons theory on the annulus by imposing asymptotic AdS boundary conditions at the inner boundary Σ_i at $r = r_i$ and at the outer boundary Σ_o at $r = r_o$. The main steps to obtain the action are similar to those in sec. 5.3.1, but the calculation is considerably more involved since SL(2,$\mathbb{R}$) is non-Abelian and there are additional constraints enforcing AdS_3 boundary conditions. Fortunately, the action was derived in [245], and we employ the result. Since our analysis of the Berry curvature draws from these results, we

present a detailed review in app. A.3, but only give the result for the action here.

Similar to the U(1) action (5.3.7), the action for the eternal AdS black hole reduces to a boundary term because there are no propagating gravitational degrees of freedom in AdS_3. The action describing the boundary dynamics in the presence of an eternal AdS black hole reads [245]

$$S[k_0, \Phi, \Psi] = \frac{k}{4\pi} \int dt d\varphi \left(\frac{1}{2} \partial_- \Phi \Phi' - \frac{1}{2} \partial_+ \Psi \Psi' + k_0 (\partial_- \Phi - \partial_+ \Psi) - k_0^2 \right). \tag{5.3.18}$$

In appearance, the action is quite similar to the U(1) action (5.3.7). There are two terms describing the dynamics of a chiral boson Φ and Ψ on each boundary. The chiral boson action emerges due to a particular choice of parameterization for the $SL(2,\mathbb{R})$ group elements. For details see app. A.3 and [245]. Furthermore, the chiral bosons are again coupled by the holonomy k_0. For an eternal AdS black hole of mass m, the holonomy is given by $k_0 = \sqrt{m}$. Its canonical conjugate momentum also takes the familiar form

$$\Pi_0 = -\frac{k}{4\pi} \int d\varphi (\Phi - \Psi). \tag{5.3.19}$$

However, in contrast to the U(1) toy model, Π_0 cannot be straightforwardly related to the radial Wilson line [245]. The phase space variables are then again given by $x^a = (\Phi, \Pi_\Phi, \Psi, \Pi_\Psi, k_0, \Pi_0)$, and the Hamiltonian of the system reads [133]

$$H = \frac{k}{4\pi} \left(\frac{1}{2} \int d\varphi \, \Phi'^2 + \frac{1}{2} \int d\varphi \, \Psi'^2 + 2\pi k_0^2 \right). \tag{5.3.20}$$

We may now proceed with step 2 and derive the symplectic form on the phase space employing (5.3.1). Following the same steps as in sec. 5.3.1, we obtain

$$\omega = d\Pi_\Phi \wedge d\Phi + d\Pi_\Psi \wedge d\Psi + d\Pi_0 \wedge dk_0. \tag{5.3.21}$$

The interpretation of this result is similar to the U(1) toy model in sec. 5.3.1. The fields Φ on the left boundary and Ψ on the right boundary give rise to two contributions seemingly analogous to $dp \wedge dq$ for a particle. However, the last term $d\Pi_0 \wedge dk_0$ prevents a factorization of the phase space in terms of fields on the left and right boundary as it is given in terms of the holonomy and its canonical conjugate. The phase space variables Π_0 and k_0 are non-local from the boundary CFT point of view as they cannot be written in terms of local fields located only on one boundary. We then obtain a non-trivial Berry phase from the symplectic form (5.3.21), which is induced by the spacetime wormhole in the bulk since the integral $\int \omega$ in (5.2.15) explicitly depends on non-local variables from the CFT point of view and therefore does not reduce to

an integral involving only boundary fields. Thus, we find that Berry phases present an ideal probe of bulk wormholes from the CFT point of view: It is a CFT measure sensitive to the wormhole in the bulk, and there is evidence of non-factorization also in the CFT as the symplectic form on the phase space does not factorize.

While it is convenient to work in the simple parameterization Φ and Ψ of the boundary fields, it hides the relation of the Berry phase obtained from (5.3.21) to the single CFT Berry phase (5.2.14). It was shown in [245] that the chiral boson action (5.3.18) may be mapped to the Virasoro coadjoint orbit action (2.1.66) by parameterizing the chiral bosons in terms of inverse Virasoro group elements F and G with $F(t, f(t,\varphi)) = \varphi$ and similarly for G,

$$\begin{aligned} \Phi &= k_0(F(t,\varphi) - \varphi) - \ln\left(-k_0 F'(t,\varphi)\right), \\ \Psi &= k_0(\varphi - G(t,\varphi)) - \ln\left(k_0 G'(t,\varphi)\right). \end{aligned} \tag{5.3.22}$$

Then, the action (5.3.18) becomes the difference of two Virasoro geometric actions

$$S = S^{L,-}_{\text{geo}}[F, b_0] - S^{R,+}_{\text{geo}}[G, b_0], \tag{5.3.23}$$

where $S^{L,-}_{\text{geo}}$ and $S^{R,+}_{\text{geo}}$ denote the geometric action obtained from the right-moving CFT sector in the left boundary and the left-moving sector in the right boundary, respectively. Furthermore, the orbit label b_0 is related to the holonomy by [245]

$$b_0 = \frac{k}{8\pi} k_0^2. \tag{5.3.24}$$

We may interpret this result as follows. From sec. 5.2.2, we know that the geometric action is equal to the Virasoro Berry phase for a single copy of the CFT up to a boundary term that we may add by hand. Similarly, (5.3.23) computes the Berry phase for two CFTs in the presence of the eternal AdS black hole. Note that in (5.3.23) it appears as if we obtain two independent Berry phases for each CFT. Upon closer inspection this is not true since the orbit labels b_0 are identical in both CFTs and act as a coupling. From a physical point of view, the equality of both orbit labels implies that observers in the left and right CFT see a black hole with exactly the same mass from both boundaries. In contrast, for two single-sided black holes with a single boundary, the Berry phases decouples, and the phase space phase is given by $\mathcal{M} = \frac{\widehat{\text{Diff}}(S^1)}{U(1)} \times \frac{\widehat{\text{Diff}}(S^1)}{U(1)}$. This phase space is factorized and upon quantization yields a factorized Hilbert space, one for each copy of the CFT dual to a single-sided black hole. Each orbit has its own independent U(1) fiber $\mathcal{K}$.

The coupling of the orbits in (5.3.23) and therefore also the coupling of the Berry phase indicates a non-factorized phase space $\mathcal{M} = \frac{\widehat{\text{Diff}}(S^1)\times\widehat{\text{Diff}}(S^1)}{U(1)}$, where the common center $U(1)$ is related to the mass of the eternal AdS black hole in the bulk. In the chiral boson model (5.3.18), this coupling is achieved by the holonomy k_0 of the annulus given in terms of the orbit label by (5.3.24). Conclusively, in the presence of a wormhole in the bulk, we obtain two coupled single orbit Virasoro Berry phases given in terms of the coupled geometric action on coadjoint orbits with a common orbit label fixed in terms of the black hole mass. This is a classical analog of a non-factorized Hilbert space. In this manner, we have shown that it is possible to see non-factorization also in the CFT in the form of coupled Berry phases.

5.4. Wormholes from Modular Berry Phases

The Berry phase for the CFT we have discussed so far is similar in nature to the standard example of a spin in a magnetic field since both arise from symmetry group transformations. As discussed in sec. 5.2.1, the SU(2) Berry phase is in fact precisely the Berry phase obtained for the spin in a magnetic field. There are, however, more possibilities to define Berry phases in CFTs which allow probing the wormhole. In particular, Berry phases may also be obtained by parallel transporting subregions in the CFT around a closed loop in the space of CFT subregions. Equivalently, this problem may be viewed as a parallel transport of the reduced density matrix ρ_A of a subregion A and its associated modular operator (3.1.3). The holonomy obtained from parallel transporting a subregion in the CFT then gives rise the the modular Berry phase [106–108] and is a probe of the entanglement structure of the global state. Since the eternal AdS black hole is dual to two entangled CFTs, the modular Berry phase presents another ideal probe of the wormhole. So far, modular Berry phases were only calculated for CFTs in the vacuum [108, 246] as the modular Hamiltonian is local and known in this case. Therefore, we first study modular Berry phases for a single thermal CFT dual to a single-sided BTZ black string. The single-sided BTZ black string is a black hole with non-compact horizon and only one boundary. We then move on to the more complicated entangled CFTs dual to the two-sided BTZ black string with two boundaries. We begin by reviewing the construction of the modular Berry phase in sec. 5.4.1 and generalize it to thermal two-dimensional CFTs on the cylinder with compact time and non-compact spatial direction. This is possible since the modular Hamiltonian may be obtained from a conformal map of the vacuum modular Hamiltonian in this case [166]. In sec. 5.4.2, we then derive the modular Berry

phase for a single CFT in a thermal state corresponding to a large interval limit dual to a single-sided black string in AdS. We then study the modular Berry phase in this system for a small interval. We observe that a relation between the symplectic form on the space of intervals and the Berry curvature observed for the vacuum continues to hold in the thermal case we consider. Based on this result, we make a tentative proposal for the modular Hamiltonian for the BTZ black hole with compact time and space directions where a map from the vacuum modular Hamiltonian does not exist as the spacetime is topologically equivalent to an annulus rather than a cylinder [166]. Drawing on these results, we finally derive the modular Berry phase for two CFTs dual to the two-sided BTZ black string and demonstrate how the Berry phase probes the wormhole.

5.4.1. Modular Berry Phase from Parallel Transport of CFT Subregions

To calculate the modular Berry phase, we need two ingredients: the modular Hamiltonian in a two-dimensional CFT for the system of interest and a notion of parallel transport for subregions on a constant time slice in the CFT. The Berry phase then follows from the holonomy of parallel transporting a subregion. We begin by briefly explaining how the modular Hamiltonian for two-dimensional CFTs on the cylinder is obtained from the Rindler modular Hamiltonian discussed in sec. 3.1.2 and then move on to describe how the Berry curvature is obtained from parallel transport of intervals. Finally, we introduce kinematic space as the space of intervals on a constant time slice in the CFT. Kinematic space plays a central role for the modular Berry phase as the modular Berry curvature is related to the symplectic form on this space.

Modular Hamiltonian in two-dimensional CFTs

If we are given a QFT in a state $|\psi\rangle$ and a subregion A, we may associate a reduced density matrix $\rho_A = \mathrm{tr}_A(|\psi\rangle\langle\psi|)$ to this subregion. Employing the formal definition (3.1.3), we may define the modular operator associated to the density matrix ρ_A. As discussed in sec. 3.1.2, for a QFT on Minkowski space, the modular operator $K = K_L - K_R$ is nothing but the Rindler-boost operator acting simultaneously in the subregions $x > 0$ and $x < 0$ with conserved charge H_{mod}. The Rindler-boost operator generates time translations with respect to the Rindler (or modular) time s by the unitary transformation $U = \rho^{is} = e^{-2\pi i s K}$. In particular, U is a symmetry of the system since it generates time translations in the Rindler time coordinate which leave

invariant expectation values of operators in the subregion A. More generally, given a subregion A with an algebra of observables $\mathcal{A}_A$, U generates an automorphism that maps the algebra to itself [108],

$$e^{iKs}\mathcal{A}_A e^{-iKs} = \mathcal{A}_A. \tag{5.4.1}$$

We are interested in the modular Hamiltonian for a subregion on a constant time slice in a two-dimensional CFT on the cylinder. In two dimensions, the constant time slice is a circle S^1 and thus the subregion A is an interval $[u, v]$. It was shown in [247] that the causal development of the half-space $x > 0$, i.e. the Rindler wedge, may be mapped to the causal development of a single interval $[-R, R]$ with modular Hamiltonian

$$H_{\text{mod},A} = \int_A \frac{R^2 - x^2}{2R} T_{tt}(x) dx. \tag{5.4.2}$$

From this result, modular Hamiltonians for CFTs on the cylinder in the vacuum or in a thermal state may be derived since they follow from employing conformal transformations [166]. In all of these cases, the modular Hamiltonian may be written as a local operator of the form [166, 248].

$$H_{\text{mod},A} = \int_A dx\, n^\mu\, T_{\mu\nu} K^\nu, \tag{5.4.3}$$

Here, n^μ is the unit normal vector normal to the subregion A, which for a subregion on a constant time slice in a two-dimensional CFT is the timelike unit normal vector, and K^μ is the Rindler boost vector mapped to the CFT or equivalently the components of the modular operator K in the CFT. It is straightforward to check that for a QFT in the vacuum on Minkowski space, we recover the modular Hamiltonian (3.1.11) upon inserting the timelike component of the Rindler boost on a constant time slice and $d\Sigma^t = dx$. Since in general the modular Hamiltonian for a CFT is only known if it can be obtained from a map of the Rindler modular Hamiltonian [166], (5.4.3) holds for the CFTs on the cylinder we consider. Note that it is not possible to construct the modular Hamiltonian for CFTs on the torus, which includes CFTs dual to the BTZ black hole, in this manner. The modular Hamiltonian in such systems is thus generally unknown and has only been computed for very simple CFTs on the torus such as for free fermions [249], where it contains contributions that generate non-local modular flows. However, for holographic CFTs, the modular Hamiltonian has the special feature that to leading order in G_N in the bulk theory, it is always local. This may be inferred from the dual bulk modular Hamiltonian, which is related to the area

operator of the Ryu-Takayanagi surface homologous to the CFT subregion to leading order in G_N [46, 250],

$$H_{\text{mod}} = \frac{\text{Area}}{4G_N} + H_{\text{bulk}}. \tag{5.4.4}$$

H_{bulk} is the modular Hamiltonian for bulk fields in the spacetime region associated to the Ryu-Takayanagi surface and is of order $\mathcal{O}(G_N)$. Since the area operator is always local to leading order in G_N, the dual modular Hamiltonian in the CFT therefore must also be local irrespective of whether a map from Rindler space exists. We will employ this feature to make a tentative suggestion for the modular Hamiltonian in the BTZ black hole geometry based on observations from modular Berry phases and compare with previous proposals obtained from different methods in [186].

Modular parallel transport

We now consider a connected, continuous set of intervals λ on a constant time slice in the CFT. To define modular parallel transport, we study how the modular Hamiltonian changes upon choosing a particular interval λ^i and deforming it into $\lambda^i + \delta\lambda^i$. To achieve this, it is necessary to associate an algebra to it. It is then convenient not to use the modular Hamiltonian H_{mod}, which is the Noether charge associated to the boost vector K^μ and given in (5.4.3), but rather the modular operator $K = K^\mu \partial_\mu$, defined in (3.1.3), itself. The modular operator K may be written in terms of the global SL(2,$\mathbb{R}$) algebra of the CFT on the cylinder [108, 246] and encodes the interval dependence of H_{mod}.

We now follow [108], which introduced modular parallel transport. To obtain modular parallel transport equations, we rewrite the operator $K \equiv K(\lambda^i)$ in the Schrödinger picture with the spectrum of eigenvalues Δ and a basis U of eigenvectors, $K = U^\dagger \Delta U$. Note, however, that the choice of basis is not unique. There are operators Q_a that commute with K,

$$[K, Q_a] = 0. \tag{5.4.5}$$

These operators are called modular zero modes in [108] and generate transformations $U_Q = e^{i\sum_a s_a Q_a}$. An example of a zero-mode operator is the modular operator K itself, $Q = -2\pi K$ with transformation $U_Q = e^{-2\pi i s K}$. Therefore, Q generates a flow with respect to the modular time. The zero mode then represents the gauge freedom to choose the modular time parameter for each interval. In the Rindler case discussed in sec. 3.1.2, this corresponds to the choice of Rindler frame. The decomposition of K into a basis is then no longer unique since the basis $\tilde{U} = (UU_Q)$ gives rise to the same operator, $K = (UU_Q)^\dagger \Delta U U_Q = U^\dagger \Delta U$. The continuous space formed by the set of all

intervals on a constant time slice in a CFT then has a fiber bundle structure as shown in fig. 5.1 with base space $\mathcal{M}$ given by the physically different modular operators K for all intervals. The fibers $\mathcal{K}$ representing the gauge choice for the basis is then generated by the zero-mode operators Q_a. Due to the gauge choice for the basis, we have to define a notion of parallel transport in the space of intervals. The holonomy is then obtained from the curvature of the fiber bundle. We now consider an interval $\lambda = [u, v]$ on a constant time slice in the CFT with its associated modular operator K and infinitesimally transform the interval to $\lambda_i + \delta\lambda_i = [u, v] + [du, dv]$. Generally under the deformation $\lambda_i + \delta\lambda_i$, both the spectrum and the basis will change,

$$\partial_\lambda K \delta\lambda = \partial_\lambda (U^\dagger \Delta U)\delta\lambda = [\partial_\lambda U^\dagger U, K]\delta\lambda + U^\dagger \partial_\lambda \Delta U \delta\lambda. \tag{5.4.6}$$

The first term encodes the change in the basis U, the second the change in the spectrum Δ. The latter is an element of the zero modes since $[K, U^\dagger \partial_\lambda \Delta U] = 0$. Next, we define a projector onto the zero-modes for some operator $\mathcal{O}$ in the interval λ by

$$P_0^\lambda[\mathcal{O}] \equiv \sum_{E, q_a, q_a'} |E, q_a\rangle \langle E, q_a|\mathcal{O}|E, q_a'\rangle \langle E, q_a'|\,, \tag{5.4.7}$$

where $|E, q_a\rangle$ is a simultaneous eigenstate of K and Q_a. The connection that encodes the change in the zero-mode frame U_Q of the basis under an infinitesimal deformation $\lambda^i + \delta\lambda^i$ is then obtained by the zero-mode projection of the first term in (5.4.6). Thus, the connection is given by

$$\Gamma\left(\lambda^i, \delta\lambda^i\right) = P_0^\lambda \left[\partial_{\lambda^i} U^\dagger U\right] \delta\lambda^i. \tag{5.4.8}$$

Given a continuous family of modular operators $K(\lambda)$ and a continuous family of bases $\tilde{U}(\lambda)$, we may relate the basis $\tilde{U}(\lambda + \delta\lambda)$ to the basis $\tilde{U}(\lambda) = U(\lambda)$ for the initial interval λ by parallel transport with the covariant derivative $D_\lambda = \partial_\lambda + \Gamma$,

$$\tilde{U}(\lambda + \delta\lambda) = U(\lambda) + D_\lambda \tilde{U}(\lambda)\delta\lambda = U(\lambda + \delta\lambda) + U(\lambda)\Gamma\delta\lambda. \tag{5.4.9}$$

Multiplication by $\tilde{U}^\dagger(\lambda) = U^\dagger(\lambda)$ on both sides yields the parallel-transport operator $V_{\delta\lambda}$ for the basis,

$$V_{\delta\lambda} = \tilde{U}^\dagger \partial_\lambda \tilde{U} = U^\dagger \partial_\lambda U + \Gamma d\lambda. \tag{5.4.10}$$

It obeys the modular Berry-transport equations [108]

$$\begin{aligned} \partial_\lambda K - P_0^\lambda \left[\partial_\lambda K\right] &= \left[V_{\delta\lambda}, K\right], \\ P_0^\lambda \left[V_{\delta\lambda}\right] &= 0. \end{aligned} \tag{5.4.11}$$

In particular, the parallel-transport operator cannot have any zero modes. Therefore, the projection $P_0^\lambda \left[V_{\delta\lambda}\right]$ has to vanish. The most convenient way to obtain the Berry-curvature operator $\hat{R}_{ij}$ is from the commutator

$$\hat{R}_{ij} = [V_{\delta\lambda_i}, V_{\delta\lambda_j}]. \tag{5.4.12}$$

Note that since we are taking the commutator of the operators $V_{\delta\lambda_i}$, the curvature is an operator in this case. For an interval on a constant time slice in a CFT on the cylinder in the vacuum [108] as well as the thermal case we discuss here, the Berry curvature operator is given in terms of the Crofton form on kinematic space. We therefore continue with a brief review of kinematic space.

Kinematic space

The kinematic space [251, 252] of a constant time slice on a two-dimensional CFT is the space of all intervals on the chosen time slice. This space is a symplectic manifold equipped with a symplectic form ω, called the Crofton form, and a metric. Given the interval endpoints λ_i and λ_j, the Crofton form and the metric are given in terms of the entanglement entropy $S(\lambda_i, \lambda_j)$ [252],

$$\begin{aligned} ds^2 &= C\partial_{\lambda_i}\partial_{\lambda_j} S(\lambda_i, \lambda_j) d\lambda_i d\lambda_j, \\ \omega &= C\partial_{\lambda_i}\partial_{\lambda_j} S(\lambda_i, \lambda_j) d\lambda_i \wedge d\lambda_j. \end{aligned} \tag{5.4.13}$$

The prefactor C is system-dependent. For instance, for a CFT in the vacuum $C = \frac{c}{12}$, where c is the central charge. Locally, we may find a symplectic potential α such that $\omega = d\alpha$. It is given by the differential entropy [252],

$$\alpha = -\partial_{\lambda_i} S(\lambda_i, \lambda_j)|_{\lambda_j} d\lambda_i. \tag{5.4.14}$$

Within the AdS/CFT correspondence, kinematic space has a dual description in terms of the Ryu-Takayanagi geodesics that connect the interval endpoints λ_i and λ_j in the dual bulk geometry. Therefore, in the bulk prescription kinematic space is the set of all Ryu-Takayanagi geodesics anchored on a constant time slice in the CFT. The symplectic form and the Crofton form are then given in terms of the length of the

geodesic $L(\lambda_i, \lambda_j)$ since the holographic entanglement entropy is given by [41]

$$S = \frac{L(\lambda_i, \lambda_j)}{4G_N}. \tag{5.4.15}$$

In particular, we will see below that the modular Berry curvature is given in terms of the Crofton form.

5.4.2. Modular Berry Curvature for Thermal CFTs on the Cylinder

Based on the approach for a CFT on a cylinder in the vacuum [108], we derive the modular Berry curvature for various interval configurations in a thermal CFT on the cylinder with compact Euclidean time and non-compact spatial direction. We will begin with simple setups that include the CFT in a thermal state and a finite interval in a CFT in a thermal state. Finally, we consider intervals in two entangled CFTs dual to the two-sided BTZ black string to study the wormhole from the CFT point of view.

To obtain the modular Berry curvature from (5.4.12), we must first find the parallel-transport operator V_{δ_i} that satisfies the modular Berry transport equations (5.4.11). This is most easily accomplished by finding eigenoperators E_κ of the modular operator with eigenvalue κ [108],

$$[E_\kappa, K] = \kappa E_\kappa. \tag{5.4.16}$$

Equation (5.4.16) hast two different types of solutions: Operators E_κ with eigenvalue $\kappa = 0$ and those with $\kappa \neq 0$. If the operator has eigenvalue $\kappa = 0$, it commutes with the modular operator K in (5.4.16). This implies the corresponding operator E_κ belongs to the zero-modes Q_a. It is therefore not a viable candidate for $V_{\delta\lambda_i}$ as it does not satisfy the modular Berry transport equations (5.4.11). Therefore, $V_{\delta\lambda_i}$ is one of the operators E_κ with $\kappa \neq 0$.

For the thermal CFTs on the cylinder we consider in this section, solutions to (5.4.16) are given by

$$\begin{aligned} E_{\kappa,1} &= K, \\ E_{\kappa,2} &= \partial_\lambda K. \end{aligned} \tag{5.4.17}$$

The solution $E_{\kappa,1}$ belongs to the zero-modes Q_a as K commutes with itself in (5.4.16). In contrast, $E_{\kappa,2}$ has a non-trivial eigenvalue $E_{\kappa,2}$ in the systems considered in this section. We may therefore construct the modular Berry transport operator $V_{\delta\lambda_i}$ from $E_{\kappa,2}$. In particular, the operator $V_{\delta\lambda_i}$ satisfying the modular Berry transport equations

(5.4.11) is given by

$$V_{\delta\lambda_i} = \frac{1}{\kappa} E_{\kappa,2} = \frac{1}{\kappa} \partial_{\lambda_i} K. \tag{5.4.18}$$

The Berry curvature may then be obtained from (5.4.12) and reads

$$\hat{R}_{ij} = [V_{\delta\lambda_i}, V_{\delta\lambda_j}] = -\frac{2}{\kappa} \partial_{\lambda_i} \partial_{\lambda_j} K. \tag{5.4.19}$$

In [108], it was observed that the Berry curvature for an interval on a constant time slice in a two-dimensional CFT in the vacuum is given in terms of the Crofton form ω defined in (5.4.13). We find that the same relation also holds for thermal CFTs on the cylinder,

$$\hat{R} = \omega K. \tag{5.4.20}$$

This relation between the modular curvature operator and the Crofton form has particularly interesting consequences in thermal CFTs. As we briefly discussed in sec. 3.2, there are transitions in the entanglement entropy when a certain interval size is exceeded. Due to (5.4.13), this induces a transition in the Crofton form, which in turn yields a transition in the modular Berry curvature. Therefore, the modular Berry phase is sensitive to transitions in the entanglement entropy. As we will see, this has particularly interesting consequences in two entangled CFTs dual to the two-sided BTZ black string. But now, let us first understand how the Berry curvature behaves in simpler thermal CFTs.

Modular Berry phase for a CFT in a thermal state

The simplest configuration we consider is a CFT in a thermal state at inverse temperature β on the cylinder described by the thermal density matrix ρ_{th}. The CFT has a compactified Euclidean time direction with $t_E \sim t_E + \beta$ and a non-compact spatial direction. Holographically, the CFT is dual to a BTZ black hole with a non-compact horizon. The metric is given by the BTZ black hole metric in Schwarzschild coordinates with horizon $r_h = \frac{2\pi}{\beta}$ [186]

$$ds^2 = -\left(\frac{r^2 - r_h^2}{\ell^2}\right) dt^2 + \left(\frac{r^2 - r_h^2}{\ell^2}\right)^{-1} dr^2 + r^2 dx^2, \tag{5.4.21}$$

but the 'angular coordinate' x is unwrapped to $-\infty < x < \infty$. Following [186], we call this geometry the BTZ black string[1]. For the thermal CFT with density matrix

[1] In contrast to the BTZ black hole, the BTZ black string is not a quotiented spacetime. The BTZ black hole is obtained from the BTZ black string by a global identification that follows by quotienting AdS_3 with a subgroup of the global symmetry group SO(2,2).

ρ_{th}, the modular Hamiltonian H_{mod} is given in terms of the system Hamiltonian H, $H_{\text{mod}} = \beta H$ [248]. This corresponds to choosing the interval large enough that it corresponds to the full time slice. The modular operator in this case is then given by

$$K = \beta(L_0 + \bar{L}_0). \tag{5.4.22}$$

For this system, the Berry-curvature operator vanishes,

$$\hat{R} = 0, \tag{5.4.23}$$

because there is no possibility to construct a modular parallel-transport operator $V_{\delta\lambda_i}$ that satisfies the modular parallel-transport equations (5.4.11). This may be seen as follows. Since $\partial_\lambda K = 0$, the first equation in (5.4.11) requires that we find an operator $V_{\delta\lambda_i}$ such that $[V_{\delta\lambda_i}, K] = 0$. This equation is solved by $V_{\delta\lambda_i} \propto (L_0 + \bar{L}_0)$. However, according to (5.4.16), $V_{\delta\lambda_i}$ is then an eigenoperator with eigenvalue $\kappa = 0$ and thus belongs to the zero modes Q_a. The second modular parallel-transport equation in (5.4.11) is then not fulfilled since $P_0^\lambda[V_{\delta\lambda_i}] \propto (L_0 + \bar{L}_0) \neq 0$. Therefore, there is no non-trivial Berry curvature in this case. The physical interpretation of this result is straightforward. If the modular Hamiltonian is given by the system Hamiltonian, this implies we do not consider a subregion but the full system. The entanglement cut specifying the subregion presents an artificial horizon: An observer located in the subregion only has access to the degrees of freedom in the subsystem, whereas the degrees of freedom outside the subregion remain hidden. Therefore, an observer in a subregion may fix a modular zero-mode frame U_Q that differs from the choice of zero-mode frame for an observer outside this subregion. The global state of the system is sensitive to the relative choice of frame. This gives rise to the Berry phase. If the observer has access to the full system as is the case here, there are no independent choices of zero-mode frames, and the frame may be fixed globally. Therefore, there is no Berry phase.

Modular Berry phase for a finite interval in a CFT in a thermal state

Here, we still consider a CFT in a thermal state on the cylinder, but study the modular Berry phase that arises from parallel transporting the interval $\lambda = [u, v]$ and its associated reduced density matrix ρ_λ rather than the thermal density matrix ρ_{th}. Just as in the preceding example, the CFT has a compactified Euclidean time direction with $t_E \sim t_E + \beta$ and a non-compact spatial direction; it is again dual to a BTZ black string. The interval $[u, v]$ is chosen on a constant time slice in the CFT. The

modular Hamiltonian may be obtained from the Rindler Hamiltonian by finding a map that maps the Rindler half-line on the plane to the interval $[u, v]$ on the cylinder with coordinates $w = x + it_E$. The map was derived in [248] and yields the modular Hamiltonian [248]

$$H_{\text{mod},\lambda} = \frac{\beta}{\pi}\int_u^v dx\, \frac{\sinh\left(\frac{\pi x}{\beta}\right)\sinh\left(\frac{\pi((v-u)-x)}{\beta}\right)}{\sinh\left(\frac{\pi(v-u)}{\beta}\right)} T_{tt}(x). \tag{5.4.24}$$

The modular operator K_λ may then be obtained from the following conditions (see for instance [253]): First, K_λ must leave invariant the interval endpoints $[u, v]$. Secondly, we know from the Rindler case that the modular time parameter, i.e. the Rindler time, is periodic with $t_E \sim t_E + 2\pi i$. Therefore, the modular flow of the coordinate x generated by K_λ with the transformation $e^{2\pi s K_\lambda}$ must obey $x(s) = x(s + i)$, where $x(s)$ is obtained by solving $\partial_s x(s) = 2\pi K_\lambda$. K_λ is an element of the global SL(2,$\mathbb{R}$) algebra. Therefore, we make an ansatz,

$$K_\lambda = K_{+,\lambda} + K_{-,\lambda}, \quad K_{+,\lambda} = a_{-1}L_{-1} + a_0 L_0 + a_1 L_1,\ K_{-,\lambda} = \bar{a}_{-1}\bar{L}_{-1} + \bar{a}_0\bar{L}_0 + \bar{a}_1\bar{L}_1. \tag{5.4.25}$$

We now focus on the holomorphic contribution K_+; K_- is obtained analogously. The representation of the SL(2,$\mathbb{R}$) generators L_{-1}, L_0, L_1 in a thermal CFT may be obtained from that on the complex plane given in (2.1.10) with the map $z = e^{\frac{2\pi}{\beta}w}$. This yields the generators

$$L_0 = -\frac{\beta}{2\pi}\partial_w \quad L_{-1} = -\frac{\beta}{2\pi}e^{-\frac{2\pi}{\beta}w}\partial_w \quad L_1 = -\frac{\beta}{2\pi}e^{\frac{2\pi}{\beta}w}\partial_w. \tag{5.4.26}$$

We now enforce that $K_{+,\lambda}$ leaves the interval endpoints $[u, v]$ on a constant time slice invariant, which yields the constraints

$$\begin{aligned} 0 &= -a_{-1}\frac{\beta}{2\pi}e^{-\frac{2\pi}{\beta}u} - a_0\frac{\beta}{2\pi} - a_1\frac{\beta}{2\pi}e^{\frac{2\pi}{\beta}u}, \\ 0 &= -a_{-1}\frac{\beta}{2\pi}e^{\frac{-2\pi}{\beta}v} - a_0\frac{\beta}{2\pi} - a_1\frac{\beta}{2\pi}e^{\frac{2\pi}{\beta}v}. \end{aligned} \tag{5.4.27}$$

We may solve these equations by fixing a_{-1} and a_1 in terms of a_0,

$$a_{-1} = -\frac{a_0 e^{\frac{2\pi}{\beta}}(u+v)}{e^{\frac{2\pi}{\beta}u} + e^{\frac{2\pi}{\beta}v}} \qquad a_1 = -\frac{a_0}{e^{\frac{2\pi}{\beta}u} + e^{\frac{2\pi}{\beta}v}}. \tag{5.4.28}$$

The remaining coefficient may then be obtained by solving $\partial_s x(s) = 2\pi K_{+,\lambda}$ and imposing $x(s) = x(s+i)$ on the solution. We obtain

$$a_0 = \coth \frac{\pi}{\beta}(v-u). \tag{5.4.29}$$

Therefore, up to an overall constant the modular operator is given by

$$\begin{gathered} K_{+,\lambda} = a_1 L_1 + a_0 L_0 + a_{-1} L_{-1}, \\ a_1 = \frac{\coth \frac{2\pi}{\beta}(v-u)/2}{e^{\frac{2\pi}{\beta}u} + e^{\frac{2\pi}{\beta}v}}, \quad a_0 = -\coth \frac{2\pi}{\beta}\frac{v-u}{2}, \quad a_{-1} = \frac{\coth \frac{2\pi}{\beta}(v-u)/2}{e^{-\frac{2\pi}{\beta}u} + e^{-\frac{2\pi}{\beta}v}}. \end{gathered} \tag{5.4.30}$$

There are two possible solution of the form (5.4.18) to the modular Berry transport equations (5.4.11) depending on whether we deform the interval endpoint u or v. The solution reads,

$$V_{+,\delta u} = \partial_u K_{+,\lambda} \quad V_{+,\delta v} = -\partial_v K_{+,\lambda}. \tag{5.4.31}$$

Therefore, we obtain the eigenvalues $\kappa = \pm 1$. Employing (5.4.19), the Berry-curvature operator for $V_{+,\delta\lambda}$ is then given by

$$\hat{R}_+ = -\frac{4\pi^2}{\beta^2}\operatorname{csch}\frac{v-u}{\beta} K_{+,\lambda} du \wedge dv. \tag{5.4.32}$$

A similar result is obtained for $\hat{R}_-$ from $V_{-,\delta\lambda}$. For an interval $[u,v]$ on a constant time slice in a thermal CFT dual to the BTZ black string, we therefore obtain the non-trivial Berry curvature operator (5.4.32). In contrast to (5.4.23), the Berry curvature for this setup is non-vanishing. The entanglement cut separating the interval $[u,v]$ from its complement acts as a horizon hiding some of the degrees of freedom of the full system. An observer in $\lambda = [u,v]$ with the reduced density matrix ρ_λ is free to choose the zero-mode frame U_Q for their modular operator K_λ. Similarly, an observer located in the complement $\bar{\lambda} = [v,u]$ may independently choose their zero-mode frame. While the choice of the zero-mode frame is a gauge choice in each subregion, the global thermal state describing the full CFT is sensitive to the relative zero-mode frame chosen in each interval. The Berry phase probes the misalignment of the zero-mode frames in the full system. A quick sanity check is to take the limit $u, v, (u-v) \gg \beta$, in which the modular Hamiltonian (5.4.24) reduces to $H_{\text{mod}} \propto H$ [248]. This corresponds to the large-interval limit in which we describe the system with the full thermal density matrix ρ_{th}. As expected, upon taking the limit $u, v, (u-v) \gg \beta$, the modular Berry curvature (5.4.32) vanishes and we recover (5.4.23).

Let us now compare the result (5.4.32) with the Crofton form ω on kinematic space,

which is given by [186]

$$\omega = \frac{4\pi^2}{\beta^2}\text{csch}\frac{v-u}{\beta}. \tag{5.4.33}$$

Therefore, the Berry-curvature operator (5.4.32) is given in terms of the Crofton form on kinematic space

$$\hat{R}_+ = \kappa\omega K_{+,\lambda} du \wedge dv. \tag{5.4.34}$$

A similar relation was observed for an interval in a CFT in the vacuum in [108]. The relation between the Berry curvature operator and the symplectic form is quite natural for the following reason: The Berry curvature is obtained by parallel transporting an interval around a closed loop. We therefore probe the space of intervals on a constant time slice of the given CFT. But this space of intervals is nothing but the kinematic space with the Crofton form as its natural symplectic form. We thus obtain a modular Berry curvature given in terms of the Crofton form.

So far, we have focused on the BTZ black string. For the BTZ black hole, the Crofton form on kinematic space is known as it can be computed from the entanglement entropy as given in (5.4.13). However, the modular Hamiltonian has not been computed since it cannot be obtained from the Rindler modular Hamiltonian by a conformal map [166]. We now use the relation between the modular Berry curvature operator and the Crofton form to make a tentative suggestion for the modular Hamiltonian of the BTZ black hole.

A tentative suggestion for the modular Hamiltonian for a CFT on the torus dual to the BTZ black hole

The BTZ black hole is obtained from the BTZ black string geometry by identifying two points P and P' by $P' = e^{k\zeta}P$, where $k \in \mathbb{Z}$ and ζ is the Killing vector $\zeta = \partial_\varphi$ [254]. This corresponds to compactifying the spatial direction with periodicity one. The Euclidean time direction is periodic with $\beta = \frac{2\pi}{r_h}$, where r_h denotes the horizon. Therefore, the spacetime has a compact space and time direction and is topologically a torus. In this case, it is not possible to obtain the modular Hamiltonian with a map from the Rindler modular Hamiltonian [166]. We do, however, know that within AdS/CFT, the modular Hamiltonian is local to leading order in G_N and given by (5.4.4). Furthermore, the Crofton form on kinematic space for an interval $[u, v]$ on a constant time slice is known. In particular, the Crofton form exhibits a transition at the critical interval size γ_C,

$$v - u = \frac{\beta}{2\pi}\log\left(\frac{1}{2} + \frac{1}{2}e^{\frac{4\pi^2}{\beta}}\right) \equiv \gamma_C. \tag{5.4.35}$$

This transition is induced by a sharp transition in the shortest geodesic yielding the entanglement entropy since the entanglement entropy and the Crofton form are related by (5.4.13). For intervals $v-u<\gamma_C$, the entanglement entropy in the dual bulk spacetime is as usual given in terms of the shortest geodesic connecting the interval endpoints. Then, at $v-u=\gamma_C$, there is a sudden jump in the geodesic configurations yielding the shortest geodesic: For intervals $v-u>\gamma_C$, the entanglement entropy is computed in terms fo two disconnected geodesics, one connecting the interval endpoints for the complement of the interval $[u,v]$ and a second geodesic wrapping around the horizon. This is shown in fig. 3.3. In sum, these two disconnected geodesics are shorter than a single geodesic connecting the endpoint $[u,v]$ if $v-u>\gamma_C$. For each configuration, we obtain a different Crofton form [186],

$$\begin{aligned}\omega_1 &= \frac{4\pi^2}{\beta^2}\operatorname{csch}^2\frac{\pi(v-u)}{\beta}du\wedge dv \quad \text{for } v-u<\gamma_C,\\ \omega_2 &= -\frac{4\pi^2}{\beta^2}\operatorname{csch}^2\frac{2\pi\left(\pi-\frac{v-u}{2}\right)}{\beta}du\wedge dv \quad \text{for } v-u>\gamma_C.\end{aligned} \tag{5.4.36}$$

At $v-u=\gamma_C$, the Crofton form is singular [186]. Since at least to leading order, the modular Hamiltonian H_{mod} must be local, the modular operator K must also be local. Furthermore, the Crofton form is the natural symplectic form on kinematic space, which we probe with modular Berry transport. Let us therefore assume that there are two modular Berry curvatures given by

$$\begin{aligned}\hat{R}_1 &= \omega_1 K_1,\\ \hat{R}_2 &= \omega_2 K_2,\end{aligned} \tag{5.4.37}$$

and that to leading order in G_N the modular Hamiltonian is of the form (5.4.3). We have hence captured the global aspect of the transition between Crofton forms, which emerges on a torus, in the existence of two modular Hamiltonians in the proposal (5.4.37). Locally, the torus is isomorphic to the complex plane, and therefore we propose that once we have captured the global properties of the torus in (5.4.37) and since we know that to leading order the modular Hamiltonian is local due to (5.4.4), we may write the modular operator in terms of the SL(2,$\mathbb{R}$) generators on the complex plane. Employing the procedure to obtain the modular Berry phase, we may then reconstruct the modular Hamiltonian and arrive at

$$H_{\text{mod,local},1}=\frac{\pi}{\beta}\int_u^v d\theta'\frac{\sinh\frac{\pi(\theta'-u)}{\beta}\sinh\frac{\pi(v-\theta')}{\beta}}{\sinh\frac{2\pi}{\beta}\left(\frac{u-v}{2}\right)}T_{tt}(\theta') \tag{5.4.38}$$

before the transition and

$$H_{\text{mod,local },2} = \frac{\pi}{\beta}\int_u^v d\theta' \frac{\sinh\frac{\pi(\pi-(\theta'-u))}{\beta}\sinh\frac{\pi(\pi-(v-\theta'))}{\beta}}{\sinh\frac{2\pi}{\beta}\left(\pi-\frac{u-v}{2}\right)} T_{tt}(\theta') \tag{5.4.39}$$

after the transition. Note that we only expect (5.4.38) and (5.4.39) to be one possible contribution to the full modular Hamiltonian valid at most to leading order in G_N. Beyond the leading order, we expect non-local contributions to the modular Hamiltonian. A first promising feature of the modular Hamiltonians obtained in this manner is that (5.4.38) has been proposed as the modular Hamiltonian before the transition in [186] employing a different procedure. In [186], a relation between the modular Hamiltonian and bulk-to-boundary propagators first observed in [255] was employed to arrive at the result (5.4.38). As a next step, the validity of the results may be verified by calculating the entanglement spectrum of the modular Hamiltonians (5.4.38) and (5.4.39). We leave this for future research.

Modular Berry phase and factorization in entangled CFTs dual to the two-sided BTZ black string

We calculated the modular Berry curvature operator for a single interval in a thermal CFT dual to the single-sided BTZ black string in (5.4.32). A single-sided geometry implies there is only one exterior region and one boundary. Similar to the BTZ black hole, the CFT in a thermal state dual to the single-sided BTZ black string may be purified by doubling the system yielding a two-sided BTZ black string dual to a CFT in a TFD state. We then obtain two identical copies of the CFT on either boundary of the two-sided bulk geometry. Note that in contrast to the BTZ black hole, the system is topologically a cylinder rather than a torus. The TFD state is constructed from the Euclidean path integral on the cylinder with two vertical cuts along the non-compact spatial direction. These cuts are identified with the left and right CFT. Therefore, a point at time $t_R = t$ in the right CFT may be mapped to a point $t_L = -t + i\frac{\beta}{2}$ in the left CFT. For more details on this construction, we refer to [256]. Since we have two copies of the CFT, one on each boundary, we now consider two disjoint intervals. The general setup is shown in fig. 5.4. We choose an interval $[u_L, v_L]$ in the left CFT and similarly an interval $[u_R, v_R]$ in the right CFT. Note that there are two possibilities to connect the interval endpoints with a Ryu-Takayanagi surface in the bulk. We may either connect interval endpoints at the same boundary leading to the red configuration in fig. 5.4 or at opposite boundaries giving rise to the blue configuration. As we discussed in sec. 3.3, it was shown in [50] that the entanglement

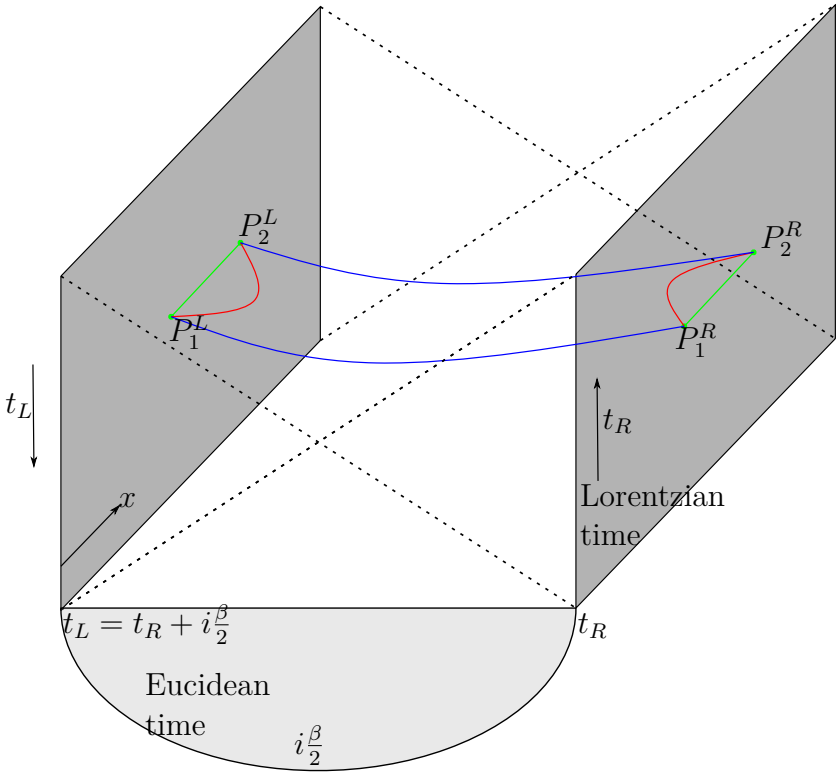

Fig. 5.4.: The two-sided BTZ black string geometry with an interval, shown in green, in each boundary. The endpoints of the interval shown in green are specified by P_1^L and P_2^L on the left boundary and P_1^R and P_2^R on the right boundary. Depending on the interval size, there are two different modular Hamiltonians describing the system. For small intervals with $\chi > 1$, the modular Hamiltonian arises from the blue configuration of the Ryu-Takayanagi geodesics yielding the entanglement entropy. For larger intervals with $\chi \leq 1$, the red configuration is appropriate. Only the modular Hamiltonian arising from the blue configuration is sensitive to the wormhole. The half-circle shaded in light gray is a part of the Euclidean cylinder that was employed to construct the system in [256].

entropy sharply transitions from the blue configuration to the red configuration. The transition occurs at $\chi = 1$, where χ is given by

$$\chi = \frac{\sinh \frac{2\pi}{\beta}\frac{u_L - v_R}{2} \sinh \frac{2\pi}{\beta}\frac{u_R - v_R}{2}}{\operatorname{csch} \frac{2\pi}{\beta}\frac{u_L - u_R}{2} \operatorname{csch} \frac{2\pi}{\beta}\frac{v_L - v_R}{2}}. \tag{5.4.40}$$

There are two different modular Hamiltonians, one for each configuration in fig. 5.4. The modular Hamiltonians were derived in [256]. Let us begin with the red configuration in fig. 5.4 which corresponds to $\chi \leq 1$. It was shown in [256] that in this case, we obtain two copies of the modular Hamiltonian for the single boundary setup given in (5.4.24). The modular operator K^L_{+,λ_L} for the interval $\lambda_L = [u_L, v_L]$ on the left

boundary is then again given by

$$K^L_{+,\lambda_L} = \frac{\coth\frac{\pi}{\beta}(v_L-u_L)}{e^{\frac{2\pi}{\beta}u_L}+e^{\frac{2\pi}{\beta}v}}L_1 - \coth\frac{\pi}{\beta}(v_L-u_L)L_0 + \frac{\coth\frac{\pi}{\beta}(v_L-u_L)}{e^{-\frac{2\pi}{\beta}u_L}+e^{-\frac{2\pi}{\beta}v_L}}L_{-1}. \quad (5.4.41)$$

We obtain an additional copy for the interval on the right boundary by exchanging the index L with R and additional contributions for the right-moving sector. The modular operator for the two-interval setup is then given by

$$K_\lambda = K^R_{+,\lambda_R} + K^R_{-,\lambda_R} + K^L_{+,\lambda_L} + K^L_{-,\lambda_L}. \quad (5.4.42)$$

We may then proceed to calculate the modular Berry curvature (5.4.19) as described for the single interval setup and obtain

$$\begin{aligned}\hat{R}_+ &= -\frac{2}{\kappa}\partial_{u_L}\partial_{v_L}K^L_{+,\lambda_L}du_L\wedge dv_L - \frac{2}{\kappa}\partial_{u_R}\partial_{v_R}K^R_{+,\lambda_R}du_R\wedge dv_R \\ &= -\frac{4\pi^2}{\beta^2}\left(\operatorname{csch}^2\frac{2\pi\left(\frac{v_L-u_L}{2}\right)}{\beta}K^L_{+,\lambda_L}du_L\wedge dv_L + \operatorname{csch}^2\frac{2\pi\left(\frac{v_R-u_R}{2}\right)}{\beta}K^R_{+,\lambda_R}du_R\wedge dv_R\right).\end{aligned} \quad (5.4.43)$$

These are two copies of the single-interval modular Berry curvature (5.4.32). We therefore obtain two decoupled Berry phases, which are unaware of the bulk wormhole that is present in the two-sided bulk spacetime, and the Berry curvature behaves as if there were two disconnected spacetimes, each with a single boundary. Before we delve deeper into the meaning of this result, let us first consider the blue configuration in fig. 5.4. The modular Hamiltonian in this case is given by [256]

$$H_{u_L,u_R} = \frac{\pi}{\beta}\int_{-t+i\frac{\beta}{2}}^{t} dw \frac{\sinh\frac{u_L-w}{\beta}\sinh\frac{u_R-w}{\beta}}{\sinh(\frac{u_L-u_R}{\beta})}T_{ww}(w). \quad (5.4.44)$$

and similarly for H_{v_L,v_R}. The integral is along the imaginary axis for $w = x + it_E$ and $t_E = -it$. Clearly, the modular Hamiltonian (5.4.44) couples the left and right CFTs as it depends on interval endpoints in each boundary. This implies that the modular operator K_λ can no longer be written as a sum of left and right modular operators as we did in (5.4.42) for the red configuration. We obtain the modular operator as follows: First, we make an ansatz that couples the left and right CFT operators appearing in the modular operator,

$$K_{+,\lambda} = a_{-1}(L^R_{-1}+L^L_{-1}) + a_0(L^R_0+L^L_0) + a_1(L^R_1+L^L_1). \quad (5.4.45)$$

Then, we calculate the coefficients a_{-1} and a_1 by requiring that $K_{+,\lambda}$ leaves invariant the interval endpoints u_L and u_R of the interval $\lambda_u = [u_L, u_R]$, which yields

$$a_{-1} = -\frac{a_0 e^{\frac{2\pi}{\beta}}(u_L + u_R)}{e^{\frac{2\pi}{\beta}u_L} + e^{\frac{2\pi}{\beta}u_R}} \qquad a_1 = -\frac{a_0}{e^{\frac{2\pi}{\beta}u_L} + e^{\frac{2\pi}{\beta}u_R}}. \tag{5.4.46}$$

Finally, we require that the point x is periodic in the modular time s, $x(s) = x(s+i)$ for $\partial_s x(s) = 2\pi K_{+,\lambda_u}$, under the modular flow generated by K_{+,λ_u} in each CFT. This fixes a_0, and we obtain the modular operator

$$K_{+,\lambda_u} = \frac{\coth\frac{2\pi}{\beta}(u_L - u_R)/2}{e^{\frac{2\pi}{\beta}u_L} + e^{\frac{2\pi}{\beta}u_R}} L_1 - \coth\frac{2\pi}{\beta}\frac{u_L - u_R}{2} L_0 + \frac{\coth\frac{2\pi}{\beta}(u_L - u_R)/2}{e^{-\frac{2\pi}{\beta}u_L} + e^{-\frac{2\pi}{\beta}u_R}} L_{-1} \tag{5.4.47}$$

and similarly for $\lambda_v = [v_R, v_L]$. Following the same procedure as before, we obtain the modular Berry curvature for $\chi > 1$,

$$\begin{aligned}\hat{R}_+ &= -\frac{2}{\kappa}\partial_{u_R}\partial_{u_L}K_{+,\lambda_u}du_L \wedge du_R - \frac{2}{\kappa}\partial_{v_R}\partial_{v_L}K_{+,\lambda_v}dv_R \wedge dv_L \\ &= -\frac{4\pi^2}{\beta^2}\left(\operatorname{csch}^2\frac{2\pi\left(\frac{u_R-u_L}{2}\right)}{\beta}K_{+,\lambda_u}du_L \wedge du_R + \operatorname{csch}^2\frac{2\pi\left(\frac{v_R-v_L}{2}\right)}{\beta}K_{+,\lambda_v}dv_L \wedge dv_R\right).\end{aligned} \tag{5.4.48}$$

In general, we therefore obtain a non-trivial Berry curvature for the blue configuration as well. Furthermore, the Berry phase exhibits a similar transition as the entanglement entropy derived in [248]. This is expected as the modular Berry phase probes the entanglement structure of the CFTs. We would now like to understand the results (5.4.43) and (5.4.48) better and in particular illuminate how the bulk wormhole appears in the CFT Berry phases. To make the discussion more tangible, it is convenient to choose specific interval endpoints. Based on the setup considered in [248] to derive the entanglement entropy, we choose the interval endpoints $P_1^L = (-\frac{x}{2}, t_L = -t)$ and $P_2^L = (\frac{x}{2}, t_L = -t)$ in the left boundary and $P_1^R = (-\frac{x}{2}, t_R = t)$ and $P_2^R = (\frac{x}{2}, t_R = t)$ in the right boundary. As depicted in fig. 5.4, the time in the left and right CFT are related by $t_L = t_R + i\frac{\beta}{2}$. For this interval configuration, the transition between the blue and red configuration at $\chi = 1$ occurs at $t = \frac{x}{2}$. For $t \geq \frac{x}{2}$, the Ryu-Takayanagi geodesic yielding the entanglement entropy connects the interval endpoints $\lambda = [-\frac{x}{2}, \frac{x}{2}]$ at fixed value t in each boundary without threading the wormhole. This yields the Berry curvature,

$$\hat{R}_+ = -2\frac{4\pi^2}{\beta^2}\operatorname{csch}\frac{2\pi x}{\beta}K^+_\lambda dx_1 \wedge dx_2, \tag{5.4.49}$$

where we introduced the indices 1 and 2 to illustrate that these points are different. The prefactor of two arises since there are two identical Berry curvatures at each boundary. This is the expected result: The Berry curvature mirrors the entanglement entropy. Both are not sensitive to the bulk wormhole and are the results obtained by equivalently considering two disconnected spacetimes each with a single boundary. We therefore have two independent modular flows $U_L = e^{-2\pi i s_L K_L}$ and $U_R = e^{-2\pi i s_R K_R}$ with an independent choice of modular time coordinate. On the other hand, for $t < \frac{x}{2}$ the entanglement entropy is given in terms of the geodesic that connects the interval endpoints $\lambda = [-t + i\frac{\beta}{2}, t]$ at fixed spatial position $\frac{x}{2}$ at opposite boundaries through the wormhole. However, since we identified the time in the left and right CFT, we schematically obtain a modular Berry curvature operator $\hat{R}_+ \propto \omega K_{+,\lambda} dt \wedge dt = 0$. This vanishes due to the wedge product between identical coordinates. Since the two-sided BTZ black string is related to the Rindler system, the modular time is secretly the physical time. Therefore, by identifying the time in both CFTs, we matched the zero-mode frames in each CFT. Then, there is no relative zero-mode frame between the left and right CFT and the Berry curvature naturally vanishes. It was argued in [238] that the identification of the time coordinate in the left and right CFT cannot hold globally. The timelike Killing vector shrinks to zero at the horizon and then flips signs. This implies that in the presence of a wormhole there is not globally well-defined Killing vector. We may then introduce a global time shift δ between the time coordinate in the left and right boundary, $t_L - \delta = t_R + i\frac{\beta}{2}$. This time shift is not a local observable since it can only measured by two observers comparing their clocks when they meet in the wormhole. With this shift, we may compute the Berry curvature for the modified interval $\lambda = [-t - \delta + i\frac{\beta}{2}, t]$. This yields the modular Berry curvature

$$\hat{R}_+ = -\frac{4\pi^2}{\beta^2} \operatorname{sech}^2\left(\frac{\pi}{\beta}(2t+\delta)\right) K_{+,\lambda} d\delta \wedge dt. \tag{5.4.50}$$

We therefore shown that the modular Berry phase probes the wormhole for $\chi > 1$ if we introduce the time shift δ. This time shift δ exists only in the presence of a wormhole due to the absence of a global Killing vector.

5.5. Gauge Berry Phase

Finally, there is a third type of Berry phase sensitive to the bulk wormhole, which we call the gauge Berry phase. We discussed the phase space of AdS_3 in sec. 2.3.3 and noted that there are two types of bulk diffeomorphisms. Bulk diffeomorphisms ξ with

$\delta_\xi g_{\mu\nu} \neq 0$ give rise to the Virasoro Berry phase (5.2.14) as these bulk diffeomorphisms do not vanish at the asymptotic boundary but change the expectation value of the energy-momentum tensor such that we move along a path on the coadjoint orbit. As discussed in sec. 5.2.1, the coadjoint orbit is the base space of the fiber bundle for the Virasoro Berry phase. Furthermore, there are bulk diffeomorphisms ζ with $\delta_\zeta g_{\mu\nu} = 0$. These are the Killing symmetries of the bulk spacetime which reduce to diffeomorphisms that leave invariant the expectation value of the energy-momentum tensor in the CFT. These diffeomorphisms form the fiber of the fiber bundle for the Virasoro Berry phase. In a spacetime such as empty AdS, the bulk diffeomorphisms ζ corresponding to Killing symmetries cannot possibly yield a Berry phase. However, the eternal AdS black hole is special due to the wormhole. The timelike Killing vector $\zeta^\mu \partial_\mu = \partial_t$ does not exist globally in such a geometry. This may be seen as follows [238]: When transporting the Killing vector around a non-contractible circle through the wormhole, it vanishes at the horizon and then switches signs such that the Killing vector comes back with the wrong sign. Therefore, we may locally identify the times t_L and t_R in the asymptotic regions near the boundary, but we cannot do so globally for the eternal AdS black hole. This allows us to introduce time shifts between the left and right boundary, $t_L = 2\delta - t_R$, as we did for the modular Berry phase in the presence of a wormhole with Berry curvature (5.4.50). This time shift allows us to generate a sequence of time-shifted eternal AdS black hole geometries by evolving the TFD state with $H_L + H_R$,

$$|\text{TFD}\rangle_\delta = e^{-i(H_L+H_R)\delta}|\text{TFD}\rangle. \tag{5.5.1}$$

Note that only the evolution with $(H_L + H_R)$ yields time-shifted spacetimes since $(H_L - H_R)$ is a symmetry of $|\text{TFD}\rangle$. The time evolution yields a new state [238],

$$|\text{TFD}\rangle_\delta = \frac{1}{\sqrt{Z}} \sum_n e^{-2iE_n\delta} e^{-\beta\frac{E_n}{2}} |E_n\rangle_L |E_n\rangle_R, \tag{5.5.2}$$

where Z denotes the partition function. This state may be interpreted as a superposition of different time-evolved eternal AdS black holes from the perspective of a global observer. However, the experience of a local observer in either exterior region of the black hole is not effected as the additional phase does not change the reduced density matrix $\rho_{L/R}$ that describes the system available to an observer. The parameter δ may then be used to define a Berry connection [243],

$$A_\delta = i_\delta \langle \text{TFD} | \partial_\delta | \text{TFD} \rangle_\delta = \frac{2}{Z} \sum_n E_n e^{-\beta E_n}. \tag{5.5.3}$$

Note that such a Berry phase can only exist in the presence of a horizon, i.e. when the local observer has access only to a part of the full system and therefore is missing information about the full system. The Berry phase with connection (5.5.3) hence is sensitive to the bulk wormhole as it is defined in terms of the time shift δ which exists due to the wormhole.

More generally, such time shifts may be defined whenever an observer only has accesses to a subsystem. To illustrate this, let us now come back to the modular Berry phases of sec. 5.4 and consider empty AdS with the dual CFT in a vacuum. On a constant time slice we again consider the subregions A and $\bar{A}$ with modular operators $K = K_A + K_{\bar{A}}$. An observer restricted to the subregion A describes their system with the reduced density matrix ρ_A and the associated modular operator K_A generating time evolution with modular time s in their subregion. The global time t with Hamiltonian H is not meaningful for an observer restricted to the subregion A. This is a general feature of the observer-dependence of gravity. In this sense, the entanglement cut between subregions A and $\bar{A}$ presents an artificial horizon that we have introduced into the system. Then, an observer in subregion A who describes the expectation values of their observables with the density matrix ρ_A and an observer in subregion $\bar{A}$ with density matrix $\rho_{\bar{A}}$ may independently choose their modular time coordinate s and s' for the modular operators K_A and $K_{\bar{A}}$. We may then also define a gauge Berry phase for this system. If the modular times s and s' of the observer in A and $\bar{A}$ are aligned, the global vacuum state for a CFT in the vacuum with modular eigenstates $|E_n\rangle_A$ for K_A and $|E_n\rangle_{\bar{A}}$ for $K_{\bar{A}}$ may be written as [107]

$$|0\rangle = \frac{1}{Z}\sum_n e^{-\pi E_n}|E_n\rangle_A|E_n\rangle_{\bar{A}}. \tag{5.5.4}$$

However, if their modular times are not aligned, the new global state then differs by a global phase from the state (5.5.4) and reads,

$$|0\rangle_{\delta'} = \frac{1}{Z}\sum_n e^{-\pi E_n}e^{iE_n\delta'}|E_n\rangle_A|E_n\rangle_{\bar{A}}, \tag{5.5.5}$$

where δ' is the difference between the modular times s and s' chosen by the local observers. In the system described by the density matrix ρ_A, the observer does not have access to the global phase in (5.5.5). Therefore, from this perspective, the information about the phase in the global state of the CFT is missing. We may then define a gauge

Berry phase with respect to the modular time shift δ' with connection

$$A_{\delta'} = {}_{\delta'}\langle 0|\partial_{\delta'}|0\rangle_{\delta'} = \frac{1}{Z}\sum_n E_n e^{-2\pi E_n}. \tag{5.5.6}$$

The Berry phase arises from a local observer in subregion A who does not have access to all information necessary to describe the global system such as the phase in the global state.

As we will see in the next section, the different types of Berry phases introduced in sec. 5.3, sec. 5.4, and sec. 5.5 probe fundamental features of the operator algebra in a black hole geometry.

5.6. Berry Phases, Factorization, and von Neumann Algebras

Within the last year, von Neumann algebras have played an increasing role in understanding the factorization problem and quantum gravity in general. We provide a brief overview over the essentials of von Neumann algebras in sec. 5.6.1. In sec. 5.6.2, we interpret our results for Virasoro, modular, and gauge Berry phases in the context of von Neumann algebras. In particular, we also propose steps to resolve the factorization problem using the Virasoro Berry phase in the presence of a wormhole obtained in sec. 5.3.2 and its interpretation in terms of von Neumann algebras. Finally, we comment in sec. 5.6.3 that Berry phases are associated to missing information for a global observer due to global symmetries in a system.

5.6.1. Overview: von Neumann Algebras

Here, we review basic aspects of von Neumann algebras based on [168, 257]. Let us consider an open set $\mathcal{U}$ in a spacetime. The Rindler wedge in fig. 3.1 is an example of such an open set in Minkowski space. The set of operators with support in $\mathcal{U}$ that acts on the Hilbert space $\mathcal{H}$ and is closed under Hermitian conjugation forms a $\star$-algebra. Furthermore, if the operators are also bounded and the algebra is closed under weak limits of a sequence of operators a_n such that $\lim_{n\to\infty} a_n = a$, the $\star$-algebra is a von Neumann algebra. From a physical point of view, the weak limit implies that a sequence of operators a_n that converges to a measured with a finite precision is indistinguishable from the operator a in a measurement if n is sufficiently large. We denote the von Neumann algebra of operators in $\mathcal{U}$ by $\mathcal{A}_\mathcal{U}$. In particular,

the algebra of operators in quantum mechanics and in a local spacetime region in QFT are von Neumann algebras. Given an algebra $\mathcal{A}_\mathcal{U}$, we may define the commutant $\mathcal{A}'$ as the algebra of operators that commutes with $\mathcal{A}_\mathcal{U}$. For instance, the algebra $\mathcal{A}_{\mathcal{U}'}$ with support in a region $\mathcal{U}'$ that is spacelike separated from $\mathcal{U}$ is contained in $\mathcal{A}'_\mathcal{U}$. Additionally, states on the algebra differ from the usual quantum mechanical description of a state as a vector on the Hilbert space. A state on the algebra is a linear functional $F_\psi(a) = \langle\psi|a|\psi\rangle$ that is

- linear: $F(\lambda a + \mu b) = \lambda F(a) + \mu F(b)$ for $a, b \in \mathcal{A}$, and $\lambda, \mu \in \mathbb{C}$,
- normalized: $F(1) = 1$,
- positive: $F(a^\dagger a) \geq 0$ for all $a \in \mathcal{A}$.

The state $F_\psi(a)$ is pure if it cannot be written as a linear combination of states F_1, F_2 such that $F_\psi(a) = p_1 F_1(a) + p_2 F_2(a)$ with $p_1, p_2 > 0$. The Hilbert space on which the algebra $\mathcal{A}$ acts is then formally constructed with the Gelfand-Naimark-Segal (GNS) construction: A vector ψ is formally associated to the identity element of the algebra. Then, we may associate a vector $a\psi$ to every $a \in \mathcal{A}$. The set of vectors obtained in this manner together with the inner product $F(a^\dagger b) = \langle a\psi|b\psi\rangle$ may be completed[2] to a Hilbert space. In this Hilbert space, ψ is the cyclic separating vector.

Furthermore, von Neumann algebras may be grouped into three types which were essential in understanding the difference between quantum mechanics and QFT at the abstract level [168].

Type I:

The algebra of observables in quantum mechanics is of type I. For type I von Neumann algebras, irreducible representations may always be found. If the Hilbert space of the quantum system has finite dimension, the algebra is of type I_n with $n < \infty$. For quantum systems with infinite-dimensional Hilbert spaces, the algebra is of type I_∞. We may always define a trace. For type I_n, the trace is defined for all operators, whereas for type I_∞ it is defined only on a subset of operators since for example the trace of the identity operator would not be finite.

From a physical point of view, in quantum mechanics there are a finite set of canonical operators satisfying canonical commutation relations. A representation of these operators acts irreducibly on the Hilbert space, and there exists a distinguished vector. An example of such a vector is the ground state of the Hamiltonian on which the ladder operators $a_k^\dagger$ act irreducibly and which is annihilated by all a_k.

[2] Completeness here refers to completeness with respect to the norm.

The remaining two types of von Neumann algebras exclusively occur in infinite-dimensional systems and may be constructed from entangled spin systems. Type II algebras have maximal entanglement; type III algebras have non-vanishing but non-maximal entanglement.

Type II:

A type II_1 algebra is obtained as follows. We consider a vector space V of 2×2 complex matrices and two copies M_2 and M_2' of the algebra of the complex matrices, where M_2 acts by left multiplication and M_2' by right multiplication on $v \in V$. Then, V is a bipartite quantum system $V = W \otimes W'$, where W are the two-component column vectors acted on by M_2 and W' are the two-component row vectors acted on by M_2'. The maximally entangled vector in V is given in terms of the 2×2 identity matrix I_2, $I_2' = \frac{1}{\sqrt{2}} I_2$. In the next step, we take an infinite product $\bigotimes_k V^{[k]}$ of the vector space with the restriction that every v_k with $k \geq n$ in $v_1 \otimes v_2 \otimes \cdots \otimes v_n \otimes \cdots \in V^{[1]} \otimes V^{[2]} \otimes \cdots \otimes V^{[n]} \otimes \cdots$ is given by I_2'. This implies all but a finite number of v_k are equal to I_2' to ensure the vector space has a countably finite dimension. A Hilbert space $\widetilde{\mathcal{H}}$ is obtained by defining the inner product $\langle v, w\rangle = \operatorname{tr} v_{[n]}^\dagger w_{[n]}$, where $v_{[n]}$ is a truncated tensor product of n vectors. The completion of $\widetilde{\mathcal{H}}$ is the Hilbert space $\mathcal{H}$ whose elements are vectors $v = v_1 \otimes v_2 \otimes \cdots \otimes v_n \otimes \cdots$, where v_n approaches I_2' for $n \to \infty$. The algebra is obtained from a similar tensor product $M_2^{[1]} \otimes M_2^{[2]} \otimes \cdots \otimes M_2^{[n]} \otimes \cdots$ with elements $a = a_1 \otimes a_2 \otimes \cdots \otimes a_n \otimes \cdots$, where all but a finite number of a_i are equal to the identity I_2. Finally, we ensure that the algebra is closed under weak limits by defining the algebra such that it includes all operators a for which $a\chi = \lim_{n\to\infty} a_{(n)}\chi$ for $\chi \in \mathcal{H}$ exists.

In a type II algebra, irreducible representations do not exist. The entanglement entropy is then divergent since the trace is only defined up to an additive infinite constant. Physically, this may be understood from the presence of an infinite amount of entanglement.

Example A very simple example for a type II_1 von Neumann algebra presented in [257] can be constructed from a countably infinite set of qubits by first entangling qubits from two copies of the system, acting with operators on a finite number of qubits, and then taking limits.

We assume the system has a Hamiltonian $H = \sum_{k=1}^{\infty} H_k$, where H_k is the Hamiltonian for a single qubit. We denote by $\mathcal{H}_r$ the Hilbert space of these k qubits and introduce a second copy of the qubit system with Hilbert space $\mathcal{H}_l$. A type II algebra

is then obtained by entangling a finite number n of qubit pairs in $\mathcal{H}_r$ and $\mathcal{H}_l$ to form a TFD state in a system with Hamiltonian $H = 0$,

$$\psi_{\text{TFD}} = \frac{1}{\sqrt{Z_n}} \bigotimes_{k=1}^{n} \sum_{i=1,2} |i\rangle_{k,r} \otimes |i\rangle_{k,\ell} = \frac{1}{\sqrt{Z_n}} \bigotimes_{k=1}^{n} \begin{pmatrix} 1 & 0 \\ 0 & 1 \end{pmatrix}, \quad Z_n = 2^n. \tag{5.6.1}$$

Here, $i = 1, 2$ denote the two states for a single spin. We consider the algebra of operators $\tilde{\mathcal{A}}_r$ that act non-trivially on only a finite number of qubits. $F(a_r) = \langle\psi_{\text{TFD}}|a_r|\psi_{\text{TFD}}\rangle$ then defines a state on the algebra for $a_r \in \tilde{\mathcal{A}}_r$. Once we include all operators satisfying the weak limit, the algebra $\tilde{\mathcal{A}}_r$ becomes the closed algebra $\mathcal{A}_r$ and is of type II_1. In particular, $F(a_r) = \langle\psi_{\text{TFD}}|a_r|\psi_{\text{TFD}}\rangle$ defines a trace, $F(a_r) = \operatorname{tr} a_r$, with property $F(1) = 1$. Therefore, a von Neumann algebra of type II is infinite dimensional, but in contrast to type I_∞, we may define a trace for all operators in the algebra. Furthermore, the algebra is not irreducible as there is always a non-trivial commutant. For instance, $\mathcal{A}_r$ and $\mathcal{A}_l$ are commutants on $\mathcal{H}_{\text{TFD}}$.

Type II_∞ is obtained as a tensor product of type II_1 and type I_∞. This algebra then inherits the property from type I_∞ that the trace is only defined on a subset of operators.

Type III:

To construct a type III algebra following [168], we proceed similarly as for type II but considers matrices $K_{\lambda,i}$ equivalent to I_2' in the type II construction. The matrices $K_{\lambda,i}$ are introduced to obtain non-maximal entanglement and read,

$$K_{2,\lambda_i} = \frac{1}{(1+\lambda_i)^{1/2}} \begin{pmatrix} 1 & 0 \\ 0 & \lambda_i^{1/2} \end{pmatrix}, \tag{5.6.2}$$

where $0 < \lambda_i < 1$. In the previous construction of the type II algebra, we then simply replace all I_2' by K_{2,λ_i}, where the λ_i form a sequence $\lambda_1, \lambda_2, \cdots$ with $0 < \lambda_i < 1$. This implies the Hilbert space $\widetilde{\mathcal{H}}_{\vec{\lambda}}$ is formed by the vector space $v_1 \otimes v_2 \otimes \cdots \otimes v_n \otimes \cdots \in V^{[1]} \otimes V^{[2]} \otimes \cdots \otimes V^{[n]} \otimes \cdots$ and the truncated inner product $\langle v, w\rangle = \operatorname{tr} v_{[n]}^\dagger w_{[n]}$, where $v_j = K_{2,\lambda_i}$ for a finite number n of v_j. The closure of the Hilbert space $\widetilde{\mathcal{H}}_{\vec{\lambda}}$ is $\mathcal{H}_{\vec{\lambda}}$. Similarly the algebra $\mathcal{A}_{\vec{\lambda}}$ is the closure of $\tilde{\mathcal{A}}_{\vec{\lambda}}$, where $\tilde{\mathcal{A}}_{\vec{\lambda}}$ is obtained as for type II, but a finite number of a_i in $a = a_1 \otimes a_2 \otimes \cdots \otimes a_n \otimes \cdots$ are equal to K_{2,λ_i}. The cyclic and separating vector for $\mathcal{A}_{\vec{\lambda}}$ and its commutant $\mathcal{A}'_{\vec{\lambda}}$ is given by $\Psi_{\vec{\lambda}} = K_{2,\lambda_1} \otimes K_{2,\lambda_2} \otimes \cdots \otimes K_{2,\lambda_n} \otimes \cdots$. Furthermore, the function $F(a) = \langle\Psi|a|\Psi\rangle$ does not define a trace since $F(ab) \neq F(ba)$. The ill-defined trace is the reason for the universal

UV divergences when calculating entanglement entropies in subregions of QFTs.

The algebra is of type III_λ if the sequence $\lambda_1, \lambda_2, \cdots$ converges to a value $0 < \lambda < 1$. If it quickly converges to 0, we recover type I_∞; if it does not converge and has a minimum of two limit points in $0 < \lambda < 1$, the algebra is then of type III_1. In particular, type III_1 algebras are distinguishable by the spectrum of their modular boost operator K, which takes all values in $[0, \infty)$. An example is the Rindler boost discussed in sec. 3.1.2, which takes any value in $[0, \infty)$. Therefore, the QFT on a local region on Minkowski space is of type III_1.

Example Following [257], we again choose a qubit system as considered for type II, but now entanglement between qubit pairs must be non-maximal. This can be achieved with a Hamiltonian $H = \sum_{k=1}^{\infty} H_k$, where the single-qubit Hamiltonian is given by

$$H_n = \begin{pmatrix} 0 & 0 \\ 0 & E \end{pmatrix}. \tag{5.6.3}$$

This yields a TFD state

$$\Psi_{\mathrm{TFD}} = \frac{1}{\sqrt{Z_N}} \bigotimes_{k=1}^{n} \begin{pmatrix} 1 & 0 \\ 0 & e^{-\beta E/2} \end{pmatrix}, \quad Z_n = \left(1 + e^{-\beta E}\right)^n. \tag{5.6.4}$$

We may then proceed as for type II to define the algebra $\mathcal{A}_r$. However, in contrast to type II, a trace does not exist for type III algebras since $F(a_r b_r) \neq F(b_r a_r)$. The algebra obtained in this example is of type III_λ with $\lambda = e^{-\beta E/2}$.

5.6.2. Factorization of the Gravity and CFT Hilbert Spaces from the Perspective of von Neumann Algebras

Recently, there have been significant advances in understanding the properties of operator algebras in a black hole geometry. In [69, 70], it was observed that in the large-N limit of the CFT or equivalently the $G_N \to 0$ limit of the bulk which we typically consider in AdS/CFT to obtain a low-energy gravity theory, the algebra of bulk observables in the left and right exterior regions of the eternal AdS black hole is a type III_1 algebra with a non-trivial center related to the black hole mass. Furthermore, [91] then showed that the type III_1 algebra may be modified to type II_∞ by including $\frac{1}{N}$ corrections in the CFT or equivalently corrections to the Newton constant G_N in the bulk. We now argue that the Berry phases discussed in sec. 5.3, sec. 5.4, and sec. 5.5 probe features of the type III von Neumann algebra in the black hole geometry. Fur-

thermore, the Virasoro Berry phases in the black hole background shed new light on the factorization problem as we now discuss.

The role of quantum corrections for the operator algebra of the eternal black hole spacetime

Let us first briefly summarize the results of [69, 70, 91]. The starting point is to choose a normalization of fields in the CFT such that they have a simple large-N dependence. Operators with a well-defined simple large-N behavior are obtained by considering subtracted single-trace operators $\mathcal{O} = \operatorname{tr} O - \langle \operatorname{tr} O \rangle$, where O are gauge-invariant polynomials of fields and derivatives with no explicit N dependence. Then, n-point correlation functions of $\mathcal{O}$ vanish for $n > 2$ and are of order one for $n = 1$ in the large-N limit. This implies commutators of single-trace operators are c-numbers, and thus are part of a generalized free field theory. The large-N CFT algebra in AdS/CFT is hence of type III_1. In the case of an eternal AdS black hole with two dual CFTs, both CFTs are then of type III_1. We denote these algebras as $\mathcal{A}_{R,0}$ and $\mathcal{A}_{L,0}$. In particular, $\mathcal{A}_{L/R,0}$ are defined with a trivial center, i.e. operators that commute with $\mathcal{A}_{L/R,0}$ are not part of $\mathcal{A}_{L/R,0}$. The boundary algebras $\mathcal{A}_{L/R,0}$ are dual to algebras $\mathcal{A}_{l/r,0}$ in the left and right exterior region of the black hole and are part of the low-energy effective field theory that is obtained in the limit $G_N \to 0$ corresponding to the $N \to \infty$ limit in the CFT. We have already argued in sec. 5.3.2 that the black hole mass encoded in the classical phase space variable k_0 is not part of the boundary algebra $\mathcal{A}_{L/R,0}$ as it is not local to either boundary. A formal proof in the context of von Neumann algebras was given in [69, 70, 91]. The mass of the black hole or equivalently its energy is the conserved charge for time translations. In the boundary, these are generated by the Hamiltonians H_L and H_R. As neither $H_{L/R}$ nor $H'_{L/R} = H_{L/R} - \langle H_{L/R} \rangle$ have a well-defined large-N limit, we employ the operator $U = \frac{H'_R}{N}$. Then for any operator $\mathcal{V} \in \mathcal{A}_{R,0}$ [69, 70, 91],

$$[U, \mathcal{V}] = \frac{1}{N}[H'_R, \mathcal{V}] = -\frac{i}{N}\frac{\partial \mathcal{V}}{\partial t}. \tag{5.6.5}$$

Clearly, the commutator vanishes in the large-N limit. However, the algebras $\mathcal{A}_{R/L,0}$ were defined with a trivial center. Since H_R belongs to the center of $\mathcal{A}_{R/L,0}$, it is hence not part of the boundary algebra. Therefore, H_L and H_R generate an outer automorphism.

In [91], it was argued that upon considering $\frac{1}{N}$ corrections, the commutator (5.6.5) no longer vanishes. Therefore, $\frac{H'_R}{N}$ is no longer central. Based on results from the mathematical literature [258], the crossed product $\mathcal{A}_R = \mathcal{A}_{r,0} \rtimes G$ with the outer automorphism group G generated by $(H_L - H_R + NU)\beta$ then deforms the algebra

to type II_∞. The crossed product indicates that the product is between two algebras which do not commute.

Another important result of [91], which will be important when interpreting the Berry phases in the context of von Neumann algebras is that the Hamiltonians H_R and H_L are not part of the TFD Hilbert space $\mathcal{H}_{\text{TFD}}$ in a type III and type II von Neumann algebra. Both H_L and H_R do not have a well-defined large-N limit as there exist divergent fluctuations. In contrast, for the operator $H = H_L - H_R$ the large-N limit exists, and the operator annihilates the TFD state, $H|\psi_{\text{TFD}}\rangle = 0$. In particular, the Hilbert space basis for the TFD Hilbert space $\mathcal{H}_{\text{TFD}}$ is then obtained by acting on the TFD state ψ_{TFD} with all $a \in \mathcal{A}_{R,0}$ or equivalently all $a \in \mathcal{A}_{L,0}$. However, H_L and H_R do not have well-defined large-N limits when acting on this Hilbert space. The existence of $H = H_L - H_R$ in the algebra but not $H_{L/R}$ individually signals that $\mathcal{H}_{\text{TFD}} \neq \mathcal{H}_L \otimes \mathcal{H}_R$ for type III and type II. In fact, factorization of the Hilbert space $\mathcal{H}_{\text{TFD}} = \mathcal{H}_L \otimes \mathcal{H}_R$ only holds for a type I von Neumann algebra.

The factorization problem from the perspective of von Neumann algebras

From the perspective of von Neumann algebras, the factorization problem can be understood as follows. In the limit $G_N \to 0$, [69, 70] showed that the algebra of bulk operators in the exterior regions of the eternal AdS black hole spacetime is a type III_1 von Neumann algebra. This algebra acts on a Hilbert space $\mathcal{H}_{\text{TFD}}$ associated to the low-energy effective gravity theory. The bulk Hilbert space does not factorize into a left and right copy since H_L and H_R individually do not have a well-defined action on the Hilbert space. Therefore, $\mathcal{H}_{\text{TFD}} \neq \mathcal{H}_L \otimes \mathcal{H}_R$. In contrast, consider the TFD state (3.2.1). The state is built in terms of energy-eigenstates of the left and right CFT. These energy-eigenstates form the Hilbert spaces $\mathcal{H}_L$ and $\mathcal{H}_R$ of the left and right CFT, respectively. The state assumes an explicit factorization of the CFT Hilbert space such that $\mathcal{H}_{\text{TFD}} = \mathcal{H}_L \otimes \mathcal{H}_R$. However, from the preceding discussion, we know that such a factorization is only correct if the operator algebra is of type I. Therefore, in the CFT (3.2.1) is the TFD state for operators that form a type I von Neumann algebra. From the bulk perspective, we already know that the operator algebra is of type III_1 and is only of type I in the full quantum regime. These contradictory assumptions about the type of von Neumann algebra describing the operators in the bulk and boundary lead to the factorization puzzle. The factorization problem may therefore be resolved by finding the non-factorized TFD Hilbert space obtained for a type III_1 operator algebra in the CFTs.

Finally, let us note that writing states such as the TFD state (3.2.1) on factorized

Hilbert spaces is common in physics to facilitate calculations, for instance of the entanglement entropy, even when this is mathematically incorrect. Typical examples include global states for complementary subregions in a QFT such as the Rindler vacuum. In fact, mathematically the entanglement entropy of a subregion in a QFT is ill-defined: The operator algebras of a local region in a QFT are of type III_1 with a non-factorized Hilbert space [168]. In such an algebra a trace necessary to calculate the entanglement entropy is ill-defined [168]. Nevertheless, in order to obtain the entanglement entropy, the Hilbert space and operator algebras are assumed to factorize into two subregions yielding a UV-divergent entanglement entropy. This UV-divergence is the consequence of an ill-defined trace for a type III_1 von Neumann algebra.

Typically, assuming a type I algebra instead of the appropriate type III algebra to have a well-defined trace is acceptable in physics as nuances such as UV divergences can be regulated and important lessons about systems can still be learned. This approach fails, however, in AdS/CFT in the presence of an eternal AdS black hole: As discussed in sec. 5.1, objects defined in the CFT which assumes a factorized Hilbert space are dual to objects in the bulk that cannot be written in terms of a factorized bulk Hilbert space such as a Wilson line or geodesic connecting both boundaries through the wormhole. At this point, it is only possible to proceed if the correct non-factorized CFT Hilbert space is obtained.

It is therefore essential to obtain the non-factorized CFT Hilbert space. For a single copy of the CFT, the Verma module forming the CFT Hilbert space is obtained by quantizing the Virasoro coadjoint orbits discussed in sec. 2.1.2. This gives an interesting interpretation to the Virasoro Berry phase in the eternal AdS black hole geometry. We argued in sec. 5.3.2 that the classical phase space $\frac{\widehat{\mathrm{Diff}}(S^1)\times\widehat{\mathrm{Diff}}(S^1)}{U(1)}$ with action (5.3.23) describes two coupled CFTs. The Berry curvature is equal to the symplectic form on a phase space of the form $\frac{\widehat{\mathrm{Diff}}(S^1)\times\widehat{\mathrm{Diff}}(S^1)}{U(1)}$, whereas for a single CFT the coadjoint obit forming the phase space is given by $\frac{\widehat{\mathrm{Diff}}(S^1)}{U(1)}$. This new phase space $\frac{\widehat{\mathrm{Diff}}(S^1)\times\widehat{\mathrm{Diff}}(S^1)}{U(1)}$ is the classical version of the appropriate Hilbert space $\mathcal{H}_{\mathrm{TFD}}$ that is dual to the non-factorized bulk Hilbert space following from the type III von Neumann algebra describing the bulk fields. Quantizing this phase space with the appropriate constraints that couple both boundaries then yields the non-factorized boundary Hilbert space $\mathcal{H}_{\mathrm{TFD}}$ appropriate for a type III algebra. Therefore, the coupled Berry phase (5.3.23) presents the first step toward obtaining the type III von Neumann algebra Hilbert space which is an essential step in resolving the factorization problem.

In contrast to the Virasoro Berry phase, the modular and gauge Berry phases given in terms of the time shift δ induced by the wormhole then probe the existence of a

non-trivial center in the von Neumann algebra but not the factorization of the bulk Hilbert space. This may be seen as follows: The time shift is a parameter that arises from the center of the type III von Neumann algebra as it is obtained from different time evolutions with H_L in the left boundary and H_R in the right boundary. We discussed above that $H_{L/R}$ do not belong to the boundary algebras $\mathcal{A}_{R/L,0}$. Therefore, the modular Berry phase with curvature (5.4.48) and the gauge Berry phase (5.5.3) probe whether the algebra has a non-trivial center. They indicate that from the boundary perspective there is a piece of missing information, which is the non-trivial center of the type III von Neumann algebra. Therefore, we expect that the modular and gauge Berry phase vanish once $\frac{1}{N}$ correction are included and the crossed product with $\mathcal{A}_{R/L,0}$ is taken. The resulting type II_∞ von Neumann algebra has a trivial center, and δ therefore no longer exists. Hence, the Berry phase must vanish.

We then conclude that the coupled Virasoro Berry phase (5.3.23) is a probe of non-factorization and shows that the Hilbert space for the type III_1 boundary von Neumann algebra does not factorize. On the other hand, the modular and gauge Berry phase in the presence of a wormhole probes the existence of a non-trivial center in the type III_1 algebra and is expected to vanish once $\frac{1}{N}$ corrections are included.

Finally, let us illuminate the relation between Berry phases and missing information alluded to in this section.

5.6.3. Berry Phases and Missing Information

In this section, we discuss that Berry phases are linked to missing information about the reference frame arising from global charges in a system in which the Berry phase is calculated. In other words, a Berry phase is obtained whenever a local observer does not have access to the full Hilbert space. A global charge allows us to distinguish between the projective Hilbert space and the full Hilbert space. In the projective Hilbert space, states that differ only by a phase in the full Hilbert space are represented by the same state. These phases are generated by global symmetries of the system and cannot be measured by a local observer. A global symmetry therefore generates a phase corresponding to a choice of reference frame from the perspective of a local observer. Consider for instance a local observer restricted to a subsystem. The observer describes their system with a reduced density matrix. If the full system has a global symmetry, the local observer in their subregion is unable to distinguish relative phases in the global state as they leave the density matrix invariant. The phase of the global state then represents missing information for an observer and is important to capture the full microscopic structure of the Hilbert space.

Let us illustrate this on the examples of the Virasoro, gauge, and modular Berry phases in the presence of a wormhole.

Virasoro Berry phase in the presence of a wormhole

The Virasoro Berry phase in the presence of a wormhole given in (5.3.23) arises from an independent choice of time coordinate for an observer in each boundary. An observer in the left exterior region is separated by a horizon from an observer in the right exterior region of the black hole. Therefore, an observer in the left exterior region may choose the origin of their time coordinate independently from an observer in the right exterior region. A misaligned choice for the origin of the time coordinate in each exterior region will result in a relative time shift between both exterior regions. This time shift yields a relative phase in the global TFD state (3.2.1) describing the full system. This phase does not effect the measurements of an observer in the exterior regions as the reduced density matrix, which the local observer employs, is invariant under the phase shift. Therefore, the relative phase associated to the choice of time coordinate for two observers separated by a horizon is missing information. The time shift is generated by a U(1) transformation, which represents the fiber of the fiber bundle with base space $\frac{\widehat{\text{Diff}}(S^1)\times\widehat{\text{Diff}}(S^1)}{U(1)}$. The global charge associated with the time shift is the black hole mass or equivalently the energy. Furthermore, as discussed in sec. 5.6, the black hole mass is related to the center of the von Neumann algebra. Therefore, the Virasoro Berry phase is related to the presence of a non-trivial center.

Gauge Berry phase

The gauge Berry phase discussed in sec. 5.5 is defined in terms of a time shift δ that arises from an independent choice of (modular) time coordinate in subregions separated by a horizon or entanglement cut. Similar to the Virasoro Berry phase, an observer located in a subregion describes their system with a reduced density matrix and does not have access to the global state. A relative time shift arising from different choices of the time coordinate in subregions therefore yields a relative phase in the global state that leaves invariant the density matrices of a local observer. This phase again represents missing information for a local observer and is directly related to the non-trivial center of the von Neumann algebra in the presence of a wormhole.

Modular Berry phase

Similar to the previous two examples, the modular Berry phase discussed in sec. 5.4 has its origin in the independent choice of modular time coordinate for observers in

subregions. We again obtain a relative time shift in the global state of the system if two observers in different subregions choose different origins of their modular time, which leaves invariant the density matrix. Similar to the gauge Berry phase, the modular Berry phase is directly related to the non-trivial center of the von Neumann algebra in the presence of a wormhole.

Note that while we have focused on missing information for Berry phases in the presence of entangled subsystems such as a wormhole geometry, the relation also holds for systems without entanglement. However, in this case, the Berry phase is no longer related to a non-trivial center in the von Neumann algebra. Consider for instance, the Virasoro Berry phase in a single CFT given in (5.2.14). At each point along the group path, there is a phase ambiguity in the state due to the existence of a global time translation symmetry. This ambiguity corresponds to the freedom to choose the time coordinate at every point along the group path. Since all expectation values measured by a local observer are invariant, the choice of time coordinate at every point represents missing information.

This concludes our discussion about the relation between Berry phases and missing information.

5.7. Summary and Discussion

We showed that we may define three different Berry phases that are sensitive to the presence of a wormhole in the bulk: the Virasoro, modular, and gauge Berry phase.

The Virasoro Berry phase arises from independent conformal transformations in each CFT dual to the eternal AdS black hole. The black hole mass, which must be equal for observers in the left and right exterior regions, acts as a coupling between the Berry phases in the left and right boundaries. This coupling yields a phase space that does not factorize between the left and right boundaries. The modular Berry phase is obtained by parallel transporting intervals in each CFT. For small intervals, the modular Hamiltonian which facilitates parallel transport depends on interval endpoints on both boundaries indicating that the appropriate Ryu-Takayanagi surface for the subregion stretches through the wormhole. We showed that this modular Berry phase vanishes unless a time shift between both boundaries is introduced. This time shift only exists if the system has a horizon. Finally, we argued that we may employ the time shift itself to define gauge Berry phases which then only exists if the system has

a physical or artificial horizon introduced by restricting the observer to a subregion such that they lose information about the global state of the system.

We furthermore interpreted these results in the context of von Neumann algebras. The operators in the CFT for which we define the Berry phases form a type III_1 von Neumann algebra which has a non-trivial center related to the black hole mass [69, 70, 91]. It has been established that the TFD Hilbert space for these algebras does not factorize in terms of the Hilbert space of the CFT in the left and right boundaries, $\mathcal{H}_{\mathrm{TFD}} \neq \mathcal{H}_L \otimes \mathcal{H}_R$ [69, 70, 91]. Similarly, the Virasoro Berry phase is defined on a non-factorized classical phase space, where non-factorization is enforced by constraint equations between the left and right boundaries. The classical non-factorized phase space associated to the Virasoro Berry phase presents a starting point for obtaining the non-factorized Hilbert space associated to the type III_1 von Neumann algebra. In contrast, the initial construction of the TFD state (3.2.1) is only valid for type I algebras as an explicit factorization of the Hilbert space is assumed. This is only true if the dual bulk gravity theory is in the quantum regime. This mismatch in the types of von Neumann algebras considered in the bulk and boundary is the source of the factorization problem. Upon quantization, we then expect that the phase space associated to the Virasoro Berry phase yields a non-factorized Hilbert space, and thus the Virasoro Berry phase is a probe of non-factorization of the CFT Hilbert space. On the other hand, the modular and gauge Berry phases do not a probe factorization but the non-trivial center of the type III_1 algebra. The non-trivial center exists because $H_{L/R}$ do not belong to the boundary algebra. Furthermore, the modular and gauge Berry phases are defined in terms of a time-shift generated by $H_{L/R}$. Therefore, the modular and gauge Berry phases probe the non-trivial center. Since it has been established in [91] that the type III_1 algebra may be deformed to a type II_∞ algebra with trivial center once $\frac{1}{N}$ corrections are considered, the modular and gauge Berry phases vanish if these corrections are included.

Furthermore, we showed that the existence of Berry phases is linked to global charges representing missing information for a local observer. An observer only has access to the projective Hilbert states but never to the full Hilbert space. Therefore, they cannot distinguish states with different phases. These phases, however, are essential to obtain the correct structure of the full Hilbert space.

It is by now clear that von Neumann algebras present a valuable tool in understanding AdS/CFT at the abstract level. In particular, they are useful in clarifying assumptions that were implicitly made in AdS/CFT calculations. The assumption that the TFD state (3.2.1) is defined in terms of a factorized Hilbert space implicitly assumes a type I algebra, whereas in the semiclassical limit where the dual bulk calcu-

lations are performed, the algebra is of type III_1. This is the source of the factorization problem. It is then clear that the puzzle can be resolved by deriving the appropriate non-factorized Hilbert space from (5.3.23) that is associated to the type III_1 algebra.

Employing the results obtained in this chapter for the non-factorized classical phase space with action (5.3.23), it becomes possible to derive the appropriate non-factorized Hilbert space for a type III_1 algebra by quantizing the classical phase space and enforcing the appropriate constraints. The non-factorized Hilbert space obtained from this quantization procedure is then the non-factorized Hilbert space associated to a type III_1 CFT Hilbert space dual to the non-factorized bulk Hilbert space. This presents a key step in resolving the factorization problem. At least in principle this non-factorized Hilbert space allows the boundary reconstruction of bulk operators such as the radial Wilson line which cannot be written in terms of a factorized Hilbert space. The non-factorized Hilbert space would thus resolve the factorization problem.

The results of this section also illustrate that Berry phases arise when there is some missing information in the description of the theory, i.e. when the theory is incomplete in the sense that we consider limits. The modular Berry phases may already be removed by including perturbative corrections and transitioning to a type II algebra with a crossed product. In a full theory of quantum gravity, where the dual CFT is considered at finite N, we expect that there are no Berry phases since there are no global charges in quantum gravity [259]. The absence of global charges and the associated symmetries prohibit the existence of Berry phases since there are no non-trivial fibers. Therefore, Berry phases are useful observables that help investigate fundamental properties of spacetime in a given limit of the gravity theory.

6 Conclusion and Outlook

Quantum information theory plays a central role in understanding the nature of spacetime also beyond the semiclassical regime. This was outlined in the introduction. The AdS/CFT correspondence [34, 38, 39] with the ER=EPR proposal [48] in particular has led to a paradigm shift, where spacetime is no longer viewed as being a fundamental ingredient to a theory of gravity but rather as emergent. In the eternal AdS black hole geometry [49], the ER=EPR proposal purports the presence of a wormhole connecting the two causally disconnected exterior regions of the eternal AdS black hole due to entanglement between two CFTs living at the boundary of each exterior region. This thesis addressed two questions the ER=EPR proposal raises:

The first concerns the growth of the bulk wormhole. It was proposed that this growth may be measured by the computational complexity of the dual CFT state [73, 74]. Several bulk observables were suggested as measures of the wormhole growth in holographic complexity conjectures [74, 81–84] and a number of proposals address how to define the complexity of the dual CFT state [75, 78, 195–197, 199, 208, 210, 216, 217, 220]. An important remaining open question is to relate CFT and bulk approaches to complexity. In this thesis, I presented a new approach that allows to derive gravity duals to quantum circuits in the CFT: A quantum circuit built from conformal transformations may be implemented as a non-trivial time evolution of the bulk spacetime. Once the dual spacetime is obtained, it becomes possible to derive gravity duals to CFT complexity measures from first principles. This framework, presented in chapter 4 and published in [1], allows to directly relate CFT complexity proposals to holographic complexity proposals in a robust manner. This presents a significant step forward in testing holographic complexity proposals.

To achieve this, I proceeded as follows: One of the main obstacles in relating quantum circuits to the gravity theory is the existence of an auxiliary parameter in the CFT quantum circuit from which the complexity is obtained. This parameter has no bulk analog. To make progress, the circuit parameter is identified with the physical time. In the next step, I then demanded that the physical Hamiltonian of the CFT governing time evolution is equal to the circuit Hamiltonian which is now parameterized by physical time. In this manner, the evolution of the quantum circuit can be encoded as a non-trivial time evolution of the boundary spacetime on which the

CFT lives. States in the quantum circuit are defined on constant time slices in the new boundary geometry. In particular, the construction ensures that the sequence of states generated by the original circuit parameterized by the auxiliary circuit parameter is exactly the same as the one obtained from the non-trivial time evolution of the spacetime. Furthermore, as the boundary spacetime remains flat at all times, the circuit is encoded in a particular choice of foliation of the spacetime. The knowledge of the boundary geometry and energy-momentum tensor that is conserved in this background then allowed me to employ the Fefferman-Graham expansion [137]. The expansion follows from a mathematical theorem that states that the bulk spacetime in three dimensions may be reconstructed from boundary data. This allowed me to derive a bulk dual to the quantum circuit.
I then employed this bulk dual to the quantum circuit to derive a holographic dual to the Fubini-Study distance. This result appeared in [2]. The bulk dual is a complicated geometric object given in terms of the boundary metric and spacelike geodesics in the bulk. It is valid for empty AdS, conical defect [128], and BTZ black hole geometries [124, 125] and holds for quantum circuits built from energy-momentum tensor insertions. The construction of a dual bulk geometry to a quantum circuit presents a new tool that allows to relate holographic complexity proposals directly to CFT complexity measures and vice versa, and therefore presents significant progress in relating CFT and bulk complexity proposals. Furthermore, the construction is easily generalizable to include other operator insertions beyond the energy-momentum tensor in the CFT, such as scalar fields or currents.

The second question I addressed in this thesis concerns the factorization problem raised by the ER=EPR proposal. The CFT state dual to the eternal AdS black hole is defined on a Hilbert space that factorizes between the left and right CFT Hilbert spaces. The Hilbert space of the effective bulk field theory in the presence of the wormhole, however, does not factorize. This contradiction is referred to as the factorization problem. So far, this problem has mainly been tackled using toy models and lower-dimensional gravity theories [89, 90, 234]. Alternatively, it has been considered from the abstract approach of von Neumann algebras describing the bulk operator algebra [69, 70, 91, 259]. In chapter 5, I introduced Berry phases as a CFT measure probing the bulk wormhole in AdS_3. The results appeared in [3, 4]. In particular, an essential result is that different types of Berry phases are sensitive to the wormhole: the Virasoro [105], modular [106–108], and gauge Berry phases. I showed that the first is defined on a non-factorized classical phase space, which I expect to yield a non-factorized Hilbert space when quantized. This is an essential step in resolving

the factorization problem. Furthermore, the gauge and modular Berry phases probe a non-trivial center in the bulk algebra in the semiclassical limit. The results therefore imply that Berry phases are a useful tool in interpreting aspects of the abstract von Neumann algebras.

Moreover, it transpired that the Virasoro Berry phase is of particular relevance for the factorization problem. The Virasoro Berry phase arises from independent conformal transformations in the CFTs and becomes coupled in the presence of a bulk wormhole. The coupling occurs due to the black hole mass which has to be equal for two observers when measured from the left and right CFTs. Employing recent results on von Neumann algebras [69, 70, 91, 257, 259], I argued in chapter 5 that this Berry phase is a genuine probe of non-factorization, as the Berry phase is given in terms of a coupled action on a non-factorized classical phase space that I expect to yield a non-factorized Hilbert space when quantized.

Furthermore, I discussed modular Berry phases, which arise from parallel transport of intervals, for thermal systems including the BTZ geometries. For the two-sided BTZ black string geometry, the Berry phase arises from an independent choice of time coordinate in the left and right boundary CFT. Similarly, a gauge Berry phase may be defined from an independent choice of time coordinate if an observer does not have access to the full system. Employing the results of [91], it becomes clear that both the modular and gauge Berry phases do not probe factorization but indicate the presence of a non-trivial center in the von Neumann algebra that may be removed by including $1/N$ corrections. These Berry phases are linked to different pieces of missing information from the perspective of an observer limited to a subregion. Gaining access to the missing information, i.e. the center of the algebra, removes the Berry phase.

More generally, the existence of Berry phases signals missing information for a local observer. This result appeared in [4]. The existence of global symmetries in a system prohibits an observer from accessing the full Hilbert space as the observer cannot distinguish between states which only differ by a phase. The observer therefore has access only to the projective Hilbert space. Without global charges, however, there is no Berry phase as the fiber of the fiber bundle on which the Berry phase is defined then has a trivial fiber. For instance, in quantum gravity, there are no Berry phases due to the absence of global charges [259]. Therefore, the Berry phase is an essential tool in understanding different limits of quantum gravity. Additionally, the non-factorized classical phase space of the Virasoro Berry phase in the presence of a wormhole presents a first step toward resolving the factorization puzzle: Quantizing the classical phase space and imposing appropriate constraints will yield the non-factorized Hilbert space appropriate for a type III von Neumann algebra. This will resolve the factorization

problem as the boundary Hilbert space then has the same non-factorized structure as the bulk Hilbert space.

Outlook

In this thesis, I derived a holographic dual to a quantum circuit and showed that the Fubini-Study metric has a geometric gravity dual. Moreover, I demonstrated the source of the factorization puzzle by deriving the symplectic form on the CFT phase space. Based on these results, there are several important questions that can now be answered:

Employing the proposal for a gravity dual to a quantum circuit, we may derive gravity duals to CFT cost functions from first principles and vice versa for the first time. For example, in [122] the expectation value of the circuit Hamiltonian was studied as a CFT cost function. Since the energy-momentum tensor appearing in the circuit Hamiltonian may be written in terms of the bulk and boundary metric, the gravity dual to this cost function is given in terms of metric components. Furthermore, the gravity dual to the circuit presents a means to derive CFT duals to the holographic complexity proposals discussed in sec. 3.3 from first principles. Establishing the CFT duals to holographic complexity proposals is an essential step in verifying these proposals. Another useful measure in circuit complexity for which we may derive a gravity dual with my proposal is the sectional curvature [260]. The sectional curvature is given in terms of the Riemann tensor and tangent vectors of the complexity geometry. It was established in [261, 262] that negative sectional curvature is indicative of the complexity growth expected of chaotic CFTs such as holographic ones. The sectional curvature for circuits considered in this thesis with the Fubini-Study metric as a cost function was studied in [86, 87].

Moreover, it is of great importance to generalize the circuits studied in this thesis. I considered circuits that implement conformal symmetry transformation. Thus, the energy-momentum tensor is the only CFT source appearing in the circuit. The circuit can straightforwardly be generalized to implement transformations that are not symmetries of the system. A good starting point is the inclusion of primary fields as these play a central role in shockwave geometries. Insertions of heavy primaries in the CFT induce shockwaves in the bulk through which the switchback effect [80, 190] may be studied. The first step in generalizing the bulk dual to a circuit is to include primaries as operators in the gate set. The circuit is then no longer comprised

solely of symmetry transformations. This is already a considerable step forward since the discussion regarding circuit complexity is mostly focused on symmetry transformations. The inclusion of primaries in the circuit then requires that in the dual bulk theory heavy operators that backreact on the geometry are considered. The dual to the Fubini-Sudy cost derived in this thesis is no longer applicable in such a setup. It will be an important step to understand the bulk dual to Fubini-Study distance for such generalized circuits.

Furthermore, an additional decisive new concept is to apply concepts of machine learning to AdS/CFT [263–267]. These important developments include understanding the information flow in neural networks from renormalization-group flow in field theories and modeling the bulk in AdS/CFT with neural networks by propagating information representing boundary values through the network. This has led to valuable new insights into AdS/CFT from machine learning and at the same time has advanced the state of the art in machine learning by applying knowledge from physics [267–269]. Applications of machine learning to quantum circuit optimization in AdS/CFT have not been discussed in the literature so far, but were employed successfully for non-holographic systems [270–272]. I believe that recent advancements in reinforcement learning, in particular the proximal policy optimization (PPO) [273], provide valuable tools in further developing these algorithms and learning about complexity in regimes where analytical calculations are hard or impossible. One suitable application is the optimization of circuits built from n-qubit gates with symmetry $\mathrm{SU}(2^n)$ [76, 77, 193]. It will be important to understand if stable reinforcement learning algorithms such as PPO are able to optimize quantum circuits by first learning the complexity geometry and then applying an action policy that leads to a geodesic motion on the group manifold from a reference state to a chosen target state. If the policy can be learned, it is important to understand if patterns arise in the complexity geometry and geodesics when increasing n. This may serve as a valuable toy model in understanding large-N complexity in CFTs, which are so far poorly understood due to strong-coupling effects. If the algorithm is not able to learn the geometry and policy, then we may employ previous knowledge about $\mathrm{SU}(2^n)$ [76, 77, 193] to advance the state of the art in reinforcement learning. However, preliminary results show promising signs that the algorithm is indeed able to learn the geometry.

My final comment concerns the factorization problem which arises from a non-factorized gravity Hilbert space in the presence of a wormhole in the semiclassical limit, whereas the dual CFT Hilbert space does not factorize. I showed that the CFT

Berry phase (5.3.23) in the presence of a wormhole is coupled and the classical phase space does not factorize between the left and right CFTs. By quantizing this classical non-factorized phase space, we will obtain the non-factorized Hilbert space $\mathcal{H}_{\text{TFD}}$ of the CFTs dual to an eternal AdS black hole. This will be a fundamental step in resolving the factorization problem. The non-factorized classical phase space may either be quanitzed by employing geometric [115] or path integral [116] quantization. In particular, constraints coupling both boundaries must then be appropriately enforced, see also [274] for a discussion. I expect this to yield a non-factorized Hilbert space that is expected of a type III_1 operator algebra describing the bulk and boundary operators in the semiclassical regime. This non-factorized CFT Hilbert space is the appropriate dual to the non-factorized bulk Hilbert space.

Answering the questions raised above presents an essential step in further understanding the relation between quantum information and gravity, with the ultimate aim to shed light on how precisely spacetime emerges from a theory of quantum gravity in the semiclassical regime. The results of this thesis present an important step in this direction.

Acknowledgements

First, I would like to thank my supervisor Johanna Erdmenger who got me excited in AdS/CFT when I first joined TP3 as a Bachelor student more then six years ago. Her continuous guidance, enthusiasm, and support were essential to the completion of my projects and this thesis.

I am also grateful to my collaborators:
Special thanks goes to Michal Heller for uncountable, invaluable discussions during our projects together. Furthermore, I am indebted to Marius Gerbershagen, who has been a collaborator since my master thesis, for the many useful discussions and suggestions. I am also particularly grateful to Moritz Dorband and Souvik Banerjee for being great collaborators and fantastic sparring partners in many discussions. I furthermore thank René Meyer for always having an open ear when I ran into problems on projects and his many useful suggestions. Finally, I would like to thank Mario Flory for his collaboration and helpful discussions.

I am thankful to Yanick Thurn for being a great office mate and always having an open ear. I would also like to thank the remaining members of TP3 who created a great environment to work in: Pablo Basteiro, Zhaohui Chen, Rathindra Nath Das, Giuseppe Di Giulio, Bastian Heß, Haye Hinrichsen, Zhuo-Yu Xian, and Suting Zhao. Moreover, I am grateful to Björn Trauzettel for insightful discussions about my projects.

I would also like to thank Nelly Meyer for helping me with paperwork and administrative issues.
I furthermore thank Pablo Basteiro, Moritz Dorband, and Tim Schuhmann for proofreading and their useful comments on this thesis.

Finally, I am grateful to my parents and my sister for their continuous support and patience.

Appendix A

A.1. Boosted Particle Trajectories in AdS_3

The timelike trajectories of massive particles in AdS_3 are easiest to determine in the covering space (2.2.4). Exploiting SL(2,$\mathbb{R}$) isometries, transformations corresponding to boundary diffeomorphisms (4.2.37) and similar right-moving diffeomorphisms yields the geodesics

$$
\begin{aligned}
X_0(\tau,t) &= -\frac{\left(-1+|\zeta|^2|\bar{\zeta}|^2\right)}{\sqrt{\left(-1+|\zeta|^2\right)\left(-1+|\bar{\zeta}|^2\right)\left(\mathrm{Im}\left(e^{2it}\zeta\bar{\zeta}\right)^2+\left(-1+\mathrm{Re}\left(e^{2it}\zeta\bar{\zeta}\right)\right)^2\right)}}\cos(t),\\
X_3(\tau,t) &= -\frac{\left(-1+|\zeta|^2|\bar{\zeta}|^2\right)}{\sqrt{\left(-1+|\zeta|^2\right)\left(-1+|\bar{\zeta}|^2\right)\left(\mathrm{Im}\left(e^{2it}\zeta\bar{\zeta}\right)^2+\left(-1+\mathrm{Re}\left(e^{2it}\zeta\bar{\zeta}\right)\right)^2\right)}}\sin(t),\\
X_1(\tau,t) &= -i\frac{e^{-it}(e^{2it}(\zeta-\bar{\zeta})+\bar{\zeta}^*+e^{2it}(|\zeta|^2\bar{\zeta}-|\bar{\zeta}|^2\zeta)-\zeta^*-|\zeta|^2\bar{\zeta}+\zeta|\bar{\zeta}|^2)}{2\sqrt{\left(-1+|\zeta|^2\right)\left(-1+|\bar{\zeta}|^2\right)\left(\mathrm{Im}\left(e^{2it}\zeta\bar{\zeta}\right)^2+\left(-1+\mathrm{Re}\left(e^{2it}\zeta\bar{\zeta}\right)\right)^2\right)}},\\
X_2(\tau,t) &= \frac{e^{-it}(-e^{2it}(\zeta+\bar{\zeta})-\bar{\zeta}^*+e^{2it}(|\zeta|^2\bar{\zeta}+|\bar{\zeta}|^2\zeta)-\zeta^*+|\zeta|^2\bar{\zeta}^*+\zeta^*|\bar{\zeta}|^2)}{2\sqrt{\left(-1+|\zeta|^2\right)\left(-1+|\bar{\zeta}|^2\right)\left(\mathrm{Im}\left(e^{2it}\zeta\bar{\zeta}\right)^2+\left(-1+\mathrm{Re}\left(e^{2it}\zeta\bar{\zeta}\right)\right)^2\right)}}.
\end{aligned}
\tag{A.1.1}
$$

Note that ζ and $\bar{\zeta}$ depend on the circuit parameter τ. The detailed derivation of these geodesics is given in [85].

A.2. Length of Spacelike Geodesics in Static Asymptotically AdS Geometries

We may write the metric for a general static AdS space as

$$ds^2 = -\left(\alpha + r^2\right) dt^2 + \frac{1}{(\alpha + r^2)} dr^2 + r^2 d\varphi^2. \tag{A.2.1}$$

For a conical defect, $\alpha = \frac{1}{n^2}$, whereas the BTZ black hole metric is obtained from $\alpha = -m$. Empty AdS is recovered upon setting $\alpha = 1$. To derive the length for a spacelike geodesic, we follow the procedure in [275]. The equations of motion follow from the constants of motion, which are the energy E and the angular momentum J and imposing $g_{\mu\nu} dx^\mu dx^\nu = 1$,

$$\begin{aligned}
\frac{\partial r}{\partial \lambda} &= \pm \frac{1}{r} \sqrt{(E^2 - J^2 + \alpha) r^2 - J^2 \alpha + r^4}, \\
\frac{\partial t}{\partial r} &= \frac{\partial t}{\partial \lambda} \frac{1}{\frac{\partial r}{\partial \lambda}} = \pm \frac{Er}{(\alpha + r^2) \sqrt{(E^2 - J^2 + \alpha) r^2 - J^2 \alpha + r^4}}, \\
\frac{\partial \varphi}{\partial r} &= \frac{\partial \varphi}{\partial \lambda} \frac{1}{\frac{\partial r}{\partial \lambda}} = \pm \frac{J}{r \sqrt{(E^2 - J^2 + \alpha) r^2 - J^2 \alpha + r^4}}.
\end{aligned} \tag{A.2.2}$$

The precise solution depends on the sign of α reflecting that the BTZ black hole is a thermal system, while the conical defect is not. Once the equations of motion have been solved, we employ the limit $\varphi(r \to \infty) = \varphi_{1/2}$ and $t(r \to \infty) = t_{1/2}$ to rewrite the boundary points $\varphi_{1/2}$ and $t_{1/2}$ in terms of the constants of motion E, J. For the conical defect, we obtain

$$\begin{aligned}
\cos((\varphi_2 - \varphi_1)\sqrt{\alpha}) &= \frac{J^2 - E^2 + \alpha}{\sqrt{-4J^2\alpha + (E^2 - J^2 + \alpha)^2}}, \\
\cos((t_2 - t_1)\sqrt{\alpha}) &= \frac{J^2 - E^2 - \alpha}{\sqrt{-4J^2\alpha + (E^2 - J^2 + \alpha)^2}}.
\end{aligned} \tag{A.2.3}$$

Note that in a conical defect geometry multiple geodesic end at the same boundary points. In the covering space with coordinates $\tilde{\varphi} = \frac{\varphi}{n}$, $\tilde{t} = \frac{t}{n}$, and $\tilde{r} = rn$, this implies leaving one endpoint fixed while the other has n copies $\tilde{\varphi}_1 + \frac{2\pi k}{n}$, where $k \in [0, n-1]$. Geodesics with these endpoints descend to geodesics with the same endpoint in the

conical defect geometry. See [71] for details. For the BTZ black hole, we obtain

$$\begin{aligned}\cosh((\varphi_2-\varphi_1)\sqrt{-\alpha}) &= \frac{J^2-E^2+\alpha}{\sqrt{-4J^2\alpha+(E^2-J^2+\alpha)^2}},\\ \cosh((t_2-t_1)\sqrt{-\alpha}) &= \frac{J^2-E^2-\alpha}{\sqrt{-4J^2\alpha+(E^2-J^2+\alpha)^2}}.\end{aligned} \tag{A.2.4}$$

The length of the geodesics then follow from

$$L=\int d\lambda=\int dr\frac{\partial\lambda}{\partial r}=\frac{1}{2}\int_{r^{*2}}^{r_\epsilon^2}\frac{dr^2}{\sqrt{(E^2-J^2+\alpha)r^2-J^2\alpha+r^4}}. \tag{A.2.5}$$

Here, r_ϵ is the value of r at the boundary cutoff. Moreover, r^* is the value of r at the turning point of the geodesic. The turning point follows from $\frac{\partial\varphi}{\partial r}\to\infty$ and is given by the zero of the square root $\sqrt{(E^2-J^2+\alpha)r^2-J^2\alpha+r^4}$ such that $r^{*2}=\frac{1}{2}(J^2-E^2-\alpha+\sqrt{(E^2-J^2-\alpha)^2-4J^2\alpha})$. The regularized geodesic length reads

$$L=-\log\left(\frac{\sqrt{-4J^2\alpha+(E^2-J^2+\alpha)^2}}{4}\right). \tag{A.2.6}$$

We may now rewrite the geodesic length in terms of the interval endpoints employing (A.2.3) and (A.2.4). For the conical defect, this yields

$$L_{\text{reg}}=\log\left(\frac{\alpha}{2}\left(\cos\Delta\tilde{t}-\cos\left(\Delta\tilde{\varphi}+\frac{2\pi k}{n}\right)\right)\right). \tag{A.2.7}$$

For $n=1$, this agrees with the result for empty AdS. Furthermore, for the BTZ black hole, we obtain

$$L_{\text{reg}}=\log\left(2\left(\frac{\beta}{2\pi}\right)^2\left(\cosh(t_2-t_1)\frac{2\pi}{\beta}\pm\cosh(\varphi_2-\varphi_1)\frac{2\pi}{\beta}\right)\right), \tag{A.2.8}$$

where the plus sign corresponds to geodesics stretching between both boundaries and the minus sign to geodesics remaining in the exterior regions.

A.3. The Eternal AdS Black Hole from Chern-Simons Theory

The eternal AdS black hole geometry may be obtained from SL(2,$\mathbb{R}$)× SL(2,$\mathbb{R}$) Chern-Simons theory on a manifold with topology $\Sigma \times \mathbb{R}$ corresponding to the annulus times time by enforcing asymptotic AdS boundary conditions. We review the derivation as presented in [245] since sec. 5.3 is based on the result. We begin with the Chern-Simons action,

$$S_{\mathrm{CS}}[A] = \frac{k}{4\pi} \int_{\Sigma\times\mathbb{R}} \mathrm{tr}\left(A \wedge dA + \frac{2}{3} A \wedge A \wedge A\right). \tag{A.3.1}$$

The two boundaries of the annulus correspond to the two boundaries of the eternal BTZ black hole. The outer boundary at r_o is identified with the right boundary of the eternal black hole and the inner boundary r_i accordingly the left boundary. The connection A is SL(2,$\mathbb{R}$)-valued. We employ the following representation for the group generators,

$$L_0 = \frac{1}{2}\begin{pmatrix} 1 & 0 \\ 0 & -1 \end{pmatrix}, \quad L_+ = \begin{pmatrix} 0 & 1 \\ 0 & 0 \end{pmatrix}, \quad L_- = \begin{pmatrix} 0 & 0 \\ 1 & 0 \end{pmatrix}. \tag{A.3.2}$$

Furthermore, the action may be rewritten as

$$S[A] = \frac{k}{4\pi} \int_{\mathcal{M}} dt d\varphi dr \, \mathrm{tr}\left(A_\varphi \dot{A}_r - A_r \dot{A}_\varphi + 2A_t F_{r\varphi}\right) + I_{\Sigma_i} + I_{\Sigma_o}, \tag{A.3.3}$$

where $F_{r\varphi}$ is the non-Abelian field strength $F_{r\varphi} = \partial_r A_\varphi - \partial_\varphi A_r + i[A_r, A_\varphi]$. The boundary terms $I_{\Sigma_i} + I_{\Sigma_o}$ ensure that the variation vanishes for a given boundary condition. A suitable boundary condition to fix time evolution in both boundaries in the upward direction is $A_- = 0 = \bar{A}_+$ on the outer boundary and $A_+ = 0 = \bar{A}_-$ on the inner boundary. To have a well-defined variation principle, the boundary terms are then fixed to

$$I_{\Sigma_{i,o}} = -\frac{k}{4\pi} \int dt d\varphi \, \mathrm{tr}(A_\varphi^2 + \bar{A}_\varphi^2), \tag{A.3.4}$$

since $A_+ = 0 = \bar{A}_-$ implies $A_t = A_\varphi$ and $\bar{A}_t = \bar{A}_\varphi$. From the equation of motion for A_t in (A.3.1), we obtain the constraint $F_{r\varphi} = 0$. This fixes the Chern-Simons connection components,

$$\begin{aligned} A_\varphi &= g^{-1}\partial_\varphi g + g^{-1}K(t)g, & \bar{A}_\varphi &= -\partial_\varphi g g^{-1} + gK(t)g^{-1}, \\ A_r &= g^{-1}\partial_r g, & \bar{A}_r &= -\partial_r g g^{-1}. \end{aligned} \tag{A.3.5}$$

Note that the additional contribution in terms of $K(t) = k_0 L_0$ to A_φ enforces that the non-contractible cycle along the φ-direction of the annulus yields a non-trivial holonomy $\oint \mathrm{tr} A_\varphi \neq 0$. In the next step, we insert (A.3.5) into the action (A.3.3), which yields

$$\begin{aligned} S_{\mathrm{CS}}[g, K(t)] = &+ \frac{k}{4\pi}\int_{\mathcal{M}} d^3x \,\mathrm{tr}\left(\partial_r\left(g^{-1}\partial_\varphi g g^{-1}\partial_t g\right)\right) + \frac{k}{12\pi}\int_{\mathcal{M}} \mathrm{tr}\left(g^{-1}dg\right)^3 \\ &+ \frac{k}{4\pi}\int_{\mathcal{M}} d^3x \,\mathrm{tr}\left(2\partial_r\left(g^{-1}K\partial_t g\right) - \partial_t\left(g^{-1}K\partial_r g\right)\right) + I_{\Sigma_i} + I_{\Sigma_o}. \end{aligned} \tag{A.3.6}$$

Note that the action may be written as a total derivative in r and therefore reduces to a boundary action. It is therefore convenient to specify the boundary values of the group elements as $h(t,\varphi) = g(t, r_o, \varphi)$ and $l(t,\varphi) = g(t, r_i, \varphi)$. We now parameterize h and l in terms of a Gauss decomposition,

$$h = e^{YL_-}e^{\Phi L_0}e^{XL_+}, \quad l = e^{VL_+}e^{\Psi L_0}e^{UL_-}, \tag{A.3.7}$$

where Y, Φ, X, V, Ψ, U are functions of the boundary coordinates t, φ. This yields the action

$$\begin{aligned} S_{CS}[G,K] &= S_o - S_i + S_{\mathrm{hol}}, \\ S_o &= \frac{k}{4\pi}\int_{\Sigma_o} dtd\varphi\left(\frac{1}{2}\partial_-\Phi\Phi' + 2e^{\Phi}\partial_- XY'\right), \\ S_i &= \frac{k}{4\pi}\int_{\Sigma_i} dtd\varphi\left(\frac{1}{2}\partial_+\Psi\Psi' + 2e^{-\Psi}\partial_+ UV'\right), \\ S_{\mathrm{hol}} &= \frac{k}{4\pi}\int dtd\varphi\left[k_0\left(\partial_-\Phi - \partial_+\Psi - 2e^{\Phi}Y\partial_- X - 2e^{-\Psi}V\partial_+ U\right) - k_0^2\right]. \end{aligned} \tag{A.3.8}$$

Finally, asymptotic AdS boundary conditions are enforced at the boundaries by requiring that at $r = r_o$,

$$A_r = 0, \quad A_\varphi = L_- + \mathcal{L}(t,\varphi)L_+, \tag{A.3.9}$$

and at $r = r_i$,

$$A_r = 0, \quad A_\varphi = L_+ + \mathcal{M}(t,\varphi)L_-, \tag{A.3.10}$$

where $\mathcal{L}$ is related to the energy-momentum tensor in the left CFT by $\mathcal{L} = \frac{c}{4}\langle T(x^+)\rangle$ and similarly for $\mathcal{M}$ in the right CFT. This yields constraints for the fields appearing

in the Gauss decomposition,

$$\begin{aligned} e^{\Phi}\left(Y' - k_0 Y\right) &= 1, \\ \Phi' + k_0 &= 2X, \\ X' + X^2 &= \mathcal{L}. \end{aligned} \tag{A.3.11}$$

These constraints may be solved with solutions

$$\begin{aligned} Y &= e^{\varphi k_0(t)} \int e^{-\varphi k_0(t) - \Phi} d\varphi, \\ X &= \frac{1}{2}(\Phi' + k_0), \\ \mathcal{L} &= \frac{1}{2}\Phi'' + \frac{1}{4}(\Phi' + k_0)^2. \end{aligned} \tag{A.3.12}$$

Following the same procedure, the constraint equations for the inner boundary are obtained. In the final step, the solutions (A.3.12) are then inserted back into the action, which yields

$$S\left[k_0, \Phi, \Psi\right] = \frac{k}{4\pi} \int dt d\varphi \left(\frac{1}{2}\partial_- \Phi \Phi' - \frac{1}{2}\partial_+ \Psi \Psi' + k_0\left(\partial_- \Phi - \partial_+ \Psi\right) - k_0^2\right). \tag{A.3.13}$$

This is the result derived in [245] and given in (5.3.18).

Bibliography

[1] J. Erdmenger et al. "Exact Gravity Duals for Simple Quantum Circuits". In: *SciPost Phys.* **13** (2022), p. 061. arXiv: 2112.12158 [hep-th].

[2] J. Erdmenger et al. "From Complexity Geometry to Holographic Spacetime". In: *arXiv* (Nov. 2022). arXiv: 2212.00043 [hep-th].

[3] S. Banerjee et al. "Berry phases, wormholes and factorization in AdS/CFT". In: *JHEP* **08** (2022), p. 162. arXiv: 2202.11717 [hep-th].

[4] S. Banerjee et al. "Geometric Phases Characterise Operator Algebras and Missing Information". In: *arXiv* (May 2023). arXiv: 2306.00055 [hep-th].

[5] W. Heisenberg. "Über quantentheoretische Umdeutung kinematischer und mechanischer Beziehungen." In: *Zeitschrift fur Physik* **33** (Dec. 1925), pp. 879–893.

[6] M. Born and P. Jordan. "Zur Quantenmechanik". In: *Zeitschrift für Physik* **34** (1925), pp. 858–888.

[7] M. Born, W. Heisenberg, and P. Jordan. "Zur Quantenmechanik. II." In: *Zeitschrift für Physik* **35** (1926), pp. 557–615.

[8] E. Schrödinger. "An Undulatory Theory of the Mechanics of Atoms and Molecules". In: *Physical Review* **28** (Dec. 1926), pp. 1049–1070.

[9] E. Schrödinger. "Quantisierung als Eigenwertproblem". In: *Annalen der Physik* **384** (1926), pp. 361–376. eprint: https://onlinelibrary.wiley.com/doi/pdf/10.1002/andp.19263840404.

[10] A. Einstein. "Zur Elektrodynamik bewegter Körper". In: *Annalen der Physik* **322** (1905), pp. 891–921. eprint: https://onlinelibrary.wiley.com/doi/pdf/10.1002/andp.19053221004.

[11] A. Einstein. "Ist die Trägheit eines Körpers von seinem Energieinhalt abhängig?" In: *Annalen der Physik* **323** (1905), pp. 639–641. eprint: https://onlinelibrary.wiley.com/doi/pdf/10.1002/andp.19053231314.

[12] A. Einstein. "Die Grundlage der allgemeinen Relativitätstheorie". In: *Annalen der Physik* **354** (Jan. 1916), pp. 769–822.

[13] A. Einstein. "Zur allgemeinen Relativitätstheorie". In: *Sitzungsberichte der Königlich Preussischen Akademie der Wissenschaften* (Jan. 1915), pp. 778–786.

[14] A. Einstein. “Erklärung der Perihelbewegung des Merkur aus der allgemeinen Relativitätstheorie”. In: *Sitzungsberichte der Königlich Preussischen Akademie der Wissenschaften* (Jan. 1915), pp. 831–839.

[15] A. Einstein. “Die Feldgleichungen der Gravitation”. In: *Sitzungsberichte der Königlich Preussischen Akademie der Wissenschaften* (Jan. 1915), pp. 844–847.

[16] T. Ando, Y. Matsumoto, and Y. Uemura. “Theory of Hall Effect in a Two-Dimensional Electron System”. In: *Journal of the Physical Society of Japan* **39** (Aug. 1975), pp. 279–288.

[17] K. v. Klitzing, G. Dorda, and M. Pepper. “New Method for High-Accuracy Determination of the Fine-Structure Constant Based on Quantized Hall Resistance”. In: *Phys. Rev. Lett.* **45** (6 Aug. 1980), pp. 494–497.

[18] J. Beringer et al. “Review of Particle Physics (RPP)”. In: *Phys. Rev. D* **86** (2012), p. 010001.

[19] G. Aad et al. “Observation of a new particle in the search for the Standard Model Higgs boson with the ATLAS detector at the LHC”. In: *Phys. Lett. B* **716** (2012), pp. 1–29. arXiv: 1207.7214 [hep-ex].

[20] S. Chatrchyan et al. “Observation of a New Boson at a Mass of 125 GeV with the CMS Experiment at the LHC”. In: *Phys. Lett. B* **716** (2012), pp. 30–61. arXiv: 1207.7235 [hep-ex].

[21] S. Chatrchyan et al. “Observation of a New Boson with Mass Near 125 GeV in pp Collisions at $\sqrt{s} = 7$ and 8 TeV”. In: *JHEP* **06** (2013), p. 081. arXiv: 1303.4571 [hep-ex].

[22] K. Schwarzschild. “On the gravitational field of a mass point according to Einstein’s theory”. In: *Sitzungsber. Preuss. Akad. Wiss. Berlin (Math. Phys.)* **1916** (1916), pp. 189–196. arXiv: physics/9905030.

[23] S. W. Hawking. “Particle Creation by Black Holes”. In: *Commun. Math. Phys.* **43** (1975). Ed. by G. W. Gibbons and S. W. Hawking. [Erratum: Commun.Math.Phys. 46, 206 (1976)], pp. 199–220.

[24] A. M. Ghez et al. “Measuring Distance and Properties of the Milky Way’s Central Supermassive Black Hole with Stellar Orbits”. In: *APJ* **689** (Dec. 2008), pp. 1044–1062. arXiv: 0808.2870 [astro-ph].

[25] B. P. Abbott et al. "Observation of Gravitational Waves from a Binary Black Hole Merger". In: *Phys. Rev. Lett.* **116** (2016), p. 061102. arXiv: 1602.03837 [gr-qc].

[26] D. Tong. "String Theory". In: *arXiv* (Jan. 2009). arXiv: 0908.0333 [hep-th].

[27] A. Ashtekar and E. Bianchi. "A short review of loop quantum gravity". In: *Rept. Prog. Phys.* **84** (2021), p. 042001. arXiv: 2104.04394 [gr-qc].

[28] J. D. Bekenstein. "Black Holes and the Second Law". In: *Jacob Bekenstein*, pp. 303–306. eprint: https://www.worldscientific.com/doi/pdf/10.1142/9789811203961_0022.

[29] J. D. Bekenstein. "Black Holes and Entropy". In: *Phys. Rev. D* **7** (8 Apr. 1973), pp. 2333–2346.

[30] A. Strominger and C. Vafa. "Microscopic origin of the Bekenstein-Hawking entropy". In: *Phys. Lett. B* **379** (1996), pp. 99–104. arXiv: hep-th/9601029.

[31] S. W. Hawking. "Breakdown of predictability in gravitational collapse". In: *Phys. Rev. D* **14** (10 Nov. 1976), pp. 2460–2473.

[32] S. W. Hawking and D. N. Page. "Thermodynamics of Black Holes in anti-De Sitter Space". In: *Commun. Math. Phys.* **87** (1983), p. 577.

[33] L. Susskind. "The World as a hologram". In: *J. Math. Phys.* **36** (1995), pp. 6377–6396. arXiv: hep-th/9409089.

[34] J. M. Maldacena. "The Large N limit of superconformal field theories and supergravity". In: *Adv. Theor. Math. Phys.* **2** (1998), pp. 231–252. arXiv: hep-th/9711200.

[35] J. D. Bekenstein. "A Universal Upper Bound on the Entropy to Energy Ratio for Bounded Systems". In: *Phys. Rev. D* **23** (1981), p. 287.

[36] G. 't Hooft. "Dimensional reduction in quantum gravity". In: *Conf. Proc. C* **930308** (1993), pp. 284–296. arXiv: gr-qc/9310026.

[37] M. Z. Hasan and C. L. Kane. "Colloquium: Topological insulators". In: *Reviews of Modern Physics* **82** (Oct. 2010), pp. 3045–3067. arXiv: 1002.3895 [cond-mat.mes-hall].

[38] E. Witten. "Anti-de Sitter space and holography". In: *Adv. Theor. Math. Phys.* **2** (1998), pp. 253–291. arXiv: hep-th/9802150.

[39] S. S. Gubser, I. R. Klebanov, and A. M. Polyakov. "Gauge theory correlators from noncritical string theory". In: *Phys. Lett. B* **428** (1998), pp. 105–114. arXiv: hep-th/9802109.

[40] O. Aharony et al. "Large N field theories, string theory and gravity". In: *Phys. Rept.* **323** (2000), pp. 183–386. arXiv: hep-th/9905111.

[41] S. Ryu and T. Takayanagi. "Holographic derivation of entanglement entropy from AdS/CFT". In: *Phys. Rev. Lett.* **96** (2006), p. 181602. arXiv: hep-th/0603001.

[42] T. Nishioka, S. Ryu, and T. Takayanagi. "Holographic Entanglement Entropy: An Overview". In: *J. Phys. A* **42** (2009), p. 504008. arXiv: 0905.0932 [hep-th].

[43] V. E. Hubeny et al. "Holographic entanglement plateaux". In: *JHEP* **08** (2013), p. 092. arXiv: 1306.4004 [hep-th].

[44] T. Faulkner, A. Lewkowycz, and J. Maldacena. "Quantum corrections to holographic entanglement entropy". In: *JHEP* **11** (2013), p. 074. arXiv: 1307.2892 [hep-th].

[45] N. Engelhardt and A. C. Wall. "Quantum Extremal Surfaces: Holographic Entanglement Entropy beyond the Classical Regime". In: *JHEP* **01** (2015), p. 073. arXiv: 1408.3203 [hep-th].

[46] D. L. Jafferis et al. "Relative entropy equals bulk relative entropy". In: *JHEP* **06** (2016), p. 004. arXiv: 1512.06431 [hep-th].

[47] M. Van Raamsdonk. "Building up spacetime with quantum entanglement". In: *Gen. Rel. Grav.* **42** (2010), pp. 2323–2329. arXiv: 1005.3035 [hep-th].

[48] J. Maldacena and L. Susskind. "Cool horizons for entangled black holes". In: *Fortsch. Phys.* **61** (2013), pp. 781–811. arXiv: 1306.0533 [hep-th].

[49] J. M. Maldacena. "Eternal black holes in anti-de Sitter". In: *JHEP* **04** (2003), p. 021. arXiv: hep-th/0106112.

[50] T. Hartman and J. Maldacena. "Time Evolution of Entanglement Entropy from Black Hole Interiors". In: *JHEP* **05** (2013), p. 014. arXiv: 1303.1080 [hep-th].

[51] J. Louko, D. Marolf, and S. F. Ross. "On geodesic propagators and black hole holography". In: *Phys. Rev. D* **62** (2000), p. 044041. arXiv: hep-th/0002111.

[52] M. Headrick et al. "Causality & holographic entanglement entropy". In: *JHEP* **12** (2014), p. 162. arXiv: 1408.6300 [hep-th].

[53] A. Hamilton et al. "Local bulk operators in AdS/CFT: A Boundary view of horizons and locality". In: *Phys. Rev. D* **73** (2006), p. 086003. arXiv: hep-th/0506118.

[54] A. Hamilton et al. "Holographic representation of local bulk operators". In: *Phys. Rev. D* **74** (2006), p. 066009. arXiv: hep-th/0606141.

[55] A. Hamilton et al. "Local bulk operators in AdS/CFT: A Holographic description of the black hole interior". In: *Phys. Rev. D* **75** (2007). [Erratum: Phys.Rev.D 75, 129902 (2007)], p. 106001. arXiv: hep-th/0612053.

[56] A. Hamilton et al. "Local bulk operators in AdS/CFT and the fate of the BTZ singularity". In: *AMS/IP Stud. Adv. Math.* **44** (2008). Ed. by E. Sharpe and A. Greenspoon, pp. 85–100. arXiv: 0710.4334 [hep-th].

[57] D. Kabat et al. "Holographic representation of bulk fields with spin in AdS/CFT". In: *Phys. Rev. D* **86** (2012), p. 026004. arXiv: 1204.0126 [hep-th].

[58] T. Faulkner and A. Lewkowycz. "Bulk locality from modular flow". In: *JHEP* **07** (2017), p. 151. arXiv: 1704.05464 [hep-th].

[59] T. Faulkner, M. Li, and H. Wang. "A modular toolkit for bulk reconstruction". In: *JHEP* **04** (2019), p. 119. arXiv: 1806.10560 [hep-th].

[60] A. Almheiri, X. Dong, and D. Harlow. "Bulk Locality and Quantum Error Correction in AdS/CFT". In: *JHEP* **04** (2015), p. 163. arXiv: 1411.7041 [hep-th].

[61] F. Pastawski et al. "Holographic quantum error-correcting codes: Toy models for the bulk/boundary correspondence". In: *JHEP* **06** (2015), p. 149. arXiv: 1503.06237 [hep-th].

[62] D. Harlow. "The Ryu–Takayanagi Formula from Quantum Error Correction". In: *Commun. Math. Phys.* **354** (2017), pp. 865–912. arXiv: 1607.03901 [hep-th].

[63] J. Cotler et al. "Entanglement Wedge Reconstruction via Universal Recovery Channels". In: *Phys. Rev. X* **9** (2019), p. 031011. arXiv: 1704.05839 [hep-th].

[64] C.-F. Chen, G. Penington, and G. Salton. "Entanglement Wedge Reconstruction using the Petz Map". In: *JHEP* **01** (2020), p. 168. arXiv: 1902.02844 [hep-th].

[65] G. Penington et al. "Replica wormholes and the black hole interior". In: *JHEP* **03** (2022), p. 205. arXiv: 1911.11977 [hep-th].

[66] A. Almheiri et al. "The entropy of bulk quantum fields and the entanglement wedge of an evaporating black hole". In: *JHEP* **12** (2019), p. 063. arXiv: 1905.08762 [hep-th].

[67] D. L. Jafferis and L. Lamprou. "Inside the hologram: reconstructing the bulk observer′s experience". In: *JHEP* **03** (2022), p. 084. arXiv: 2009.04476 [hep-th].

[68] J. de Boer, D. L. Jafferis, and L. Lamprou. "On black hole interior reconstruction, singularities and the emergence of time". In: *arXiv* (Nov. 2022). arXiv: 2211.16512 [hep-th].

[69] S. Leutheusser and H. Liu. "Emergent times in holographic duality". In: *arXiv* (Dec. 2021). arXiv: 2112.12156 [hep-th].

[70] S. Leutheusser and H. Liu. "Causal connectability between quantum systems and the black hole interior in holographic duality". In: *arXiv* (Oct. 2021). arXiv: 2110.05497 [hep-th].

[71] V. Balasubramanian et al. "Entwinement and the emergence of spacetime". In: *JHEP* **01** (2015), p. 048. arXiv: 1406.5859 [hep-th].

[72] M. Gerbershagen. "Illuminating entanglement shadows of BTZ black holes by a generalized entanglement measure". In: *JHEP* **10** (2021), p. 187. arXiv: 2105.01097 [hep-th].

[73] L. Susskind. "Butterflies on the Stretched Horizon". In: *arXiv* (Nov. 2013). arXiv: 1311.7379 [hep-th].

[74] L. Susskind. "Computational Complexity and Black Hole Horizons". In: *Fortsch. Phys.* **64** (2016). [Addendum: Fortsch.Phys. 64, 44–48 (2016)], pp. 24–43. arXiv: 1403.5695 [hep-th].

[75] P. Caputa and J. M. Magan. "Quantum Computation as Gravity". In: *Phys. Rev. Lett.* **122** (2019), p. 231302. arXiv: 1807.04422 [hep-th].

[76] M. A. Nielsen. "A geometric approach to quantum circuit lower bounds". In: *arXiv e-prints* (Feb. 2005), quant–ph/0502070. arXiv: quant-ph/0502070 [quant-ph].

[77] M. A. Nielsen et al. "Quantum Computation as Geometry". In: *Science* **311** (Feb. 2006), pp. 1133–1135. arXiv: quant-ph/0603161 [quant-ph].

[78] S. Chapman et al. "Toward a Definition of Complexity for Quantum Field Theory States". In: *Phys. Rev. Lett.* **120** (2018), p. 121602. arXiv: 1707.08582 [hep-th].

[79] J. M. Magán. "Black holes, complexity and quantum chaos". In: *JHEP* **09** (2018), p. 043. arXiv: 1805.05839 [hep-th].

[80] D. Stanford and L. Susskind. "Complexity and Shock Wave Geometries". In: *Phys. Rev. D* **90** (2014), p. 126007. arXiv: 1406.2678 [hep-th].

[81] A. R. Brown et al. "Holographic Complexity Equals Bulk Action?" In: *Phys. Rev. Lett.* **116** (2016), p. 191301. arXiv: 1509.07876 [hep-th].

[82] J. Couch, W. Fischler, and P. H. Nguyen. "Noether charge, black hole volume, and complexity". In: *JHEP* **03** (2017), p. 119. arXiv: 1610.02038 [hep-th].

[83] A. Belin et al. "Does Complexity Equal Anything?" In: *Phys. Rev. Lett.* **128** (2022), p. 081602. arXiv: 2111.02429 [hep-th].

[84] A. Belin et al. "Complexity Equals Anything II". In: *arXiv* (Oct. 2022). arXiv: 2210.09647 [hep-th].

[85] N. Chagnet et al. "Complexity for Conformal Field Theories in General Dimensions". In: *Phys. Rev. Lett.* **128** (2022), p. 051601. arXiv: 2103.06920 [hep-th].

[86] M. Flory and M. P. Heller. "Conformal field theory complexity from Euler-Arnold equations". In: *JHEP* **12** (2020), p. 091. arXiv: 2007.11555 [hep-th].

[87] M. Flory and M. P. Heller. "Geometry of Complexity in Conformal Field Theory". In: *Phys. Rev. Res.* **2** (2020), p. 043438. arXiv: 2005.02415 [hep-th].

[88] M. Banados. "Three-dimensional quantum geometry and black holes". In: *AIP Conf. Proc.* **484** (1999). Ed. by H. Falomir, R. E. Gamboa Saravi, and F. A. Schaposnik, pp. 147–169. arXiv: hep-th/9901148.

[89] D. Harlow. "Wormholes, Emergent Gauge Fields, and the Weak Gravity Conjecture". In: *JHEP* **01** (2016), p. 122. arXiv: 1510.07911 [hep-th].

[90] D. Harlow and D. Jafferis. "The Factorization Problem in Jackiw-Teitelboim Gravity". In: *JHEP* **02** (2020), p. 177. arXiv: 1804.01081 [hep-th].

[91] E. Witten. "Gravity and the crossed product". In: *JHEP* **10** (2022), p. 008. arXiv: 2112.12828 [hep-th].

[92] E. Gesteau and M. J. Kang. "Nonperturbative gravity corrections to bulk reconstruction". In: *arXiv* (Dec. 2021). arXiv: 2112.12789 [hep-th].

[93] V. Chandrasekaran, G. Penington, and E. Witten. "Large N algebras and generalized entropy". In: *arXiv* (Sept. 2022). arXiv: 2209.10454 [hep-th].

[94] E. Bahiru et al. "Holography and Localization of Information in Quantum Gravity". In: *arXiv* (Jan. 2023). arXiv: 2301.08753 [hep-th].

[95] E. Gesteau. "Large N von Neumann algebras and the renormalization of Newton's constant". In: *arXiv* (Feb. 2023). arXiv: 2302.01938 [hep-th].

[96] J. von Neumann. "Zur Algebra der Funktionaloperationen und Theorie der normalen Operatoren". In: *Mathematische Annalen* **102** (1930), pp. 370–427.

[97] J. v. Neumann. "On a Certain Topology for Rings of Operators". In: *Annals of Mathematics* **37** (1936), pp. 111–115.

[98] F. J. Murray and J. v. Neumann. "On Rings of Operators". In: *Annals of Mathematics* **37** (1936), pp. 116–229.

[99] F. J. Murray and J. von Neumann. "On Rings of Operators. II". In: *Transactions of the American Mathematical Society* **41** (1937), pp. 208–248.

[100] J. v. Neumann. "On Rings of Operators. III". In: *Annals of Mathematics* **41** (1940), pp. 94–161.

[101] J. von Neumann. "On Some Algebraical Properties of Operator Rings". In: *Annals of Mathematics* **44** (1943), pp. 709–715.

[102] F. J. Murray and J. von Neumann. "On Rings of Operators. IV". In: *Annals of Mathematics* **44** (1943), pp. 716–808.

[103] J. V. Neumann. "On Rings of Operators. Reduction Theory". In: *Annals of Mathematics* **50** (1949), pp. 401–485.

[104] J. von Neumann and A. Taub. *Collected Works. Volume III: Rings of Operators.* Pergamon Press, 1961.

[105] B. Oblak. "Berry Phases on Virasoro Orbits". In: *JHEP* **10** (2017), p. 114. arXiv: 1703.06142 [hep-th].

[106] B. Czech et al. "Modular Berry Connection for Entangled Subregions in AdS/CFT". In: *Phys. Rev. Lett.* **120** (2018), p. 091601. arXiv: 1712.07123 [hep-th].

[107] B. Czech, L. Lamprou, and L. Susskind. "Entanglement Holonomies". In: *arXiv* (July 2018). arXiv: 1807.04276 [hep-th].

[108] B. Czech et al. "A modular sewing kit for entanglement wedges". In: *JHEP* **11** (2019), p. 094. arXiv: 1903.04493 [hep-th].

[109] P. Di Francesco, P. Mathieu, and D. Senechal. *Conformal Field Theory.* Graduate Texts in Contemporary Physics. New York: Springer-Verlag, 1997. ISBN: 978-0-387-94785-3, 978-1-4612-7475-9.

[110] P. H. Ginsparg. "Applied Conformal Field Theory". In: *Les Houches Summer School in Theoretical Physics: Fields, Strings, Critical Phenomena.* Sept. 1988. arXiv: hep-th/9108028.

[111] P. Caputa et al. "Liouville Action as Path-Integral Complexity: From Continuous Tensor Networks to AdS/CFT". In: *JHEP* **11** (2017), p. 097. arXiv: 1706.07056 [hep-th].

[112] K. Nguyen. "Reparametrization modes in 2d CFT and the effective theory of stress tensor exchanges". In: *JHEP* **05** (2021), p. 029. arXiv: 2101.08800 [hep-th].

[113] Y. I. Benoit Estienne. *Conformal field theory for 2d statistical mechanics*. URL: https://www.lpthe.jussieu.fr/~ikhlef/CFT.pdf.

[114] A. Kirillov. *Lectures on the Orbit Method*. Graduate studies in mathematics. American Mathematical Society, 2004. ISBN: 9780821835302.

[115] E. Witten. "Coadjoint Orbits of the Virasoro Group". In: *Commun. Math. Phys.* **114** (1988), p. 1.

[116] A. Alekseev and S. L. Shatashvili. "Path Integral Quantization of the Coadjoint Orbits of the Virasoro Group and 2D Gravity". In: *Nucl. Phys. B* **323** (1989), pp. 719–733.

[117] B. Rai and V. G. J. Rodgers. "From Coadjoint Orbits to Scale Invariant WZNW Type Actions and 2-D Quantum Gravity Action". In: *Nucl. Phys. B* **341** (1990), pp. 119–133.

[118] A. Alekseev and S. L. Shatashvili. "From geometric quantization to conformal field theory". In: *Commun. Math. Phys.* **128** (1990), pp. 197–212.

[119] B. Oblak. "BMS Particles in Three Dimensions". PhD thesis. U. Brussels, Brussels U., 2016. arXiv: 1610.08526 [hep-th].

[120] M. Schottenloher. *A Mathematical Introduction to Conformal Field Theory*. Vol. 759. Aug. 2008. ISBN: 978-3-540-68625-5.

[121] R. Bott. "On the characteristic classes of groups of diffeomorphisms". In: *Enseign. Math.* (1977), pp. 209–220.

[122] J. Erdmenger, M. Gerbershagen, and A.-L. Weigel. "Complexity measures from geometric actions on Virasoro and Kac-Moody orbits". In: *JHEP* **11** (2020), p. 003. arXiv: 2004.03619 [hep-th].

[123] M. Ammon and J. Erdmenger. *Gauge/gravity duality: Foundations and applications*. Cambridge: Cambridge University Press, Apr. 2015. ISBN: 978-1-107-01034-5, 978-1-316-23594-2.

[124] M. Banados, C. Teitelboim, and J. Zanelli. "The Black hole in three-dimensional space-time". In: *Phys. Rev. Lett.* **69** (1992), pp. 1849–1851. arXiv: hep-th/9204099.

[125] M. Banados et al. "Geometry of the (2+1) black hole". In: *Phys. Rev. D* **48** (1993). [Erratum: Phys.Rev.D 88, 069902 (2013)], pp. 1506–1525. arXiv: gr-qc/9302012.

[126] L. Fidkowski et al. "The Black hole singularity in AdS / CFT". In: *JHEP* **02** (2004), p. 014. arXiv: hep-th/0306170.

[127] D. S. Ageev, I. Y. Aref'eva, and M. D. Tikhanovskaya. "(1+1)-Correlators and moving massive defects". In: *Theor. Math. Phys.* **188** (2016), pp. 1038–1068. arXiv: 1512.03362 [hep-th].

[128] S. Deser and R. Jackiw. "Three-dimensional cosmological gravity: Dynamics of constant curvature". In: *Ann. Phys. (N.Y.); (United States)* **153:2** (Apr. 1984).

[129] R. Bousso. "The Holographic principle". In: *Rev. Mod. Phys.* **74** (2002), pp. 825–874. arXiv: hep-th/0203101.

[130] P. Kraus. "Lectures on black holes and the AdS(3) / CFT(2) correspondence". In: *Lect. Notes Phys.* **755** (2008), pp. 193–247. arXiv: hep-th/0609074.

[131] J. M. Maldacena. "Black holes in string theory". PhD thesis. Princeton U., 1996. arXiv: hep-th/9607235.

[132] J. D. Brown and M. Henneaux. "Central Charges in the Canonical Realization of Asymptotic Symmetries: An Example from Three-Dimensional Gravity". In: *Commun. Math. Phys.* **104** (1986), pp. 207–226.

[133] M. Henningson and K. Skenderis. "The Holographic Weyl anomaly". In: *JHEP* **07** (1998), p. 023. arXiv: hep-th/9806087.

[134] V. Balasubramanian and P. Kraus. "A Stress tensor for Anti-de Sitter gravity". In: *Commun. Math. Phys.* **208** (1999), pp. 413–428. arXiv: hep-th/9902121.

[135] S. de Haro, S. N. Solodukhin, and K. Skenderis. "Holographic reconstruction of space-time and renormalization in the AdS / CFT correspondence". In: *Commun. Math. Phys.* **217** (2001), pp. 595–622. arXiv: hep-th/0002230.

[136] D. Marolf, W. Kelly, and S. Fischetti. "Conserved Charges in Asymptotically (Locally) AdS Spacetimes". In: *Springer Handbook of Spacetime*. Ed. by A. Ashtekar and V. Petkov. 2014, pp. 381–407. arXiv: 1211.6347 [gr-qc].

[137] Collectif. "Conformal invariants". en. In: *Élie Cartan et les mathématiques d'aujourd'hui - Lyon, 25-29 juin 1984*. Astérisque S131. Société mathématique de France, 1985.

[138] G. Compère et al. "Symplectic and Killing symmetries of AdS_3 gravity: holographic vs boundary gravitons". In: *JHEP* **01** (2016), p. 080. arXiv: 1511.06079 [hep-th].

[139] M. M. Sheikh-Jabbari and H. Yavartanoo. "On quantization of AdS_3 gravity I: semi-classical analysis". In: *JHEP* **07** (2014), p. 104. arXiv: 1404.4472 [hep-th].

[140] M. M. Sheikh-Jabbari and H. Yavartanoo. "On 3d bulk geometry of Virasoro coadjoint orbits: orbit invariant charges and Virasoro hair on locally AdS_3 geometries". In: *Eur. Phys. J. C* **76** (2016), p. 493. arXiv: 1603.05272 [hep-th].

[141] L. Susskind, L. Thorlacius, and J. Uglum. "The Stretched horizon and black hole complementarity". In: *Phys. Rev. D* **48** (1993), pp. 3743–3761. arXiv: hep-th/9306069.

[142] C. R. Stephens, G. 't Hooft, and B. F. Whiting. "Black hole evaporation without information loss". In: *Class. Quant. Grav.* **11** (1994), pp. 621–648. arXiv: gr-qc/9310006.

[143] L. Susskind and L. Thorlacius. "Gedanken experiments involving black holes". In: *Phys. Rev. D* **49** (1994), pp. 966–974. arXiv: hep-th/9308100.

[144] S. Ryu and T. Takayanagi. "Aspects of Holographic Entanglement Entropy". In: *JHEP* **08** (2006), p. 045. arXiv: hep-th/0605073.

[145] A. Reynolds and S. F. Ross. "Complexity in de Sitter Space". In: *Class. Quant. Grav.* **34** (2017), p. 175013. arXiv: 1706.03788 [hep-th].

[146] S. Chapman, D. A. Galante, and E. D. Kramer. "Holographic complexity and de Sitter space". In: *JHEP* **02** (2022), p. 198. arXiv: 2110.05522 [hep-th].

[147] S. B. Giddings. "The deepest problem: some perspectives on quantum gravity". In: *arXiv* (Feb. 2022). arXiv: 2202.08292 [hep-th].

[148] T. Faulkner et al. "Snowmass white paper: Quantum information in quantum field theory and quantum gravity". In: *2022 Snowmass Summer Study*. Mar. 2022. arXiv: 2203.07117 [hep-th].

[149] J. de Boer et al. "Frontiers of Quantum Gravity: shared challenges, converging directions". In: *arXiv* (July 2022). arXiv: 2207.10618 [hep-th].

[150] R. Bousso and G. Penington. "Holograms In Our World". In: *arXiv* (Feb. 2023). arXiv: 2302.07892 [hep-th].

[151] P. Hayden and J. Preskill. "Black holes as mirrors: Quantum information in random subsystems". In: *JHEP* **09** (2007), p. 120. arXiv: 0708.4025 [hep-th].

[152] Y. Sekino and L. Susskind. "Fast Scramblers". In: *JHEP* **10** (2008), p. 065. arXiv: 0808.2096 [hep-th].

[153] L. Susskind. "Singularities, Firewalls, and Complementarity". In: *arXiv* (Aug. 2012). arXiv: 1208.3445 [hep-th].

[154] D. Harlow and P. Hayden. "Quantum Computation vs. Firewalls". In: *JHEP* **06** (2013), p. 085. arXiv: 1301.4504 [hep-th].

[155] G. Penington. "Entanglement Wedge Reconstruction and the Information Paradox". In: *JHEP* **09** (2020), p. 002. arXiv: 1905.08255 [hep-th].

[156] A. Almheiri et al. "The Page curve of Hawking radiation from semiclassical geometry". In: *JHEP* **03** (2020), p. 149. arXiv: 1908.10996 [hep-th].

[157] X. Dong, D. Harlow, and A. C. Wall. "Reconstruction of Bulk Operators within the Entanglement Wedge in Gauge-Gravity Duality". In: *Phys. Rev. Lett.* **117** (2016), p. 021601. arXiv: 1601.05416 [hep-th].

[158] S. H. Shenker and D. Stanford. "Black holes and the butterfly effect". In: *JHEP* **03** (2014), p. 067. arXiv: 1306.0622 [hep-th].

[159] J. Maldacena, S. H. Shenker, and D. Stanford. "A bound on chaos". In: *JHEP* **08** (2016), p. 106. arXiv: 1503.01409 [hep-th].

[160] C. Murthy and M. Srednicki. "Bounds on chaos from the eigenstate thermalization hypothesis". In: *Phys. Rev. Lett.* **123** (2019), p. 230606. arXiv: 1906.10808 [cond-mat.stat-mech].

[161] A. R. Brown et al. "Complexity, action, and black holes". In: *Phys. Rev. D* **93** (2016), p. 086006. arXiv: 1512.04993 [hep-th].

[162] A. Belin, A. Lewkowycz, and G. Sárosi. "Complexity and the bulk volume, a new York time story". In: *JHEP* **03** (2019), p. 044. arXiv: 1811.03097 [hep-th].

[163] B. Chen, B. Czech, and Z.-z. Wang. "Quantum information in holographic duality". In: *Rept. Prog. Phys.* **85** (2022), p. 046001. arXiv: 2108.09188 [hep-th].

[164] M. A. Nielsen and I. L. Chuang. *Quantum Computation and Quantum Information*. Cambridge University Press, 2000.

[165] M. Rangamani and T. Takayanagi. *Holographic Entanglement Entropy*. Vol. 931. Springer, 2017. arXiv: 1609.01287 [hep-th].

[166] J. Cardy and E. Tonni. "Entanglement hamiltonians in two-dimensional conformal field theory". In: *J. Stat. Mech.* **1612** (2016), p. 123103. arXiv: 1608.01283 [cond-mat.stat-mech].

[167] P. Calabrese and J. L. Cardy. "Entanglement entropy and quantum field theory". In: *J. Stat. Mech.* **0406** (2004), P06002. arXiv: hep-th/0405152.

[168] E. Witten. "APS Medal for Exceptional Achievement in Research: Invited article on entanglement properties of quantum field theory". In: *Rev. Mod. Phys.* **90** (2018), p. 045003. arXiv: 1803.04993 [hep-th].

[169] D. Harlow. "Jerusalem Lectures on Black Holes and Quantum Information". In: *Rev. Mod. Phys.* **88** (2016), p. 015002. arXiv: 1409.1231 [hep-th].

[170] H. Reeh and S. Schlieder. "Bemerkungen zur unitäräquivalenz von lorentzinvarianten feldern". In: *Nuovo Cim.* **22** (1961), pp. 1051–1068.

[171] J. J. Bisognano and E. H. Wichmann. "On the Duality Condition for Quantum Fields". In: *J. Math. Phys.* **17** (1976), pp. 303–321.

[172] W. G. Unruh. "Notes on black-hole evaporation". In: *Phys. Rev. D* **14** (4 Aug. 1976), pp. 870–892.

[173] P. Calabrese and J. Cardy. "Entanglement entropy and conformal field theory". In: *J. Phys. A* **42** (2009), p. 504005. arXiv: 0905.4013 [cond-mat.stat-mech].

[174] A. Lewkowycz and J. Maldacena. "Generalized gravitational entropy". In: *JHEP* **08** (2013), p. 090. arXiv: 1304.4926 [hep-th].

[175] T. Takayanagi. "Holographic Spacetimes as Quantum Circuits of Path-Integrations". In: *JHEP* **12** (2018), p. 048. arXiv: 1808.09072 [hep-th].

[176] V. E. Hubeny, M. Rangamani, and T. Takayanagi. "A Covariant holographic entanglement entropy proposal". In: *JHEP* **07** (2007), p. 062. arXiv: 0705.0016 [hep-th].

[177] T. Faulkner et al. "Gravitation from Entanglement in Holographic CFTs". In: *JHEP* **03** (2014), p. 051. arXiv: 1312.7856 [hep-th].

[178] A. Saha, S. Karar, and S. Gangopadhyay. "Bulk geometry from entanglement entropy of CFT". In: *Eur. Phys. J. Plus* **135** (2020), p. 132. arXiv: 1807.04646 [hep-th].

[179] J. Hammersley. "Numerical metric extraction in AdS/CFT". In: *Gen. Rel. Grav.* **40** (2008), pp. 1619–1652. arXiv: 0705.0159 [hep-th].

[180] T. Hartman. *Lectures on Quantum Gravity and Black Holes*. 2015. URL: http://www.hartmanhep.net/topics2015/gravity-lectures.pdf.

[181] J. B. Hartle and S. W. Hawking. "Path-integral derivation of black-hole radiance". In: *Phys. Rev. D* **13** (8 Apr. 1976), pp. 2188–2203.

[182] E. Witten. "Anti-de Sitter space, thermal phase transition, and confinement in gauge theories". In: *Adv. Theor. Math. Phys.* **2** (1998). Ed. by L. Bergstrom and U. Lindstrom, pp. 505–532. arXiv: hep-th/9803131.

[183] W. Israel. "Thermo field dynamics of black holes". In: *Phys. Lett.* **A57** (1976), pp. 107–110.

[184] A. Einstein and N. Rosen. "The Particle Problem in the General Theory of Relativity". In: *Phys. Rev.* **48** (1 July 1935), pp. 73–77.

[185] H. Verlinde. "Wormholes in Quantum Mechanics". In: *arXiv* (May 2021). arXiv: 2105.02129 [hep-th].

[186] C. T. Asplund, N. Callebaut, and C. Zukowski. "Equivalence of Emergent de Sitter Spaces from Conformal Field Theory". In: *JHEP* **09** (2016), p. 154. arXiv: 1604.02687 [hep-th].

[187] M. Karliner, I. R. Klebanov, and L. Susskind. "Size and Shape of Strings". In: *Int. J. Mod. Phys. A* **3** (1988), p. 1981.

[188] A. Mezhlumian, A. W. Peet, and L. Thorlacius. "String thermalization at a black hole horizon". In: *Phys. Rev. D* **50** (1994), pp. 2725–2730. arXiv: hep-th/9402125.

[189] I. R. Klebanov and L. Susskind. "Continuum Strings From Discrete Field Theories". In: *Nucl. Phys. B* **309** (1988), pp. 175–187.

[190] L. Susskind and Y. Zhao. "Switchbacks and the Bridge to Nowhere". In: *arXiv* (Aug. 2014). arXiv: 1408.2823 [hep-th].

[191] J. Watrous. "Quantum Computational Complexity". In: *arXiv e-prints* (Apr. 2008). arXiv: 0804.3401 [quant-ph].

[192] S. Aaronson. "The Complexity of Quantum States and Transformations: From Quantum Money to Black Holes". In: *arXiv* (July 2016). arXiv: 1607.05256 [quant-ph].

[193] M. R. Dowling and M. A. Nielsen. "The geometry of quantum computation". In: *arXiv* (Dec. 2006). arXiv: quant-ph/0701004 [quant-ph].

[194] X. Mo. *An Introduction to Finsler Geometry*. World Scientific, 2006.

[195] R. Jefferson and R. C. Myers. "Circuit complexity in quantum field theory". In: *JHEP* **10** (2017), p. 107. arXiv: 1707.08570 [hep-th].

[196] L. Hackl and R. C. Myers. "Circuit complexity for free fermions". In: *JHEP* **07** (2018), p. 139. arXiv: 1803.10638 [hep-th].

[197] R. Khan, C. Krishnan, and S. Sharma. "Circuit Complexity in Fermionic Field Theory". In: *Phys. Rev. D* **98** (2018), p. 126001. arXiv: 1801.07620 [hep-th].

[198] M. Guo et al. "Circuit Complexity for Coherent States". In: *JHEP* **10** (2018), p. 011. arXiv: 1807.07677 [hep-th].

[199] P. Bueno, J. M. Magan, and C. S. Shahbazi. "Complexity measures in QFT and constrained geometric actions". In: *JHEP* **09** (2021), p. 200. arXiv: 1908.03577 [hep-th].

[200] M. Flory and N. Miekley. "Complexity change under conformal transformations in AdS_3/CFT_2". In: *JHEP* **05** (2019), p. 003. arXiv: 1806.08376 [hep-th].

[201] M. Flory. "WdW-patches in AdS_3 and complexity change under conformal transformations II". In: *JHEP* **05** (2019), p. 086. arXiv: 1902.06499 [hep-th].

[202] M. Alishahiha. "Holographic Complexity". In: *Phys. Rev. D* **92** (2015), p. 126009. arXiv: 1509.06614 [hep-th].

[203] M. Miyaji et al. "Distance between Quantum States and Gauge-Gravity Duality". In: *Phys. Rev. Lett.* **115** (2015), p. 261602. arXiv: 1507.07555 [hep-th].

[204] C. A. Agón, M. Headrick, and B. Swingle. "Subsystem Complexity and Holography". In: *JHEP* **02** (2019), p. 145. arXiv: 1804.01561 [hep-th].

[205] H. A. Camargo et al. "Complexity as a novel probe of quantum quenches: universal scalings and purifications". In: *Phys. Rev. Lett.* **122** (2019), p. 081601. arXiv: 1807.07075 [hep-th].

[206] E. Caceres et al. "Complexity of Mixed States in QFT and Holography". In: *JHEP* **03** (2020), p. 012. arXiv: 1909.10557 [hep-th].

[207] G. Di Giulio and E. Tonni. "Complexity of mixed Gaussian states from Fisher information geometry". In: *JHEP* **12** (2020), p. 101. arXiv: 2006.00921 [hep-th].

[208] P. Caputa et al. “Anti-de Sitter Space from Optimization of Path Integrals in Conformal Field Theories”. In: *Phys. Rev. Lett.* **119** (2017), p. 071602. arXiv: 1703.00456 [hep-th].

[209] A. Bhattacharyya et al. “Path-Integral Complexity for Perturbed CFTs”. In: *JHEP* **07** (2018), p. 086. arXiv: 1804.01999 [hep-th].

[210] H. A. Camargo et al. “Path integral optimization as circuit complexity”. In: *Phys. Rev. Lett.* **123** (2019), p. 011601. arXiv: 1904.02713 [hep-th].

[211] P. Caputa and I. MacCormack. “Geometry and Complexity of Path Integrals in Inhomogeneous CFTs”. In: *JHEP* **01** (2021). [Erratum: JHEP 09, 109 (2022)], p. 027. arXiv: 2004.04698 [hep-th].

[212] P. Caputa, D. Das, and S. R. Das. “Path integral complexity and Kasner singularities”. In: *JHEP* **01** (2022), p. 150. arXiv: 2111.04405 [hep-th].

[213] H. A. Camargo, P. Caputa, and P. Nandy. “Q-curvature and path integral complexity”. In: *JHEP* **04** (2022), p. 081. arXiv: 2201.00562 [hep-th].

[214] J. Boruch, P. Caputa, and T. Takayanagi. “Path-Integral Optimization from Hartle-Hawking Wave Function”. In: *Phys. Rev. D* **103** (2021), p. 046017. arXiv: 2011.08188 [hep-th].

[215] J. Boruch et al. “Holographic path-integral optimization”. In: *JHEP* **07** (2021). [Erratum: JHEP 09, 111 (2022)], p. 016. arXiv: 2104.00010 [hep-th].

[216] A. R. Chandra et al. “Spacetime as a quantum circuit”. In: *JHEP* **21** (2021), p. 207. arXiv: 2101.01185 [hep-th].

[217] A. R. Chandra et al. “Cost of holographic path integrals”. In: *arXiv* (Mar. 2022). arXiv: 2203.08842 [hep-th].

[218] D. E. Parker et al. “A Universal Operator Growth Hypothesis”. In: *Phys. Rev. X* **9** (2019), p. 041017. arXiv: 1812.08657 [cond-mat.stat-mech].

[219] E. Rabinovici et al. “Operator complexity: a journey to the edge of Krylov space”. In: *JHEP* **06** (2021), p. 062. arXiv: 2009.01862 [hep-th].

[220] P. Caputa, J. M. Magan, and D. Patramanis. “Geometry of Krylov complexity”. In: *Phys. Rev. Res.* **4** (2022), p. 013041. arXiv: 2109.03824 [hep-th].

[221] A. Kar et al. “Random matrix theory for complexity growth and black hole interiors”. In: *JHEP* **01** (2022), p. 016. arXiv: 2106.02046 [hep-th].

[222] A. Dymarsky and M. Smolkin. “Krylov complexity in conformal field theory”. In: *Phys. Rev. D* **104** (2021), p. L081702. arXiv: 2104.09514 [hep-th].

[223] V. Balasubramanian et al. "Quantum chaos and the complexity of spread of states". In: *Phys. Rev. D* **106** (2022), p. 046007. arXiv: 2202.06957 [hep-th].

[224] E. Rabinovici et al. "Krylov complexity from integrability to chaos". In: *JHEP* **07** (2022), p. 151. arXiv: 2207.07701 [hep-th].

[225] P. Caputa and D. Ge. "Entanglement and geometry from subalgebras of the Virasoro". In: *arXiv* (Nov. 2022). arXiv: 2211.03630 [hep-th].

[226] S. Chapman and G. Policastro. "Quantum computational complexity from quantum information to black holes and back". In: *Eur. Phys. J. C* **82** (2022), p. 128. arXiv: 2110.14672 [hep-th].

[227] P. Zanardi, M. Cozzini, and P. Giorda. "Ground state fidelity and quantum phase transitions in free Fermi systems". In: *Journal of Statistical Mechanics: Theory and Experiment* **2007** (Feb. 2007), pp. L02002–L02002.

[228] W.-L. You, Y.-W. Li, and S.-J. Gu. "Fidelity, dynamic structure factor, and susceptibility in critical phenomena". In: *Physical Review E* **76** (Aug. 2007).

[229] A. Trivella. "Holographic Computations of the Quantum Information Metric". In: *Class. Quant. Grav.* **34** (2017), p. 105003. arXiv: 1607.06519 [hep-th].

[230] R. Abt et al. "Topological Complexity in AdS_3/CFT_2". In: *Fortsch. Phys.* **66** (2018), p. 1800034. arXiv: 1710.01327 [hep-th].

[231] R. Abt et al. "Holographic Subregion Complexity from Kinematic Space". In: *JHEP* **01** (2019), p. 012. arXiv: 1805.10298 [hep-th].

[232] J. M. Maldacena and L. Maoz. "Wormholes in AdS". In: *JHEP* **02** (2004), p. 053. arXiv: hep-th/0401024.

[233] D. Harlow. "Aspects of the Papadodimas-Raju Proposal for the Black Hole Interior". In: *JHEP* **11** (2014), p. 055. arXiv: 1405.1995 [hep-th].

[234] D. L. Jafferis and D. K. Kolchmeyer. "Entanglement Entropy in Jackiw-Teitelboim Gravity". In: *arXiv* (Nov. 2019). arXiv: 1911.10663 [hep-th].

[235] P. Saad, S. Shenker, and S. Yao. "Comments on wormholes and factorization". In: *arXiv* (July 2021). arXiv: 2107.13130 [hep-th].

[236] T. G. Mertens, J. Simón, and G. Wong. "A proposal for 3d quantum gravity and its bulk factorization". In: *arXiv* (Oct. 2022). arXiv: 2210.14196 [hep-th].

[237] T. G. Mertens and G. J. Turiaci. "Solvable Models of Quantum Black Holes: A Review on Jackiw-Teitelboim Gravity". In: *arXiv* (Oct. 2022). arXiv: 2210.10846 [hep-th].

[238] H. Verlinde. "ER = EPR revisited: On the Entropy of an Einstein-Rosen Bridge". In: *arXiv* (Mar. 2020). arXiv: 2003.13117 [hep-th].

[239] L. J. Boya, A. M. Perelomov, and M. Santander. "Berry phase in homogeneous Kähler manifolds with linear Hamiltonians". In: *Journal of Mathematical Physics* **42** (Nov. 2001), pp. 5130–5142.

[240] H. Verlinde. "Deconstructing the Wormhole: Factorization, Entanglement and Decoherence". In: *arXiv* (May 2021). arXiv: 2105.02142 [hep-th].

[241] M. V. Berry. "Quantal phase factors accompanying adiabatic changes". In: *A Half-Century of Physical Asymptotics and Other Diversions*. Chap. 1.6, pp. 72–84.

[242] M. Nakahara. *Geometry, topology and physics*. 2003.

[243] F. S. Nogueira et al. "Geometric phases distinguish entangled states in wormhole quantum mechanics". In: *Phys. Rev. D* **105** (2022), p. L081903. arXiv: 2109.06190 [hep-th].

[244] E. Witten. "A New Look At The Path Integral Of Quantum Mechanics". In: *arXiv* (Sept. 2010). arXiv: 1009.6032 [hep-th].

[245] M. Henneaux, W. Merbis, and A. Ranjbar. "Asymptotic dynamics of AdS_3 gravity with two asymptotic regions". In: *JHEP* **03** (2020), p. 064. arXiv: 1912.09465 [hep-th].

[246] X. Huang and C.-T. Ma. "Berry Curvature and Riemann Curvature in Kinematic Space with Spherical Entangling Surface". In: *Fortsch. Phys.* **69** (2021), p. 2000048. arXiv: 2003.12252 [hep-th].

[247] H. Casini, M. Huerta, and R. C. Myers. "Towards a derivation of holographic entanglement entropy". In: *JHEP* **05** (2011), p. 036. arXiv: 1102.0440 [hep-th].

[248] T. Hartman and N. Afkhami-Jeddi. "Speed Limits for Entanglement". In: *arXiv* (Dec. 2015). arXiv: 1512.02695 [hep-th].

[249] P. Fries and I. A. Reyes. "Entanglement and relative entropy of a chiral fermion on the torus". In: *Phys. Rev. D* **100** (2019), p. 105015. arXiv: 1906.02207 [hep-th].

[250] D. L. Jafferis and S. J. Suh. "The Gravity Duals of Modular Hamiltonians". In: *JHEP* **09** (2016), p. 068. arXiv: 1412.8465 [hep-th].

[251] B. Czech and L. Lamprou. "Holographic definition of points and distances". In: *Phys. Rev. D* **90** (2014), p. 106005. arXiv: 1409.4473 [hep-th].

[252] B. Czech et al. "Integral Geometry and Holography". In: *JHEP* **10** (2015), p. 175. arXiv: 1505.05515 [hep-th].

[253] L. Apolo et al. "Modular Hamiltonians in flat holography and (W)AdS/WCFT". In: *JHEP* **09** (2020), p. 033. arXiv: 2006.10741 [hep-th].

[254] G. Compère and A. Fiorucci. "Advanced Lectures on General Relativity". In: *arXiv* (Jan. 2018). arXiv: 1801.07064 [hep-th].

[255] J. de Boer et al. "Holographic de Sitter Geometry from Entanglement in Conformal Field Theory". In: *Phys. Rev. Lett.* **116** (2016), p. 061602. arXiv: 1509.00113 [hep-th].

[256] Y. O. Nakagawa, G. Sárosi, and T. Ugajin. "Chaos and relative entropy". In: *JHEP* **07** (2018), p. 002. arXiv: 1805.01051 [hep-th].

[257] E. Witten. "Why Does Quantum Field Theory In Curved Spacetime Make Sense? And What Happens To The Algebra of Observables In The Thermodynamic Limit?" In: *arXiv* (Dec. 2021). arXiv: 2112.11614 [hep-th].

[258] M. Takesaki. "Duality for crossed products and the structure of von Neumann algebras of type III". In: *Acta Mathematica* **131** (1973), pp. 249–310.

[259] E. Witten. "Algebras, Regions, and Observers". In: *arXiv* (Mar. 2023). arXiv: 2303.02837 [hep-th].

[260] J. Milnor. "Curvatures of left invariant metrics on lie groups". In: *Advances in Mathematics* **21** (1976), pp. 293–329.

[261] A. R. Brown, L. Susskind, and Y. Zhao. "Quantum Complexity and Negative Curvature". In: *Phys. Rev. D* **95** (2017), p. 045010. arXiv: 1608.02612 [hep-th].

[262] A. R. Brown and L. Susskind. "Second law of quantum complexity". In: *Phys. Rev. D* **97** (2018), p. 086015. arXiv: 1701.01107 [hep-th].

[263] V. Balasubramanian, J. J. Heckman, and A. Maloney. "Relative Entropy and Proximity of Quantum Field Theories". In: *JHEP* **05** (2015), p. 104. arXiv: 1410.6809 [hep-th].

[264] K. Hashimoto et al. "Deep learning and the AdS/CFT correspondence". In: *Phys. Rev. D* **98** (2018), p. 046019. arXiv: 1802.08313 [hep-th].

[265] K. Hashimoto et al. "Deep learning and the AdS/CFT correspondence". In: *Physical Review D* **98** (2018), p. 046019.

[266] K. Hashimoto. "AdS/CFT correspondence as a deep Boltzmann machine". In: *Physical Review D* **99** (2019), p. 106017.

[267] J. Erdmenger, K. T. Grosvenor, and R. Jefferson. "Towards quantifying information flows: relative entropy in deep neural networks and the renormalization group". In: *SciPost Phys.* **12** (2022), p. 041. arXiv: 2107.06898 [hep-th].

[268] C. Bény. "Deep learning and the renormalization group". In: *arXiv* (Jan. 2013). arXiv: 1301.3124 [quant-ph].

[269] P. Mehta and D. J. Schwab. "An exact mapping between the variational renormalization group and deep learning". In: *arXiv* (2014). arXiv: 1410.3831 [hep-th].

[270] K. Guy and G. Perdue. "Using Reinforcement Learning to Optimize Quantum Circuits in the Presence of Noise". In: *Fermilab Technical Publications* (Aug. 2020).

[271] T. Fösel et al. "Quantum circuit optimization with deep reinforcement learning". In: *arXiv* (2021).

[272] E.-J. Kuo, Y.-L. L. Fang, and S. Y.-C. Chen. "Quantum architecture search via deep reinforcement learning". In: *arXiv* (2021).

[273] J. Schulman et al. "Proximal policy optimization algorithms". In: *arXiv* (2017).

[274] J. Cotler and K. Jensen. "A theory of reparameterizations for AdS_3 gravity". In: *JHEP* **02** (2019), p. 079. arXiv: 1808.03263 [hep-th].

[275] J. Aparicio and E. Lopez. "Evolution of Two-Point Functions from Holography". In: *JHEP* **12** (2011), p. 082. arXiv: 1109.3571 [hep-th].